ECOLOGY OF PHOTOSYNTHETIC PICOEUKARYOTES IN THE OLIGOTROPHIC OCEAN: DIVERSITY, ACTIVITY, AND DYNAMICS

A DISSERTATION SUBMITTED TO THE GRADUATE DIVISION OF THE UNIVERSITY OF HAWAI‘I AT MĀNOA IN PARTIAL FULFILLMENT OF THE REQUIREMENTS FOR THE DEGREE OF

DOCTOR OF PHILOSOPHY

IN

OCEANOGRAPHY

MAY 2016

By

Yoshimi M. Rii

Dissertation Committee:
Matthew J. Church, Chairperson
Robert R. Bidigare
David M. Karl
Michael S. Rappé
Alison R. Sherwood

Keywords: Picoplankton, picoeukaryotes, phytoplankton diversity, 18S rRNA gene, photosynthetic pigments, primary productivity, flow cytometry, North Pacific Subtropical Gyre, South Pacific Subtropical Gyre

DEDICATION

This dissertation is dedicated to my family, in particular:
my mother, who has provided me with unconditional love and support throughout my life, and instilled in me an endless thirst for knowledge, curiosity about all things close and beyond, and determination to always do my best;
my sister, who radiates peace and overcomes obstacles and pain with a smile;
my grandmother-in-law, who expertly balanced being a mother to five while obtaining her PhD;
my mother-in-law, whose love and kindness I will hold in my heart forever;
and finally my husband, who dreams big and works hard to achieve his goals.

ACKNOWLEDGMENTS

This dissertation could not have been possible without the generosity and kindness of numerous individuals and organizations. Chapter-specific acknowledgments are included within each chapter in this dissertation. Funding for this research was provided by National Science Foundation grants for the Hawaii Ocean Time-series (HOT) program, Center for Microbial Oceanography: Research and Education (C-MORE), and the Dimensions of Biodiversity project, as well as by the Simons Collaboration in Ocean Processes and Ecology. Thanks also to the University of Hawai‘i Foundation and Hawai‘i Institute of Geophysics and Planetology for graduate funding through the Denise B. Evans Research Fellowship in Oceanography. A very special thanks to the administrative support staff of the Department of Oceanography in the School of Ocean and Earth Science and Technology, especially Catalpa Kong, Anne Lawyer, Nancy Koike, and Kristin Momohara, and to the C-MORE staff, especially Georgia Tanaka, Jennifer Kondo, Lisa Lum, Sharon Sakamoto, Steve Poulos, and Eric Grabowski.

I extend my deepest gratitude to Matt Church, my primary advisor, who has, from day 1, “had my back” and supported me throughout this work. His thoroughness, attention to detail, and dedication to producing high quality work are merits I hope to carry on as I move forward in my career. He is an amazing teacher, advisor, and mentor, and I cannot thank him enough for being by my side every step of the way. His unwavering belief in me truly helped to overcome many of the academic as well as psychological obstacles in my PhD journey.

Many thanks to my dissertation committee members for being extremely supportive and helpful throughout my research. Dave Karl has provided me with a home within C-MORE, and always offered comments and questions that helped put my work in perspective. Thanks to Bob Bidigare, who has supported my oceanographic research career throughout my Master’s and now through my PhD, and was always available for interesting discussions. I am continually humbled by their intelligence and breadth of knowledge. Mike Rappé has always been generous, with his time and with the support he provided on a number of techniques used in this dissertation. Finally, thanks to Alison Sherwood, who provided helpful comments to my dissertation as well as advice on careers.

This work could not have been possible without the hard work of the past and present researchers of the HOT program. They are a dedicated group of oceanographers who I have had

the utmost pleasure of working with, and consider myself extremely lucky to have had this experience. Many thanks also to the captains and crew of various research vessels, and to the researchers who have led expeditions on the research cruises I have participated in, including Sam Wilson, Jessica Fitzsimmons, Dan Repeta, Solange Duhamel, Jamie Becker, Tara Clemente, Susan Curless, Dan Sadler, and Fernando Santiago-Mandujano. Particular to some of the methods used in this work, I would like to extend gratitude to Ken Doggett, Karin Björkman, Anne Thompson, Edward DeLong, John Eppley, Markus Lindh, Christine Shulse, Sean Jungbluth, Brianne Maillot, Brenner Wai, Anna Neuheimer, Craig Nelson, Everett Omori, Bob Bowers, and Stephanie Christensen. I am extremely grateful to my lab mates, especially Donn Viviani and Daniela Böttjer who have helped me with countless things at sea and in the lab.

Thank you to many of my advisors and mentors throughout the years, including Paul Bienfang for always providing sage advice; Susan Brown, Kathleen Ruttenberg, and Margaret McManus for supporting me through a transition period; and Barbara Bruno, Michele Guannel, and Malia Rivera for nurturing my outreach and communication efforts outside of research. My graduate career would not have been as fulfilling without the knowledge I've gained from working with these excellent advisors. This is also true for colleagues and cohorts, especially Michelle Jungbluth and Elisha Wood-Charlson and the rest of the Science Communicators ʻOhana who have partnered with me to improve science communication amongst scientists; Anela Choy, Tatiana Oje, and Jennifer Wong-Ala for irreplaceable experiences within the Maile Mentoring Bridge and beyond; and my officemates, especially Chris Schvarcz, Olivia Nigro, Donn Viviani, and others for science discussions, jokes, and support. Thanks also to other colleagues near and far, including Alli Fong, Fenina Buttler, Sandra Martinez, Sue Defelice Slaughter, Tara Clemente, Susan Curless, Jackie Miranda, Angel White, Stuart Goldberg, Flavienne Bruyant, and Xuemei Bai, for continuous encouragement.

Lastly, I acknowledge my family and friends for being there and understanding my choice to embark on this journey. To my friends from various paths in life, including Lōkahi, ʻIolani, and UCLA, thank you for providing balance and love. I am eternally grateful to my family, the Rii's, the Claborn's, and the Stewart's, for cheering me on with kindness and patience. I hope to continue exploring our oceans for many years to come, and am grateful for the opportunity to contribute knowledge that could result in preserving the wonder that is our planet Earth.

ABSTRACT

Picophytoplankton (≤3 μm), including cyanobacteria and photosynthetic picoeukaryotes (PPE), account for ~60% of total phytoplankton biomass and are responsible for greater than 40% of total net primary production in large regions of the world's oceans. Eukaryotic picophytoplankton are globally significant contributors to primary productivity; however, to date, relatively little is known about the temporal dynamics underlying their production and diversity. In this dissertation, picophytoplankton contributions to ^{14}C primary productivity and group-specific contributions by *Prochlorococcus*, *Synechococcus*, and PPE were determined along a transect spanning a large trophic gradient in the South East Pacific Ocean (SEP) and during monthly scale sampling over a one-year period at Station ALOHA in the North Pacific Subtropical Gyre (NPSG). Results revealed that cell-specific rates of PPE carbon fixation were elevated in the well-lit regions of the euphotic zone (<75 m). In addition, depth-dependent variability in PPE taxa composition was determined in biogeochemically distinct regions of the SEP, and depth- and time-dependent variability was examined throughout the euphotic zone (0-175 m) at Station ALOHA in the NPSG over a two-year period. Diverse and distinct PPE taxa were observed in the SEP and in the NPSG between the well-lit and the dimly lit regions of the euphotic zone. Moreover, PPE taxa composition in the NPSG varied seasonally, with taxa typically residing near the deep chlorophyll maximum entrained into the upper euphotic zone during periods of winter and spring convective mixing. Such variations in PPE communities appeared to influence the types of organisms best poised to respond to nutrient perturbations in the surface waters at Station ALOHA at different times of the year. Overall, results revealed greater diversity of PPE taxa in oligotrophic environments with potentially mixotrophic taxa more prevalent in these low-nutrient regions. This dissertation contributes knowledge to understanding the ecology of picoeukaryotes in the euphotic zone of the open ocean, and lends insight into the contributions of these microorganisms to carbon cycling in these oligotrophic habitats.

TABLE OF CONTENTS

LIST OF TABLES

LIST OF FIGURES

CHAPTER 1 – Introduction, Rationale, and Research Objectives

1.1 Introduction

Subtropical ocean gyres occupy ~40% of Earth's surface (Longhurst, 1998; Karl, 1999) and ~60% of the total ocean area (Eppley and Peterson, 1979; Emerson et al., 1997). Primary production in the ocean, estimated to be ~50 Gt C y^{-1}, accounts for nearly half of the net global carbon fixation (Field et al., 1998; Carr et al., 2006), and the low nutrient waters of the subtropical ocean gyres are the site of a major fraction of this productivity (Martin et al., 1987; Longhurst et al., 1995; Karl et al., 1996; Falkowski et al., 1998; Behrenfeld et al., 2006). Picophytoplankton, operationally defined as photosynthetic organisms smaller than 2-3 μm in diameter, are dominant contributors to productivity and plankton biomass in these oligotrophic ocean gyres (Sieburth et al., 1978; Campbell et al., 1994; Li, 1994; Marañon et al. 2001). Their light-harvesting physiologies and high surface area-to-volume ratios make them efficient competitors for low nutrient concentrations that typify oligotrophic oceanic regions (Raven, 1986; Chisholm, 1992).

The picophytoplankton community in the subtropical ocean gyres is dominated in numerical abundance by prokaryotic marine cyanobacteria belonging to the genera *Prochlorococcus* (Chisholm et al., 1988) and *Synechococcus* (Waterbury et al., 1979). In the North Pacific Subtropical Gyre (NPSG), *Prochlorococcus* contributes up to 82% to total gross primary production (Liu et al., 1997; Karl, 1999). However, select studies in the past 20 years have reported that a diverse group of eukaryotic picophytoplankton may contribute significantly to carbon biomass and primary production despite their relatively low abundance in oligotrophic regions (Li, 1994; Zubkov et al., 2000; Grob et al., 2007; Li et al., 2011). Studies conducted in both coastal (Worden et al. 2004) and open ocean waters (Goericke, 1998; Jardillier et al., 2010) supported a seminal study by Li (1994), which indicated that small eukaryotic phytoplankton maintain high (cell- or taxon-specific) rates of carbon fixation despite generally low population sizes. Such reports suggest that PPE may be highly responsive to changes in nutrients and light, constituting essential components of microbial food webs and playing significant roles in global nutrient cycles.

Picoeukaryotes are single-celled organisms that, unlike cyanobacteria, possess a nucleus and minimal organelles (*e.g.* mitochondrion, chloroplast if photosynthetic), and like all

eukaryotes, their cellular components are the evolutionary products of one or several endosymbiosis events (Delwiche, 1999). This group consists of planktonic protists possessing diverse metabolic capabilities (including autotrophy, heterotrophy, and mixotrophy), with different trophic interactions and variable roles in marine food webs (Jones et al., 1993, Granéli et al., 1999, Zubkov and Tarran, 2008; Hartmann et al., 2012). Picoeukaryotes capable of photosynthesis are often perceived as occupying similar functional niches as prokaryotic cyanobacteria; however, they are phenotypically, phylogenetically, and metabolically diverse, containing subgroups that are scattered throughout at least five branches of the eukaryotic tree (Baldauf, 2003). Hence, photosynthetic picoeukaryotes (PPE) likely demonstrate different responses to variations in nutrient resources and experience varying top-down controls in comparison to those of cyanobacteria. To date, oceanic PPE are underrepresented in culture collections and hence laboratory characterization of their physiologies is lacking (Campbell et al., 1994; Worden et al., 2004). Thus, identifying the diversity of PPE communities and the factors influencing PPE population structure provides important information on the functioning of contemporary marine ecosystems.

1.2 Methods for PPE identification

Due in part to their small cell sizes, PPE can be difficult to distinguish morphologically using microscopy-based methods. In the open ocean, most PPE are lacking in distinctive morphological characteristics, occurring as coccoid or flagellated cell forms. Light microscopy thus has limited utility for taxonomic differentiation of these organisms (Simon et al., 1995). The use of high-resolution scanning and transmission electron microscopes has provided more detailed information on the surface morphology of these cells and cross-sectional views of cell types and organelles; however, sample preparation for these analyses can be time-consuming and cell losses during such preparations are often large.

Since the 1980s, enumeration of marine picoplankton using flow cytometric techniques has become increasingly popular. Such tools led to the discovery and enumeration of *Prochlorococcus,* the most abundant photosynthetic organism in the oligotrophic oceans (Chisholm et al., 1988). When distinguishing organisms by fluorescence and light scatter (proxy for size) on the flow cytometer, “picoeukaryotes” appear as an operationally defined group of

picoplankton containing higher chlorophyll fluorescence and having slightly larger cell sizes than the cyanobacteria *Prochlorococcus* and *Synechococcus*.

Separation and quantification of photosynthetic pigments with high performance liquid chromatography (HPLC) have proven useful for distinguishing distributions and biomass of various phytoplankton taxa (*e.g.*, Letelier et al., 1993; Bidigare and Ondrusek, 1996). However, phytoplankton taxa cannot be discriminated using pigment concentrations beyond the class level, and cell pigment composition varies by species and depends in part on the light and nutrient history of the cells (Dimier et al., 2009; Jeffrey et al., 2011). Laboratory cultures of representative organisms are needed to characterize the pigment content of specific species or genera, and many lineages of marine phytoplankton have proven difficult to isolate. Hence, relationships between pigment content and biomass are not well resolved. For example, the most abundant eukaryotic carotenoid in tropical waters is 19'-hexanoyloxyfucoxanthin (Letelier et al., 1993; Bidigare and Ondrusek, 1996), the diagnostic pigment for prymnesiophytes, which are commonly found in the nano-plankton size range (2-20 μm; Sieburth et al., 1978). However, recent studies have discovered a multitude of unique prymnesiophyte taxa in the pico-size range from subpolar and subtropical oceans that have yet to be identified (Moon-van der Staay et al., 2000; Liu et al., 2009; Cuvelier et al., 2010).

Culture-independent techniques, including those relying on sequencing or amplification of specific genetic markers, have been widely utilized for characterizing the microbial biodiversity of prokaryotes (*e.g.*, Giovannoni et al., 1990). In the last decade, the use of nucleic acid-based techniques has revealed an unexpected diversity of picoeukaryotes in all oceans and has greatly improved our understanding of the distribution and possible function of the PPE assemblage (*e.g.*, Moon-van der Staay et al., 2001; Vaulot et al., 2008; Worden and Not, 2008; Cuvelier et al., 2010; Kirkham et al., 2011; 2013). Ribosomal RNA genes (rRNA) are widely used as phylogenetic markers to distinguish Bacteria, Archaea, and Eukaryotes (Pace, 1997). The slow and known rate of evolution of rRNA genes allows for the construction of evolutionary relationships between distantly related organisms. Moreover, the 18S rRNA gene contains highly conserved and rapidly evolving regions, permitting discriminations of eukaryotic organisms at many different taxonomic levels, from phylum to species. In addition to rRNA genes, other genes have been utilized as phylogenetic markers for discriminating phytoplankton, including the plastid 16S rRNA genes (Rappé et al., 1995; 1998; Shi et al., 2011; Treusch et al., 2012), as well

as functional genes such as *rbcL*, which codes for the large subunit of the RuBisCO protein (Paul et al., 1999; Wawrik et al., 2002; 2003).

By targeting such genes, techniques such as the polymerase chain reaction, cloning, and sequencing have provided new insights into the diversity, distribution, and abundance of uncultivated groups of organisms, such as picoeukaryotes. Numerous studies have found that 18S rRNA gene sequences are often dominated by the presence of heterotrophic eukaryotes, including alveolates (Syndiniales group I and II which are parasites of larger phytoplankton) and heterotrophic stramenopiles (MAST predators; Diéz et al., 2001; Massana et al., 2004; Caron et al., 2009). Thus, the combination of methods, such as sorting of chlorophyll-containing cells using a flow cytometer and subsequent amplification and sequencing of eukaryote rRNA genes, has proven useful in revealing subgroups of PPE (Cuvelier et al., 2010; Shi et al., 2011). Alternatively, surveys of eukaryotic diversity based on high-throughput sequencing of 18S rRNA genes have improved our knowledge of eukaryotic plankton diversity and biogeographic distributions in the world's oceans (*e.g.*, Pernice et al., 2013; Logares et al., 2014; de Vargas et al, 2015).

1.3 PPE contribution to carbon fixation

Determinations of the contributions of different plankton size fractions to primary production rely in large part on studies examining ^{14}C incorporation into cells captured on size-fractionated filter membranes. However, determining the contribution of different groups to primary production, especially between picoplanktonic prokaryotes and eukaryotes, has proven difficult. Li (1994) used a combination of flow cytometric sorting coupled with ^{14}C tracer experiments, and concluded that picoeukaryotes are important contributors to primary production in spite of their relatively low numerical abundance. Recently, by combining flow cytometry, radioactive tracer experiments, and molecular techniques, Jardillier et al. (2010) revealed that small eukaryotes (dominated by prymnesiophytes) contributed as much as 44% to total carbon fixation in the open sea. In this way, flow cytometric sorting of ^{14}C-radiolabeled cells can provide estimates of group-specific rates of ^{14}C primary production and allow linkage of taxonomic information with function.

1.4 Rationale for this study

Many eukaryotic phytoplankton have been described from coastal waters and relatively eutrophic oceanic waters (Moon-van der Staay 2000; 2001; Guillou et al., 2004); however, there are few studies describing the composition of picoeukaryote assemblages or their vertical distribution in the water column in the oligotrophic Pacific Ocean. Picophytoplankton are responsible for a large fraction of primary production in the subtropical gyres, but the fraction of picoeukaryotic contribution to primary production, and temporal and vertical variability associated with their productivity has not been examined (Vaulot et al., 2008). Moreover, PPE appear to respond significantly in terms of growth and biomass to nutrient enrichment, but the taxonomic identity of the organisms that respond to such perturbations remains unknown (McAndrew et al., 2007; Duhamel and Moutin, 2009; Mahaffey et al., 2012). Hence, identifying the key groups of PPE and examining their ecological significance in the oligotrophic Pacific Ocean will further understanding of planktonic carbon cycling in the oligotrophic oceans.

1.5 Research objectives and structure

The overall goals of this dissertation research are to 1) examine the population dynamics (abundance and diversity) of PPE in the oligotrophic oceans, and 2) elucidate the role of PPE in ocean carbon cycling.

Specific objectives of this dissertation are:

1) Describe the spatial and temporal variability of PPE population structure (abundance and diversity) in the oligotrophic Pacific Ocean;
2) Determine the contribution of PPE to rates of carbon fixation in the oligotrophic ocean;
3) Investigate how differing nitrogenous substrates influence PPE biomass, diversity, and productivity.

This dissertation consists of six chapters built around the three specific objectives. **Chapter 1** is this introductory chapter, with the aim to provide background information about previously known knowledge of PPE and the rationale for this study. **Chapter 2** investigated the spatial dynamics of PPE taxa composition and their contributions to picophytoplankton productivity between biogeochemically distinct regions in the South East Pacific Ocean. This

work was published in *Limnology and Oceanography* (Y.M. Rii, S. Duhamel, R.R. Bidigare, D.M. Karl, D.J. Repeta, M.J. Church, 2016. Diversity and productivity of photosynthetic picoeukaryotes in biogeochemically distinct regions of the South East Pacific Ocean. doi:10.1002/lno.10255). Chapters 3, 4, and 5 examined the dynamics of PPE population structure and productivity at Station ALOHA, a well-characterized field site of the Hawaii Ocean Time-series program in the NPSG. In **Chapter 3**, contributions of PPE to picophytoplankton carbon fixation and their depth and time variability over a period of one year (2012-2013) were examined at Station ALOHA. This chapter will be submitted to *Marine Ecology Progress Series* under the authorship of Y.M. Rii, D.M. Karl, and M.J. Church. **Chapter 4** used next generation sequencing to examine the temporal and depth variability of picoeukaryote populations at Station ALOHA over a period of two years (2011-2013). Chapter 4 will be submitted to *The ISME Journal* under the authorship of Y.M. Rii, M. Lindh, and M.J. Church. In **Chapter 5**, nutrient addition experiments were performed to determine the response of PPE assemblages to the addition of differing nitrogenous substrates and how the magnitude and time-scales of their response influence phytoplankton successional patterns. Five experiments were conducted during different times of the year from 2011- 2013. Chapter 5 will be submitted to *Environmental Microbiology* under the authorship of Y.M. Rii, R.R. Bidigare, D.M. Karl, and M.J. Church. Finally, **Chapter 6** provides an integrated synthesis and overall insights gained from the research conducted as part of this dissertation. Significance of this work and ideas for future research are also discussed.

1.6 References

Baldauf, S. 2003. The deep roots of eukaryotes. Science **300**: 1703-1706.

Behrenfeld, M. J., R. T. O'Malley, D. A. Siegel, and others. 2006. Climate-driven trends in contemporary ocean productivity. Nature **444**: 752-755.

Bidigare, R. R., and M. E. Ondrusek. 1996. Spatial and temporal variability of phytoplankton pigment distributions in the central equatorial Pacific Ocean. Deep-Sea Res. II **43**: 809-833.

Campbell, L., H. A. Nolla, and D. Vaulot, D. 1994. The importance of *Prochlorococcus* to community structure in the central North Pacific Ocean. Limnol. Oceanogr. **39**: 954-961.

Caron, D. A., A. Z. Worden, P. D. Countway, E. Demir, and K. B. Heidelberg. 2009. Protists are microbes too: a perspective. ISME J. **3**: 4-12.

Carr, M. E., M. A. M. Friedrichs, M. Schmeltz, and others. 2006. A comparison of global estimates of marine primary production from ocean color. Deep-Sea Res. II **53**: 741-770.

Chisholm, S. W., R. J. Olson, E. R. Zettler, R. Goericke, J. B. Waterbury, and N. A. Welschmeyer. 1988. A novel free-living prochlorophyte abundant in the oceanic euphotic zone. Nature **334**: 340-343.

Chisholm, S. W. 1992. Phytoplankton size, p. 213-237. In P. G. Falkowski and A. D. Woodhead [eds.], Primary productivity and biogeochemical cycles in the sea. Springer.

Cuvelier, M. L., A. E. Allen, A. Monier, and others. 2010. Targeted metagenomics and ecology of globally important uncultured eukaryotic phytoplankton. Proc. Natl. Acad. Sci. U.S.A. **107**: 14679-14684.

Delwiche, C. F. 1999. Tracing the thread of plastid diversity through the tapestry of life. Am. Nat. **154**: S164-S177.

de Vargas, C., S. Audic, N. Henry, and others. 2015. Ocean plankton. Eukaryotic plankton diversity in the sunlit ocean. Science **348**: 1261605. doi:10.1126/science.1261605.

Diéz, B., C. Pedrós-Alió, and R. Massana. 2001. Study of genetic diversity of eukaryotic picoplankton in different oceanic regions by small-subunit rRNA gene cloning and sequencing. Appl. Environ. Microbiol. **67**: 2932-2941.

Dimier, C., C. Brunet, R. Geider, and J. Rave. 2009. Growth and photoregulation dynamics of the picoeukaryote *Pelagomonas calceolata* in fluctuating light. Limnol. Oceanogr. **54**: 823-836.

Duhamel, S., and T. Moutin. 2009. Carbon and phosphate incorporation rates of microbial assemblages in contrasting environments in the Southeast Pacific. Mar. Ecol. Progr. Ser. **375**: 53-64.

Emerson, S., P. Quay, D. M. Karl, C. Winn, L. Tupas, and M. Landry. 1997. Experimental determination of the organic carbon flux from open-ocean surface waters. Nature **389**: 951-954.

Eppley, R. W., and B. J. Peterson. 1979. Particulate organic matter flux and planktonic new production in the deep ocean. Nature **282**: 677-680.

Falkowski, P. G., R. T. Barber, and V. Smetacek. 1998. Biogeochemical controls and feedbacks on ocean primary production. Science **282**: 200-206.

Field, C. B., M. J. Behrenfeld, J. T. Randerson, and P. G. Falkowski. 1998. Primary production of the biosphere: integrating terrestrial and oceanic components. Science **281**: 237-240.

Giovannoni, S. J., E. F. DeLong, T. M. Schmidt, and N. R. Pace. 1990. Tangential flow filtration and preliminary phylogenetic analysis of marine picoplankton. Appl. Environ. Microbiol. **56**: 2572-2575.

Goericke, R. 1998. Response of phytoplankton community structure and taxon-specific growth rates to seasonally varying physical forcing in the Sargasso Sea off Bermuda. Limnol. Oceanogr. **43**: 921-935.

Granéli, E., P. Carlsson, and C. Legrand. 1999. The role of C, N and P in dissolved and particulate organic matter as a nutrient source for phytoplankton growth, including toxic species. Aquat. Ecol. **33**: 17-27.

Grob, C., O. Ulloa, H. Claustre, Y. Huot, G. Alarcón, and D. Marie. 2007. Contribution of picoplankton to the total particulate organic carbon concentration in the eastern South Pacific. Biogeosciences **4**: 837-852.

Guillou, L., W. Eikrem, M. J. Chrétiennot-Dinet, F. Le Gall, R. Massana, K. Romari, C. Pedrós-Alió, and D. Vaulot. 2004. Diversity of picoplanktonic prasinophytes assessed by direct nuclear SSU rDNA sequencing of environmental samples and novel isolates retrieved from oceanic and coastal marine ecosystems. Protist **155**: 193-214.

Hartmann, M., C. Grob, G. A. Tarran, A. P. Martin, P. H. Burkill, D. J. Scanlan, and M. V. Zubkov. 2012. Mixotrophic basis of Atlantic oligotrophic ecosystems. Proc. Natl. Acad. Sci. U.S.A. **109**: 5756–5760.

Jardillier, L., M. V. Zubkov, J. Pearman, and D. J. Scanlan. 2010. Significant CO_2 fixation by small prymnesiophytes in the subtropical and tropical northeast Atlantic Ocean. ISME J. **4**: 1180-1192.

Jeffrey, S. W., S. W. Wright, and M. Zapata. 2011. Microalgal classes and their signature pigments, p. 3-77. In S. Roy, C. A. Llewellyn, E. Skarstad Egeland, and G. Johnsen [eds.], Phytoplankton pigments. Characterization, Chemotaxonomy, and Applications in Oceanography. Cambridge University Press, Cambridge.

Jones, H. L. J., B. S. C. Leadbeater, and J. C. Green. 1993. Mixotrophy in marine species of *Chrysochromulina* (Prymnesiophyceae): ingestion and digestion of a small green flagellate. J. Mar. Biol. Assoc. U. K. **73**: 283-296.

Karl, D. M., 1999. A sea of change: biogeochemical variability in the North Pacific Subtropical Gyre. Ecosystems **2**: 181-214.

Karl, D. M., J. R. Christian, J. E. Dore, D. V. Hebel, R. M. Letelier, L. M. Tupas, and C. D. Winn. 1996. Seasonal and interannual variability in primary production and particle flux at Station ALOHA. Deep-Sea Research II 43: 539-568.

Kirkham, A. R., L. E. Jardillier, A. Tiganescu, J. Pearman, M. V. Zubkov, and D. J. Scanlan. 2011. Basin-scale distribution patterns of photosynthetic picoeukaryotes along an Atlantic Meridional Transect. Environ. Microbiol. **13**: 975-990. doi:10.1111/j.1462-2920.2010.02403.x.

Kirkham, A. R., C. Lepère, L. E. Jardillier, F. Not, H. Bouman, A. Mead, and D. J. Scanlan. 2013. A global perspective on marine photosynthetic picoeukaryote community structure. ISME J. **7**: 922-936. doi:10.1038/ismej.2012.166.

Letelier, R. M., R. R. Bidigare, D. V. Hebel, M. E. Ondrusek, C. D. Winn, and D. M. Karl. 1993. Temporal variability of phytoplankton community structure based on pigment analysis. Limnol. Oceanogr. **38**: 1420-1437.

Li, B., D. M. Karl, R. M. Letelier, and M. J. Church. 2011. Size-dependent photosynthetic variability in the North Pacific Subtropical Gyre. Mar. Ecol. Prog. Ser. **440**: 27-40.

Li, W. K. W. 1994. Primary production of prochlorophytes, cyanobacteria, and eukaryotic ultraphytoplankton: measurements from flow cytometric sorting. Limnol. Oceanogr. **39**: 169-175.

Liu, H., H. A. Nolla, and L. Campbell. 1997. *Prochlorococcus* growth rate and contribution to primary production in the equatorial and subtropical North Pacific Ocean. Aquatic Microbial Ecology 12: 39-47.

Liu, H., Probert, I., Uitz, J., Claustre, H., Aris-Brosou, S., Frada, M., Not, F., de Vargas, C., 2009. Extreme diversity in noncalcifying haptophytes explains a major pigment paradox in open oceans. Proc. Natl. Acad. Sci. U.S.A. **106**: 12803-12808.

Logares, R., S. Audic, D. Bass, and others (2014). Patterns of rare and abundant marine microbial eukaryotes. Curr. Biol. **24**: 813-821.

Longhurst, A., 1998. Ecological Geography of the Sea. Academic Press, San Diego, 542 pp.

Longhurst, A., S. Sathyendranath, T. Platt, and C. Caverhill. 1995. An estimate of global primary production in the ocean from satellite radiometer data. J. Plankton Res. **17**: 1245-1271.

Mahaffey, C., K. M. Björkman, and D. M. Karl. 2012. Phytoplankton response to deep seawater nutrient addition in the North Pacific Subtropical Gyre. Mar. Ecol. Prog. Ser. **460**: 13-34.

Marañon, E., P. M. Holligan, R. Barciela, N. González, B. Mouriño, M. J. Pazó, and M. Varela. 2001. Patterns of phytoplankton size structure and productivity in contrasting open-ocean environments. Mar. Ecol. Prog. Ser. **216**: 43-56.

Martin, J. H., G. A. Knauer, D. M. Karl, and W. W. Boenkow. 1987. VERTEX: Carbon cycling in the northeast Pacific. Deep-Sea Res. **34**: 267-285.

Massana, R., V. Balagué, L. Guillou, and C. Pedrós-Alioó. 2004. Picoeukaryotic diversity in an oligotrophic coastal site studied by molecular and culturing approaches. FEMS Microbiol. Ecol. **50**: 231-243.

McAndrew, P. M., K. M. Björkman, M. J. Church, P. J. Morris, N. Jachowski, P. J. le B. Williams, and D. M. Karl. 2007. Mar. Ecol. Prog. Ser. **332**: 63-75.

Moon-van der Staay, S. Y., R. De Wachter, and D. Vaulot. 2001. Oceanic 18S rDNA sequences from picoplankton reveal unsuspected eukaryotic diversity. Nature **409**: 607-610.

Moon-van der Staay, S. Y., G. W. M. van der Staay, L. Guillou, D. Vaulot, H. Claustre, and L. Medlin. 2000. Abundance and diversity of prymnesiophytes in the picoplankton community from the equatorial Pacific Ocean inferred from 18S rDNA sequences. Limnol. Oceanogr. **45**: 98-109.

Pace, N. R., 1997. A molecular view of microbial diversity and the biosphere. Science **276**: 734-740.

Paul, J. H., S. L. Pichard, J. B. Kang, G. M. F. Watson, and F. R. Tabita. 1999. Evidence for a clade-specific temporal and spatial separation in ribulose biphosphate carboxylase gene expression in phytoplankton populations off Cape Hatteras and Bermuda. Limnol. Oceanogr. **44**: 12-23.

Pernice, M. C., R. Logares, L. Guillou, and R. Massana. 2013. General patterns of diversity in major marine microeukaryote lineages. PLoS ONE **8**: e57170. doi:10.1371/journal.pone.0057170.s008.

Rappé M. S., P. F. Kemp, and S. J. Giovannoni. 1995. Chromophyte plastid 16S ribosomal RNA genes found in a clone library from Atlantic Ocean seawater. J. Phycol. **31**: 979-988.

Rappé M. S., M. T. Suzuki, K. L. Vergin, and S. J. Giovannoni. 1998. Phylogenetic diversity of ultraplankton plastid small-subunit rRNA genes recovered in environmental nucleic acid samples from the Pacific and Atlantic coasts of the United States. Appl. Environ. Microb. **64**: 294-303.

Raven, J. A. 1986. Physiological consequences of extremely small size for autotrophic organisms in the sea, p. 1-70. In T. Platt and W. K. W. Li [eds.], Photosynthetic picoplankton. Can. Bull. Fish. Aquat. Sci. 214.

Rii, Y. M., S. Duhamel, R. R. Bidigare, D. M. Karl, D. Repeta, and M. J. Church. 2016. Diversity and productivity of photosynthetic picoeukaryotes in biogeochemically distinct regions of the South East Pacific Ocean. Limnol. Oceanogr. doi:10.1002/lno.10255.

Shi, X. L., C. Lepére, D. J. Scanlan, and D. Vaulot. 2011. Plastid 16S rRNA gene diversity among eukaryotic picophytoplankton sorted by flow cytometry from the South Pacific Ocean. PLoS ONE **6**: e18979.

Sieburth, J. M., V. Smetacek, and J. Lenz. 1978. Pelagic ecosystem structure: Heterotrophic compartments of the plankton and their relationship to plankton size fractions. Limnol. Oceanogr. **23**: 1256-1263.

Simon, N., N. LeBot, D. Marie, F. Partensky, and D. Vaulot. 1995. Fluorescent *in situ* hybridization with rRNA-targeted oligonucleotide probes to identify small phytoplankton by flow cytometry. Appl. Environ. Microb. **61**: 2506-2513.

Treusch, A. H., E. Demir-Hilton, K. L. Vergin, A. Z. Worden, C. A. Carlson, M. G. Donatz, R. M. Burton, and S. J. Giovannoni. 2012. Phytoplankton distribution patterns in the northwestern Sargasso Sea revealed by small subunit rRNA genes from plastids. ISME J. **6**: 481-492.

Vaulot, D., W. Eikrem, and M. Viprey. 2008. The diversity of small eukaryotic phytoplankton (≤3 μm) in marine ecosystems. FEMS Microbiol. Rev. **32**: 795-820.

Waterbury, J. B., S. W. Watson, R. R. L. Guillard, and L. E. Brand. 1979. Widespread occurrence of a unicellular, marine, planktonic, cyanobacterium. Nature **277**: 293-294.

Wawrik, B., J. H. Paul, L. Campbell, D. Griffin, L. Houchin, A. Fuentes-Ortega, and F. Muller-Karger. 2003. Vertical structure of the phytoplankton community associated with a coastal plume in the Gulf of Mexico. Mar. Ecol. Prog. Ser. **251**: 87-101.

Wawrik, B., J. H. Paul, and F. R. Tabita. 2002. Real-time PCR quantification of *rbcL* (ribulose-1,5-biphosphate carboxylase/oxygenase) mRNA in diatoms and pelagophytes. Appl. Environ. Microb. **68**: 3771-3779.

Worden, A. Z., J. K. Nolan, and B. Palenik. 2004. Assessing the dynamics and ecology of marine picophytoplankton: The importance of the eukaryotic component. Limnol. Oceanogr. **49**: 168-179.

Worden, A. Z., and F. Not. 2008. Ecology and diversity of picoeukaryotes. In: Kirchman, D.L. (ed.), Microbial Ecology of the Oceans. John Wiley & Sons, Inc., Hoboken, pp. 159-205.

Zubkov, M. V., M. A. Sligh, P. H. Burkill, and R. J. G. Leakey. 2000. Picoplankton community structure on the Atlantic Meridional Transect: a comparison between seasons. Prog. Oceanogr. **45**: 369-386.

Zubkov, M. V., and G. A. Tarran. 2008. High bacterivory by the smallest phytoplankton in the North Atlantic Ocean. Nature **455**: 224-226. doi:10.1038/nature07236.

CHAPTER 2

Diversity and productivity of photosynthetic picoeukaryotes in biogeochemically distinct regions of the South East Pacific Ocean

Yoshimi M. Rii, Solange Duhamel, Robert R. Bidigare, David M. Karl, Daniel J. Repeta, Matthew J. Church. (2016). *Limnology and Oceanography* doi:10.1002/lno.10255

2.1. Abstract

Picophytoplankton, including photosynthetic picoeukaryotes (PPE) and unicellular cyanobacteria, are important contributors to plankton biomass and primary productivity. In this study, phytoplankton composition and rates of carbon fixation were examined across a large trophic gradient in the South East Pacific Ocean (SEP) using a suite of approaches: photosynthetic pigments, rates of ^{14}C-primary productivity, and phylogenetic analyses of partial 18S rRNA genes PCR amplified and sequenced from flow cytometrically sorted cells. While phytoplankton >10 μm (diatoms and dinoflagellates) were prevalent in the upwelling region off the Chilean coast, picophytoplankton consistently accounted for 55-92% of the total chlorophyll *a* inventories and >60% of ^{14}C-primary productivity throughout the sampling region. Estimates of rates of ^{14}C-primary productivity derived from flow cytometric sorting of radiolabeled cells revealed that the contributions of PPE and *Prochlorococcus* to euphotic zone depth-integrated picoplankton productivity were nearly equivalent (ranging 36-57%) along the transect, with PPE comprising a larger share of picoplankton productivity than cyanobacteria in the well-lit (>15% surface irradiance) region compared to in the lower regions (1-7% surface irradiance) of the euphotic zone. 18S rRNA gene sequence analyses revealed the taxonomic identities of PPE; *e.g.*, Mamiellophyceae (*Ostreococcus*) were the dominant PPE in the upwelling-influenced waters, while members of the Chrysophyceae, Prymnesiophyceae, Pelagophyceae, and Prasinophyceae Clades VII and IX flourished in the oligotrophic South Pacific Subtropical Gyre. Our results suggest that, despite low numerical abundance in comparison to cyanobacteria, diverse members of PPE are significant contributors to carbon cycling across biogeochemically distinct regions of the SEP.

2.2. Introduction

Primary production in the ocean accounts for nearly half of the net global carbon fixation and a substantial fraction of this productivity occurs in the oligotrophic subtropical gyres (Field et al., 1998; Carr et al., 2006). Picophytoplankton (typically defined as microorganisms <2-3 μm) include unicellular cyanobacteria and photosynthetic picoeukaryotes (PPE) and are significant contributors to productivity and plankton biomass, particularly in the subtropical ocean gyres (Sieburth et al., 1978; Li, 1994; Massana, 2011). Due to their numerical dominance, *Prochlorococcus* and *Synechococcus* have long been thought to be responsible for a majority of the picophytoplankton productivity in oligotrophic waters. However, several studies have reported that, despite generally low abundances, diverse members of PPE can contribute significantly to biomass and primary production due to their larger cell biovolumes and rapid growth rates (Li, 1994; Worden et al., 2004; Jardillier et al., 2010). For example, Worden et al. (2004) estimated that despite small differences in their cell diameters (PPE = ~2.0 μm, *Prochlorococcus* = ~0.7 μm, and *Synechococcus* = ~1.1 μm), PPE carbon content was 6.5- to 14-fold greater than that of pico-cyanobacteria. Combined, PPE's larger biovolume and rapid growth rates indicate that PPE can be active and significant components of picophytoplankton population dynamics in the ocean.

Photosynthetic picoeukaryotes include taxonomically diverse populations, with members scattered widely across many branches of the eukaryotic tree of life (Baldauf, 2003; Vaulot et al., 2008; Massana, 2011). Studies examining PPE diversity in various regions of the world's oceans show that members of the prasinophyte algae (Mamiellophyceae) have been found to be abundant in nutrient-enriched, coastal regions (Guillou et al., 2004; Romari and Vaulot, 2004; Worden, 2006), while groups of uncultured prymnesiophytes, chrysophytes, and pelagophytes are often more dominant in open ocean waters (Fuller et al., 2006; Shi et al., 2009; Cuvelier et al., 2010). The cosmopolitan distribution of PPE may reflect their metabolic flexibility. Many PPE taxa appear capable of mixotrophy, combining photosynthetic growth with phagotrophic consumption of other picoplankton for nutrition, thereby complicating characterization of the ecological roles of these organisms (Zubkov and Tarran, 2008; Caron et al., 2009; Hartmann et al., 2012). To date, whether or how variability in the composition of picophytoplankton assemblages influences productivity remains unclear. For example, a recent study in the Atlantic

Ocean concluded that biomass-specific rates of primary production by PPE appeared largely unaffected by changes in the phylogenetic structure of PPE assemblages (Grob et al., 2011).

In this study, we examined spatial variation in PPE diversity and contributions to productivity across diverse habitats of the South East Pacific Ocean (SEP). This study was conducted as part of the research expedition Biogeochemical Gradients: Role in Arranging Planktonic Assemblages (BiG RAPA), which focused on examining microplankton ecology in the SEP. We sampled biogeochemically distinct regions of the SEP that spanned the productive waters in the permanent upwelling zone off the coast of Chile to the oligotrophic waters of the South Pacific Subtropical Gyre (SPSG). We utilized a suite of approaches to characterize spatial variability in PPE population structure, including photosynthetic pigment-based analyses and assessment of 18S rRNA genes derived from flow cytometrically sorted PPE cells. In addition, we evaluated spatial changes in size-fractionated and PPE group-specific rates of primary productivity. Collectively, we aimed to evaluate the contributions of specific picophytoplankton to plankton biomass and the roles they play in productivity across various nutrient regimes.

2.3. Methods

2.3.1. Study site and sample collections

Sampling for this study occurred aboard R/V *Melville* from 18 November (Arica, Chile) to 14 December 2010 (Rapa Nui, Chile). Three main stations were sampled within biogeochemically distinct regions of the SEP: station 1UP in the high productivity, coastal upwelling region; station 7GY in the low productivity, oligotrophic SPSG; and station 4TR in the transitional region between 1UP and 7GY (Figure 1, Table 1). Additional stations (Stations 2, 3, 5, and 6), located between these main stations, were sampled for a subset of measurements.

A 24-bottle rosette sampler equipped with a Sea-Bird 911+ conductivity, temperature, and depth profiler was used to collect seawater samples. Water samples were collected on specific isopleth surfaces (50, 25, 15, 7, 3, 1, and 0.1% of the sea surface photosynthetically active radiation, or PAR), with additional samples collected at specific biological features, including the depth of the chlorophyll maximum (Chl max). Isopleths were calculated based on vertical profiles of downwelling PAR, measured using a Biospherical Instruments QSP-2300 PAR sensor mounted on the rosette frame. The depths of integration representing the euphotic zone were selected for each station to capture the downwelling light field (down to 0.1% surface

PAR), including the Chl max. Thus, the depths of integration used for our calculations were determined to be the depth of the 0.1% surface PAR for stations 1UP-6 and the depth of the Chl max for station 7GY.

2.3.2. Macronutrient analyses

Determination of nitrate plus nitrite ($NO_3^- + NO_2^-$) and phosphate (PO_4^{3-}) in seawater samples were measured on board the R/V *Melville* using a 5-channel, Alpkem and Technicon II™ continuous segmented flow autoanalyzer (Armstrong et al., 1967; Gordon et al., 1994). Detection limits for the instrumental settings used, determined as three times the concentration of our lowest resolvable standard, were 0.16 μM $NO_3^- + NO_2^-$ and 0.011 μM PO_4^{3-}. All nutrient data are available through the Center for Microbial Oceanography: Research and Education (C-MORE) Data System (http://hahana.soest.hawaii.edu/cmoreDS/interface.html).

2.3.3. Photosynthetic pigments

Seawater samples (2 L) were collected for subsequent determination of photosynthetic pigments from eight depths in the euphotic zone (from stations 1UP, 2, 4TR, 5, 6, and 7GY) and vacuum-filtered separately onto 25 mm diameter filters of three pore sizes including glass fiber microfilters (Whatman® GF/F) and 3 and 10 μm polycarbonate membrane filters (Millipore Isopore™). Filters were immediately flash-frozen in liquid nitrogen and stored at -80°C until analysis. Pigments were extracted in 100% acetone and analyzed on a Varian 9012 high performance liquid chromatography (HPLC) system (Waters Spherisorb® 5 μm ODS-2 C_{18} column, 200 μL injection) with SpectraSYSTEM Thermo Separation Products dual wavelength UV/VIS UV2000 and fluorescence FL2000 detectors (Bidigare et al., 2005). Pigment identifications were based on absorbance spectra and retention time comparison with a monovinyl chlorophyll *a* (Chl *a*) standard and representative culture extracts. Spectra-Physics WOW® software was used to calculate peak area and a dichromatic equation was used to spectrally resolve mixtures of monovinyl and divinyl Chl *a* (Latasa et al., 1996). Total chlorophyll *a* (TChl *a*) was calculated as the sum of monovinyl Chl *a*, divinyl Chl *a*, and chlorophyllide *a*. The limits of detection were determined as 0.6 ng per injection for chlorophylls and 0.4 ng per injection for carotenoids, which corresponded to an in situ concentration of 0.0045 mg m^{-3} (chlorophylls) and 0.003 mg m^{-3} (carotenoids) for this data set (calculated with 3

mL extract volume and filtered volume of 2 L seawater). Abbreviations and significance of photosynthetic pigments referred to in this study are described in Table 2. All pigment data are available through the C-MORE Data System (http://hahana.soest.hawaii.edu/cmoreDS/interface.html).

2.3.4. Picophytoplankton cell counts

Seawater samples for flow cytometric analyses were collected in 2 mL cryogenic vials containing a final concentration of 0.24% (w/v) paraformaldehyde (PFA, in water, Alfa Aesar 43368). The vials were kept for 15 minutes in the dark, then flash-frozen in liquid nitrogen and stored at -80°C until analysis. Abundances of PPE, *Prochlorococcus*, and *Synechococcus* were enumerated from PFA-preserved seawater samples based on fluorescence and cell scattering characteristics using a BD Influx™ flow sorter and the data acquisition software Spigot. *Prochlorococcus* cells were enumerated based on forward scatter (FSC) and chlorophyll-based red fluorescence (692 nm center wavelength) signatures using a 488 nm laser, *Synechococcus* cells were identified based on FSC and phycoerythrin-based orange fluorescence (585 nm center wavelength), and PPE cells were defined by their greater FSC, higher red fluorescence, and low orange fluorescence signatures using the data analysis software FlowJo 10.0.7. All flow cytometry cell abundance data are available through the C-MORE Data System (http://hahana.soest.hawaii.edu/cmoreDS/interface.html).

2.3.5. Photosynthetic picoeukaryote cell sorting

Seawater samples were collected, concentrated, and preserved to examine the taxonomic identities of PPE assemblages at the depths of the 50% surface PAR (5 m, 15 m, and 12 m) and the Chl max (48 m, 118 m, and 150 m) of the three main stations (1UP, 4TR, and 7GY, respectively). Seawater samples (2 L) were filtered through in-line 25 mm diameter polycarbonate membranes (pore size 3 μm, Millipore Isopore™), and 2 mL of each pre-filtered sample was collected and preserved in 0.24% (w/v) PFA for subsequent cell enumeration. Pre-filtered seawater was then concentrated to ~50-60 mL (~40-fold) by tangential flow filtration (using Millipore Pellicon® XL 50 Cassette Membranes, Durapore 0.22 μm). During concentration, the inlet pressure of the original water feed was kept constant at 25-30 psig, with the retentate (concentrate) flow at least 2x faster than the permeate flow. The retentate was first

backflushed with 10 mL of permeate, then collected in 2 and 5 mL cryogenic vials for flow cytometric analyses, containing either 0.24% (w/v) PFA for cell counting, or 7% (v/v) glycerol for sorting and subsequent molecular analyses of PPE cells. All samples were kept for 15 minutes in the dark, then flash-frozen in liquid nitrogen, and stored at -80°C until analysis.

Cell counts were determined (using the protocol previously described) for samples prior to and after tangential flow concentration to evaluate cell loss deriving from the concentration procedure. For subsequent amplification of the 18S rRNA genes, cell populations were sorted using the BD Influx™ flow sorter from glycerol-preserved samples into 1.5 mL microcentrifuge tubes containing sterile, nuclease-free water totaling up to 10 µL in volume (FSC trigger, 100 µm nozzle tip, 1X BioSure® sheath solution, 1.0 drop purity mode, two tube sort).
Triplicate samples containing 250-1000 PPE cells were collected from the sorting procedure. In addition, the following samples were collected and analyzed as negative controls in the 18S rRNA gene PCR reactions to test for contamination in the flow sorting process: sheath fluid only, 500 1 µm fluorescent microspherical beads (Fluoresbrite, Polysciences), and 250-500 cells of *Prochlorococcus* and *Synechococcus.* All picophytoplankton cells were distinguished using the same FSC and fluorescence-based properties described in the previous section. Tubes containing sorted cells were stored at -80°C until amplification.

2.3.6. Photosynthetic picoeukaryotes sequence analysis

Eukaryote 18S rRNA genes (~1527 bp) were amplified by polymerase chain reaction (PCR) using oligonucleotide primers complementary to regions of conserved sequences close to the respective 5' and 3' termini of the 18S rRNA gene (forward: 5'-ACC TGG TTG ATC CTG CCA G-3' *Escherichia coli* position 7 and reverse: 5'-TGA TCC TTC YGC AGG TTC AC-3' *E. coli* position 1534; Moon-van der Staay et al., 2000). PCR reaction mixes contained the same reagent concentrations described in Moon-van der Staay et al. (2000) except for 200 nM total deoxyribose nucleoside triphosphates (dNTPs; Life Technologies). Thermal cycling conditions were optimized for direct cell amplification and involved a 15-minute hold at 95°C proceeded by 40 cycles at 94°C for 1 minute, 55°C annealing for 1 minute, and 72°C extension for 1 minute, with a final extension at 72°C for 10 minutes. PCR products were gel-purified (Qiagen MinElute) and cloned into TOPO-TA 4 vectors (Invitrogen). Sequencing was performed using an Applied Biosystems 3730XL DNA Analyzer using the internal sequencing primer 502f (5'-

GGA GGG CAA GTC TGG T-3') targeting the V4 hypervariable region of the 18S rRNA gene (Worden, 2006).

Partial 18S rRNA gene sequences (averaging 680 bp) were checked for chimeras using USEARCH61 (Edgar et al., 2011) and clustered into distinct operational taxonomic units (OTUs) based on the SILVA 119 eukaryote database using similarity thresholds of 97 and 99% (Caporaso et al., 2010; Quast et al., 2013). Clustering at both thresholds yielded equivalent proportions of taxa composition based on class and genus level; for this study, OTUs clustered at 99% are described. Nucleotide sequences were aligned with CLUSTALW (Thompson et al., 1994) and manually inspected and edited. Distance matrices of aligned sequences were generated using CLUSTALW applying the Jukes-Cantor model. The 18S rRNA gene sequences determined in the present study have been filed in GenBank under accession numbers KR063739-KR064299.

2.3.7. Rates of ^{14}C-bicarbonate assimilation

Seawater samples for ^{14}C-based primary production measurements were collected from pre-dawn CTD hydrocasts at six depths in the euphotic zone at stations 1UP, 2, 4TR, 6, and 7GY. Duplicate samples from each depth were collected into 75 mL polycarbonate bottles and transferred to a shipboard radiation lab van where samples were inoculated (under subdued light) with a ^{14}C-bicarbonate solution to a final activity of 0.09 MBq mL^{-1}. Bottles were placed in screened bags to simulate in situ light levels and incubated in an on-deck, blue-shielded, surface seawater-cooled Plexiglas container (Arkema 2069, 6.4 mm thickness) for the full photoperiod.

Each bottle was sampled for size-fractionated and cell-specific ^{14}C activities (Duhamel et al., 2006). The total ^{14}C radioactivity added to each bottle was determined by placing 100 µL sample aliquots into 20 mL borosilicate scintillation vials containing 500 µL β-phenylethylamine and 6 mL scintillation cocktail (Perkin Elmer Ultima Gold^{TM} LLT). For size-fractionated ^{14}C activities, 10 mL of inoculated seawater was separately vacuum-filtered onto 25 mm diameter 0.2, 0.6, and 2 µm pore size polycarbonate membranes. Filters were acidified with 150 µL of 1N hydrochloric acid for 24 hours, followed by the addition of 6 mL scintillation cocktail. Samples were counted within 6-12 hours of the addition of the cocktail in a shipboard Beckman LS6500 liquid scintillation counter for determination of radioactivity. Daily rates of carbon fixation were

calculated based on the measured dissolved inorganic carbon concentrations and correcting for isotope fractionation (Steemann Nielsen, 1952).

For cell-specific ^{14}C activity measurements, duplicate 5 mL aliquots from the inoculated seawater were preserved in cryovials containing 0.24% (w/v) PFA and stored at -80°C. Cell-specific rates of carbon fixation by PPE, *Prochlorococcus*, and *Synechococcus* were determined by measuring the ^{14}C assimilated into cell populations that had been sorted using a BD Influx™ sorter (FSC trigger, 70 μm nozzle tip, 1X BioSure® sheath solution, 1.0 drop purity mode, two tube sort) into 6.5 mL HDPE scintillation vials (Li, 1994; Jardillier et al., 2010; Grob et al., 2011). Each picophytoplankton group was sorted using the same sorting parameters described for molecular analyses, except that an additional laser (457 nm, focused into the 488 nm laser pinhole) was used to improve the detection of dim *Prochlorococcus* cells, particularly in surface samples. Each group was sorted in duplicate ($2.7 \times 10^3 – 20 \times 10^3$ PPE cells, $3.0 \times 10^4 – 20 \times 10^4$ *Prochlorococcus* cells, and $2.0 \times 10^3 – 75 \times 10^3$ *Synechococcus* cells), and linearity between increasing numbers of cells sorted and radioactivity was checked regularly. The radioactivity of the sorted cells was measured following the same procedures as previously described for filtered samples but with 4 mL scintillation cocktail. Resulting radioactivity was normalized to the number of cells sorted (Bq $cell^{-1}$), and ^{14}C-assimilation rates were converted to mmol C m^{-3} d^{-1} using cell abundance, total added activity, and measured dissolved inorganic carbon concentrations (Moutin et al., 1999; Duhamel and Moutin, 2009).

While the samples for the derived 18S rRNA gene sequence information of flow cytometrically sorted PPE populations had been pre-concentrated prior to sorting, samples utilized for the ^{14}C-based rate measurements were not pre-concentrated prior to sorting. However, sort conditions were nearly identical and the fluorescence and scatter characteristics for the picophytoplankton populations did not change for the pre- and post-concentrated samples, supporting the notion that the same groups of organisms were targeted by both approaches.

2.3.8. Hierarchical clustering

Hierarchical clustering based on the Jaccard dissimilarity index (using the 'vegan' package in R 3.1.1; Oksanen et al., 2013) was used to compare the relative proportions of photosynthetic pigments (normalized to TChl *a*) and 18S rRNA gene-based assessment of PPE populations at two depths of the three main process stations.

2.4. Results

2.4.1. Spatial variability in upper ocean biogeochemistry

The sampling area for this study included diverse hydrographic and biogeochemical regions in the SEP, with strong vertical and longitudinal gradients in upper ocean temperature, nutrient, dissolved oxygen, and TChl *a* concentrations (Figure 1). Shoaling of isopycnal surfaces due to upwelling along the coast introduced cooler, nutrient-enriched, low oxygen waters to the euphotic zone, with concomitant impacts on phytoplankton biomass, diversity, and productivity. Influences of this upwelling were most evident at the eastern-most stations of the sampling region (stations 1UP and 2), where euphotic zone (vertically-integrated to the 0.1% surface PAR isopleth for stations 1UP to 6, and to the Chl max for station 7GY) inventories of $NO_3^- + NO_2^-$ and PO_4^{3-} ranged 248-625 mmol N m^{-2} and 69-100 mmol P m^{-2} (Table 1). Shoaling of low oxygen waters resulted in suboxic (<10 μM O_2) levels immediately below the subsurface Chl max (~50 m), becoming anoxic at ~100-400 m (Figure 1). With greater distance offshore, the upper ocean waters became warmer, stratified, and increasingly oligotrophic, with a deepening of this low oxygen waters into the SPSG. The resulting penetration of light through the upper ocean increased westward along the transect, with the 0.1% surface PAR isopleth ranging 57-96 m at stations 1UP and 2, and extending to 165 m into the SPSG (Figure 1, Table 1). Euphotic zone nutrient inventories decreased into the SPSG, with integrated $NO_3^- + NO_2^-$ concentrations decreasing more than 70-fold from station 1UP to stations 4TR-7GY (Table 1). Euphotic zone inventories of PO_4^{3-} decreased ~2-fold from station 1UP to station 3, then remained relatively consistent at ~37-50 mmol P m^{-2} throughout the oceanic gyre stations (Table 1).

Near-surface ocean TChl *a* concentrations decreased more than an order of magnitude into the oligotrophic waters of the SPSG, with concentrations ranging between 0.2-0.6 mg Chl m^{-3} at stations 1UP and 2, decreasing to 0.02-0.06 mg Chl m^{-3} at stations 4TR-7GY (Table 1). The resulting euphotic zone inventories of TChl *a* varied by 3.4-fold between stations 1UP and 7GY (40.0 mg m^{-2} and 11.6 mg m^{-2}, respectively; Table 1). The depth of the Chl max also deepened westward, shoaling to ~24 m at station 1UP, and deepening to ~160 m at 7GY (Table 1). The vertical positioning of the Chl max was associated with different isopleth surfaces along the transect, ranging from 7% at station 1UP to 0.1% surface PAR at station 7GY.

2.4.2. Spatial variability in phytoplankton composition

Size-fractionated photosynthetic pigment measurements provided insight into the size distribution of phytoplankton taxa. Consistent with the spatial variability observed in upper ocean biogeochemistry, the size structure, composition, and abundance of phytoplankton varied markedly between the sampling regions. Euphotic zone inventories of size-fractionated TChl *a* revealed that >10 μm cells comprised 37% of TChl *a* at station 1UP and ≤8% of TChl *a* at other stations sampled (Table 1). Picophytoplankton (cells <3 μm) accounted for 55% of the euphotic zone TChl *a* inventories at station 1UP and 82-92% at other stations (Table 1). Contributions by the 3-10 μm size fraction were consistent and relatively low (5-10%) at all stations sampled, with most of the variability in phytoplankton TChl *a* attributable to spatial changes in the >10 μm and picophytoplankton fractions of TChl *a*. Profiles of size-fractionated TChl *a* also indicated vertical variability associated with phytoplankton size structure among the sampling stations. At station 1UP, the picophytoplankton size fraction was dominant in the upper euphotic zone (<40 m; above the 1% surface PAR) and the >10 μm fraction dominated in the lower euphotic zone (~40-59 m; near the 0.1% surface PAR; Figure 2). At all other stations, the pico-size fraction dominated in the Chl max (Figure 2).

Hierarchical clustering analyses (based on presence-absence and dissimilarity using the Jaccard index) of TChl *a*-normalized photosynthetic pigments revealed large differences between the phytoplankton sampled at station 1UP, especially in the larger size fraction, compared to other stations (Figure 3). For example, absolute concentrations of peridinin and fucoxanthin were elevated at 1UP (9.7 and 6.0 mg m^{-2}, respectively), particularly in the >10 μm fraction, indicating a greater presence of dinoflagellates and diatoms in the upwelled water (Table 2, Figure 3). Pigment to TChl *a* ratios for photosynthetic pigments diagnostic of prymnesiophytes (19'-hexanoyloxyfucoxanthin) and pelagophytes (19'-butanoyloxyfucoxanthin) remained relatively consistent across the cruise-track, with a majority of these pigments observed in the picophytoplankton size fraction (Figure 3). Phytoplankton types were partitioned amongst the picophytoplankton and the larger size fraction, as indicated by the clustering together of photosynthetic pigments in the picophytoplankton size fractions, separately from pigments measured in the >3 μm fractions (Figure 3). Concentrations of prasinoxanthin and lutein, pigment biomarkers indicative of the presence of prasinophytes and chlorophytes, respectively, were below the limit of detection at all stations except 1UP (Table 2). Concentrations of

alloxanthin, a biomarker diagnostic of cryptophytes, were detectable only at stations 1UP and 4TR. Concentrations of divinyl Chl *a*, a pigment diagnostic of *Prochlorococcus*, were highest at the oceanic stations 4TR and 7GY but in relatively low concentration at station 1UP. However, concentrations of zeaxanthin, an accessory pigment found in all cyanobacteria, were elevated and relatively stable across the transect, including station 1UP (Table 2, Figure 3).

Flow cytometric quantification of PPE, *Prochlorococcus*, and *Synechococcus* demonstrated spatial changes in picophytoplankton abundance across the sampling transect. Euphotic zone inventories of *Prochlorococcus* were low at station 1UP (5.24 x 10^{11} cells m^{-2}), becoming increasingly abundant into the SPSG (17.4-143 x 10^{11} cells m^{-2} at stations 2-7GY; Table 1). Abundances of *Synechococcus* revealed an opposite trend, with abundances greatest in the upwelling region (abundances at stations 1UP and 2 ranged 19.3-20 x 10^{11} cells m^{-2}), and nearly 50-fold lower (0.71-3.45 x 10^{11} cells m^{-2}) into the SPSG. In contrast, euphotic zone abundances of PPE were much less variable than that of cyanobacteria, ranging ~6 fold over the transect (1.5-6.8 x 10^{11}cells m^{-2}; Table 1), with PPE abundances peaking at stations 2 and 3.

2.4.3. Composition of PPE assemblages

We amplified and sequenced partial 18S rRNA genes from flow cytometrically sorted PPE populations from the near-surface (50% surface PAR) and the Chl max at stations 1UP, 4TR, and 7GY to examine changes in taxonomic composition. We employed this method of combining molecular analyses with flow-sorted cells in order to specifically target PPE, as 18S rRNA gene sequences retrieved from filtered seawater samples are often dominated by non-photosynthetic (presumably heterotrophic) picoeukaryotes. No amplification was observed in the control reactions (containing sheath fluid, sorted beads, or sorted cyanobacteria cells). A total of 561 sequences were obtained from flow-sorted PPE assemblages, and sequences were clustered at a 99% sequence similarity threshold into 32 OTUs. Six of these OTU clusters (totaling 35 sequences) derived from taxa not known to be photosynthetic: 2 Ciliophora OTUs (consisting of 21 sequences closely related to ciliates Cryptocaryon JX188358 and Scuticociliatia AY665059), 3 Fungi OTUs (10 sequences affiliated with the genus Malassezia FJ000217, FJ000238, KC673661), and 1 Rhizaria OTU (4 sequences clustering among the Acantharea Group I GU821070). Given our interests in PPE, we removed these sequences from subsequent analyses in this study. Of the remaining 26 OTUs (526 sequences in total), 8 distinct OTUs (108

sequences total) clustered among the Haptophyta, 8 OTUs (280 sequences total) among the Chlorophyta, 5 OTUs (121 sequences total) with the Stramenopiles, 2 OTUs (2 sequences total) with the Cryptophyta, and 3 OTUs (15 sequences total) with the Alveolata (Table 3).

The dominant PPE taxa derived from these flow-sorted cell 18S rRNA gene amplifications differed spatially between the three stations and vertically between the near-surface waters and at the Chl max. Hierarchical clustering analyses (based on the Jaccard index) of the 18S rRNA gene sequences revealed that the PPE assemblages at station 1UP clustered separately from those at 4TR and 7GY (Figure 4). A large proportion (74-95%) of the sequences retrieved from station 1UP in both near-surface waters and the Chl max were closely related (99.7% sequence identity) to *Ostreococcus* (Mamiellophyceae), which were not detected at any of the other stations sampled (Table 3). In addition, ~15% of sequences from the near-surface and ~2% from the Chl max sequences from station 1UP clustered among haptophytes belonging to the genus *Chrysochromulina*. These *Chrysochromulina* sequences formed two clusters that differed by >97.8% sequence identity, one of which was closely related to *Chrysochromulina simplex*. Other sequences retrieved at station 1UP clustered (>97% sequence identity) among chlorophytes *Nannochloris* and *Micromonas* (~5% and 3% of the sequences from the near-surface water sample, respectively) and cryptophytes *Teleaulax* (~2% of the sequences from the near-surface water sample). In the Chl max, the assemblage included sequences closely related (99.5% sequence identity) to the pelagophyte *Pelagomonas calceolata* (~3% of the sequences from this sample; Table 3).

Photosynthetic picoeukaryote assemblages at both depths at station 4TR clustered together (along with assemblages at the Chl max at station 7GY) according to the Jaccard index, though the dominant sequence-types found at each depth differed (Figure 4). Sequences closely related (>99% sequence identity) to *Pelagomonas calceolata* and Prasinophyceae clade VII subclade B were retrieved from both depths, but sequences most similar to *Pelagomonas calceolata* comprised 62% of the sequences in the near-surface sample, while the Prasinophyceae clade VII subclade B comprised 52% of the Chl max sequences (Table 3). The assemblage at the Chl max was composed of a greater number of distinct OTUs than the surface assemblage, with a mixture of sequences clustering among Prasinophyceae, Prymnesiophyceae, and Pelagophyceae (Table 3). In addition, 24% of the sequences retrieved from the Chl max at

station 4TR grouped among the Alveolata, including those closely related (>98% sequence identity) to Syndiniales Group V, an uncultivated group of presumed parasitic marine alveolates.

We observed a greater number of total distinct OTUs in the oligotrophic SPSG station 7GY than at other stations. The near-surface phytoplankton assemblage clustered separately from the assemblage at the Chl max (Figure 4), with the near-surface assemblage including Prasinophyceae (4 OTU totaling ~63% of sequences; >97% identity) and Chrysophyceae (~31% of total sequences; 99.6% identity;), with small contributions from the haptophyte *Chrysochromulina* and dictyochophyte *Pedinella* (Figure 4, Table 3). The PPE sequences from the Chl max were dominated (70% of sequences from this depth) by diverse groups of prymnesiophytes (4 distinct OTUs) that included sequences closely related (>98% sequence identity) to *Phaeocystis globosa*, *Helicosphaera*, *Chrysochromulina*, and *Imantonia* (Figure 4, Table 3).

2.4.4. Rates of total and group-specific primary production

Euphotic zone rates of ^{14}C-bicarbonate assimilation varied ~6-fold across the sampling region, with elevated rates (128-137 mmol C m^{-2} d^{-1}) observed at stations 1UP and 2 and rates decreasing to 18-23 mmol C m^{-2} d^{-1} at stations 6 and 7GY in the oligotrophic SPSG (Figure 5a). Despite large differences in rates of ^{14}C-based primary production between stations, the picophytoplankton size fraction (0.2-0.6 and 0.6-2 μm, combined) consistently accounted for 61-73% of the total (>0.2 μm) ^{14}C-based productivity (Figure 5b). Rates of ^{14}C-bicarbonate assimilation by the >2 μm size fraction accounted for the remaining 27-38% of the depth-integrated productivity (Figure 5b).

Group- and cell-specific contributions of PPE, *Prochlorococcus*, and *Synechococcus* to rates of primary productivity were examined based on flow cytometric sorting of ^{14}C-radiolabeled cells at stations 2, 4TR, 6, and 7GY. Rates of ^{14}C-based primary production by PPE and *Prochlorococcus* were approximately equivalent to each other throughout the sampling region, while rates of production by *Synechococcus* were consistently 2- to 6-fold lower than either rates of PPE or *Prochlorococcus* production (Table 4). The resulting cell-specific rates of ^{14}C-based primary production by PPE (~16-34 fmol C $cell^{-1}$ d^{-1}) were considerably greater than the rates by *Prochlorococcus* (~0.3-2 fmol C $cell^{-1}$ d^{-1}) or *Synechococcus* (~5-11 fmol C $cell^{-1}$ d^{-1}; Table 4). In total, cumulative rates of primary production by sorted picophytoplankton cells

(sum of group-specific rates of primary productivity by PPE, *Prochlorococcus*, and *Synechococcus*) accounted for 63-111% of the measured picoplankton (0.2-2 μm) primary productivity, and 42-70% of total (>0.2 μm) primary productivity measured on filters (Table 4).

There was also vertical variability in picoplankton contributions to rates of ^{14}C-primary production. At the upwelling-influenced station 2, productivity by PPE and cyanobacteria were comparable in the well-lit waters above 15% surface PAR, with contributions by cyanobacteria increasing in the lower euphotic zone (<7% surface PAR isopleth; Figure 6). Along the western end of the sampling transect (stations 4TR, 6, and 7GY), PPE contribution to production was greatest in the well-lit upper ocean (>15% surface PAR), with contributions by *Prochlorococcus* increasing deeper in the euphotic zone (<7% surface PAR isopleth; Figure 6).

2.5. Discussion

We identified vertically and longitudinally distinct patterns in picophytoplankton biomass, productivity, and taxonomic diversity across widely differing trophic states in the SEP using a combination of approaches that included size-fractionated photosynthetic pigments and rates of ^{14}C-productivity, flow cytometric sorting of ^{14}C-radiolabeled picoplankton cells, and 18S rRNA gene amplification and sequencing of sorted PPE cells. The upwelling-influenced waters supported a phytoplankton standing stock that consisted of both large (>3 μm) and pico-sized phytoplankton, with approximately equal contributions (45% and 55%, respectively) by both size classes to TChl *a* inventories. In comparison, in the oligotrophic waters, picophytoplankton dominated (88-92%) TChl *a* inventories, while phytoplankton >3 μm comprised 8-12% of TChl *a* inventories. Despite these large differences in the size structure of phytoplankton assemblages between the upwelling-influenced and oligotrophic waters, the size partitioning of primary productivity appeared largely consistent across the transect. Larger (>2 μm) phytoplankton and picophytoplankton accounted for ~30-40% and ~60-70%, respectively, of the >0.2 μm ^{14}C-based productivity. Thus, while the contributions of different phytoplankton sizes to biomass and productivity are comparable to each other in the upwelling region, larger phytoplankton appeared, on a biomass-normalized basis, disproportionately active in oligotrophic waters. These observations, which imply that significant changes occur in photosynthetic activities of large phytoplankton without accompanying variations in biomass, have been observed in studies conducted in other ocean ecosystems (Malone, 1980; Marañón et al., 2001; Li et al., 2011).

Latasa et al. (2005), in a study that derived estimates of phytoplankton taxa-specific growth and grazing through measurements of pigment biomarkers, dilution experiments, and ^{14}C-based primary production, showed that specific taxa, such as diatoms, played a disproportionate role in carbon flux compared to their biomass due to their high growth and grazing rates. Similarly, it is likely that recycling of biomass must intensify in low nutrient waters to sustain productivity, with population sizes presumably under tight control by top-down processes such as microzooplankton grazing, viral lysis, and disease.

One of the striking observations made in our study was the consistent dominance of picophytoplankton as contributors to the measured rates of >0.2 μm ^{14}C-based productivity across the biogeochemically diverse sampling regions. The observed increases in the biomass and productivity of larger phytoplankton in nutrient-enriched waters appear superimposed against a background of active picophytoplankton in these regions, a finding consistent with an active microbial food web across varying trophic states of the ocean (Margalef, 1969; Yentsch and Phinney, 1989; Chisholm, 1992). Closer examination of picophytoplankton group-specific rates of ^{14}C-primary productivity provided further insight into productivity dynamics between PPE and cyanobacteria. Cellular abundances of *Prochlorococcus* were two orders of magnitude greater than PPE at all stations except at the upwelling station 1UP. Yet, cell-specific rates of productivity by *Prochlorococcus* were relatively low (ranging 0.3-2.0 fmol C cell^{-1} d^{-1}), while activities by PPE and *Synechococcus* were considerably greater (averaging 28 and 9 fmol C cell^{-1} d^{-1}, respectively, Table 4). In fact, PPE cell-specific rates of productivity remained fairly consistent across the transect, while *Prochlorococcus* rates decreased into the SPSG; cell-specific PPE rates were 17-fold greater than *Prochlorococcus* at station 2, increasing to 93-fold greater at station 7GY (Table 4).

These results are consistent with the findings of Jardillier et al. (2010), who reported cell-specific PPE rates as much as 82-fold greater than those of *Prochlorococcus* in the subtropical and tropical northeast Atlantic Ocean. When taking into account their cell abundances, the proportional contributions by PPE and *Prochlorococcus* to rates of >0.2 μm ^{14}C-primary production were equivalent, with each group responsible for ~17-22% of the productivity at the main process stations in the study region (Table 4). This observation of their equal contributions to rates of >0.2 μm ^{14}C-primary productivity in biogeochemically distinct regions of the study region reveals that the partitioning of their photosynthetic activities remains surprisingly

consistent despite large changes in cell biomass. However, the derived contributions to rates of ^{14}C-based primary productivity by these two groups of picophytoplankton varied with depth, with PPE appearing more active in the upper ocean and *Prochlorococcus* becoming increasingly important in the dimly-lit waters.

The important role of PPE in carbon cycling in the upper open ocean likely derives from the larger cell biovolumes of these cells relative to unicellular cyanobacteria (Zubkov et al., 2000; Worden et al., 2004; Jardillier et al., 2010). Similar to our results, Grob et al. (2011) concluded that cell-specific carbon uptake rates by PPE varied as a function of cell size, following the rule of isometric scaling of production (Marañón et al., 2007). While our estimates of PPE cell-specific rates of ^{14}C-productivity were on average 25-fold greater than those of *Prochlorococcus*, the biomass-normalized rates of productivity (using biovolume carbon conversion factors from Worden et al., 2004) were at least 2-fold greater among PPE (0.68 d^{-1}) than *Prochlorococcus* (0.35 d^{-1}) throughout the euphotic zones in the regions sampled for this study. These derived growth rates are highly dependent on volume-specific carbon conversion factors and equations used for biovolume and carbon content calculations, particularly for PPE, which can differ greatly in cell size. However, our rates are comparable to those reported in previous studies using varying techniques (Li, 1994; Worden et al., 2004; Jardillier et al., 2010).

Similar to phytoplankton >3 μm in the oligotrophic SPSG, PPE were observed to have high growth rates without proportional biomass accumulation in each of the regions studied, implying that PPE assemblages are closely regulated by an analogous mortality rate. In a study examining growth and grazing mortality rates of picophytoplankton groups, Worden et al. (2004) found that a significant fraction of the net carbon produced was consumed immediately (*e.g.*, more than 2.5 times the carbon equivalent to the visible PPE standing stock was produced and consumed without changes in standing stock measurements). Thus, despite the lower numerical abundance of PPE in various regions of the world's ocean, PPE appear to actively transfer carbon to higher trophic levels. Furthermore, picophytoplankton removal from the upper ocean may be a result of viral lysis and other causes of mortality (Baudoux et al., 2008; Bidle and Vardi, 2011) as well as accelerated sinking through particle aggregation and mesozooplankton grazing, contributing to carbon export at rates proportional to their rates of production (Richardson and Jackson, 2007).

We combined a suite of approaches to identify key PPE taxa observed to be responsible for this relatively large fraction of picophytoplankton production in the near-surface waters of the SEP. The PPE assemblage structure observed in this study is similar to previous reports of PPE assemblages found in upwelling regions of the SEP (Lepère et al., 2009; Shi et al., 2009; Kirkham et al., 2013). In the near-surface waters of station 1UP, pigments retrieved in the picophytoplankton size fraction included those diagnostic of prymnesiophytes, prasinophytes, and cryptophytes. The 18S rRNA gene sequence analyses revealed more taxa-specific results, with *Ostreococcus* (Mamiellophyceae) appearing as the dominant member of the PPE assemblage at station 1UP amongst other chlorophytes (*Micromonas* and *Nannochloris*), haptophytes (*Chrysochromulina*), and cryptophytes (*Teleaulax*). The sequences clustering among *Ostreococcus* appeared closely related to the "low-light" ecotype Clade OII (RCC393 and 143), and our results are consistent with known biogeographical distributions of these organisms (Demir-Hilton et al., 2011; Acosta et al., 2013). Clade OII have been previously described occurring in the deep chlorophyll maximum of warm (22 ± 3 °C) oligotrophic waters and in the surface waters during periods of euphotic zone mixing, suggesting nutrient availability to be a determinant of OII vertical distribution in addition to light (Demir-Hilton et al., 2011). Quantitative PCR amplification of different clades of *Ostreococcus* indicates a cosmopolitan distribution of clade OII in offshore waters, including the relatively nutrient-enriched waters of the Gulf Stream (Demir-Hilton et al., 2011). Similarly, the *Ostreococcus* sequences retrieved in the current study were dominant in the nutrient-enriched waters of station 1UP where water temperatures remained relatively warm (~19˚C).

In the oligotrophic waters of the SPSG, the combined use of pigment biomarkers and 18S rRNA gene sequences revealed that the near-surface PPE assemblages consisted of prasinophytes Clades VII and IX, diverse groups of stramenopiles such as Ochrophyta MOCH-2 and *Pelagomonas calceolata*, uncultivated marine chrysophytes, and various haptophytes including *Helicosphaera*, *Imantonia*, *Phaeocystis globosa*, and several uncultured *Chrysochromulina*. Many of these organisms have also been previously reported from similar oceanic habitats, including the SEP (Lepère et al., 2009; Shi et al., 2009; Kirkham et al., 2013). While taxa such as *Chrysochromulina* appeared to be ubiquitous along the transect, other taxa were region-specific, presumably reflecting taxon-specific balance between growth and removal. In particular, the biogeographic partitioning of different clades of Prasinophyceae suggests

differing adaptations to bottom-up and top-down processes (*e.g.*, nutrient acquisition, light availability, and mortality) among the Prasinophyceae class.

The relatively large proportion of sequences clustering among pico-haptophytes in the current study (108 total sequences out of 526 total) is notable, given the known mixotrophic capabilities of these organisms, obtaining nutrition and energy through bacterivory and/or photosynthesis (Estep and MacIntyre, 1989; Liu et al., 2009; Kirkham et al., 2013). In addition, sequences retrieved among the PPE in the present study were closely related to various groups of prymnesiophytes and stramenopiles (Dictyochophyceae and Chrysophyceae), taxa that have been reported to feed on *Prochlorococcus* and *Synechococcus* (Frias-Lopez et al., 2009). It has been hypothesized that mixotrophs display such behavior to increase their relative fitness by reducing competitors in low-nutrient environments (Acosta et al., 2013). The prevalence of potentially mixotrophic taxa in the more oligotrophic waters of the study region may be indicative of a switch in metabolism among the PPE from photoautotrophy to mixotrophy along the gradient from high to low nutrient concentrations. If this is true, the amount of ^{14}C measured in mixotrophic cells retrieved from a ^{14}C-labeled incubation experiment may be slightly greater not only as a result of the assimilation of ^{14}C via autotrophy but also of the consumption of ^{14}C-labeled organic matter (*e.g.*, other autotrophic cells). We expect the contribution of this 'consumed' ^{14}C to be relatively small in magnitude, given the low cell-specific rates of carbon assimilation of cyanobacteria observed in this study and reported by others (Li, 1994; Jardillier et al., 2010). However, if PPE are rapidly consuming cyanobacterial biomass, as suggested by Zubkov and Tarran (2008) and Hartmann et al. (2012), quantifying the contributions of photosynthetic and heterotrophic ^{14}C assimilation by these organisms may be an important consideration for future experiments.

From the Chl max at the transition station 4TR and from the near-surface at station 1UP, we retrieved sequences clustering among the Syndiniales (*Amoebophrya* and Group V), a parasitic group of alveolates. These organisms have been frequently retrieved from 18S rRNA gene sequencing analyses in marine ecosystems (with groups II, III, and V largely found in the photic zone) and hypothesized to be important generalist parasites (Massana et al., 2004; Guillou et al., 2008, Acosta et al., 2013). Our finding of these sequences from flow-sorted PPE populations was somewhat surprising, but may reflect the presence of parasites carried by the PPE cells themselves, or the simultaneous sorting of an undetected non-photosynthetic cell

alongside a photosynthetic organism (Shi et al., 2009). Furthermore, it is possible that members of the Syndiniales retained ancestral traits such as photosynthetic capabilities, pigmentation, and/or phagotrophy (Guillou et al., 2008).

There are several potentially important methodological considerations that emerged from our measurements. First, the flow-sorting methodology may underestimate picophytoplankton production, as evidenced by the collective (flow-sorted PPE, *Prochlorococcus*, and *Synechococcus* cells) carbon fixation rates accounting for 63-111% of the productivity measured in the picoplanktonic fraction (0.2-2 μm) on filters. This underestimation is possibly due to low cell abundances of certain PPE taxa, resulting in the under-representation of rarer organisms, or due to cell breakage of fragile taxa occurring as a result of the preservation process. Secondly, for the 18S rRNA gene analyses, we sorted PPE cells that had been concentrated after excluding organisms >3 μm. However, for the filtration-based estimates of ^{14}C-productivity, picoplankton activity was quantified based on organisms <2 μm. Hence, if there were PPE with cell diameters in the 2-3 μm size range, they would have been included in the production rate measurements for the >2 μm fraction, thereby potentially underestimating the measured contributions by PPE to the 0.2-2 μm filter fraction. Finally, an additional source of methodological uncertainty in this study lies with the flow cytometric sorting of specific populations for phylogenetic information. It is possible that losses of more fragile PPE cells could have occurred as a result of the tangential flow filtration process, though samples were processed as quickly as possible (within 4-6 hours of collection) at gentle flow rates. In an attempt to collect as many cells as possible for low abundance populations such as PPE, a delicate balance must be sought to maintain sample integrity while collecting a sufficient amount of material for subsequent analyses.

In summary, our study confirms that picophytoplankton are significant contributors to biomass and primary production in distinct biogeochemical regions of the South East Pacific Ocean. We found that despite cellular abundances that are lower by orders of magnitude, PPE contributed a nearly equivalent proportion to measured ^{14}C-primary productivity as the numerically dominant *Prochlorococcus*, a finding consistent with the presumed larger cell-carbon content of the PPE. Moreover, we found that in the well-lit upper regions (>15% surface PAR) of the SPSG, rates of ^{14}C-productivity by PPE exceeded productivity by cyanobacteria. Cyanobacteria have long been thought to be the dominant picophytoplankton, numerically due to their high abundance as well as functionally due to their affinity for utilizing low concentrations

of nutrients; yet, unique characteristics of prominent PPE taxa (haptophytes, cryptophytes, prasinophytes, and stramenopiles), such as their slightly larger size and reportedly mixotrophic metabolism, may allow them to thrive across the biogeochemically distinct regions sampled as part of this study. Moreover, the apparently high growth rates of PPE observed in the current study, without concomitant accumulation of biomass, suggests these organisms are rapidly removed via top-down processes and/or sinking. Combined, our study highlights the multifaceted ecology of PPE in different regions of the world's oceans, and provides new insight into the important role of these organisms in ocean carbon cycling.

2.6. Acknowledgments

The authors would like to thank the captain and crew of R/V *Melville* and the participants of the BiG RAPA expedition for assistance with data collection for this project. We also acknowledge Ken Doggett, Brandon Carter, Anne Thompson, and Karin Björkman for help with cell sorting, Mariona Segura-Noguera for measurements of dissolved inorganic carbon used in calculations of primary production, and Joe Jennings for macronutrient analyses. Support for this work derived from U.S. National Science Foundation grants to C-MORE (EF-0424599; DMK) and OCE-1241263 (MJC). Additional support was received from the University of Hawai'i Denise B. Evans Research Fellowship in Oceanography (YMR), the Gordon and Betty Moore Foundation (DMK), and the Simons Foundation via the Simons Collaboration on Ocean Processes and Ecology (SCOPE).

2.7. References

Acker, J. G., and G. Leptoukh. 2007. Online analysis enhances use of NASA earth science data. EOS, Trans. AGU **88**: 14-17.

Acosta, F., D. K. Ngugi, and U. Stingl. 2013. Diversity of picoeukaryotes at an oligotrophic site off the Northeastern Red Sea Coast. Aquat. Biosyst. **9**: 16.

Andersen, R. A., G. W. Saunders, M. P. Paskind, and J. P. Sexton. 1993. Ultrastructure and 18S rRNA gene sequence for *Pelagomonas calceolata* gen. et. sp. nov. and the description of a new algal class, the Pelagophyceae classis nov. J. Phycol. **29**: 701-715.

Armstrong, F. A. J., C. R. Stearns, and J. D. H. Strickland. 1967. The measurement of upwelling and subsequent biological processes by means of the Technicon AutoAnalyzer™ and associated equipment. Deep-Sea Res. **14**: 381-389.

Baldauf, S. 2003. The deep roots of eukaryotes. Science **300**: 1703–1706.

Balzano, S., D. Marie, P. Gourvil, and D. Vaulot. 2012. Composition of the summer photosynthetic pico and nanoplankton communities in the Beaufort Sea assessed by T-RFLP and sequences of the 18S rRNA gene from flow cytometry sorted samples. ISME J. **6**: 1480-1498.

Baudoux, A. C., M. Veldhuis, A. Noordeloos, G. Van Noort, and C. Brussaard. 2008. Estimates of virus- vs. grazing induced mortality of picophytoplankton in the North Sea during summer. Aquat. Microb. Ecol. **52**: 69-82.

Bidigare, R. R., L. Van Heukelem, and C. C. Trees. 2005. Analysis of algal pigments by high-performance liquid chromatography, p. 327-345. In R. A. Anderson [ed.], Algal culturing techniques. Academic Press.

Bidle, K. D., and A. Vardi. 2011. A chemical arms race at sea mediates algal host–virus interactions. Curr. Op. Microb. **14**: 449-457.

Caporaso, J. G., J. Kuczynski, J. Stombaugh, and others. 2010. QIIME allows analysis of high-throughput community sequencing data. Nat. Methods **7**: 335-336.

Caron, D.A., A. Z. Worden, P. D. Countway, E. Demir, and K. B. Heidelberg. 2009. Protists are microbes too: a perspective. ISME J. **3**: 4-12.

Carr, M. E., M. A. M. Friedrichs, M. Schmeltz, and others. 2006. A comparison of global estimates of marine primary production from ocean color. Deep-Sea Res. II **53**: 741-770.

Chisholm, S. W. 1992. Phytoplankton size, p. 213-237. In P. G. Falkowski and A. D. Woodhead [eds.], Primary productivity and biogeochemical cycles in the sea. Springer.

Cuvelier, M. L., A. E. Allen, A. Monier, and others. 2010. Targeted metagenomics and ecology of globally important uncultured eukaryotic phytoplankton. Proc. Natl. Acad. Sci. U.S.A. **107**: 14679-14684.

Decelle, J., I. Probert, L. Bittner, and others. 2012. An original mode of symbiosis in open ocean plankton. Proc. Natl. Acad. Sci. U.S.A. **109**: 18000-18005.

Demir-Hilton, E., S. Sudek, M. L. Cuvelier, C. L. Gentemann, J. P. Zehr, and A. Z. 2011. Global distribution patterns of distinct clades ofthe photosynthetic picoeukaryote *Ostreococcus*. ISME J. **5**, 1095–1107.

Duhamel, S., and T. Moutin. 2009. Carbon and phosphate incorporation rates of microbial assemblages in contrasting environments in the Southeast Pacific. Mar. Ecol. Prog. Ser. **375**: 53-64.

Duhamel, S., F. Zeman, and T. Moutin. 2006. A dual-labeling method for the simultaneous measurement of dissolved inorganic carbon and phosphate uptake by marine planktonic species. Limnol. Oceanogr.: Methods **4**: 416-425.

Edgar, R. C., B. J. Haas, J. C. Clemente, C. Quince, and R. Knight. 2011. UCHIME improves sensitivity and speed of chimera detection. Bioinformatics **27**: 2194-2200.

Edgcomb, V. P., D. T. Kysela, A. Teske, A. de Vera Gomez, and M. L. Sogin. 2002. Benthic eukaryotic diversity in the Guaymas Basin hydrothermal vent environment. Proc. Natl. Acad. Sci. U.S.A. **99**: 7658-7662.

Edgcomb, V. P., W. Orsi, J. Bunge, and others. 2011. Protistan microbial observatory in the Cariaco Basin, Caribbean. I. Pyrosequencing vs Sanger insights into species richness. ISME J. **5**:1344-1356.

Estep, K. W., and F. MacIntyre. 1989. Taxonomy, life cycle, distribution and dasmotrophy of *Chrysochromulina:* a theory accounting for scales, haptonema, muciferous bodies and toxicity. Mar. Ecol. Prog. Ser. **57**: 11-21.

Field, C. B., M. J. Behrenfeld, J. T. Randerson, and P. G. Falkowski. 1998. Primary production of the biosphere: integrating terrestrial and oceanic components. Science **281**: 237-240.

Frias-Lopez, J., A. Thompson, J. Waldbauer, and S. W. Chisholm. 2009. Use of stable isotope-labelled cells to identify active grazers of picocyanobacteria in ocean surface waters. Environ. Microbiol. **11**: 512-525.

Fuller, N. J., C. Campbell, D. J. Allen, F. D. Pitt, K. Zwirglmaier, F. Le Gall, D. Vaulot, and D. J. Scanlan. 2006. Analysis of photosynthetic picoeukaryote diversity at open ocean sites in the Arabian Sea using a PCR biased towards marine algal plastids. Aquat. Microb. Ecol. **43**: 79-93.

Gordon, L. I., J. C. Jennings, A. A. Ross, and J. M. Krest, 1994. A suggested protocol for continuous flow analysis of seawater nutrients (phosphate, nitrate, nitrite, and silicic acid) in the WOCE Hydrographic Program and Joint Global Ocean Fluxes Study. WHP Office Report 91-1.

Grob, C., M. Hartmann, M. V. Zubkov, and D. J. Scanlan. 2011. Invariable biomass-specific primary production of taxonomically discrete picoeukaryote groups across the Atlantic Ocean. Environ. Microbiol. **13**: 3266-3274.

Guillou, L., W. Eikrem, M.-J. Chrétiennot-Dinet, F. Le Gall, R. Massana, K. Romari, C. Pedrós-Alió, and D. Vaulot. 2004. Diversity of picoplanktonic prasinophytes assessed by direct

nuclear SSU rDNA sequencing of environmental samples and novel isolates retrieved from oceanic and coastal marine ecosystems. Protist **155**: 193-214.

Guillou, L., M. Viprey, A. Chambouvet, R. M. Welsh, A. R. Kirkham, R. Massana, D. J. Scanlan, and A. Z. Worden. 2008. Widespread occurrence and genetic diversity of marine parasitoids belonging to Syndiniales (Alveolata). Environ. Microbiol. **10**: 3349-3365.

Hartmann, M., C. Grob, G. A. Tarran, A. P. Martin, P. H. Burkill, D. J. Scanlan, and M. V. Zubkov. 2012. Mixotrophic basis of Atlantic oligotrophic ecosystems. Proc. Natl. Acad. Sci. U.S.A. **109**: 5756–5760.

Jardillier, L., M. V. Zubkov, J. Pearman, and D. J. Scanlan. 2010. Significant CO_2 fixation by small prymnesiophytes in the subtropical and tropical northeast Atlantic Ocean. ISME J. **4**: 1180-1192.

Jeffrey, S. W., S. W. Wright, and M. Zapata. 2011. Microalgal classes and their signature pigments. p. 3-77. In S. Roy, A. Llewellyn, E. S. Egeland, and G. Johnsen [eds.], Phytoplankton pigments: characterization, chemotaxonomy, and applications in oceanography. Cambridge University Press.

Kirkham, A. R., L. E. Jardillier, A. Tiganescu, J. Pearman, M. V. Zubkov, and D. J. Scanlan. 2011. Basin-scale distribution patterns of photosynthetic picoeukaryotes along an Atlantic Meridional Transect. Environ. Microbiol. **13**: 975-990.

Kirkham, A. R., C. Lepère, L. E. Jardillier, F. Not, H. Bouman, A. Mead, and D. J. Scanlan. 2013. A global perspective on marine photosynthetic picoeukaryote community structure. ISME J. **7**: 922-936.

Latasa, M., R. R. Bidigare, M. E. Ondrusek, and M. C. Kennicutt II. 1996. HPLC analysis of algal pigments: A comparison exercise among laboratories and recommendations for improved analytical performance. Mar. Chem. **51**: 315-324.

Latasa, M., X. A. G. Morán, R. Scharek, and M. Estrada. 2005. Estimating the carbon flux through main phytoplankton groups in the northwestern Mediterranean. Limnol. Oceanogr. **50**: 1447-1458.

Laza-Martinez, A., J. Arluzea, I. Miguel, and E. Orive. 2012. Morphological and molecular characterization of *Teleaulax gracilis* sp. nov. and *T. minuta* sp. nov. (Cryptophyceae). Phycologia **51**: 649-661.

Lepère, C., D. Vaulot, and D. J. Scanlan. 2009. Photosynthetic picoeukaryote community structure in the South East Pacific Ocean encompassing the most oligotrophic waters on earth. Environ. Microbiol. **11**: 3105-3117.

Li, B., D. M. Karl, R. M. Letelier, and M. J. Church. 2011. Size-dependent photosynthetic variability in the North Pacific Subtropical Gyre. Mar. Ecol. Prog. Ser. **440**: 27-40.

Li, W. K. W. 1994. Primary production of prochlorophytes, cyanobacteria, and eukaryotic ultraphytoplankton: measurements from flow cytometric sorting. Limnol. Oceanogr. **39**: 169-175.

Liu, H., I. Probert, J. Uitz, H. Claustre, S. Aris-Brosou, M. Frada, F. Not, and C. de Vargas. 2009. Extreme diversity in noncalcifying haptophytes explains a major pigment paradox in open oceans. Proc. Natl. Acad. Sci. U.S.A. **106**: 12803-12808.

Malone, T. C. 1980. Size-fractionated primary productivity of marine phytoplankton, p. 301-319. In P. G. Falkowski [ed.], Primary productivity in the sea. Plenum Press.

Marañón, E., P. Holligan, R. Barciela, N. González, B. Mouriño, M. Pazó, and M. Varela. 2001. Patterns of phytoplankton size structure and productivity in contrasting open-ocean environments. Mar. Ecol. Prog. Ser. **216**: 43-56.

Marañón E., V. Pérez, E. Fernández, and others. 2007. Planktonic carbon budget in the eastern subtropical North Atlantic. Aquat. Microb. Ecol. **48**: 261-275.

Margalef, R. 1969. Size of centric diatoms as an ecological indicator. Mitt. Internat. Verein. Limnol. **17**: 202-210.

Massana, R. 2011. Eukaryotic picoplankton in surface oceans. Annu. Rev. Microbiol. **65**: 91-110.

Massana, R., V. Balagué, L. Guillou, and C. Pedrós-Alió. 2004. Picoeukaryotic diversity in an oligotrophic coastal site studied by molecular and culturing approaches. FEMS Microbiol. Ecol. **50**: 231-243.

Massana, R., J. del Campo, M. E. Sieracki, S. Audic, and R. Logares. 2014. Exploring the uncultured microeukaryote majority in the oceans: reevaluation of ribogroups within stramenopiles. ISME J. **8**: 854-866.

Moon-van der Staay, S. Y., G. W. M. van der Staay, L. Guillou, D. Vaulot, H. Claustre, and L. K. Medlin. 2000. Abundance and diversity of prymnesiophytes in the picoplankton community from the equatorial Pacific Ocean inferred from 18S rDNA sequences. Limnol. Oceanogr. **45**: 98-109.

Moutin, T., P. Raimbault, and J. C. Poggiale. 1999. Primary production in surface waters of the western Mediterranean sea. Calculation of daily production. C.R. Acad. Sci. III-Vie. **322**: 651-659.

Oksanen, J., F. G. Blanchet, R. Kindt, and others. 2013. Package 'vegan': community ecology package. R package version 2.0-10. http://cran.r-project.org/web/packages/vegan/.

Orsi, W., Y. C. Song, S. Hallam, and V. Edgcomb. 2012. Effect of oxygen minimum zone formation on communities of marine protists. ISME J. **6**: 1586-1601.

Potter, D., T. C. LaJeunesse, G. W. Saunders, and R. A. Anderson. 1997. Convergent evolution masks extensive biodiversity among marine coccoid picoplankton. Biodivers. Conserv. **6**: 99-107.

Quast, C., E. Pruesse, P. Yilmaz, J. Gerken, T. Schweer, P. Yarza, J. Peplies, and F. O. Glöckner. 2013. The SILVA ribosomal RNA gene database project: improved data processing and web-based tools. Nucl. Acids Res. **41**: D590-D596.

Richardson, T. L., and G. A. Jackson. 2007. Small phytoplankton and carbon export from the surface ocean. Science **315**: 838-840.

Romari, K., and D. Vaulot. 2004. Composition and temporal variability of picoeukaryote communities at a coastal site of the English Channel from 18S rDNA sequences. Limnol. Oceanogr. **49**: 784-798.

Shi, X. L., D. Marie, L. Jardillier, D. J. Scanlan, D. Vaulot. 2009. Groups without cultured representatives dominate eukaryotic picophytoplankton in the oligotrophic South East Pacific Ocean. PLoS ONE **4**: e7657.

Sieburth, J. M., V. Smetacek, and J. Lenz. 1978. Pelagic ecosystem structure: Heterotrophic compartments of the plankton and their relationship to plankton size fractions. Limnol. Oceanogr. **23**: 1256-1263.

Steemann Nielsen, E. 1952. The use of radioactive carbon (^{14}C) for measuring organic production in the sea. J. Conseil. **18**: 117-140.

Stoeck, T., G. T. Taylor, and S. S. Epstein. 2003. Novel eukaryotes from the permanently anoxic Cariaco Basin (Caribbean Sea). Appl. Environ. Microbiol. **69**: 5656-5663.

Thompson, A. W., R. A. Foster, A. Krupke, B. J. Carter, N. Musat, D. Vaulot, M. M. M. Kuypers, and J. P. Zehr. 2012. Unicellular cyanobacterium symbiotic with a single-celled eukaryotic alga. Science **337**: 1546-1550.

Thompson, J. D., D. G. Higgins, and T. J. Gibson. 1994. CLUSTAL W: Improving the sensitivity of progressive multiple sequence alignment through sequence weighting, position-specific gap penalties and weight matrix choice. Nucl. Acids Res. **22**: 4673-4680.

Vaulot, D., W. Eikrem, and M. Viprey. 2008. The diversity of small eukaryotic phytoplankton (≤3 μm) in marine ecosystems. FEMS Microbiol. Rev. **32**: 795-820.

Worden, A. Z. 2006. Picoeukaryote diversity in coastal waters of the Pacific Ocean. Aquat. Microb. Ecol. **43**: 165-175.

Worden, A. Z., J. K. Nolan, and B. Palenik. 2004. Assessing the dynamics and ecology of marine picophytoplankton: The importance of the eukaryotic component. Limnol. Oceanogr. **49**: 168-179.

Wu, W., B. Huang, and C. Zhong. 2014. Photosynthetic picoeukaryote assemblages in the South China Sea from the Pearl River estuary to the SEATS station. Aquat. Microb. Ecol. **71**: 271-284.

Yentsch, C. S, and D. A. Phinney. 1989. A bridge between ocean optics and microbial ecology. Limnol. Oceanogr. **34**: 1694-1705.

Zubkov, M. V., M. A. Sligh, P. H. Burkill, and R. J. G. Leakey. 2000. Picoplankton community structure on the Atlantic Meridional Transect: a comparison between seasons. Prog. Oceanogr. **45**: 369-386.

Zubkov, M. V., and G. A. Tarran. 2008. High bacterivory by the smallest phytoplankton in the North Atlantic Ocean. Nature **455**: 224-226.

Table 2.1. Station summary data during the BiG RAPA cruise (18 Nov – 14 Dec 2010)

	Station ID						
	7GY	**6**	**5**	**4TR**	**3**	**2**	**1UP**
Station location (Lat, Lon)	26.248°S, 103.961°W	25.551°S, 100.136°W	24.560°S, 94.725°W	23.458°S, 88.768°W	22.261°S, 82.348°W	21.178°S, 76.573°W	20.083°S, 70.800°W
Distance from Arica (km)	3637	3249	2695	2078	1407	798	185
$Z_{0.1\%}$ (m)*	137	165	157	141	116	96	57
Chl max (m)	160 ± 13	126 ± 4	123 ± 4	113 ± 7	59 ± 15	40 ± 8	24 ± 3
TChl a_{SFC} (mg Chl m^{-3})†	0.025	0.029	0.041	0.066	0.108	0.207	0.632
TChl a_{EZ} (mg Chl m^{-2})‡	11.6	17.8	20.6	21.8	n/a	26.3	40.0
TChl *a* >10 µm‡††	0.1 [1%]	0.9 [5%]	0.8 [4%]	0.7 [3%]	n/a	2.0 [8%]	14.6 [37%]
TChl *a* 3-10 µm‡††	0.8 [7%]	1.2 [7%]	1.0 [5%]	1.9 [9%]	n/a	2.7 [10%]	3.2 [8%]
TChl *a* <3 µm‡††	10.7 [92%]	15.8 [88%]	18.8 [91%]	19.2 [88%]	n/a	21.5 [82%]	22.2 [55%]
PPE ($x10^{11}$ cells m^{-2})‡	1.59 ± 0.05	2.81	1.86	3.30 ± 0.43	6.55	6.76	2.99 ± 1.36
Prochlorococcus ($x10^{11}$ cells m^{-2})‡	143 ± 10.0	120	142	80.9 ± 13.9	17.4	116	5.24 ± 1.91
Synechococcus ($x10^{11}$ cells m^{-2})‡	0.77 ± 0.03	0.71	2.07	2.56 ± 0.21	3.45	20.0	19.3 ± 10.6
$NO_3^- + NO_2^-$ (mmol N m^{-2})‡	32.4 ± 30.9	8.07	13.5	17.9 ± 11.0	57.4	248	625 ± 57.0
PO_4^{3-} (mmol P m^{-2})‡	36.7 ± 2.50	39.4	44.9	49.7 ± 0.10	55.3	69.3	100 ± 4.00

*Depth of the 0.1% Surface PAR

†TChl *a* at surface depth of each station (~5-15 m)

‡Euphotic zone depth-integrated (0.1% surface PAR for St. 1UP-6 and Chl max for St. 7GY)

††(mg Chl m^{-2}), [% total TChl *a*]

Table 2.2. Euphotic zone depth-integrated* photosynthetic pigment concentrations (mg m^{-2})

		7GY				4TR				1UP			
Pigment	**Dominant pigment in:†**	**>10 µm**	**3-10 µm**	**<3 µm**	**Total**	**>10 µm**	**3-10 µm**	**<3 µm**	**Total**	**>10 µm**	**3-10 µm**	**<3 µm**	**Total**
Divinyl Chl *a* (DVChl *a*)	*Prochlorococcus*	0.06	0.24	3.53	**3.83**	0.02	0.13	6.97	**7.12**	BLD‡	BLD	0.98	**0.98**
Zeaxanthin (Zea)	Cyanobacteria	BLD	BLD	5.06	**5.06**	0.39	0.03	4.86	**5.28**	0.07	0.12	2.99	**3.18**
Lutein (Lut)	Chlorophytes	BLD	BLD	BLD	**BLD**	BLD	BLD	BLD	**BLD**	0.01	0.03	0.36	**0.40**
Prasinoxanthin (Pras)	Prasinophytes	BLD	BLD	BLD	**BLD**	BLD	BLD	BLD	**BLD**	BLD	0.02	0.35	**0.37**
19'-hexanoyloxy-fucoxanthin (Hex)	Prymnesiophytes	0.11	0.25	2.37	**2.73**	0.21	0.90	5.21	**6.32**	BLD	BLD	6.06	**6.06**
19'-butanoyloxy-fucoxanthin (But)	Pelagophytes	0.02	0.05	1.32	**1.39**	0.02	0.20	2.77	**2.99**	BLD	0.03	1.33	**1.36**
Fucoxanthin (Fuco)	Diatoms	BLD	BLD	0.55	**0.55**	BLD	0.08	0.47	**0.55**	2.19	0.88	2.95	**6.02**
Alloxanthin (Allo)	Cryptophytes	BLD	BLD	BLD	**BLD**	BLD	BLD	0.20	**0.20**	BLD	0.06	0.36	**0.42**
Peridinin (Peri)	Dinoflagellates	BLD	BLD	0.23	**0.22**	BLD	0.24	0.21	**0.45**	9.22	0.31	0.20	**9.73**

*Euphotic zone depth-integrated (0.1% surface PAR for St. 1UP and 4TR, and Chl max for St. 7GY)

†Pigment descriptions from Jeffrey et al. (2011)

‡BLD: Below the limit of detection (LOD); LOD = 0.0045 mg m^{-3} for chlorophylls, 0.003 mg m^{-3} for carotenoids

Table 2.3. Distribution of 18S rRNA gene clones of PPE as percent of total number of sequences* recovered from each station / depth

Phylum	Class	Genus (Species)	Accession No. (% Identity)	Sta. 7GY Chl max	Sta. 7GY 50% PAR	Sta. 4TR Chl max	Sta. 4TR 50% PAR	Sta. 1UP Chl max	Sta. 1UP 50% PAR	Reference
Chlorophyta	Mamiellophyceae	*Ostreococcus*	KC583118 (99.7%)	--†	--	--	--	95.2%	74.1%	Red Sea, 10 m; Acosta et al. (2013)
Chlorophyta	Mamiellophyceae	*Micromonas*	GQ863805 (99.3%)	--	--	--	--	--	2.5%	Atlantic Meridional Transect, 10 m; Kirkham et al. (2011)
Chlorophyta	Trebouxiophyceae	*Nannochloris*	AY256258 (99.3%)	--	--	--	--	--	4.9%	Anoxic deep sea basin; Stoeck et al. (2003)
Chlorophyta	Prasinophyceae	Clade IX	FJ537345 (99.1%)	--	5.6%	--	--	--	--	BIOSOPE T65.111, STB12, 40 m; Shi et al. (2009)
Chlorophyta	Prasinophyceae	Clade IX	KF031641 (99.2%)	--	31.5%	1.7%	--	--	--	South China Sea, surface; Wu et al. (2014)
Chlorophyta	Prasinophyceae	Clade IX	JX291959 (97.6%)	--	7.9%	1.7%	--	--	--	North Pacific Ocean; Thompson et al. (2012)
Chlorophyta	Prasinophyceae	Clade VII Subclade A	U40921 (99.5%)	--	18.0%	--	--	--	--	CCMP1205; Potter et al. (1997)
Chlorophyta	Prasinophyceae	Clade VII Subclade B	FJ537357 (99.2%)	--	--	51.7%	7.1%	--	--	BIOSOPE, Oligo station, 150 m; Shi et al. (2009)
Haptophyta	Prymnesiophyceae	*Chrysochromulina*	FJ000253 (97.9%)	--	--	--	--	1.6%	3.7%	Mediterranean; Edgcomb et al. (unpub.)
Haptophyta	Prymnesiophyceae	*Chrysochromulina*	JF698758 (98.9%)	--	--	--	--	--	11.1%	Beaufort Sea, 3 m; Balzano et al. (2012)

Haptophyta	Prymnesiophyceae	*Chrysochromulina*	HM581603 (99.1%)	--	2.2%	--	--	--	--	N. Atlantic, 75 m; Cuvelier et al. (2010)
Haptophyta	Prymnesiophyceae	*Chrysochromulina*	FJ537355 (98.8%)	5.7%	--	--	--	--	--	BIOSOPE T84.038, 5 m; Shi et al. (2009)
Haptophyta	Prymnesiophyceae	Prymnesiales OLI16029	JX291794 (98.6%)	--	--	--	30.6%	--	--	Open ocean, Thompson et al. (2012)
Haptophyta	Prymnesiophyceae	*Phaeocystis* (*globosa*)	JX660986 (99.7%)	18.4%	--	--	--	--	--	Atlantic Ocean; Decelle et al. (2012)
Haptophyta	Prymnesiophyceae	*Imantonia*	AJ402351 (98.3%)	3.4%	--	--	--	--	--	Equatorial Pacific; Moon-van der Staay (2000)
Haptophyta	Prymnesiophyceae	*Helicosphaera*	FJ537311 (99%)	42.5%	--	8.6%	--	--	--	BIOSOPE T33.008, 180 m; Shi et al. (2009)
Stramenopiles	Chrysophyceae	Marine chrysophyte	AY046864 (99.6%)	--	31.5%	--	--	--	--	Guaymas Basin hydrothermal vent; Edgcomb et al. (2002)
Stramenopiles	Dictyochophyceae	*Pedinella*	JX291705 (99.6%)	--	2.2%	--	--	--	--	N. Pacific Ocean; Thompson et al. (2012)
Stramenopiles	Ochrophyta	MOCH-2	GQ382461 (99.8%)	1.1%	--	3.4%	--	--	--	NW Pacific; Caron et al. (2009); Massana et al. (2014)
Stramenopiles	Pelagophyceae	*Pelagomonas* (*calceolata*)	U14389 (99.5%)	28.7%	--	8.6%	62.4%	3.2%	--	CCMP1214; Andersen et al. (1993)
Stramenopiles	Labyrinthulomycetes	Marine stramenopile	GU824965 (97.8%)	--	1.1%	--	--	--	--	Micro-oxic water, Cariaco Basin; Edgcomb et al. (2011)
Cryptophyta	Cryptophyceae	*Teleaulax* (*minuta*)	JQ966996 (99.3%)	--	--	--	--	--	1.2%	Cr8EHU, estuarine, Spain; Laza-Martinez et al. (2012)

Cryptophyta	Cryptophyceae	*Teleaulax*	HQ865081 (97.5%)	--	--	--	--	--	1.2%	Saanich Inlet, 10 m; Orsi et al. (2012)
Alveolata	Dinophyceae	Uncultured dinoflagellate	KC488419 (98.6%)	--	--	1.7%	--	--	--	Atlantic Ocean, station BBL6, 3 m; Dasilva et al. (unpub.)
Alveolata	Syndiniales	*Amoebophrya*	AY129038 (97.9%)	--	--	--	--	--	1.2%	Coastal Pacific Ocean; Worden (2006)
Alveolata	Syndiniales	Group V	EU793265 (99.3%)	--	--	22.4%	--	--	--	Mediterranean, PROSOPE, 25 m; Guillou et al. (2008)
*Total excludes sequences of non-photosynthetic taxa				100%	100%	100%	100%	100%	100%	
†-- denotes 0%			**Total # of PPE sequences:**	**87**	**89**	**58**	**85**	**126**	**81**	

Table 2.4. Picophytoplankton ^{14}C-productivity and group- and cell-specific contributions

	7GY	6	4TR	2
^{14}C-Primary production rates (mmol C m^{-2} d^{-1}), [% sum of sorts]*				
PPE	4.5 [48%]	4.6 [36%]	10.8 [44%]	23.6 [41%]
Prochlorococcus	4.3 [45%]	7.3 [57%]	11.6 [48%]	23.6 [41%]
Synechococcus	0.7 [7%]	0.8 [7%]	2.0 [8%]	10.6 [18%]
Group contribution to CO_2 fixation (%)*†				
PPE	21%	25%	20%	17%
Prochlorococcus	20%	40%	22%	17%
Synechococcus	3%	5%	4%	8%
Cell-specific primary production rates (fmol C cell^{-1} d^{-1})*				
PPE	28.6	16.3	32.8	34.9
Prochlorococcus	0.30	0.61	1.44	2.04
Synechococcus	9.40	11.8	7.69	5.32
Contribution to ^{14}C Primary production rates (%)*				
Sum of sorted cells / picoplankton productivity on filters	69	111	63	66
Sum of sorted cells / total (>0.2 µm) productivity on filters	43	70	46	42

*Rates and cellular stocks depth-integrated to the 0.1% surface PAR for St. 1UP-6 and to the Chl max for St. 7GY

†Contributions are calculated as percent of >0.2 µm primary productivity captured on filters (see Figure 5).

Figure 2.1 Contour plots depicting spatial distributions of biogeochemical properties at seven stations along the BiG RAPA transect (produced with Ocean Data View 4.6.2). Left: Map depicting the sampling locations for this study, superimposed on MODIS chlorophyll data obtained from the Giovanni online data system (NASA GES DISC; Acker and Leptoukh, 2007); top: Temperature (°C, color) and potential density anomaly (sigma-t; contour lines); center: NO_3^- + NO_2^- (µM, color) and dissolved oxygen (µM, contour lines); bottom: TChl *a* (mg m^{-3}, color) and % surface PAR (white circles darkening in order; 50, 25, 15, 7, 3, 1, 0.1). Black dots indicate depths where samples were collected.

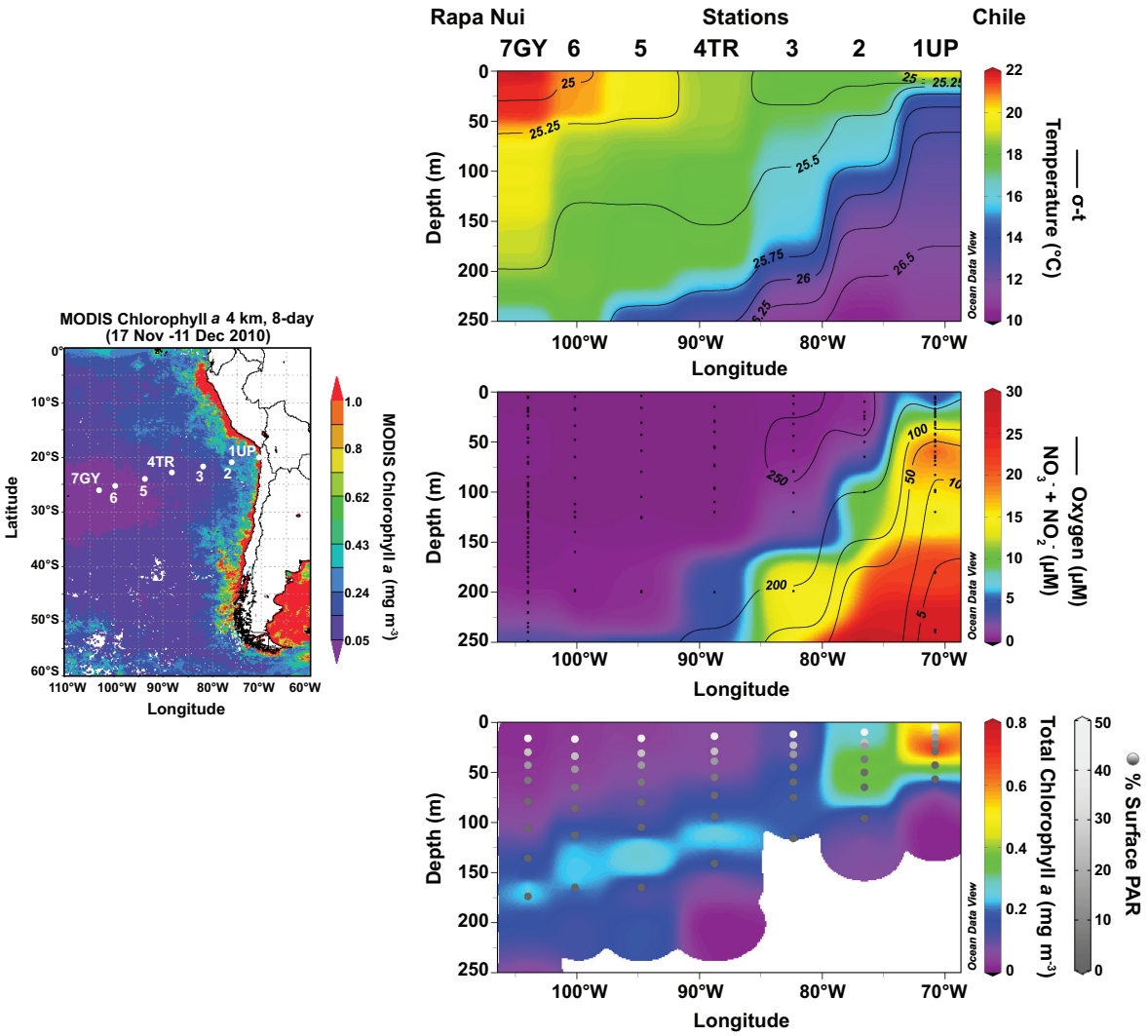

Figure. 2.2. Depth profiles of size-fractionated TChl *a* concentrations (mg m^{-3}) at stations 1UP, 2, 4TR, 5, 6, and 7GY. Dashed horizontal lines indicate depths of the 0.1% surface PAR.

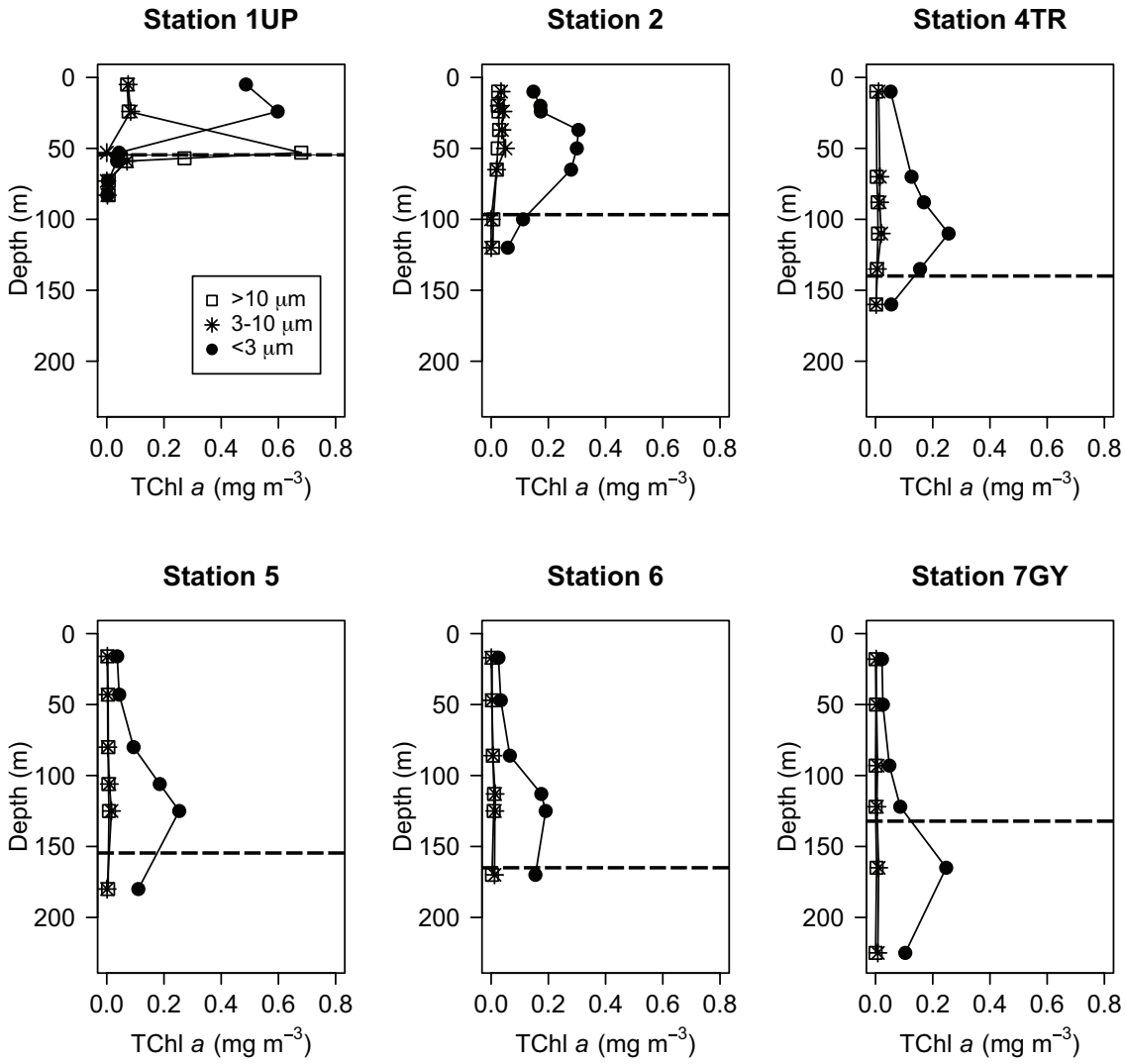

Figure 2.3. Horizontal and vertical distributions of photosynthetic pigments (as a ratio to TChl *a*) measured at stations 1UP, 4TR, and 7GY. Relative pigments are binned by station, depth (50% surface PAR isopleth or the Chl max), and size fraction (>3 µm or pico = <3 µm). The dendrogram, at height 1.0 being the most dissimilar, depicts clustering based on the Jaccard index.

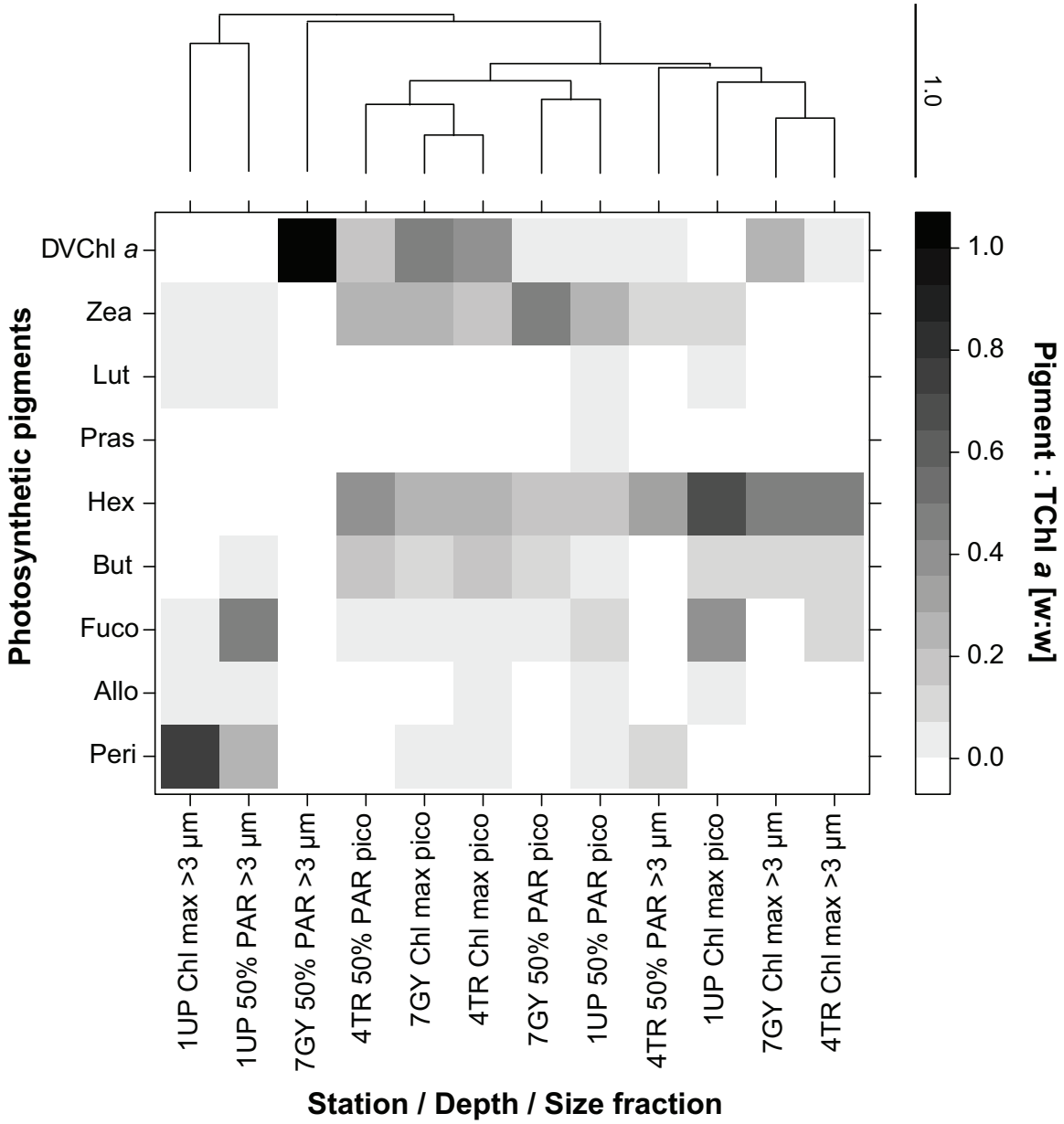

Figure 2.4. Taxonomic composition of PPE assemblages based on 18S rRNA gene sequences obtained from flow cytometrically sorted cells from the 50% surface PAR isopleth and the Chl max at stations 1UP, 4TR, and 7GY. A total of 526 sequences were clustered at the 99% similarity threshold into OTUs by open reference picking with the SILVA 119 eukaryote database. The dendrogram, at height 1.0 being the most dissimilar, depicts clustering based on the Jaccard index.

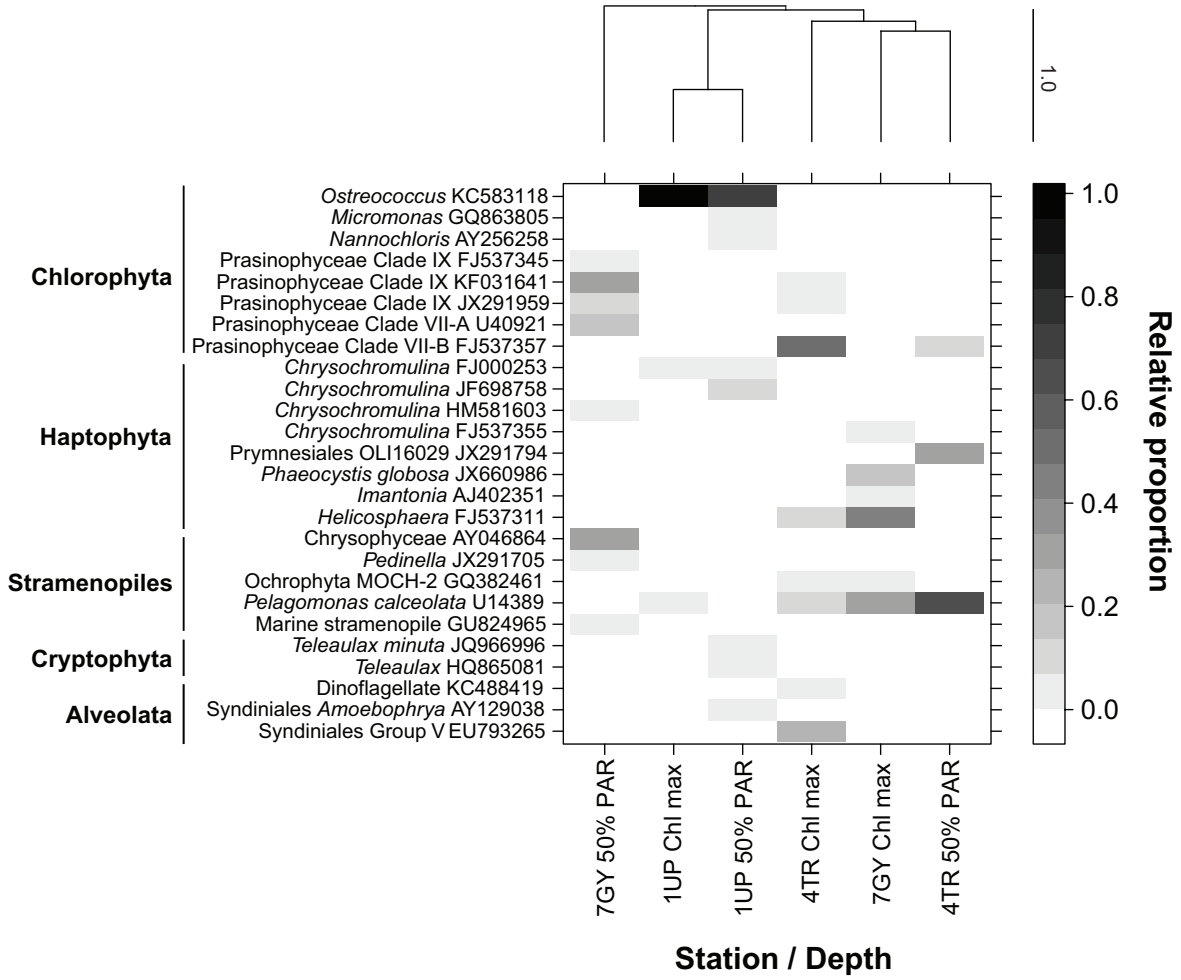

Figure 2.5. a) Euphotic zone depth-integrated (0.1% surface PAR for stations 1UP, 2, 4TR, and 6; depth of Chl max for St. 7GY) rates of ^{14}C-based primary production in three size fractions (>2 μm, 0.6-2 μm, and 0.2-0.6 μm) at station 1UP, 2, 4TR, 6, and 7GY. b) Contributions of size-fractionated rates to >0.2 μm ^{14}C-primary production.

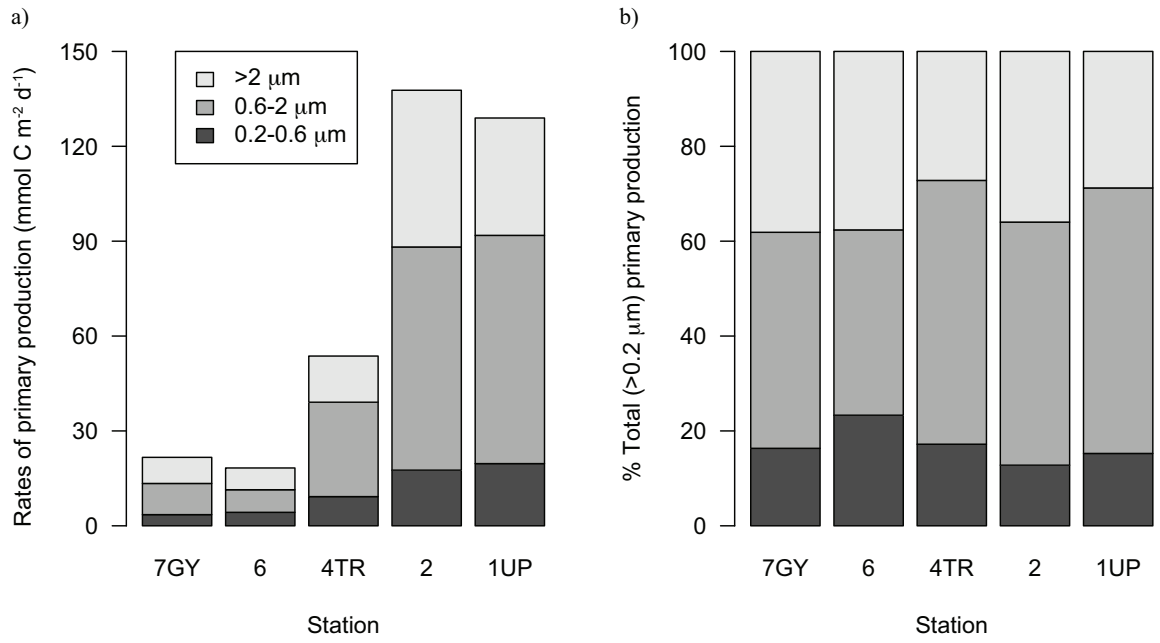

Figure 2.6. Depth profiles of PPE, *Prochlorococcus*, and *Synechococcus* ^{14}C-based primary production rates at stations 2, 4TR, 6, and 7GY. Rates of primary production are binned by vertical isopleths (% surface PAR). Missing data indicate samples where there were too few cells to sort.

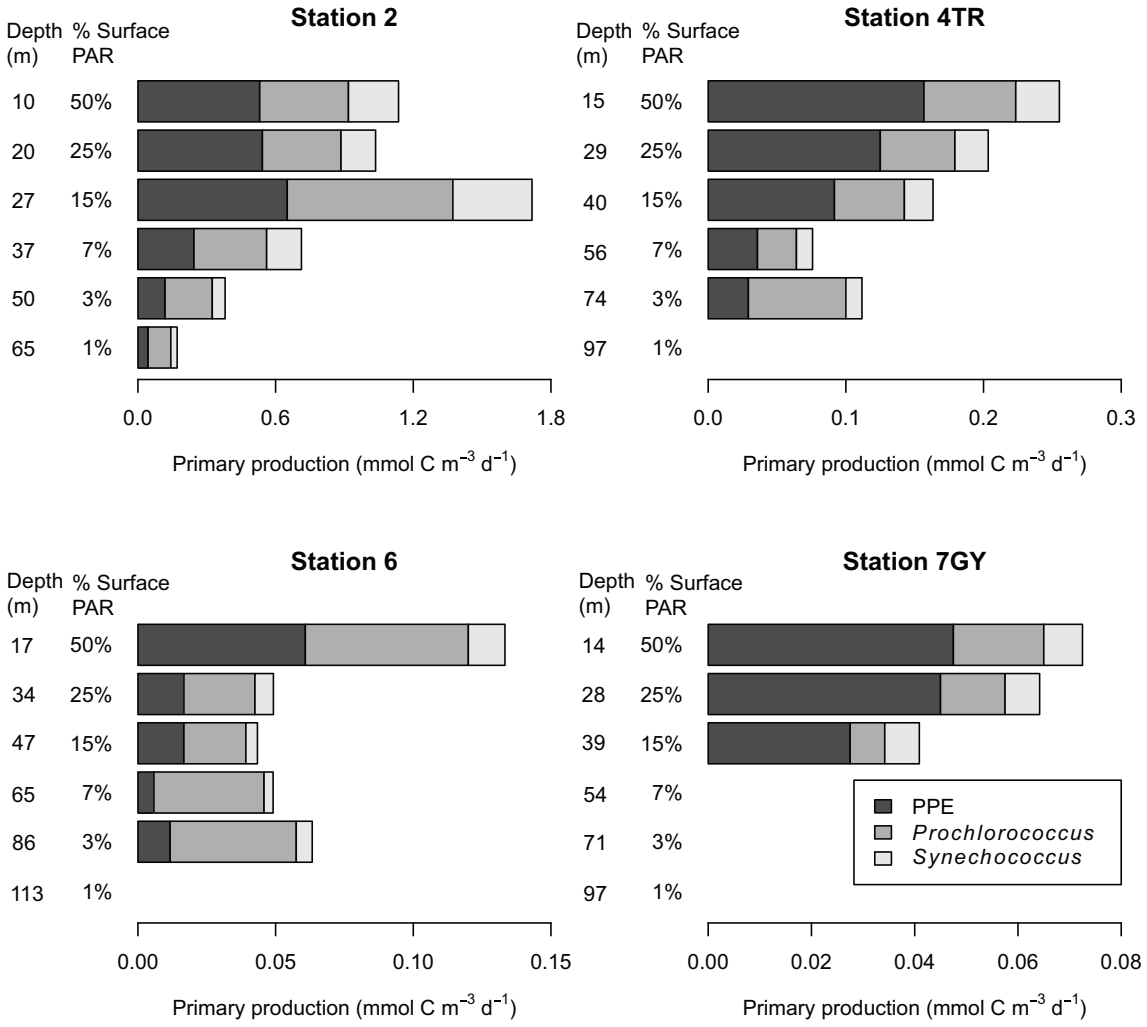

CHAPTER 3

Temporal and vertical variability in picoplankton primary productivity in the North Pacific Subtropical Gyre

Yoshimi M. Rii, David M. Karl, Matthew J. Church

3.1. Abstract

Picophytoplankton (≤3 μm) are major contributors to plankton biomass and primary productivity in the subtropical oceans. Over a one year period (May 2012-May 2013), we examined vertical and temporal variability of picophytoplankton primary productivity at near-monthly time scales in the North Pacific Subtropical Gyre based on filter size-fractionated and flow cytometric sorting of radiolabeled (^{14}C) picoplankton cells. Primary productivity by picophytoplankton comprised ~68-83% of >0.2 μm ^{14}C-based productivity, with the lowest rates observed between September and December and highest between March and August. Group-specific rates of *Prochlorococcus*, *Synechococcus*, and photosynthetic picoeukaryotes (PPE) averaged ~39%, ~2%, and ~11% of the >0.2 μm ^{14}C-productivity, respectively. Despite comparatively low numerical cell abundances, cell-normalized rates of production by PPE (averaging 15.2 fmol C cell^{-1} d^{-1}) were 25- to 90-fold greater than those by *Prochlorococcus* and *Synechococcus* (averaging 0.36 and 1.56 fmol C cell^{-1} d^{-1}, respectively). Moreover, PPE were more active per cell (3.5-fold greater cell-specific rates of ^{14}C-productivity) in the upper euphotic zone (0-45 m) than in the lower euphotic zone (75-125 m), despite greater cell abundances in the lower euphotic zone. Combined, our results suggest that PPE grow rapidly in the well-lit, low-nutrient region of the euphotic zone, likely supported by multiple nutrient acquisition strategies. Furthermore, their rapid growth and presumed removal in the upper euphotic zone indicate that PPE are active contributors to upper ocean carbon cycling in the NPSG.

3.2. Introduction

Picophytoplankton (≤3 μm) are dominant contributors to plankton biomass and net global productivity, particularly in the oligotrophic subtropical ocean gyres (Sieburth et al. 1978, Emerson et al. 1997, Marañón et al. 2001, Carr et al. 2006). In the North Pacific Subtropical Gyre (NPSG), one of the largest ocean ecosystems on Earth (Sverdrup et al. 1946), persistent thermal stratification of the upper ocean and a relatively deep, permanent pycnocline prevents

nutrient-enriched deep waters from penetrating the well-lit waters of the euphotic zone (Eppley et al. 1973, Karl & Lukas 1996). The combination of stratification and perennially high flux of photosynthetically active radiation (PAR) results in extremely low concentrations of inorganic nutrients throughout the upper ocean. As a result, a large fraction of primary productivity appears to be sustained by the rapid recycling of nutrients through microbial food webs (Karl 2002), which is likely facilitated in part by diverse mixotrophic microbial physiologies prevalent in such habitats (Caron 2000, Sherr & Sherr 2002, Zubkov & Tarran 2008).

A diverse assemblage of photosynthetic picoeukaryotes (PPE) and cyanobacteria belonging to the genera *Prochlorococcus* and *Synechococcus* dominate phytoplankton biomass (60-90%) and account for >70% of net primary production in the NPSG (Campbell & Vaulot 1993, Vaulot et al. 1995, Li et al. 2011). The significant contributions of picophytoplankton to biomass and primary production appear linked to efficient nutrient acquisition and light-harvesting capabilities enabled by their small cell sizes (Takahashi & Bienfang 1983, Raven 1986, Chisholm 1992, Raven 1998). Though *Prochlorococcus* cellular abundances are typically orders of magnitude greater than those of PPE in the open ocean, studies from various regions in the Atlantic Ocean suggest rapid growth rates by PPE results in significant contributions to carbon fixation (Li 1994, Jardillier et al. 2010). Moreover, studies in the North Atlantic indicate a large fraction of PPE growth may be supported through assimilation of nitrate (Fawcett et al. 2011), making these picoplanktonic organisms potentially important contributors to new production.

Since 1988, the Hawaii Ocean Time-series (HOT) program has measured a suite of properties and processes to characterize ocean physics and biogeochemistry on near-monthly time scales at Station ALOHA (22.75°N, 158°W), a site representative of the NPSG (Karl & Lukas 1996). The resulting 27+-years of measurements have proven invaluable for characterizing temporal dynamics of bioelemental stocks and fluxes in this ecosystem. The HOT program measurements of ^{14}C-based primary productivity indicate well-resolved seasonal variations that co-vary with changes in solar radiation (Karl & Church 2014). Superimposed on this seasonal dynamic are annually recurring summertime phytoplankton blooms, which are often linked to episodic mesoscale forcing (Dore et al. 2008, Church et al. 2009) and appear to be large contributors to particulate carbon export to the deep sea (Karl et al. 2012). In addition, decreased flux of light to the lower euphotic zone during the winter months permits the

accumulation of nitrate with a subsequent accumulation of phytoplankton biomass in these dimly lit waters triggered by increased light during the spring (Letelier et al. 2004). To date, however, there is limited information on the contributions of major groups of photosynthetic organisms to such temporal variations in primary productivity at Station ALOHA, or on how time-varying changes in the upper ocean habitat influence phytoplankton production and growth in this ecosystem.

Examination of picoplankton contributions to primary productivity has been typically conducted through the size-partitioning of productivity using a range of filter pore sizes to separate plankton biomass (e.g., Marañón et al. 2001, Duhamel & Moutin 2009, Li et al. 2011). Studies have additionally characterized the specific contributions of picoplankton assemblages to rates of primary production through particle size distributions (Barone et al. 2015, White et al. 2015), specific photosynthetic pigment-based labeling (Goericke and Welschmeyer 1993, Pinckney et al. 1996), and flow cytometric sorting of radiolabeled cells (Li 1994, Jardillier et al. 2010, Lomas et al. 2011, Bjorkman et al. 2015, Rii et al. 2016). In the current study, we relied on combined size-fractionated measurements of ^{14}C-bicarbonate assimilation and flow cytometric sorting of ^{14}C-labeled picoplankton populations to examine vertical and temporal patterns in carbon fixation on 11 near-monthly cruises to Station ALOHA. The resulting measurements provided quantitative information on the contributions of dominant groups of picophytoplankton to carbon fixation in this persistently oligotrophic ecosystem, and provided insights into how monthly-scale changes in the upper ocean habitat influences rates of production by these organisms.

3.3. Methods

3.3.1. Sample collection

Seawater was collected in 12 L polyvinylchloride bottles affixed to a rosette sampler equipped with a Sea-Bird 911+ conductivity, temperature, and pressure sensors. Size-fractionated and group-specific rates of ^{14}C-assimilation were collected between May 2012 and May 2013 on ten HOT program (H242-H243, H245-H252) cruises and one Center for Microbial Oceanography: Research and Education (C-MORE) research cruise (termed HOE-DYLAN V) to Station ALOHA (Table 1).

3.3.2. In situ *measurements of ^{14}C-bicarbonate assimilation*

Rates of size-fractionated (>3 μm and 0.2-3 μm) and group-specific ^{14}C-based primary production were obtained using a free-drifting *in situ* array at Station ALOHA (Letelier et al. 1996). Triplicate samples of seawater from six discrete depths (5, 25, 45, 75, 100, and 125 m) were collected into 30 mL polycarbonate centrifuge tubes (Nalgene™ Oak Ridge) from a pre-dawn cast, spiked under subdued light with 70 μL of $NaH^{14}CO_3^-$ (MP Biomedicals 17441H) to a final activity of ~0.14 MBq mL^{-1}. The tubes were incubated over the full photoperiod (~12-14 hours) in white mesh bags affixed to the floating *in situ* array at the corresponding depths where the water was collected. At the end of the incubation period (after sundown), each polycarbonate tube was sampled for size-fractionated and group-specific rates of ^{14}C primary productivity.

Aliquots (25 ml) were subsampled from each tube and stored in 20 mL glass scintillation vials containing 500 μL of β–phenylethylamine to determine the total activity of ^{14}C added to each sample. Next, 5 mL of each sample was preserved in cryotubes containing 30 μl of 16% (final concentration 0.24% w/v) microscopy-grade paraformaldehyde (PFA, Alfa Aesar 43368), flash-frozen in liquid nitrogen, and stored at -80°C for subsequent flow cytometric sorting. The remaining sample volume (~25 mL) was vacuum-filtered onto 25 mm diameter 3 μm pore size polycarbonate membranes (Millipore Isopore™). The filtrate was then vacuum-filtered onto 25 mm diameter 0.2 μm pore size polycarbonate membrane filters (GE Osmonics). After filtration, each filter was placed into a 20 mL glass scintillation vial and stored at -20°C until analyzed back at the shore-based laboratory. Upon return back to shore, vials were uncapped, 1 mL of 2 M hydrochloric acid was added to each filter, and vented for at least 24 hours to remove remaining inorganic ^{14}C. After venting, 10 mL of Ultima Gold liquid scintillation cocktail was added to each vial, and vials were placed in a liquid scintillation counter (Packard TRI-Carb 4640) for the determination of ^{14}C activities.

Group-specific rates of ^{14}C-assimilation by *Prochlorococcus*, *Synechococcus*, and PPE were determined by measuring the amount of ^{14}C assimilated into populations sorted into 6.5 mL HDPE scintillation vials using the BD Influx™ (triggered on forward scatter or FSC, two tube sort, 100 μm nozzle tip, 1X BioSure® sheath solution, 1.0 drop purity mode). Fluorescent microspherical beads (1 μm, Fluoresbrite, Polysciences) were included with the samples for size reference, and 0.2 x 10^3 - 4 x 10^3 beads were sorted for the determination of background levels of radioactivity (both organic ^{14}C in the seawater and ^{14}C absorbed to the beads).

Picophytoplankton cells were enumerated (using the data acquisition software Spigot) based on FSC and side scatter, chlorophyll-based red fluorescence (692 ± 20 nm), and phycoerythrin-based orange fluorescence (585 ± 20 nm) following excitation with two lasers, 488 nm and 457 nm. *Synechococcus* cells were identified based on orange fluorescence signatures, while *Prochlorococcus* cells were defined by their low FSC, side scatter, and orange fluorescence signals relative to *Synechococcus*. Lastly, PPE cells were distinguished based on high FSC, high red fluorescence, and low orange fluorescence (typical population gates depicted in Fig. 1). For each picophytoplankton group, the number of cells sorted ranged 25 x 10^3 - 100 x 10^3 for *Prochlorococcus*, 0.1 x 10^3 - 10 x 10^3 for *Synechococcus*, and 0.36 x 10^3 - 3.5 x 10^3 for PPE. Linearity between cells sorted and radioactivity was checked regularly. For all cruises except H250 (March 2013), we were unable to sort a sufficient number of *Synechococcus* cells at and below 100 m for detection of radioactivity. After sorting, 200 µL of 2 M hydrochloric acid was added to each vial containing the cells, and vials were vented for 48 hours to remove adsorbed and residual ^{14}C-bicarbonate. Then, 4 mL of Ultima Gold liquid scintillation cocktail were added to each vented vial, and after 1 hour, the vials were placed in a liquid scintillation counter (Packard TRI-Carb 4640) for the determination of ^{14}C activities (30 min count time per sample). The resulting radioactivity was converted to cell-normalized and group-specific ^{14}C-assimilation rates based on total added radioactivity, measured dissolved inorganic carbon concentrations (following HOT program procedures and methodologies, Winn et al. 1998), a correction for preferential assimilation of ^{12}C relative to ^{14}C (Steeman Nielsen 1952), the number of cells sorted, and the measured cell abundances.

3.3.3. Picophytoplankton cell abundance

Seawater (2 mL) was collected into cryotubes (Corning) containing a final concentration of 0.24% (w/v) microscopy-grade PFA. Cryotubes were stored at room temperature for 15 minutes in the dark, then flash-frozen in liquid nitrogen and stored at -80°C until analysis. Each picophytoplankton population was distinguished with the same fluorescence and scatter parameters described above, and cell counts were determined using the data analysis software FlowJo 10.0.7.

3.3.4. Mixing, light, nutrients, and pigments

Physical and biogeochemical characteristics of the water column were obtained as part of the near-monthly HOT program core measurements at Station ALOHA (http://hahana.soest.hawaii.edu/hot/hot-dogs/). Samples were collected from eight discrete depths (5, 25, 45, 75, 100, 125, 150, 175 m) in the upper ocean. The mixed layer depths (MLD) for each research cruise were defined as the depth where a 0.125 potential density offset was observed relative to the surface ocean waters (Brainerd & Gregg 1995). A HyperPro radiometer (Satlantic) was used to collect daily vertical profiles of midday downwelling PAR, and coincident measurements of incident PAR were collected using a deckboard radiometer (Satlantic). Together, these measurements were used to compute the downwelling PAR attenuation coefficient (K_{PAR}). Daily-integrated PAR (400 to 700 nm) at the sea-surface was measured with a LI-COR LI-1000 cosine collector and data logger. The flux of downwelling PAR at the discrete depths where productivity measurements were conducted was derived from measured K_{PAR} values and the daily-integrated incident PAR measurements. Seawater samples for the determination of nitrate + nitrite ($NO_3^- + NO_2^-$) in the upper 125 m were analyzed following a high-sensitivity chemiluminescent method (Garside 1982, Dore & Karl 1996). HOT program measurements of high performance liquid chromatography (HPLC)-derived chlorophyll *a* (Chl *a*) were obtained following the protocols of Bidigare et al. (2005).

3.3.5. Statistical analyses

Data sets were tested for normality using the Shapiro-Wilk Test (Royston 1982) and quantile-quantile plots, and those that rejected the null hypothesis ($P>0.05$) were log-transformed. When log transformation was not successful in attaining normality, non-parametric methods (Kruskal-Wallis test, Hollander & Wolfe 1973) were used to test for significant differences between data sets.

3.4. Results

3.4.1. Variability in upper ocean biogeochemistry

Biogeochemical conditions in the upper ocean during our study period (May 2012 to May 2013) were consistent with the long-term HOT program climatology at Station ALOHA (Fig. 2). Inventories of $NO_3^- + NO_2^-$ in the well-lit regions of the upper ocean (0-45 m) were persistently

low and demonstrated no apparent seasonality (one-way ANOVA, P=0.97, Fig. 2A). In contrast, $NO_3^- + NO_2^-$ inventories in the lower euphotic zone (75-125 m) were more temporally variable, with elevated concentrations in November, December, and February (pairwise Tukey and Kramer, P<0.05, Fig. 2B). The depth of the mixed layer ranged from ~36-60 m through the late spring through fall, deepening to ~77-126 m between December to April (Table 1). PAR flux to the upper euphotic zone (<25 m) was greatest from April to August, with lower fluxes (~3-fold lower) in December (Table 1, Fig. 2C). Incident PAR flux at 100 m tended to be greatest between April and June, declining steadily thereafter (Fig. 2D). The depth of the 1% surface PAR isopleth during our study period averaged 112 m, shoaling to 106-110 m from August to February and deepening to 115-118 m from March to June (Table 1). Inventories of HOT program Chl *a* in the upper euphotic zone (0-45 m) were temporally variable (Kruskal-Wallis, P<0.0001), with generally elevated concentrations from November to February compared to the other months (pairwise Tukey and Kramer, P<0.05, Fig. 2E). Monthly-binned Chl *a* inventories in the lower euphotic zone (75-125 m) were not significantly variable across monthly time scales (ANOVA, P=0.18, Fig. 2F).

3.4.2. Variability in picophytoplankton cell abundances

Depth profiles of *Prochlorococcus*, *Synechococcus*, and PPE cell abundances measured during our study were consistent with the historical HOT program measurements of the abundances of these organisms. *Prochlorococcus* cell abundances ranged 36.8 x 10^9 - 336.3 x 10^9 cells m^{-3}, while *Synechococcus* cell abundances ranged 0 - 5.4 x 10^9 cells m^{-3} and PPE cell abundances ranged 0.5 x 10^9 - 2.3 x 10^9 cells m^{-3} (Fig. 3A-C). Throughout the current study, depth-integrated *Prochlorococcus* and *Synechococcus* cell inventories in the upper euphotic zone (0-45 m) were ~1.2- and ~1.4-fold greater than in the lower euphotic zone (75-125 m), respectively (Kruskal-Wallis, P<0.005, Fig. 3D-E). In contrast, PPE cell inventories were ~1.3-fold greater in the lower euphotic zone than in the upper euphotic zone (Kruskal-Wallis, P<0.005, Fig. 3F).

3.4.3. Size partitioning of ^{14}C primary productivity

During this study, we examined the contributions of two plankton size fractions (0.2-3 μm and >3 μm) to rates of ^{14}C-based primary productivity using different filter pore sizes. In

general, the picophytoplankton (0.2-3 μm) contributions to depth-integrated (0-125 m) rates of ^{14}C assimilation were ~3-fold greater (ranging 8.8 and 26.4 mmol C m^{-2} d^{-1}) than contributions by phytoplankton >3 μm (ranging 2.5 to 8.8 mmol C m^{-2} d^{-1}; Table 2). Nearly half (41-59%) of the 0-125 m picophytoplankton ^{14}C-based productivity occurred in the upper euphotic zone (0-45 m), while greater than half (55-75%) of the >3 mm production occurred in the well-lit upper ocean waters (Fig. 4). Picophytoplankton comprised ~68-83% of >0.2 μm (sum of both fractions) euphotic zone depth-integrated (0-125 m) rates of productivity, with their contributions to rates of >0.2 μm ^{14}C primary productivity greater (76-90% vs 65-78%) in the lower (75-125 m) than in the well-lit (0-45 m) regions of the euphotic zone (Table 2). Rates of >0.2 μm ^{14}C - productivity were greatest in July 2012 and lowest in December 2012 (Table 2). In the picophytoplankton fraction, rates of primary productivity in the upper euphotic zone were greatest between May and July 2012, and between March and May 2013 (Table 2, Fig. 4). In the lower euphotic zone, lowest rates of primary production were observed in December 2012 (~1.5 mmol C m^{-2} d^{-1}), followed by a ~3-fold increase in March 2013 (Table 2).

3.4.4. Group- and cell-specific rates of ^{14}C-assimilation

As groups, *Prochlorococcus*, *Synechococcus*, and PPE comprised 39 ± 20%, 1.6 ± 1.7%, and 11 ± 6% of the >0.2 μm ^{14}C primary productivity, respectively, accounting for 52% (on average) of the >0.2 μm ^{14}C primary productivity and 70 ± 32% of picophytoplankton (0.2-3 μm filters) ^{14}C-based primary productivity. *Prochlorococcus* accounted for 63-86% of the depth-integrated (0-125 m) rates of sorted picophytoplankton ^{14}C-production (sum of sorted populations), with *Synechococcus* and PPE accounting for the remaining 1-8% and 12-36%, respectively (Table 3). The largest increases in productivity occurred in March and April 2013 (Fig. 5), and much of this increase appeared attributable to *Prochlorococcus* and *Synechococcus* (~2- to 4-fold increases in group-specific rates compared to February 2013, Table 3). PPE group-specific rates of ^{14}C-production remained fairly consistent throughout the year, except for 3-fold lower rates in October and December. In addition, contributions by PPE were consistently greater in the upper 45 m of the euphotic zone than in the lower euphotic zone (Fig. 5).

Normalizing the sort-based rates of productivity to cell abundances highlighted large differences in cell-specific production by these groups of picophytoplankton. Cell-specific rates of ^{14}C-production by *Prochlorococcus* were consistently lowest (0.2-0.7 fmol C $cell^{-1}$ d^{-1}), with

Synechococcus exhibited somewhat higher rates (0.8-3.8 fmol C $cell^{-1}$ d^{-1}), and PPE demonstrating rates (6.5-26.7 fmol C $cell^{-1}$ d^{-1}) that were 25-95-fold greater than those of *Prochlorococcus* (Table 3). Throughout this study period, depth-integrated (0-125 m) cell-specific rates peaked in March 2013 for both groups of cyanobacteria and in May 2013 for PPE (Table 3). *Prochlorococcus* and *Synechococcus* cell-specific rates of ^{14}C-assimilation appeared temporally dynamic, with rates lowest between August and October, increasing between February and March (Fig. 6A, C). In contrast, cell-specific rates of production by PPE tended to be less variable, with the greatest changes in cell-specific productivity occurring in the upper euphotic zone (Fig. 6E). PPE cell-specific rates were significantly greater (average 3.5-fold) in the well-lit waters (<45 m) than in the lower euphotic zone (Kruskal-Wallis, $P<0.005$, Fig. 6F). In comparison, cell-specific rates of ^{14}C-primary productivity for both *Prochlorococcus* and *Synechococcus* in the upper euphotic zone were ~1.7-fold greater than rates in the lower euphotic zone (Kruskal-Wallis, $P<0.005$, Fig. 6B, D).

3.5. Discussion

We examined the vertical and temporal variability in rates of picophytoplankton ^{14}C-based primary productivity at Station ALOHA in the oligotrophic NPSG. Our observations indicate that picophytoplankton (0.2-3 mm) were consistently responsible for >70% of the ^{14}C-based primary productivity throughout the year, accounting for as much as 90% of the productivity in the lower euphotic zone. This finding is consistent with past studies that have observed the importance of the picophytoplankton fraction to carbon cycling in the ocean, in both oligotrophic and nutrient-rich waters (Li 1994, Agawin et al. 2000, Marañón et al. 2001, Li et al. 2011, Rii et al. 2016). Flow cytometric cell sorting of radiolabeled phytoplankton groups revealed that the majority of sorted picophytoplankton productivity (based on the sum of the sorted cells) at Station ALOHA was attributable to growth by *Prochlorococcus* (76 ± 6%), with PPE and *Synechococcus* accounting for 22 ± 7% and 3 ± 2% of the sorted picophytoplankton productivity, respectively. The resulting contributions to filter-based (>0.2 mm) estimates of productivity by *Prochlorococcus*, *Synechococcus*, and PPE were 39 ± 20%, 2 ± 2%, and 11 ± 6%, respectively. These estimates are comparable to the contribution by *Prochlorococcus* to ^{14}C-assimilation (30-40%) at Station ALOHA reported by Björkman et al. (2015).

In the current study, the sum of ^{14}C primary productivity by sorted cells accounted for 70 ± 32% of the 0.2-3 μm filter size fraction, indicating that not all of the picophytoplankton ^{14}C primary productivity captured on filters was accounted for through cell sorting of picoplankton groups. This apparent underestimation may reflect loss of labeled cell compounds that may have occurred after preservation with PFA (Silver and Davoll 1978), or underrepresented contributions by less abundant, but highly active, members of the PPE. In a study in the Atlantic Ocean, Jardillier et al. (2010) sorted ^{14}C-labeled nucleic acid-stained PPE and observed rates of production nearly equivalent to filter-based measurements. We did not sort and count non-pigmented picoplankton in our study, and some of the filter-based activity could reflect assimilation of ^{14}C by heterotrophs, chemoautotrophs, and weakly fluorescing photoautotrophs.

Vertical differences in the contributions of picophytoplankton groups to euphotic zone productivity were notable in this study. Contributions by *Prochlorococcus* increased with depth, accounting for 81 ± 5% of the productivity in the lower euphotic zone (75-125 m) compared to 72 ± 9% in the upper euphotic zone (0-45 m). In contrast, relative contributions by PPE tended to be greater in the upper euphotic zone relative to the lower euphotic zone (25 ± 9% versus 17 ± 6%), highlighting their potential importance to productivity in the upper ocean. *Synechococcus* contributions remained relatively low and vertically consistent, averaging 3 ± 2% throughout the euphotic zone. Despite the relative increase in the contribution of *Prochlorococcus* to productivity with depth, cell-specific rates of production by *Prochlorococcus* and *Synechococcus* were ~1.7-fold greater in the upper euphotic zone than at depth. Meanwhile, PPE cell-specific rates of production were ~3.5-fold greater in the well-lit regions compared to rates in the lower euphotic zone (Kruskal-Wallis, $P<0.005$).

These results indicate that PPE appear adapted to rapid growth in warm, well-lit regions of the euphotic zone, which is consistent with previous studies demonstrating positive correlations between PPE growth and temperature and irradiance (Bec et al. 2005). PPE taxa can rely on various photophysiological strategies to optimize growth in high light environments, including synthesis and accumulation of photoprotective carotenoids and rapid modification of intracellular Chl *a* concentrations (Dimier et al. 2009, Brunet et al. 2011). Such photophysiological adaptations may provide PPE with competitive advantages over some cyanobacteria or larger phytoplankton in the well-lit upper ocean (Ferris & Christian 1991, Dimier et al. 2009). However, the observation that cell-specific rates of carbon fixation by PPE

were maximal in the upper ocean where vertical supply of nitrate is persistently limited suggests a large fraction of PPE productivity at ALOHA derives from active recycling. Various studies now indicate that diverse taxa of PPE can rely on mixotrophy to obtain nutrients (Caron 2000, Zubkov & Tarran 2008, Frias-Lopez et al. 2009). In a study using RNA stable isotope probing, Frias-Lopez et al. (2009) found that major groups of Prymnesiophyceae, Dictyochophyceae, Bolidomonas, and Dinophyceae actively consumed picocyanobacteria in the surface waters at Station ALOHA. Similarly, in the surface waters of the tropical northeast Atlantic, 37-70% of total bacterivory was attributable to PPE (Zubkov & Tarran 2008). Such mixotrophic metabolism could fuel rapid recycling of nutrients in the upper ocean (Hartmann et al. 2012) and serve to decrease competition with cyanobacteria for available nutrients, while simultaneously diminishing prey concentrations of potential phagotrophic competitors (Thingstad et al. 1996, Tittel et al. 2003). The consideration of a large proportion of PPE as mixotrophs significantly alters their ecological roles, not just as primary producers but also as top-down control of bacterioplankton abundance and producers of organic matter into the microbial food web.

In addition to their presumed importance in regenerated production, various studies suggest PPE may also contribute to new production. Studies using nitrogen isotopes to examine the nitrogen uptake capacities of cyanobacteria and PPE in the North Atlantic found that the $\delta^{15}N$ signatures of flow-sorted PPE were consistently higher than bulk $\delta^{15}N$ of particulate matter and $\delta^{15}N$ of prokaryote biomass in the upper 100 m during the summer, suggesting a seasonal reliance by PPE on the assimilation of nitrate introduced from below the euphotic zone than on nitrogen recycled in the euphotic zone (Fawcett et al. 2011, 2014). PPE may also access nitrogen through short-lived transport events that occur at near-monthly frequencies in the spring and summer (Johnson et al. 2010); however, such features appear largely restricted to the lower euphotic zone. In addition, PPE productivity may be partly sustained by nitrogen fixation through local nitrification (Dore & Karl 1996) and through symbiotic interactions such as those reported between unicellular nitrogen-fixing cyanobacteria and picoeukaryotic prymnesiophytes (Thompson et al. 2012).

Despite the high cell-specific activities in the upper euphotic zone, cell abundances of PPE were significantly greater in the lower euphotic zone. Together, the observed vertical distributions of cell abundances and rates of carbon fixation suggest that the coupling between growth and mortality among cyanobacteria may be less vertically variable than observed for

PPE, with both growth and removal (presumably via predation or viral lysis) of PPE being more rapid throughout the upper euphotic zone than in the dimly lit lower euphotic zone waters. Such results are consistent with Worden et al. (2004), who found that rates of grazing on PPE could exceed growth rates. Other studies have also observed tight coupling between growth and grazing for PPE, suggesting that PPE growth may be critical to transfer of material through the food web (Reckermann & Veldhuis 1997, Brown et al. 1999).

Our observations that cell specific rates of carbon fixation by PPE were consistently greater than rates by cyanobacteria suggest that rates of productivity in this ecosystem may not scale on cellular biomass. For example, cell-specific rates of production by PPE in the euphotic zone were 25- to 95-fold greater than *Prochlorococcus* and 4- to 23-fold greater than *Synechococcus*. Assuming average cell diameters of *Prochlorococcus*, *Synechococcus*, and PPE of 0.7 mm, 1.2 mm, and 2 mm, respectively (Worden et al. 2004), yields equivalent spherical volumes of 0.18 mm^3, 0.70 mm^3, and 4.19 mm^3. Assuming biomass scales with cell volume, such estimates would imply that on a per-cell basis, PPE biomass could be ~20-fold greater than *Prochlorococcus* biomass. Normalizing the per-cell production rates in the current study to cell biomass (converted from measured cell abundances assuming 39 fg C $cell^{-1}$, 82 fg C $cell^{-1}$, and 530 fg C $cell^{-1}$, Worden et al. 2004) yields growth rates of 0.11 ± 0.05 d^{-1}, 0.23 ± 0.13 d^{-1}, and 0.35 ± 0.12 d^{-1}, for *Prochlorococcus*, *Synechococcus*, and PPE, respectively. These estimated rates suggest that PPE may be growing ~1.5- to 3-fold more rapidly than *Prochlorococcus* and *Synechococcus*. Such derived estimates of growth rates are subject to large uncertainty, in part due to the wide range of cell sizes and carbon conversion factors reported for these picophytoplankton groups (Casey et al. 2013, Hartmann et al. 2014). Nonetheless, our results are generally consistent with previous studies in other regions of the world's oceans based on various methodological approaches. For example, Jardillier et al. (2010) reported average PPE cell-specific rates of carbon fixation that were 81-fold and 10-fold greater than rates by *Prochlorococcus* and *Synechococcus*, respectively, in the tropical and subtropical northeast Atlantic Ocean. Dilution grazing experiment results conducted in coastal waters of the Pacific Ocean yielded growth rates of 0.33 ± 0.14 d^{-1}, 0.66 ± 0.13 d^{-1}, and 0.99 ± 0.28 d^{-1} for *Prochlorococcus*, *Synechococcus*, and PPE, respectively (Worden et al. 2004), complementing the proportional differences of growth rates derived from the present study. In a recent study at Station ALOHA, Björkman et al. (2015) measured rates of 0.12-0.52 fmol C $cell^{-1}$ d^{-1} for

Prochlorococcus at 75 m, similar to rates measured in this study (averaging ~0.34 fmol C cell^{-1} d^{-1} at 75 m).

For this study period, we observed high group- and cell-specific rates of primary production in the cell sorts of all three picophytoplankton groups in the early spring of 2013 (March and April). Cell-specific rates of ^{14}C primary production by *Prochlorococcus* and *Synechococcus* increased 4-fold during this period, coincident with a ~1.3-fold increase in inventories of Chl *a* in the lower euphotic zone. The apparent increase in net picophytoplankton growth may reflect the previously documented seasonal interaction of light and nutrients in the lower euphotic zone. Letelier et al. (2004) hypothesized that deepening of isolumes during the spring period alleviates light-limited phytoplankton production and results in rapid consumption of nutrients in the lower euphotic zone. Thus, similar to hypothesized controls on temperate ecosystem spring blooms, seasonal changes in the availability of light appear to be a primary control on net picophytoplankton growth in the lower regions of euphotic zone at Station ALOHA. Interestingly, cell-specific rates of production and cell inventories of *Prochlorococcus* and *Synechococcus* both appeared most responsive during the spring of 2013, coincident with the period of rapid nitrate consumption. Although many of the dominant ecotypes of *Prochlorococcus* appear to prefer reduced nitrogen substrates (Moore et al. 2002, Fawcett et al. 2014), various studies have demonstrated the capacity for nitrate assimilation by *Prochlorococcus* (Casey et al. 2007, Martiny et al. 2009, Berube et al. 2014, 2015). In addition, *Synechococcus* have been reported to respond significantly to nanomolar changes in nitrate concentration (Glover et al. 1988, 2007). Although the activities and biomass of *Prochlorococcus* and *Synechococcus* increased most during the spring in the lower euphotic zone, proportional contributions of PPE to group-specific rates of primary production and cell abundances increased in the upper euphotic zone during March and April. The accumulation of PPE cells in the upper euphotic zone could reflect a decoupling of growth and grazing interactions during this period, perhaps triggered by a slight deepening of the mixed layer (77-126 m) from December to April. Such mixed layer deepening may have resulted in some dilution of predator-prey interactions, thereby allowing the accumulation of PPE cell abundances in the upper euphotic zone for a brief period (Behrenfeld 2010). Alternatively, the deepening of the mixed layer, together with the accumulation of nitrate in the lower euphotic zone due to low light, may increase the vertical supply of nitrate to the upper waters of the euphotic zone.

In summary, we examined variability in size-fractionated rates of carbon fixation, as well as group- and cell-specific rates of picophytoplankton primary productivity over a period of one year at Station ALOHA. An increase in picophytoplankton productivity was observed in the lower euphotic zone in March and April 2013, which appears consistent with the seasonal light-triggered drawdown of nutrients during this period. In addition, PPE cell-specific rates of ^{14}C productivity in the upper euphotic zone remained consistently higher than rates in the lower euphotic zone, though their cell inventories increased in the lower euphotic zone, indicating that controls on PPE population size may be vertically variable. Collectively, these results reveal significant vertical variability in picophytoplankton cell-specific rates of primary production. As the oceans warm and stratify with future projected changes to Earth's climate (Sarmiento et al. 1998, Behrenfeld et al. 2006, Gruber 2011), our results suggest that these altered states, with increased light in the upper water column, may favor PPE growth, significantly influencing carbon cycling throughout low productivity ecosystems such as the NPSG.

3.6. Acknowledgments

We are grateful to the HOT program science team for the collection and analyses of data used in this study. Sam Wilson and Jessica Fitzsimmons served as chief and junior chief scientists for the HOE-DYLAN expedition V. Thanks also to Ken Doggett and Karin Björkman for the technical support and advice on the flow sorting methodology. We acknowledge the captains and crew of the various research vessels that have supported the Hawaii Ocean Time-series, including the University of Hawai‘i vessels R/V *Kilo Moana* and R/V *Ka‘imikai-O-Kanaloa*. Support for this work derived from U.S. National Science Foundation grants OCE-1241263 and OCE-1260164 (MJC), C-MORE (EF-0424599; DMK), Gordon and Betty Moore Foundation (DMK), the Simons Collaboration on Ocean Processes and Ecology (SCOPE; DMK and MJC), and the University of Hawai‘i Denise B. Evans Research Fellowship in Oceanography (YMR).

3.7. References

Agawin NSR, Duarte CM, Agusti S (2000) Nutrient and temperature control of the contribution of picoplankton to phytoplankton biomass and production. Limnol Oceanogr 45: 591-600

Barone B, Bidigare RR, Church MJ, Karl DM, Letelier RM, White AE (2015) Particle distributions and dynamics in the euphotic zone of the North Pacific Subtropical Gyre. J Geophys Res Oceans 120: 3229-3247

Bec B, Husseini-Ratrema J, Collos Y, Souchu P, Vaquer A (2005) Phytoplankton seasonal dynamics in a Mediterranean coastal lagoon: emphasis on the picoeukaryote community. J Plankton Res 27: 881–894

Behrenfeld MJ (2010) Abandoning Sverdrup's critical depth hypothesis on phytoplankton blooms. Ecology 91: 977–989

Behrenfeld MJ, O'Malley RT, Siegel DA, McClain CR and others (2006) Climate-driven trends in contemporary ocean productivity. Nature 444: 752-755

Berube PM, Biller SJ, Kent AG, Berta-Thompson JW and others (2014). Physiology and evolution of nitrate acquisition in *Prochlorococcus*. ISME J 9: 1195-1207

Berube PM, Coe A, Roggensack SE, Chisholm SW (2015). Temporal dynamics of *Prochlorococcus* cells with the potential for nitrate assimilation in the subtropical Atlantic and Pacific oceans. Limnol Oceanogr doi:10.1002/lno.10226

Bidigare RR, Van Heukelem L, Trees CC (2005) Analysis of algal pigments by high-performance liquid chromatography. In: Andersen RA (ed) Algal culturing techniques. Academic Press, New York, p 327–345

Björkman KM, Church MJ, Doggett JK, Karl DM (2015) Differential assimilation of inorganic carbon and leucine by *Prochlorococcus* in the oligotrophic North Pacific Subtropical Gyre. Front Mar Sci doi:10.3389/fmicb.2015.01401

Brainerd KE, Gregg MC (1995) Surface mixed and mixing layer depths. Deep-Sea Res I 42: 1521-1543

Brown SL, Landry M, Barber RT, Campbell L, Garrison D, Gowing M (1999) Picophytoplankton dynamics and production in the Arabian Sea during the 1995 Southwest Monsoon. Deep-Sea Res II 46: 1745-1768

Brunet C, Johnsen G, Lavaud J, Roy S (2011) Pigments and photoacclimation processes. In: Roy S, Llewellyn CA, Egeland ES, Johnsen G (eds) Phytoplankton pigments: characterization, chemotaxonomy and applications in oceanography. Cambridge University Press, New York, p 445-471

Campbell L, Vaulot D (1993) Photosynthetic picoplankton community structure in the subtropical North Pacific Ocean near Hawaii (station ALOHA) Deep-Sea Res I 40: 2043-2060

Caron DA (2000) Symbiosis and mixotrophy among pelagic microorganisms. In: Kirchman DL (ed) Microbial ecology of the oceans. Wiley, Hoboken, p 495-523

Carr ME, Friedrichs MAM, Schmeltz M, Noguchi Aita M and others (2006) A comparison of global estimates of marine primary production from ocean color. Deep-Sea Res II 53: 741-770

Casey JR, Aucan JP, Goldberg SR, Lomas MW (2013) Changes in partitioning of carbon amongst photosynthetic pico- and nano-plankton groups in the Sargasso Sea in response to changes in the North Atlantic Oscillation. Deep-Sea Res II 93: 58-70

Casey JR, Lomas MW, Mandecki J, Walker DE (2007) *Prochlorococcus* contributes to new production in the Sargasso Sea deep chlorophyll maximum. Geophys Res Lett 34: doi:10.1029/2006GL028725

Chisholm SW (1992) Phytoplankton size. In: Falkowski PG, Woodhead AD (eds), Primary productivity and biogeochemical cycles in the sea, Plenum Press, New York, pp 213-237

Church MJ, Mahaffey C, Letelier RM, Lukas R, Zehr JP, Karl DM (2009) Physical forcing of nitrogen fixation and diazotroph community structure in the North Pacific subtropical gyre. Global Biogeochem Cy 23: doi:10.1029/2008GB003418

Dimier C, Giovanni S, Ferdinando T, Brunet C (2009) Comparative ecophysiology of the xanthophyll cycle in six marine phytoplanktonic species. Protist 160: 397-411

Dore JE, Karl DM (1996) Nitrification in the euphotic zone as a source for nitrite, nitrate, and nitrous oxide at Station ALOHA. Limnol Oceanogr 41: 1619-1628

Dore JE, Letelier RM, Church MJ, Lukas R, Karl DM (2008) Summer phytoplankton blooms in the oligotrophic North Pacific Subtropical Gyre: Historical perspective and recent observations. Prog Oceanogr 76: 2-38

Duhamel S, Moutin T (2009) Carbon and phosphate incorporation rates of microbial assemblages in contrasting environments in the Southeast Pacific. Mar Ecol Prog Ser 375: 53-64

Emerson S, Quay P, Karl DM, Winn C, Tupas L, Landry M (1997) Experimental determination of the organic carbon flux from open-ocean surface waters. Nature 389: 951-954

Eppley RW, Renger H, Venrick L, Mullin M (1973) A study of phytoplankton dynamics and nutrient cycling in the central gyre of the North Pacific Ocean. Limnol Oceanogr 18: 534-551

Fawcett SE, Lomas MW, Casey JR, Ward BB, Sigman DM (2011) Assimilation of upwelled nitrate by small eukaryotes in the Sargasso Sea. Nature Geosci 4: 717-722

Fawcett SE, Lomas MW, Ward BB, Sigman DM (2014) The counterintuitive effect of summer-to-fall mixed layer deepening on eukaryotic new production in the Sargasso Sea. Global Biogeochem Cy 28: 86-102

Ferris JM, Christian R (1991) Aquatic primary production in relation to microalgal responses to changing light: a review. Aquat Sci 53: 187-217

Frias-Lopez J, Thompson A, Waldbauer J, Chisholm SW (2009) Use of stable isotope-labelled cells to identify active grazers of picocyanobacteria in ocean surface waters. Environ Microbiol 11: 512-525

Garside C (1982) A chemiluminescent technique for the determination of nanomolar concentrations of nitrate and nitrite in seawater. Mar Chem 11: 159–167

Glover HE, Garside C, Trees CC (2007). Physiological responses of Sargasso Sea picoplankton to nanomolar nitrate perturbations. J Plankton Res 29: 263-274

Glover HE, Prezelin BB, Campbell L, Campbell M (1988) A nitrate-dependent *Synechococcus* bloom in surface Sargasso Sea water. Nature 331: 161-163

Goericke R, Welschmeyer NA (1993) The marine prochlorophyte *Prochlorococcus* contributes significantly to phytoplankton biomass and primary production in the Sargasso Sea. Deep-Sea Res I 40: 2283-2294

Gruber N (2011) Warming up, turning sour, losing breath: ocean biogeochemistry under global change. Philos Trans A Math Phys Eng Sci 369: 1980-1996

Hartmann M, Gomez-Pereira P, Grob C, Ostrowski M, Scanlan DJ, Zubkov MV (2014) Efficient CO_2 fixation by surface *Prochlorococcus* in the Atlantic Ocean. ISME J 8: 2280-2289

Hartmann M, Grob C, Tarran GA, Martin AP, Burkill PH, Scanlan DJ, Zubkov MV (2012) Mixotrophic basis of Atlantic oligotrophic ecosystems. Proc Natl Acad Sci USA 109: 5756-5760

Hollander M, Wolfe DA (1973) Nonparametric statistical procedures. Wiley, New York.

Jardillier L, Zubkov MV, Pearman J, Scanlan DJ (2010). Significant CO2 fixation by small prymnesiophytes in the subtropical and tropical northeast Atlantic Ocean. ISME J 4: 1180-1192

Johnson KS, Riser SC, Karl DM (2010) Nitrate supply from deep to near-surface waters of the North Pacific subtropical gyre. Nature 465: 1062-1065

Karl DM (2002) Nutrient dynamics in the deep blue sea. Trends Microbiol 10: 410-418

Karl DM, Church MJ (2014) Microbial oceanography and the Hawaii Ocean Time-series programme. Nat Rev Microbiol 12: 699-713

Karl DM, Church MJ, Dore JE, Letelier R, Mahaffey C (2012) Predictable and efficient carbon sequestration in the North Pacific Ocean supported by symbiotic nitrogen fixation. Proc Natl Acad Sci USA 109: 1842-1849

Karl DM, Lukas R (1996) The Hawaii Ocean Time-series (HOT) program: Background, rationale and field implementation. Deep-Sea Res II 43: 129-156

Letelier R, Dore JE, Winn C, Karl DM (1996) Seasonal and interannual variations in photosynthetic carbon assimilation at Station. Deep-Sea Res II 43: 467-490

Letelier R, Karl DM, Abbott MR, Bidigare RR (2004) Light driven seasonal patterns of chlorophyll and nitrate in the lower euphotic zone of the North Pacific Subtropical Gyre. Limnol Oceanogr 49: 508–519

Li B, Karl DM, Letelier R, Church MJ (2011) Size-dependent photosynthetic variability in the North Pacific Subtropical Gyre. Mar Ecol Prog Ser 440: 27-40

Li WKW (1994) Primary production of prochlorophytes, cyanobacteria, and eukaryotic ultraphytoplankton - measurements from flow cytometric sorting. Limnol Oceanogr 39: 169-175

Lomas MW, Bronk DA, van den Engh G (2011) Use of flow cytometry to measure biogeochemical rates and processes in the ocean. Ann Rev Mar Sci 3: 537–566

Marañón E, Holligan PM, Barciela R, González N, Mouriño B, Pazó M, Varela M (2001) Patterns of phytoplankton size structure and productivity in contrasting open-ocean environments. Mar Ecol Prog Ser 216: 43-56

Martiny AC, Kathuria S, Berube PM (2009) Widespread metabolic potential for nitrite and nitrate assimilation among *Prochlorococcus* ecotypes. Proc Natl Acad Sci USA 106: 10787-10792

Moore LR, Post AF, Rocap G, Chisholm SW (2002) Utilization of different nitrogen sources by marine cyanobacteria. Limnol Oceanogr 47: 989-996

Pickney JL, Millie DF, Howe, KE, Paerl HW, Hurley JP (1996) Flow scintillation counting of ^{14}C-labeled microalgal photosynthetic pigments. J Plankton Res 18: 1867-1880

Raven JA (1986) Physiological consequences of extremely small size for autotrophic organisms in the sea. In: Platt T, Li WKW (eds), Photosynthetic Picoplankton, Can Bull Fish Aquat Sci 214: 1-70

Raven JA (1998) Small is beautiful: the picophytoplankton. Funct Ecol 12: 503-513

Reckermann M, Veldhuis M (1997) Trophic interactions between picophytoplankton and micro- and nanozooplankton in the western Arabian Sea during the NE monsoon 1993. Aquat Microb Ecol 12: 263-273

Rii YM, Duhamel S, Bidigare RR, Karl DM, Repeta DJ, Church MJ (2016) Diversity and productivity of photosynthetic picoeukaryotes in biogeochemically distinct regions of the South East Pacific Ocean. Limnol Oceanogr doi:10.1002/lno.10255

Royston JP (1982) An extension of Shapiro and Wilk's W test for normality to large samples. Appl Stat 31: 115–124

Sarmiento JL, Hughes T, Stouffer RJ, Manabe S (1998) Simulated response of the ocean carbon cycle to anthropogenic climate warming. Nature 393: 245-249

Sherr EB, Sherr BF (2002) Significance of predation by protists in aquatic microbial food webs. Antonie Van Leeuwenhoek 81: 293-308

Sieburth JM, Smetacek V, Lenz J (1978) Pelagic ecosystem structure: Heterotrophic compartments of the plankton and their relationship to plankton size fractions. Limnol Oceanogr 23: 1256-1263

Silver MW, Davoll PJ (1978) Loss of ^{14}C activity after chemical fixation of phytoplankton: Error source for autoradiography and other productivity measurements. Limnol Oceanogr 23: 362-368

Steeman Nielsen E (1952) The use of radioactive carbon (^{14}C) for measuring organic production in the sea. J Cons Int Explor Mer 18: 117-140

Sverdrup HU, Johnson MW, Fleming RH (1946) The oceans: their physics, chemistry and general biology. Prentice-Hall.

Takahashi M, Bienfang PK (1983) Size structure of phytoplankton biomass and photosynthesis in subtropical Hawaiian waters. Mar Biol 76: 203-211

Thingstad TF, Havskum H, Garde K, Riemann B (1996) On the strategy of "eating your competitor": A mathematical analysis of algal mixotrophy. Ecology 77: 2108-2118

Thompson AW, Foster RA, Krupke A, Carter BJ and others (2012). Unicellular cyanobacterium symbiotic with a single-celled eukaryotic alga. Science 337: 1546-1550

Tittel J, Bissinger V, Zippel B, Gaedke U, Bell E, Lorke A, Kamjunke N (2003) Mixotrophs combine resource use to outcompete specialists: Implications for aquatic food webs. Proc Natl Acad Sci USA 100: 12776-12781

Vaulot D, Marie D, Olson RJ, Chisholm SW (1995) Growth of *Prochlorococcus*, a photosynthetic prokaryote, in the Equatorial Pacific Ocean. Science 268: 1480-1482

White AE, Letelier RM, Whitmire AL, Barone B, Bidigare RR, Church MJ, Karl DM (2015) Phenology of particle size distributions and primary productivity in the North Pacific subtropical gyre (Station ALOHA). J Geophys Res Oceans 120: 7381-7399

Winn CD, Li Y-H, Mackenzie FT, Karl DM (1998) Rising surface ocean dissolved inorganic carbon at the Hawaii Ocean Time-series site. Mar Chem 60: 33-47

Worden A, Nolan J, Palenik B (2004) Assessing the dynamics and ecology of marine picophytoplankton: The importance of the eukaryotic component. Limnol Oceanogr 49: 168-179

Zubkov MV, Tarran GA (2008) High bacterivory by the smallest phytoplankton in the North Atlantic Ocean. Nature 455: 224-226

Table 3.1. Sampling dates, light, mixed layer depths, inventories of chlorophyll *a* (Chl *a*), and cell inventories of *Prochlorococcus*, *Synechococcus*, and photosynthetic picoeukaryotes (PPE) measured during this study

Cruise*	Date	Surface PAR (mol quanta m^{-2} d^{-1})	1% Surface PAR Depth (m)	Mixed Layer Depth† (m)	[Chl *a*]‡ (mg m^{-2})	*Prochlorococcus*‡ (x 10^{11} cells m^{-2})	*Synechococcus*‡ (x 10^{11} cells m^{-2})	PPE‡ (x 10^{11} cells m^{-2})
H242	30 May 2012	48.42	n/a	36 ± 6	14.59	214.52	1.44	1.17
H243	25 Jun 2012	42.76	118	73 ± 8	14.74	201.63	1.38	1.65
HD5	12 Jul 2012	44.34	n/a	58 ± 13	18.04	208.35	1.31	1.36
H245	17 Aug 2012	n/a	110	34 ± 6	14.07	256.74	1.96	1.34
H246	14 Sep 2012	41.67	109	59 ± 7	15.16	180.98	0.97	1.26
H247	07 Oct 2012	35.83	106	60 ± 8	15.36	208.80	1.63	0.90
H248	3 Dec 2012	15.17	109	92 ± 11	19.92	232.71	0.89	1.22
H249	12 Feb 2013	24.06	109	111 ± 37	13.01	275.34	3.47	1.95
H250	6 Mar 2013	38.99	117	126 ± 45	22.24	226.19	4.57	1.88
H251	5 Apr 2013	38.17	115	77 ± 28	21.24	275.61	2.80	1.86
H252	17 May 2013	n/a	116	39 ± 10	17.14	285.85	1.60	1.73

*H = HOT, HD = HOE-DYLAN
†Mean ± standard deviation (s.d.)
‡Depth-integrated (0-125 m) inventories

Table 3.2. Rates of size-fractionated ^{14}C primary production

		Upper (0-45 m)*		Lower (75-125 m)*		Total (0-125 m)*	
Cruise	Date	0.2-3 µm	>3 µm	0.2-3 µm	>3 µm	0.2-3 µm	>3 µm
H242	30 May 2012	9.31 ± 1.93†	4.67 ± 0.63	4.07 ± 0.40	1.13 ± 0.07	18.61 ± 2.00	7 .93 ± 0.76
		[67 ± 17%]‡	[33 ± 7%]	[78 ± 10%]	[22 ± 2%]	[70 ± 9%]	[30 ± 4%]
HD5	12 Jul 2012	15.33 ± 1.53	5.29 ± 0.84	4.04 ± 0.28	1.10 ± 0.09	26.37 ± 1.74	8.75 ± 0.98
		[74 ± 10%]	[26 ± 5%]	[79 ± 7%]	[21 ± 2%]	[75 ± 7%]	[25 ± 3%]
H245	17 Aug 2012	6.10 ± 0.70	3.12 ± 0.18	4.03 ± 0.44	0.53 ± 0.02	13.57 ± 1.29	4.85 ± 0.18
		[66 ± 9%]	[34 ± 3%]	[88 ± 13%]	[12 ± 1%]	[74 ± 9%]	[26 ± 2%]
H246	14 Sep 2012	4.30 ± 0.38	1.72 ± 0.17	3.14 ± 0.10	0.52 ± 0.02	10.08 ± 0.44	3.13 ± 0.23
		[71 ± 8%]	[29 ± 3%]	[86 ± 4%]	[14 ± 1%]	[76 ± 4%]	[24 ± 2%]
H247	7 Oct 2012	3.94 ± 0.74	2.02 ± 0.16	2.60 ± 0.30	0.50 ± 0.04	8.84 ± 0.87	3.58 ± 0.25
		[66 ± 15%]	[34 ± 5%]	[84 ± 13%]	[16 ± 2%]	[71 ± 9%]	[29 ± 3%]
H248	3 Dec 2012	5.31 ± 0.61	1.88 ± 0.11	1.47 ± 0.31	0.19 ± 0.02	9.01 ± 0.76	2.49 ± 0.15
		[74 ± 11%]	[26 ± 3%]	[89 ± 25%]	[11 ± 2%]	[78 ± 8%]	[22 ± 2%]
H249	12 Feb 2013	6.21 ± 1.24	3.33 ± 0.17	2.40 ± 0.42	0.45 ± 0.03	11.87 ± 1.31	4.90 ± 0.24
		[65 ± 16%]	[35 ± 5%]	[84 ± 19%]	[16 ± 3%]	[71 ± 10%]	[29 ± 3%]
H250	6 Mar 2013	10.51 ± 0.22	3.00 ± 0.14	6.69 ± 0.75	0.76 ± 0.11	25.39 ± 0.95	5.05 ± 0.22
		[78 ± 2%]	[22 ± 1%]	[90 ± 14%]	[10 ± 2%]	[83 ± 4%]	[17 ± 1%]
H251	5 Apr 2013	9.13 ± 0.70	2.82 ± 0.29	4.74 ± 0.35	0.83 ± 0.04	19.15 ± 1.13	5.07 ± 0.31
		[76 ± 8%]	[24 ± 3%]	[85 ± 8%]	[15 ± 1%]	[79 ± 6%]	[21 ± 2%]
H252	17 May 2013	9.38 ± 0.77	4.54 ± 0.50	2.72 ± 0.42	0.86 ± 0.06	16.13 ± 0.94	7.71 ± 0.53
		[67 ± 7%]	[33 ± 4%]	[76 ± 15%]	[24 ± 3%]	[68 ± 5%]	[32 ± 3%]

*Depth of integration

†Mean ± s.d. of triplicate bottles (in mmol C m^{-2} d^{-1})

‡[% of each size fraction relative to the sum of 0.2-3 µm and >3 µm fractions ± s.d.]

Table 3.3. Depth-integrated (0-125 m) rates of group- and cell-specific picophytoplankton carbon fixation

		Group-specific (mmol C m^{-2} d^{-1})			Cell-specific (fmol C $cell^{-1}$ d^{-1})		
Cruise	Date	*Prochlorococcus*	*Synechococcus*	PPE	*Prochlorococcus*	*Synechococcus*	PPE
H242	30 May 2012	4.71 [73%]*	0.12 [2%]	1.65 [25%]	0.22	0.83	14.12
H243	25 Jun 2012	10.38 [77%]	0.28 [2%]	2.77 [21%]	0.51	2.00	16.79
HD5	12 Jul 2012	9.71 [79%]	0.29 [2%]	2.34 [19%]	0.49	2.08	19.28
H245	17 Aug 2012	9.47 [81%]	0.30 [3%]	1.93 [16%]	0.37	1.53	14.38
H246	14 Sep 2012	5.03 [75%]	0.06 [1%]	1.63 [24%]	0.28	0.59	12.93
H247	07 Oct 2012	3.10 [74%]	0.13 [3%]	0.96 [23%]	0.15	0.80	10.65
H248	3 Dec 2012	5.76 [86%]	0.13 [2%]	0.78 [12%]	0.25	1.45	6.45
H249	12 Feb 2013	7.34 [69%]	0.42 [4%]	2.88 [27%]	0.27	1.20	14.75
H250	6 Mar 2013	16.52 [76%]	1.74 [8%]	3.46 [16%]	0.73	3.79	18.37
H251	5 Apr 2013	11.38 [80%]	0.47 [3%]	2.45 [17%]	0.41	1.68	13.17
H252	17 May 2013	8.05 [63%]	0.19 [1%]	4.63 [36%]	0.28	1.19	26.74

*[% Contribution of each group relative to the summed contributions of *Prochlorococcus*, *Synechococcus*, and PPE]

Figure 3.1. Flow cytograms depicting depth-dependent (0-125 m) changes in forward scatter (FSC) and red fluorescence (488-RED) characteristics of *Prochlorococcus* (Pro), *Synechococcus* (Syn), and PPE. The locations of the reference beads (1 µm) are indicated in the 25 m and 125 m cytograms. Approximate gates around populations are depicted, though specific fluorescence and FSC characteristics were used to distinguish populations while counting and sorting (see Methods text).

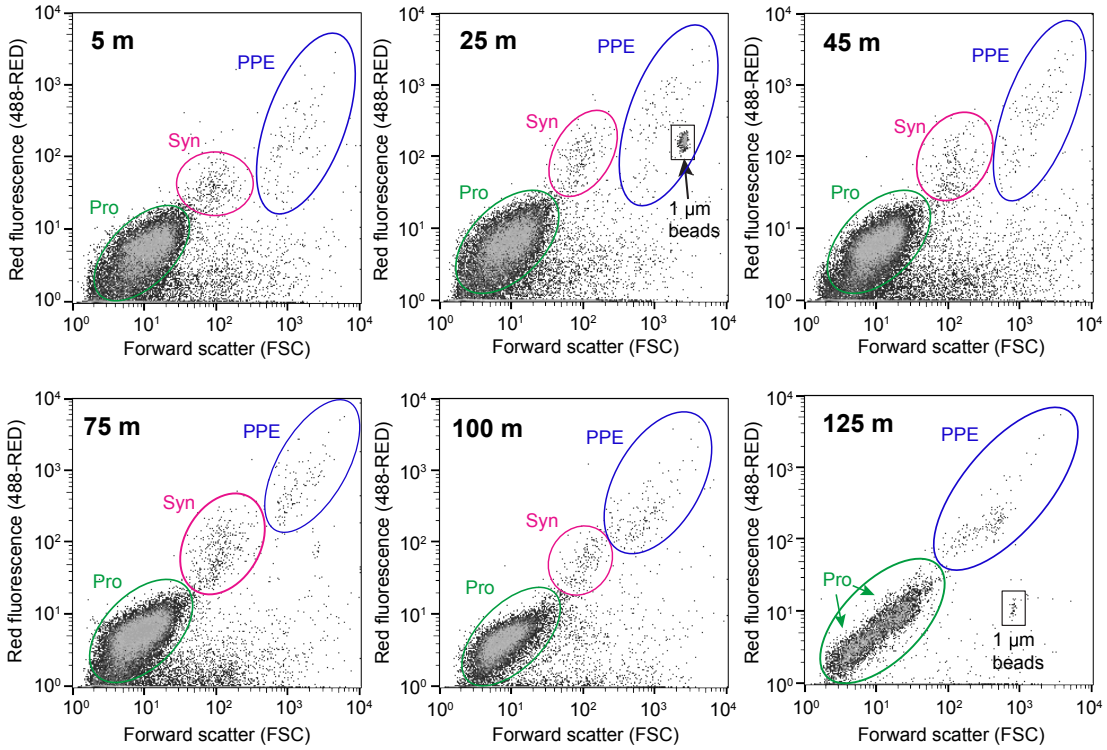

Figure 3.2. Temporal (monthly binned) variability in biogeochemical properties based on HOT program sampling at Station ALOHA, for the upper (0-45 m) and lower (75-125 m) euphotic zone: $NO_3^- + NO_2^-$ (A-B, 1989-2013); daily PAR flux (1998-2013) at 25 m (C) and 100 m (D); and inventories of Chl *a* (E-F, 1989-2013). Measurements conducted as part of the current study (May 2012-May 2013) are symbolized as stars (✳). For each boxplot: dark horizontal line indicates the median, the box boundaries span the 1st (25th percentile) to the 3rd quartile (75th percentile), and the whiskers extend to the maximum and minimum (boundary +/- 1.5*interquartile range) of the selected measurements. Outlier observations, considered to be beyond the maximum and minimum limits of the observations, are depicted as open circles, and observations falling outside the scale of the plot region are indicated by arrows and measurement value (A, F).

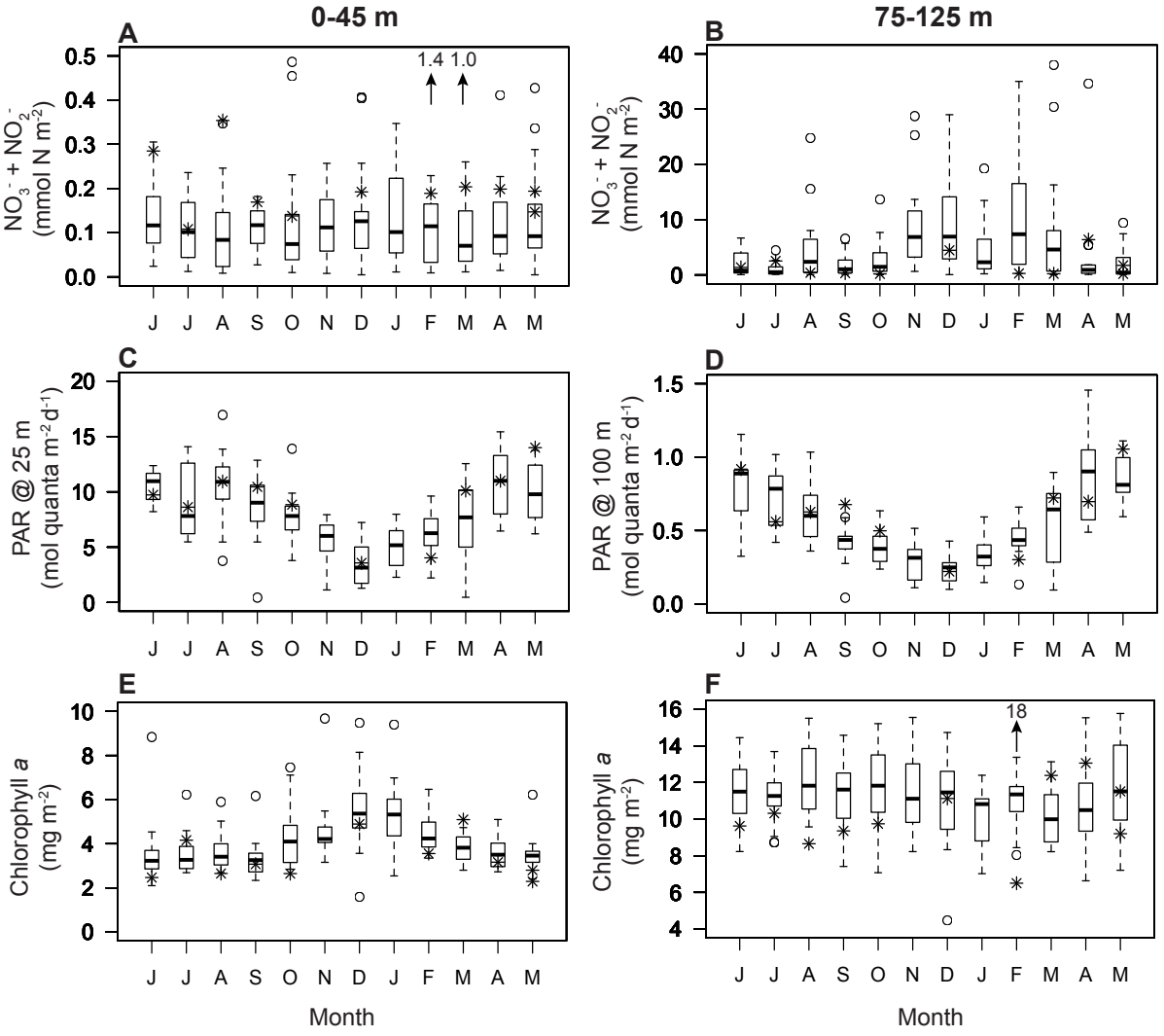

Figure 3.3. Upper ocean *Prochlorococcus* (A), *Synechococcus* (B), and PPE (C) cell abundances at Station ALOHA between 2006 and 2013 (gray circles), with overlay of black circles (mean) and error bars (standard deviations) for measurements obtained during the current study period (May 2012-May 2013). Boxplots show depth-integrated cell abundances of *Prochlorococcus* (D), *Synechococcus* (E), and PPE (F) in the upper (0-45 m) and lower (75-125 m) regions of the euphotic zone from 2006-2013. Boxplot boundaries are the same as those described in Fig. 2.

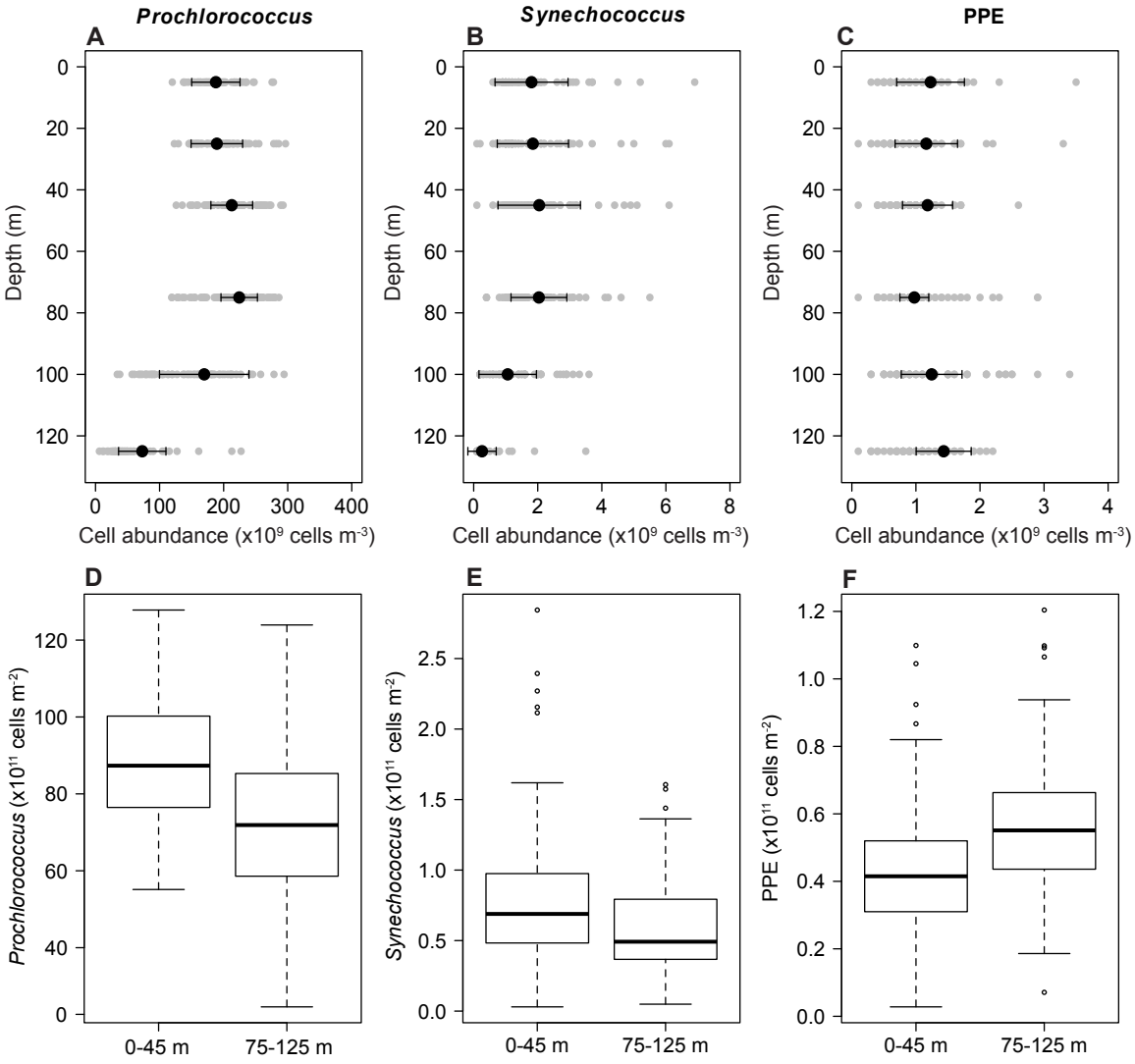

Figure 3.4. Pico- (0.2-3 µm; A) and larger phytoplankton (>3 µm; B) rates of ^{14}C primary production between May 2012 and May 2013. Black circles indicate sampling depths, and values reflect mean of triplicate samples.

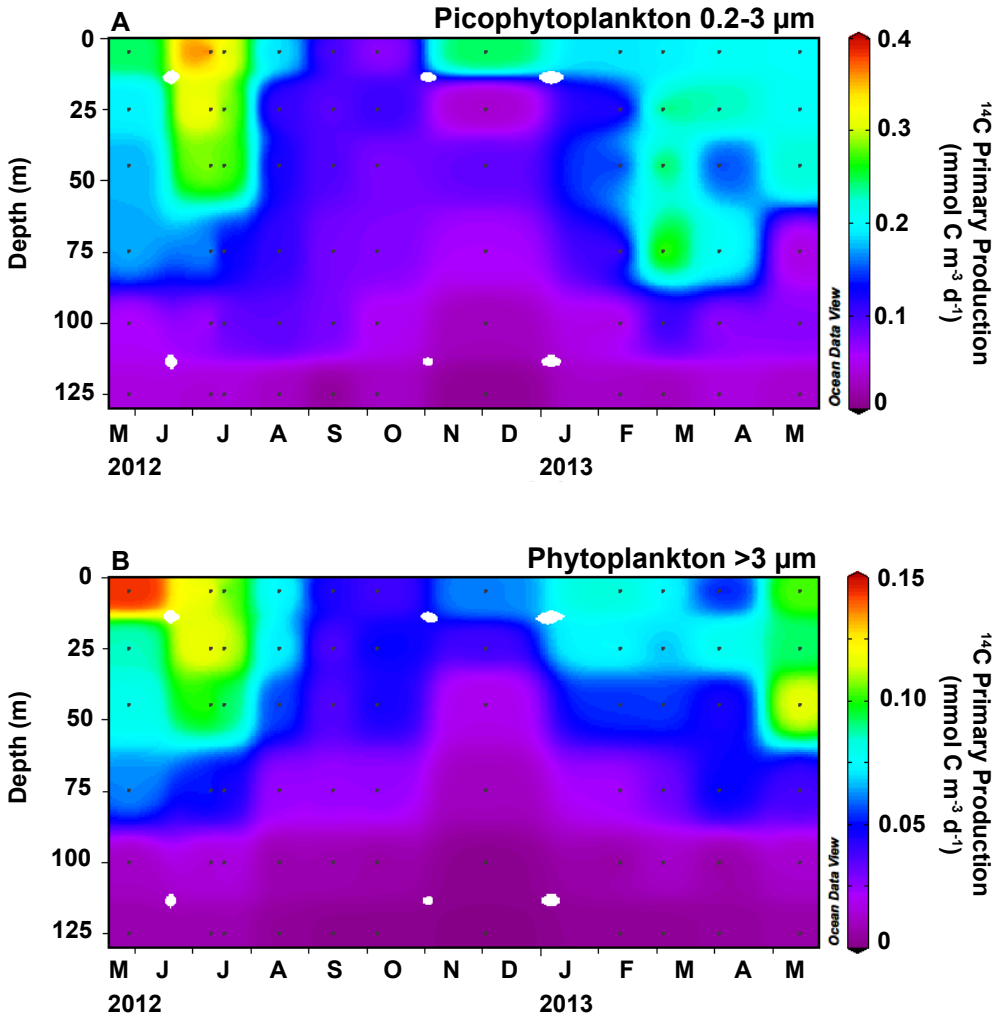

Figure 3.5. Vertical profiles of group-specific rates of ^{14}C-based primary productivity by *Prochlorococcus* (dark grey bars), *Synechococcus* (medium grey bars), and PPE (light grey bars) between May 2012 and May 2013. *Synechococcus* contributions were not measured at 100 m and 125 m except during H250 (March 2013) due to insufficient number of cells sorted.

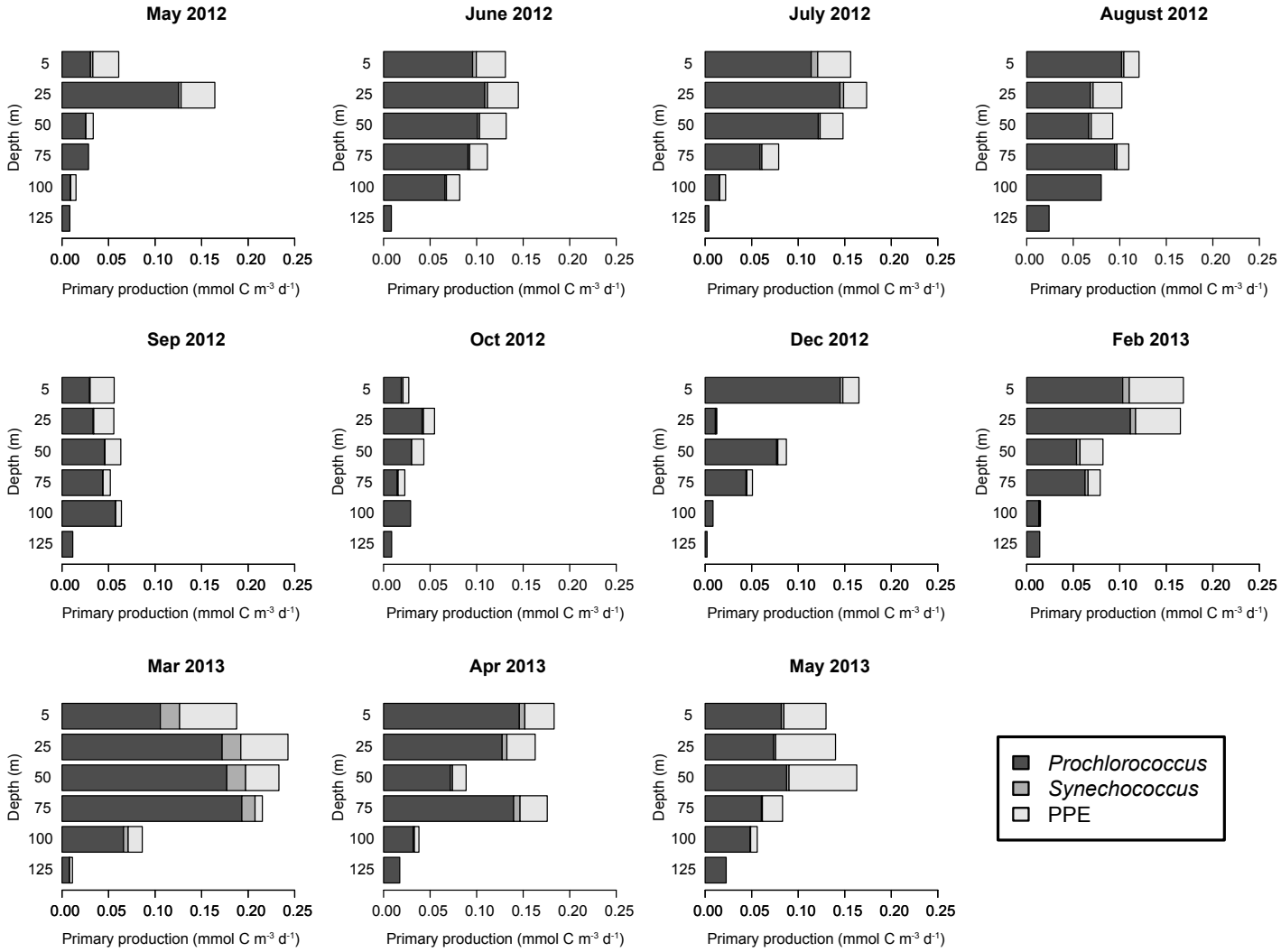

Figure 3.6. Depth profiles of cell-specific rates of ^{14}C primary productivity by *Prochlorococcus* (A, B), *Synechococcus* (C, D), and PPE (E, F) between May 2012 and May 2013. Black circles in A, C, and E indicate sampling depths. Symbols and error bars depicted in panels B, D, and F are time-averaged means and standard deviations.

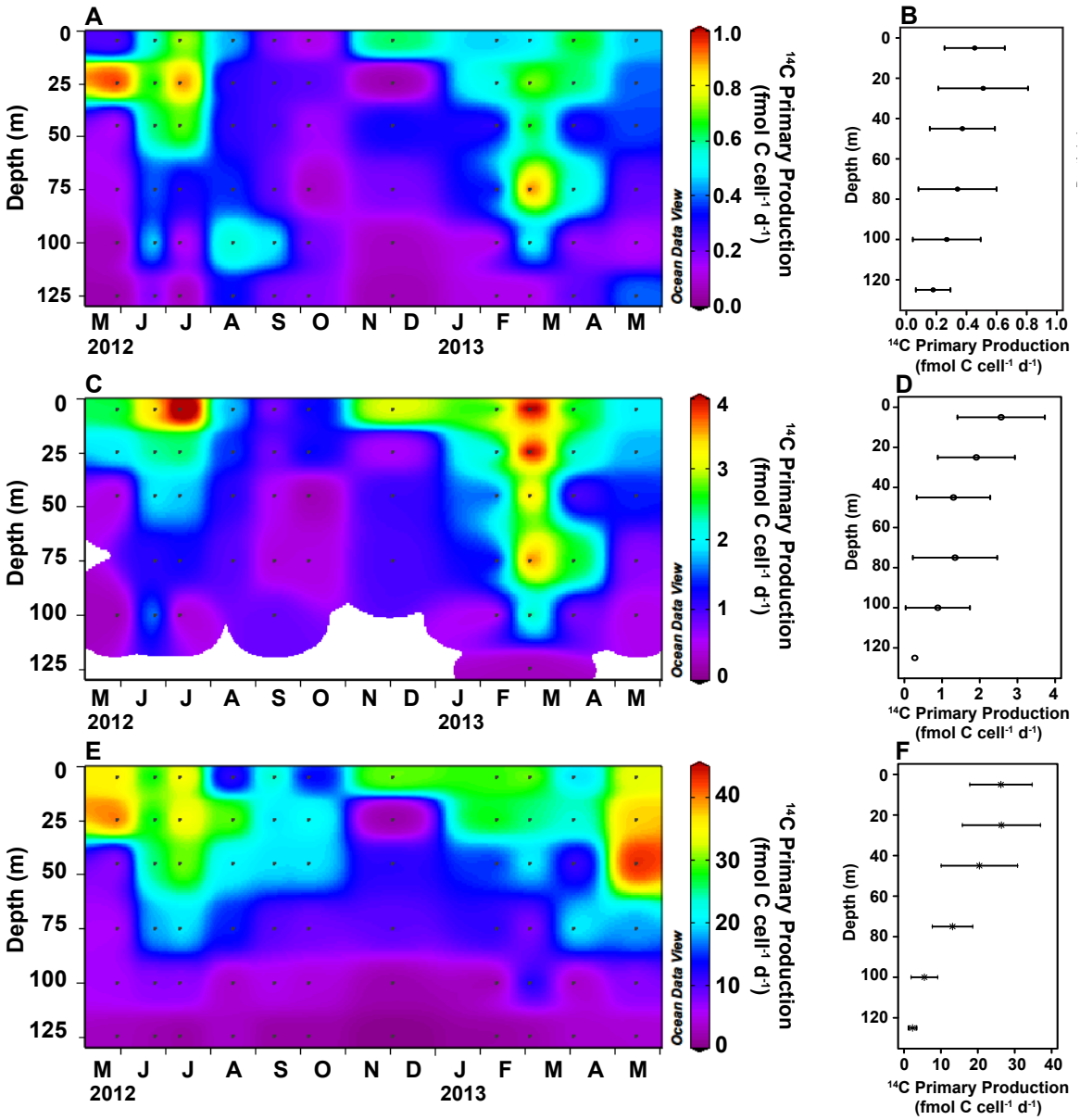

CHAPTER 4

Diversity and dynamics of eukaryotic picoplankton in the North Pacific Subtropical Gyre

Yoshimi M. Rii, Markus V. Lindh, Matthew J. Church

4.1. Abstract

Eukaryotic picoplankton are highly diverse and have a substantial impact on ocean ecosystems, contributing to both photosynthetic energy capture and heterotrophic consumption of organic matter. To date, there are relatively few studies examining the temporal variability of picoeukaryote community structure in the open sea. We examined the dynamics of upper ocean (<200 m) picoeukaryote community diversity through high-throughput sequencing of 18S rRNA gene fragments from near-monthly sampling between February 2011 and May 2013 in the North Pacific Subtropical Gyre. Alveolata comprised on average 58% of total picoeukaryote sequences, with Syndiniales Groups I and II, Dinophyceae, and Syndiniales Amoebophora as the dominant representatives of these sequences. OTUs classified as Het (non-alveolate, non-photosynthetic picoeukaryotes) comprised 17% of total picoeukaryote sequences and were mainly affiliated with marine stramenopiles (MAST) and Rhizaria. OTUs assigned as previously reported photosynthetic picoeukaryotes (PPE) comprised ~8% of the total picoeukaryote sequences and included Pelagophyceae, Prymnesiophyceae, Mamiellophyceae, Chrysophyceae, Cryptophyceae, Dictyochophyceae, and Bolidophyceae. While alpha diversity of the Alveolata and non-photosynthetic picoeukaryotes remained relatively stable with depth, the PPE community exhibited greater diversity in the well-lit upper ocean than in the dimly lit regions of the euphotic zone. Furthermore, PPE assemblages in the upper (5-75 m) and lower (100-175 m) euphotic zone were distinct, suggesting strong vertical structuring likely related to environmental controls. However, the two-layer structuring of PPE assemblages diminished during winter and spring when specific PPE assemblages in the lower euphotic zone (Pelagophyceae, Mamiellophyceae, Prymnesiophyceae) appeared to be entrained via convective mixing into the upper euphotic zone. Collectively, our results highlight temporal variability in picoeukaryote taxonomic composition and diversity, providing insights into the dynamics of bottom-up and top-down controls of picoplankton in the North Pacific Subtropical Gyre.

4.2. Introduction

Picoplanktonic eukaryotes (≤3 μm) are ubiquitous and contribute significantly to biomass and nutrient cycling in the ocean (Sieburth et al., 1978; Stockner et al., 1988; Worden and Not, 2008; Caron et al., 2009). Recent studies have shown that these organisms rely on metabolisms that include photoautotrophy, chemoheterotrophy, and mixotrophy (e.g., Jones, 2000; Zubkov and Tarran, 2008; Massana, 2011), and may play important roles in the marine food web through parasitism (Guillou et al., 2008). Moreover, picoeukaryotes are phylogenetically diverse and include nine major supergroups (Baldauf, 2003; Massana, 2011) that contain numerous lineages poorly represented in culture collections (e.g., Diez et al., 2001; Moon-van der Staay et al., 2001; Worden and Not, 2008; de Vargas et al., 2015). Thus, investigations of the diversity and temporal dynamics of picoeukaryotes can provide insights into various pathways of energy and matter in marine ecosystems.

Photosynthetic picoeukaryotes (PPE), along with marine cyanobacteria, comprise a substantial portion of plankton biomass in various open ocean and coastal eutrophic environments (Campbell et al., 1994; Worden et al., 2004; Vaulot et al., 2008; Not et al., 2012). In particular, PPE contribute significantly to primary production due to high cell-specific rates of carbon fixation (Li, 1994; Jardillier et al., 2010; Rii et al., 2016), despite their relatively low cell abundances (~10^2 -10^3 cells mL^{-1} in the oligotrophic subtropical gyres). Various phylogenetically distinct taxa comprise the PPE (Moon-van der Staay et al., 2000; Worden and Not, 2008; Shi et al. 2009; Treusch et al., 2011; Dasilva et al., 2013; Kirkham et al., 2013) and this diverse group of organisms have been shown to respond rapidly to episodic to seasonal-scale changes in light and nutrients (Fouilland et al., 2004; Rodriguez et al., 2005; McAndrew et al., 2007; Mahaffey et al., 2012). Thus, identifying the diversity, stability, and factors influencing picoeukaryote communities provides important information on the functioning of contemporary marine ecosystems. Surveys of eukaryote diversity based on sequencing of 18S rRNA genes and plastid 16S rRNA genes have improved our knowledge of eukaryotic plankton diversity and biogeographic distributions in the world's oceans (Moon-van der Staay et al., 2001; Rusch et al., 2007; Worden and Not, 2008; Not et al., 2009; Shi et al., 2009; Massana, 2011; Kirkham et al., 2013; de Vargas et al, 2015). The resulting datasets reveal diverse eukaryotic plankton communities. However, there are limited studies to date evaluating temporal variability in eukaryotic plankton communities.

The current study was conducted at Station ALOHA (22.75° N, 158° W), the study site of the Hawaii Ocean Time-series (HOT) program (Karl and Lukas, 1996) in the North Pacific Subtropical Gyre (NPSG). Station ALOHA is characterized by perennially high flux of photosynthetically active radiation (PAR) and extremely low concentrations of inorganic nutrients throughout the upper ocean (Karl and Lukas, 1996; Karl and Church, 2014), where a large fraction of primary productivity appears to be sustained by the rapid recycling of nutrients (Karl, 2002). Picophytoplankton dominate photosynthetic biomass and productivity in this ecosystem (Campbell et al., 1997, Corno et al., 2008; Pasulka et al., 2013); however, little is known about the picoeukaryote community composition and its variability in this region. Our aim was to investigate the temporal and vertical variability in the diversity of picoeukaryote assemblages at Station ALOHA through high-throughput sequencing of 18S rRNA genes. By placing the resulting analyses in the context of the time-resolved HOT program measurements, we sought to identify factors shaping euphotic zone picoeukaryote community structure over a two-year period (2011-2013). We focused our analyses on dominant members of the PPE in order to identify variability associated with these functionally important members of the community.

4.3. Methods

4.3.1. Light, nutrient, and pigment measurements

Samples were collected from eight discrete depths (5, 25, 45, 75, 100, 125, 150, 175 m) on 19 research cruises to Station ALOHA between February 2011 and May 2013. This sampling period captured the range of seasonally variable upper ocean conditions (Table 1). Seawater was collected in 12-L polyvinylchloride bottles affixed to a 24-bottle rosette sampler, equipped with a Sea-Bird 911+ conductivity, temperature, and pressure profiler. Physical and biogeochemical measurements were obtained from the HOT program (data available at http://hahana.soest.hawaii.edu/hot/hot-dogs/interface). Daily vertical profiles of midday downwelling PAR (400 to 700 nm) and incident PAR were collected using a Satlantic HyperPro radiometer and a deckboard radiometer, respectively. Daily PAR fluxes at discrete depths were calculated based on the measured attenuation coefficients (K_{PAR}) together with the daily-integrated incident PAR measurements. Determinations of nitrate + nitrite (NO_3^- + NO_2^-) and phosphate (PO_4^{3-}) concentrations in the upper 100 m relied on high-sensitivity chemiluminescent

methods (Garside, 1982; Dore and Karl, 1996) and the MAGnesium Induced Co-precipitation (MAGIC; Karl and Tien, 1992), respectively. Concentrations of $NO_3^- + NO_2^-$, PO_4^{3-}, and silicic acid at depths >100 m were measured colorimetrically using a 3-channel Bran+Luebbe Autoanalyzer III. PPE cells were distinguished and enumerated based on high forward scatter signals, high red fluorescence, and low orange fluorescence on a BD Influx flow cytometer. Concentrations of total chlorophyll *a* (TChl *a*, monovinyl chlorophyll *a* + divinyl chlorophyll *a*) were obtained from filter extracts detected using high performance liquid chromatography following protocols described in Bidigare et al. (2005).

4.3.2. Nucleic acid sample collection and extraction

Seawater samples (2-L) for subsequent extraction of planktonic DNA were subsampled from the rosette sampler into acid-washed polyethylene bottles. Seawater samples were sequentially filtered using a peristaltic pump onto 25-mm diameter, 3-µm pore size polycarbonate membranes (Millipore Isopore™), followed by filtration through 25-mm diameter, 0.2-µm pore size polyethersulfone membranes (Pall Supor®). After filtration, filters were placed in 1.5-mL microcentrifuge tubes, immediately flash frozen in liquid nitrogen, and stored at -80°C until analysis. Back in the shore-based laboratory, DNA from the 0.2-µm filter membranes was extracted and purified using the QIAGEN DNeasy Plant Mini Kit including a bead-beating step (with 0.1- and 0.5-mm beads) and Proteinase K (QIAGEN) for additional cell disruption and lysing (Paerl et al., 2008). Extracts were eluted in 200 µL of nuclease-free PCR grade water and quantified using the Qubit® fluorometer.

4.3.3. PCR amplification

We amplified the hypervariable V9 region of 18S rRNA genes using the polymerase chain reaction (PCR) primers 1391F (5'-GTACACACCGCCCGTC-3'; *S. cerevisiae* NCBI GenBank Accession #U53879 position 1629-1644; Lane, 1991) and Euk Br (5'-TGATCCTTCTGCAGGTTCACCTAC-3'; *S. cerevisiae* NCBI GenBank Accession #U53879 position 1774-1797; Medlin et al., 1988; Amaral-Zettler et al., 2009). Each PCR reaction contained both primers (0.2 µM final concentration), 1X 5 PRIME HotMasterMix (Cat# 2200410), and ~5 ng of template DNA in a 25 µL reaction. Thermal cycling conditions consisted of an initial activation step at 94°C for 3 min, followed by 35 cycles of 45 sec at 94°C, 60 sec at

57°C, and 90 sec at 72°C, ending with a final extension of 10 min at 72°C. Amplifications were conducted in triplicate and PCR products were pooled and checked to verify amplification and specificity on an agarose gel. Triplicate-pooled products were quantified, with ~50 ng of product from each sample combined into a single tube and purified using the MoBio UltraClean PCR Clean-Up Kit (Cat# 12500).

4.3.4. Sequence analyses

The quality of the combined PCR products was determined on a Bioanalyzer 2100 (Agilent) and paired-end sequencing was conducted (300 cycles) on an Illumina MiSeq at the University of Hawai‘i Core Functional Genomics Facility at the Hawai‘i Institute of Marine Biology. Paired-end sequencing reads were merged using PEAR (Zhang et al., 2014), with 14,424,491 merged reads recovered from a total of 191 samples. All merged sequences were quality filtered with the following parameters: reads were trimmed to 100-150 bp in size, maximum expected error of 1%, no ambiguous bases allowed, and an average Phred quality threshold >34. Reference-based and *de novo* detection of chimeras was performed with USEARCH v7.0.1090 (Edgar et al., 2011) with the SILVA 119 database pre-clustered at 97% (Quast et al., 2013), and all chimeras were removed. Remaining reads were clustered using UCLUST v1.2.22q (max accepts = 20, max rejects = 500) into operational taxonomic units (OTUs) using subsampled open-reference OTU picking through the QIIME pipeline (Caporaso et al., 2010b). OTUs were first clustered with the SILVA 119 database and then clustered *de novo* at the 95, 97, and 99% similarity thresholds. The centroid sequence within each OTU was selected as the representative sequence, and sequences that failed to align using PyNAST (minimum percent identification 0.75, Caporaso et al., 2010a) were removed. Singletons (OTUs composed of only one sequence in the data set) and OTUs present in only one sample, comprising 38%, 48%, and 63% of the total OTUs when clustered at the 95%, 97%, and 99% similarity thresholds, respectively (Table 2), were subsequently removed. The number of OTUs increased 2- to 7-fold with increasing similarity thresholds, resulting in 14,254; 33,342; and 111,964 quality-filtered OTUs for 95%, 97%, and 99% similarity, respectively (Table 2). For further analyses, OTUs clustered at 97% were used in order to limit inflation of species richness (Kunin et al., 2010). Taxonomy was assigned to representative sequences at 90% identity with BLAST (max E value threshold at $1e^{-30}$) using the SILVA 119 and the PR^2 databases (Guillou et

al., 2012) pre-clustered at the respective similarity thresholds, and manually curated for consensus assignments. Bacteria and Metazoa comprised 17% and 4% of the quality-filtered reads, respectively, and were removed from further analyses.

The final OTU table of total picoeukaryotes consisted of 29,241 OTUs and 5,983,390 sequences (Table 2). Of these, taxonomy was not assigned for 8,943 OTUs (955,354 or 16% of total picoeukaryote sequences), consistent with the stringent BLAST E value utilized. Rarefaction analyses were conducted for all samples up to 25,000 reads. The total picoeukaryote OTU table was divided into three additional taxonomy-based OTU categories in order to examine specific taxa in closer detail: Alveolata OTUs contained all OTUs assigned as Alveolata, including Syndiniales, Ciliophora, Apicomplexa, and Dinophyceae; Het OTUs contained presumed non-photosynthetic picoeukaryotes, including Excavata, marine stramenopiles (MAST), Rhizaria, Picozoa, Opisthokonta, Amoebozoa, and Apusozoa, while excluding the Alveolata; and PPE OTUs consisted of OTUs assigned as known photosynthetic (and mixotrophic) organisms including Archaeplastida, Cryptophyta, Haptophyta, Chlorarachniophyceae, and Ochrophyta. Subsampling for calculations of species richness was conducted on the minimum number of sequences per OTU table and category: 9,165 for total picoeukaryote OTUs, 4,591 for Alveolata OTUs, 1,111 for Het OTUs and 271 for PPE OTUs. For phylogenetic analyses of the 20 most abundant PPE OTUs, representative sequences (90-150 bp) were aligned with reference sequences using CLUSTALW (Thompson et al., 1994) and manually inspected. A distance matrix was calculated based on the sequence alignment (Table 3). Final quality-filtered sequences will be deposited into NCBI's Sequence Read Archive.

4.3.5. Statistical analyses

Community analyses including alpha and beta diversity were performed in R 3.1.1 with the package *Vegan* (Oksanen et al., 2013; R Core Development Team, 2014) and graphical outputs were constructed with the package *ggplot2* (Wickham, 2009). The dataset was seasonally binned and analyzed as follows: spring (March, April, May), summer (June, July, August), fall (September, October, November), and winter (December, January, February). Differences in picoeukaryote community composition between seasons and depths were tested using permutational analysis of variance (PERMANOVA) on Bray-Curtis distances. Absolute shifts in picoeukaryote community structure (estimated from Bray-Curtis dissimilarity) were correlated

with absolute changes in environmental properties (estimated from Euclidean distances) and significance was tested using Mantel tests. Hierarchical clustering of PPE OTUs was performed with Bray-Curtis dissimilarity and bootstrap values were calculated using the package *pvclust* (Suzuki and Shimodaira, 2006).

4.4. Results

4.4.1. Biogeochemical parameters

During this study, upper ocean temperatures varied seasonally, with warmest temperatures measured between June and November, and cooler waters observed in winter and early spring (Fig. 1A). Similarly, the upper ocean, which was stratified during summer and fall, became increasingly well mixed in the winter and spring periods (Fig. 1). Surface incident PAR was highest in spring and summer months (averaging 42 ± 5 and 43 ± 1 mol quanta m^{-2} d^{-1}, respectively), decreasing to 38 ± 4 and 53 ± 5 mol quanta m^{-2} d^{-1} in fall and winter, respectively (Table 1). Daily-integrated downwelling PAR in the lower region of the euphotic zone increased ~2- to 4-fold through the spring and summer relative to the winter (Fig. 1C). Concentrations of NO_3^- + NO_2^- were persistently low in the well-lit upper ocean (<75 m), increasing in the lower euphotic zone where concentrations often co-varied with vertical oscillations in isopycnal surfaces (Fig. 1B). 0-175 m inventories of NO_3^- + NO_2^- were highest in winter and lowest in spring (averaging 57 ± 33 and 18 ± 6 m, respectively; Table 1). Concentrations of TChl *a* were typically maximal in the lower regions of the euphotic zone where the PAR flux decreased to ~1% of the surface irradiance (~0.5-1 mol quanta m^{-2} d^{-1}; Fig. 1C). PPE cell inventories in the 0-175 m of the water column remained relatively stable over time (Table 1).

4.4.2. Alpha and beta diversity

A total of 29,241 distinct picoeukaryotic OTUs were retrieved from high-throughput sequencing of 18S rRNA gene fragments delineated at 97% sequence similarity (Table 2). Each sample contained on average 31,327 sequences, and rarefaction analyses showed saturation of mean species richness at ~25,000 sequences per sample (Fig. S1). Examination of Shannon index across depth bins for the total picoeukaryotes (n = 29,241) revealed that alpha diversity was relatively constant throughout the upper 100 m (increasing slightly in the mid-euphotic zone = 75-100 m), with somewhat lower diversity observed at the deepest depth sampled (175 m; Fig.

2A). For each of the additional OTU categories (Alveolata, Het, and PPE), alpha diversity varied as a result of different number of OTUs in each table (Fig. 2B-D). For example, Alveolata OTUs (n = 14,767) had greater alpha diversity than Het OTUs (n = 3,921) and PPE OTUs (n = 1,610). Within each category, however, Shannon index for the Alveolata OTUs revealed similar alpha diversity patterns as the total picoeukaryote OTUs, with diversity of the Alveolata remaining relatively constant throughout the euphotic zone and decreasing in the lower regions of the upper ocean (150-175 m, Fig. 2B). The Shannon index for the non-alveolate, non-photosynthetic picoeukaryotes (Het OTUs) also demonstrated relatively weak depth-dependence, increasing slightly in waters 75-150 m (Fig. 2C). In contrast, the Shannon index for PPE OTUs was greatest at depths <100 m, decreasing sharply in the lower regions of the euphotic zone (125-175 m; Fig. 2D).

Analyses of beta diversity revealed how absolute shifts in community composition coincided with absolute changes in environmental conditions (Table 3). For example, significant correlations were observed between absolute shifts in species composition and absolute changes in temperature ($Mantel_{samples|temperature}$, Pearson r = 0.67 to 0.73, P = 0.001), σ-t ($Mantel_{samples|\sigma\text{-}t}$, Pearson r = 0.57 to 0.70, P = 0.001), and daily-integrated PAR ($Mantel_{samples|PAR}$, Pearson r = 0.36 to 0.44, P = 0.001; Table 3). Moreover, variations in concentrations of NO_3^- were more strongly correlated with changes in the Alveolata and other non-photosynthetic picoeukaryotes ($Mantel_{samples|NO3^-}$, Pearson r = 0.52 and 0.64, P = 0.001) compared to the PPE ($Mantel_{samples|NO3^-}$, Pearson r = 0.27, P = 0.001). Shifts in species composition were moderately but significantly correlated with changes in PO_4^{3-}, silicic acid, and TChl *a* concentration ($Mantel_{samples|PO4^{3-}, Si, TChl\ a}$, Pearson r = 0.09 to 0.59, P = 0.001; Table 3).

Mantel tests were conducted to examine the extent that variations in photosynthetic pigment concentrations reflected shifts in PPE species composition (Table 3). There was a significant correlation between PPE species composition and 19'-butanoyloxyfucoxanthin (19'-But; $Mantel_{samples|19'\text{-}But}$, Pearson r = 0.34, P = 0.001), a carotenoid synthesized by pelagophytes. Changes in other photosynthetic pigments (fucoxanthin, 19'-hexanoyloxyfucoxanthin, zeaxanthin, and divinyl chlorophyll *a*) often used as diagnostic biomarkers for diatoms, haptophytes, cyanobacteria, and *Prochlorococcus*, respectively, were weakly but significantly correlated with variations in species composition ($Mantel_{samples|other\ pigments}$, Pearson r = 0.03 to 0.10, P = 0.001).

Differences in community composition of PPE OTUs in the upper (<75 m) and lower (100-175 m) regions of the euphotic zone was examined, and revealed to be distinct (PERMANOVA, $P < 0.001$). Seasonal differences in alpha diversity examined for PPE in the upper and lower euphotic zones revealed little to no seasonal variability in the lower euphotic zone (Fig. S2). In contrast, alpha diversity in the upper euphotic zone was lower in winter and spring and highest during fall. Moreover, there were significant seasonal differences in community composition (PERMANOVA, $P < 0.001$). Hierarchical clustering analyses based on the Bray-Curtis dissimilarity index demonstrated compositional similarities within the communities in the upper (<75 m) euphotic zone, as well as within the communities in the lower (100-175 m) euphotic zone, throughout much of the year (Fig. S3). Notably, the depth-dependent partitioning of picoeukaryote communities from samples collected during the spring demonstrated mixing of communities between the upper and lower euphotic zone (Fig. S3).

4.4.3. Vertical and temporal variability in picoeukaryote community composition

Overall, picoeukaryotes at Station ALOHA were dominated by Alveolata (average 58% of total picoeukaryote sequences), followed by Stramenopiles (~10%), Rhizaria (~9%), and Hacrobia (~5%; Table 4). Opisthokonta, Excavata, Archaeplastida, and Amoebozoa/Apusozoa each comprised ≤1% of the relative abundance in the full (0-175 m) euphotic zone. Community composition varied vertically within the euphotic zone, with relative abundances of various taxa differing between the well-lit (<75 m) and dimly lit regions of the euphotic zone (100-175 m; Fig. 3A). For example, the relative abundance of Alveolata OTUs (including Syndiniales, Amoebophora, and Dinophyceae) comprised ~63% of the total sequences in the upper euphotic one (<75 m), decreasing to ~53% in the lower euphotic zone (100-175 m; Table 4). Similarly, Hacrobia (including cryptophytes and haptophytes) decreased in relative abundance between the upper and lower euphotic zone (from ~6% to ~3%), while the relative abundances of Rhizaria (including the radiolaria and foraminifera) increased (from ~3% to ~15%) in the lower regions of the euphotic zone (Fig. 3A). Archaeplastida OTUs (including chlorophytes and rhodophytes) increased ~2-fold in the lower euphotic zone from ~0.4% to ~1%. Relative abundances of the various taxa demonstrated very little temporal variability at this broad taxonomic level (*e.g.*, alveolate taxa comprised between 53% and 61% of the total picoeukaryote sequences throughout the study; Fig. 3B).

The proportions of various Alveolata in its own category displayed remarkable consistency in relative abundance with depth (Fig. 4A, Table 4). On average, 38% of alveolate only sequences were dominated by Syndiniales Group II, a group of uncultured organisms hypothesized to be parasitic (Table 4). In addition, other dominant alveolates included Syndiniales Group I (~25%), Dinophyceae (~13%), and Syndiniales Amoebophora (~13%). Ciliophora and Syndiniales Groups III-V comprised the remaining Alveolata taxa (summing to ~11% of alveolate sequences). Relative abundances of the alveolate taxa appeared stable in time throughout the study. For example, Syndiniales Group II and Dinophyceae comprised 20-25% and 6-11% of the alveolates, respectively (Fig. 4B).

The non-photosynthetic taxa excluding the alveolates (Het OTUs) comprised ~17% of the total picoeukaryote sequences. Relative abundances within this category of non-photosynthetic, non-alveolate taxa were highly variable with depth (Fig. 5, Table 4). Marine stramenopiles MAST-1 to -11 comprised a majority (~53% on average of the non-alveolate, non-photosynthetic sequences) of the non-photosynthetic picoeukaryotes at depths <75 m, with MAST-3 being the most dominant group (averaging ~23%; Fig. 5A, Table 4). Proportions of MAST decreased in the lower euphotic zone to ~21% (on average) of the non-alveolate, non-photosynthetic sequences, while taxa affiliated with Rhizaria (radiolarian and foraminifera) increased from ~17% in waters <75 m to ~58% in the deeper euphotic zone waters (100-175 m; Fig. 5A, Table 4). The groups Excavata, Hacrobia (including Telonema, Centroheliozoa, and Picozoa), choanoflagellates, fungi, and other stramenopiles (including Labyrinthulomycetes, Bicosoecida, Pirsonia, and Peronosporomycetes) averaged ~25% of the non-alveolate, non-photosynthetic picoeukaryotes throughout the upper 175 m water column. Relative abundances of the non-photosynthetic picoeukaryote taxa appeared to be most temporally dynamic during the late summer and early fall months (Fig. 5B).

PPE OTUs comprised ~8% of the total sequences and were highly variable with depth and time (Fig. 6, Table 4). Haptophyta OTUs dominated (averaging 46% of the PPE sequences) in the upper 75 m of the water column, while those classified as Pelagophyceae were the dominant (averaging ~43% of the PPE sequences) PPE OTUs in the deeper waters of the euphotic zone (100-175 m; Fig. 6, Table 4). Members of the Chrysophyceae and Bolidophyceae demonstrated apparent depth-dependence, with elevated relative abundances at depths <100 m of the euphotic zone (Fig. 6, Table 4). Archaeplastida comprised higher proportions (averaging

~14% of the PPE sequences) in the deeper waters of the euphotic zone compared to ~4% in the upper euphotic zone (<75 m; Fig. 6). Relative abundances of the Cryptophyceae remained relatively consistent (averaging ~7% of the PPE sequences) throughout the euphotic zone. Several PPE taxa demonstrated considerable temporal variability. For example, the Pelagophyceae, which were generally observed in low proportions in the upper 75 m, increased in proportion in the late winter and spring months (Fig. 6). Haptophyta OTUs increased in proportion during the summer months in the mid-to lower regions of the euphotic zone (75-100 m; Fig. 6). Archaeplastida increased during the winter and spring months, with relative abundances increasing in the spring and summer in the deeper regions of the euphotic zone (150-175 m).

4.4.4. Most abundant photosynthetic picoeukaryote OTUs

Among the PPE OTUs, the relative abundances of the 100 most abundant OTUs (out of 1,610 total PPE OTUs) accounted for ~92% of the PPE sequences, with the 20 most abundant PPE OTUs comprising ~71% of the PPE sequences. These 20 most abundant PPE OTUs included members of the pelagophytes, dictyochophytes, prymnesiophytes, chrysophytes, chlorophytes, cryptophytes, and bolidophytes (Table 5). An OTU closely related to *Pelagomonas calceolata* (AL-KC001) was the most abundant PPE at Station ALOHA, comprising ~24% of the PPE sequences, followed by an OTU closely related to prymnesiophyte *Coccolithus pelagicus* (AL-AB002; averaging ~11% of PPE sequences) and Mamiellophyceae *Bathycoccus* (AL-FR003; averaging ~5% of PPE sequences; Table 5). Relative abundances (% of the total picoeukaryote sequences) of the 20 most abundant PPE OTUs, sorted vertically by depth, showed that the communities in the upper euphotic zone (<75 m) were considerably different from those in the lower euphotic zone, with 15 out of 20 OTUs being more prevalent in the upper euphotic zone (Fig. 7). Members of prymnesiophytes, chrysophytes, cryptophytes, and dictyochophytes were most abundant in the upper euphotic zone, with the dominant OTU being closely related to the prymnesiophyte *C. pelagicus* (AL-AB002). In contrast, *P. calceolata* (AL-KC001), cryptophyte *Proteomonas* (AL-JF011), Mamiellophyceae *Ostreococcus* and *Bathycoccus* (AL-GQ006 and AL-FR003), and a prymnesiophyte (AL-1473) were all more prevalent in the lower euphotic zone (Fig. 7). Of these taxa, pelagophyte AL-KC001,

Mamiellophyceae AL-FR003, and prymnesiophyte AL-1473 increased in relative abundance during the spring in both the upper and lower euphotic zones (Fig. 7).

We selected 8 of the 20 most abundant PPE OTUs to examine, in detail, vertical and temporal dynamics associated with several classes of PPE in this ecosystem (Table 5, Fig. 8). Stramenopile OTUs closely affiliated with the pelagophyte *P. calceolata* (AL-KC001) and the dictyochophyte *Florenciella* (AL-AB004) were present throughout the year. These OTUs demonstrated different vertical patterns, with *P. calceolata* prominent in the lower regions of the euphotic zone (5-10% of total picoeukaryote sequences; Fig. 8A) and *Florenciella* residing in the upper 100 m of the euphotic zone at an order of magnitude lower relative abundances (0.4-1% of total picoeukaryote sequences; Fig. 8B). Two different Prymnesiophyceae OTUs closely affiliated with *C. pelagicus* (AL-AB002; Fig. 8D) and an uncultured prymnesiophyte (AL-AF009; Fig. 8C) also demonstrated vertically different distributions within the euphotic zone. While *C. pelagicus* was proportionally more abundant in the well-lit upper ocean at ~2-6% of total picoeukaryote sequences, the uncultured prymnesiophyte OTU (AL-AF009) was much less abundant (~0.2-1% of total picoeukaryote sequences) and occurred in the lower euphotic zone. Both OTUs appeared to increase in relative abundance in the spring and summer months. Two different Mamiellophyceae OTUs (AL-FR003 and AL-GQ006, Fig. 8E and G, respectively) were both more prevalent in the deeper regions of the euphotic zone averaging ~1% of the total picoeukaryote sequences, increasing to ~2-4% during various times of the year. Chrysophyceae (AL-235; Fig. 8F) occurred at low relative abundances (~0.2-0.8% of total picoeukaryote sequences) in the upper 50 m and appeared to vary seasonally, with greatest relative abundances observed in the spring (March to May). Relative abundances of Cryptophyceae (AL-2762; Fig. 8H) were also persistently low (0.05-0.25% of total picoeukaryote sequences) and homogenously distributed throughout the euphotic zone, with no apparent seasonal dynamic.

4.5. Discussion

The sequenced 18S rRNA gene fragments collected from euphotic zone plankton assemblages at Station ALOHA revealed vertical and temporal variations in the diversity of major picoeukaryote taxa. OTUs classified as Alveolata dominated (58% on average of the total picoeukaryote sequences) the community, followed by various taxa from other eukaryote supergroups such as Hacrobia, Stramenopiles, and Rhizaria. PPE OTUs comprised 8% (on

average) of total picoeukaryote sequences. While Alveolata community composition remained relatively stable over depth and time, other picoeukaryote taxa were highly dynamic in time and with depth. Comparisons of estimated alpha and beta diversity metrics also revealed distinct shifts in community composition correlated with depth and associated changes in environmental conditions. Moreover, examination of the relative abundances of the 20 most abundant PPE OTUs provided insights into the temporal variations of diverse taxa in both the high-light (but persistently low-nutrient) and the dimly lit (but relatively nutrient-enriched) regions of the euphotic zone. Collectively, our observations revealed distinct depth- and time-dependent variability in the different picoeukaryote OTU categories, suggesting that associated changes in environmental parameters and/or taxa composition strongly dictate the spatial and temporal patterns of picoeukaryote taxa distributions.

Our finding that members of the Alveolata dominated the detected sequences is consistent with several previous studies suggesting that these organisms may have a cosmopolitan distribution in the world's oceans (Guillou et al., 2008; Not et al., 2009; Massana et al., 2011; deVargas et al., 2015). In the current study, the majority of the Alveolata OTUs were classified as Syndiniales Group II, organisms suspected to be parasites of marine plankton, including dinoflagellates (Chambouvet et al., 2008). Syndiniales Group I, which composed ~20-25% of the Alveolata OTUs, are also suspected to be parasitic, infecting diverse hosts including radiolarians, ciliates, and fish (Harada et al., 2007; Chambouvet et al., 2008). Notably, in our study, OTUs affiliated with the Dinophyceae and Ciliophora comprised <20% of the Alveolata sequences, likely reflecting the exclusion of these larger organisms by our sampling methodology of sampling <3 μm plankton size fractions. Relative abundances and alpha diversity of Alveolata OTUs displayed little vertical or temporal variability, making it difficult to discern possible factors regulating these organisms. However, Guillou et al. (2010) reported that dinospores of Syndiniales may be actively grazed by microzooplankton, suggesting that there may be a trophic loss term associated with these populations. Conceptualization of the role of parasitism in the oligotrophic marine food web may include additional pathways of carbon (from small and large eukaryotes) being re-routed into the dissolved organic matter pool, thereby potentially fueling the microbial food web. Although parasitism may promote diversity and further complicates the classic predator-prey roles in the food web, the ecological role of parasitism has yet to be included in biogeochemical and food web models (Guillou et al., 2008; Dunne et al., 2013;

Lima-Mendez, 2015). The relatively consistent vertical and temporal dynamic of the Alveolata that we observed in our study suggests that the unique trophic modes of these picoeukaryotes are likely widespread and important considerations in future studies of euphotic zone plankton community dynamics.

Various studies have suggested that PCR amplification of different variable regions of the 18S rRNA gene may result in preferential amplification of certain taxa (Van de Peer et al., 1997; Stoeck et al., 2010), such as the high representation of Alveolata in the present study and several other studies (Massana, 2011; de Vargas et al., 2015). However, a study examining the barcoded DNA fragments amplified from both the V4 and V9 regions compared to full-length 18S rRNA genes (containing both hypervariable regions) found that Alveolata and close relatives dominated sequence reads irrespective of the region amplified (Stoeck et al., 2010). Furthermore, a study comparing 18S rRNA genes derived from metagenomic sequencing (a PCR-independent approach) to those derived based on PCR amplification and sequencing found no major biases in the diversity of taxa introduced via the PCR-based approach (Not et al., 2009). In addition to biases related to the variable regions, the notably high representation of Alveolata in the current and previous 18S rDNA studies may reflect high rDNA copy numbers known to occur in various members of the Alveolata (Zhu et al., 2005; Not et al., 2009; Medinger et al., 2010).

In the current study, we evaluated the diversity of presumed non-alveolate, non-photosynthetic taxa (Het OTUs) by excluding the alveolates. By analyzing these groups separately, we were able to detect large depth-dependent changes in the relative abundances of the presumed non-photosynthetic picoeukaryotes. The well-lit regions of the euphotic zone were dominated by several members of MAST groups, including MAST-1 and MAST-3. In comparison, a study of picoeukaryote diversity in the oligotrophic Northeastern Red Sea found that MAST groups accounted for ~10% of the sequences derived from 18S rRNA gene clone libraries (Acosta et al., 2013), similar to the proportions of these groups in our study. MAST groups are known bacterivores and have been reported to regulate *Synechococcus* population size (Dasilva et al., 2013). Members of MAST groups have also been observed to graze on eukaryotic picophytoplankton such as *Micromonas pusilla* and *Ostreococcus* (Massana et al., 2009). MAST-3, the dominant group found in our study, has been reported to be the most abundant of the MAST clades globally (Gómez et al., 2011; Logares et al., 2012), consistent with their potential role as grazers of photosynthetic picoplankton. In such ways, MAST groups appear to have a

significant impact as top-down control of ecologically important picophytoplankton communities.

Observations of the PPE OTUs in our study suggested strong vertical structuring of the PPE community, including distinct assemblages of organisms dwelling in the upper compared to lower regions of the euphotic zone. Prymnesiophyceae were amongst the most dominant PPE groups in the upper euphotic zone, with smaller contributions by Dictyochophyceae, Bolidophyceae, Cryptophyceae, and Chrysophyceae. Furthermore, Prymnesiophyceae (7 OTUs) and Chrysophyceae (5 OTUs) were highly represented among the 20 most abundant PPE OTUs, averaging ~71% of the total PPE sequences. Previous studies at Station ALOHA, based on phytoplankton pigment analyses, identified prymnesiophytes as important contributors to phytoplankton biomass in this ecosystem (Letelier et al., 1993; Bidigare and Ondrusek, 1996; Mackey et al., 2002). Moreover, both prymnesiophytes (Moon-van der Staay et al., 2000; Liu et al., 2009; Cuvelier et al., 2010) and chrysophytes (Fuller et al., 2006; Massana et al., 2011; Rii et al., 2016) have previously been reported to be diverse, broadly distributed groups of organisms, including many uncultivated phylotypes. The apparent dominance of prymnesiophytes and chrysophytes in diverse ocean environments has been attributed to their potentially mixotrophic physiologies (Zubkov and Tarran, 2008; Hartmann et al., 2012). In fact, 15 out of the 20 most abundant OTUs were classified as taxa that have been previously reported as mixotrophic, and a large fraction of these taxa were prevalent in the upper euphotic zone. For example, both cryptophytes (Jones, 2000) and dictyochophytes are known to be capable of mixotrophy; in particular, dictyochophyte *Florenciella*, which was the fifth most abundant PPE OTU, has been reported to be an active grazer of picocyanobacteria, especially *Prochlorococcus* (Frias-Lopez et al., 2009). As such, mixotrophy by these organisms would likely confer competitive advantages in the nutrient-deprived upper ocean waters at Station ALOHA, with predation serving as a means to acquire nutrients (Caron, 2000). Phagotrophic predation by mixotrophic and heterotrophic picoeukaryotes can be a significant source of mortality for suspended bacteria (Arenovski et al., 1995; Sherr and Sherr, 2002); for example, in surface waters of the tropical Northeast Atlantic Ocean, small (<5 μm) phytoplankton were responsible for 37-70% of measured rates of bacterivory (Zubkov and Tarran, 2008). Hence, picoeukaryotes appear to be important consumers of picocyanobacteria, the dominant phytoplankton in subtropical ocean

gyres, but likely also constitute a significant food source for higher trophic levels and may be important suppliers of regenerated nutrients to the upper ocean (Sherr and Sherr, 2002).

Relative abundances of PPE OTUs in the deeper waters of the euphotic zone were dominated by Pelagophyceae, with smaller contributions from Mamiellophyceae and Prymnesiophyceae. These taxa were largely confined to the deep chlorophyll maximum, a region where light decreases to <1% of the surface flux and experiences light-driven seasonal changes in concentrations of inorganic nutrients (Letelier et al. 2004). The dominant PPE OTU (AL-KC001) in our study classified with *P. calceolata*, which has previously been reported as a low-light adapted picoplankton abundant in the deep chlorophyll maximum (Timmermans et al., 2005, Dupont et al., 2014) and whose transcriptional patterns revealed elevated expression of nitrate transporter genes, suggesting these organisms rely heavily on nitrate assimilation for nutritional demands (Dupont et al., 2014). Concentrations of 19'-butanoyloxyfucoxanthin, carotenoid pigment diagnostic of pelagophytes, often appear maximal in the lower euphotic zone at Station ALOHA (Letelier et al., 1993; Andersen et al., 1996; Bidigare and Ondrusek, 1996). Several Mamiellophyceae clades are also known to reside in high nutrient regions and have been observed in high abundances in the lower euphotic zone (Demir-Hilton et al., 2011). These observations, combined with lower alpha diversity of the PPE OTUs in the lower euphotic zone, indicate that the lower euphotic zone is comprised of specialist PPE taxa that are best adapted to growth in low-light, high-nutrient regions.

The near-monthly sampling frequency in the current study provided insight into seasonal-scale variability of some of the major taxa in the upper and lower euphotic zones of this ecosystem. Both Prymnesiophyceae *C. pelagicus* (AL-AB002), the dominant OTU in the upper euphotic zone, and Chrysophyceae (AL-235), which occurred at much lower relative abundances, demonstrated apparent seasonal variability, increasing ~6- to 8-fold in relative abundance from late winter through summer (January to September). While Prymnesiophyceae AL-AB002 appeared prevalent throughout the upper ~100 m, Chrysophyceae AL-235 were largely confined to the mixed layer. Moreover, Dictyochophyceae *Florenciella* (AL-AB004), Cryptophyceae (AL-2767), and Bolidophyceae (AL-KC005) all appeared to be prevalent throughout the upper 150 m at low relative abundances. In the lower euphotic zone, three primary members of the PPE showed notable seasonal changes in their relative abundances. Pelagophyceae *P. calceolata* (AL-KC001) was the dominant OTU throughout the year; however,

P. calceolata increased in relative abundance during the late winter to early spring, coincident with an upward shift in the distributions of these organisms, perhaps associated with entrainment due to deep mixing during this period. Relative abundances of *P. calceolata* remained elevated in the upper euphotic zone throughout the spring, decreasing as the water warmed and stratified in the summer months. Similar temporal dynamics were observed for Prymnesiophyceae AL-AF009, which increased ~5-fold coincident with winter and spring mixing, persisting until early summer. Mamiellophyceae *Bathycoccus* (AL-FR003) appeared relatively abundant (~1-2.5%) throughout the year in the deeper euphotic zone, but was also shifted upwards in the water column (into 25-100 m) during the spring months. *Ostreococcus* (AL-GQ006) was low in relative abundance throughout the year, but increased to ~1-4% in the summer (May to August) while remaining at depth (100-150 m). The increase in *Ostreococcus* relative abundance persisted until fall, indicating a possible succession of species in the lower euphotic zone.

Collectively, these results reveal a highly diverse and temporally dynamic upper euphotic zone community of PPE including dictyochophytes, cryptophytes, and bolidophytes, with seasonal variance of specific prymnesiophytes and chrysophytes from January to August. The increase in specific taxa in the upper euphotic zone may reflect seasonal increases in the daily flux of light to the upper ocean between winter and spring months. In fact, we suggest that the temporal variability of these organisms in the upper euphotic zone is influenced by light availability. On the other hand, the appearance of pelagophytes, prymnesiophytes, and *Bathycoccus* (all taxa dominant in the lower euphotic zone) in the upper euphotic zone specific to late winter and early spring months was likely due to deep mixing resulting in the redistribution of organisms upward into regions of higher light, and subsequent growth. This mixing of communities was also evident in the examination of compositional similarity of PPE communities, which showed distinct clustering between the upper and lower euphotic zones except during spring. Our results suggest that these lower euphotic zone taxa are growing and persisting in the upper euphotic zone after being physically mixed upwards. Rapid adaptations to variable light conditions, such as *P. calceolata*'s capability for xanthophyll cycling (Dimier et al., 2009; Bidigare et al., 2014), as well as the increased supply of nutrients entrained from the lower euphotic zone, likely aided the proliferation of these organisms in the upper euphotic zone. By May, when mixed layer depths have shoaled and the nutrient supply has likely decreased, Pelagophyceae and Mamiellophyceae were relegated to the low-light, nutrient-enriched regions

of the lower euphotic zone. If vertical mixing was the only mechanism responsible for their appearance in the upper euphotic zone, other lower euphotic zone taxa (*e.g.*, cryptophytes) would appear in the upper euphotic zone as well, and taxa typically residing in the upper euphotic zone would also be mixed deeper into the lower euphotic zone. The absence of these other taxa, we well as the stability of alpha diversity metrics in both the upper and lower euphotic zone during the winter and spring, suggest that *P. calceolata*, *Bathycoccus*, and Prymnesiophyceae (AL-1473) are mixed upwards into regions of higher light and persisting on a seasonal scale at Station ALOHA.

In contrast to the upper euphotic zone, the lower euphotic zone appears to be less dynamic and diverse than the upper euphotic zone, supporting the same group of taxa throughout the year with only a few specific taxa undergoing seasonal-scale changes in relative abundances. Such seasonal variability in the lower euphotic zone may be linked to the progressive increase in solar irradiance occurring throughout the spring (Letelier et al., 2004). Temporal dynamics of specific PPE OTUs, like the ones we observed, provide insight into the environmental controls of these organisms, their nutrient acquisition capabilities, and further understanding of successive processes within the food web.

Oligotrophic ocean ecosystems appear to support greater diversity of plankton compared to more nutrient-enriched waters (Hulburt, 1963; Longhurst, 1967; McGowan & Walker, 1985), and several theories have been proposed to explain the differential diversity, such as selective removal processes and niche differentiation (Longhurst, 1967; Timonin, 1969). High diversity of PPE OTUs in the well-lit upper ocean may be promoted by the persistent scarcity of inorganic nutrients, resulting in the proliferation of diverse populations capable of mixotrophic capabilities. Such intense competition for nutrients may promote niche differentiation, thereby increasing diversity (Hutchinson, 1961), such as during the fall for PPE in the upper euphotic zone. In turn, lower alpha diversity of PPE observed in the deeper euphotic zone may reflect the selective pressures imposed by the episodic interaction of nutrient and light gradients in this region of the water column, winnowing down diversity to those organisms best adapted to capitalize on variability in growth-requiring resources (Hardin, 1960). Thus, our results suggest that in this persistently oligotrophic system, competition for nutrients promotes diversity to a greater extent than competition for light. In addition, removal processes promoting higher turnover of species

are important considerations that likely aids in maintaining elevated diversity in the upper euphotic zone.

We hypothesized various mechanisms driving the diversity of PPE in the upper and lower regions of the euphotic zone, contributed by limitations in light and nutrients, high growth rates, and frequency of removal processes. The Intermediate Disturbance Hypothesis states that high diversity is maintained at intermediate frequencies of disturbances caused by non-uniform distributions of organisms or by external physical processes (winter mixing and subsequent stratification in the upper waters), halting successional processes that would typically result in the exclusion of the 'best fit' (Richerson et al., 1970; Connell, 1978; Flöder and Sommer, 1999). Since the upper ocean undergoes moderate seasonal changes in nutrients and temperatures in comparison to greater seasonal changes in the lower euphotic zone, it may be possible that disturbances occur at relatively 'intermediate' frequencies in the upper ocean, promoting greater diversity. Moreover, it may be likely that the frequency of disturbances in the lower euphotic zone (e.g., internal wave forcing at diurnal scales or eddy forcing at monthly scales) is high, thereby reducing diversity throughout the year. As the Intermediate Disturbance Hypothesis rests on the balance between net growth (turnover) and frequency and/or intensity of the disturbance, perhaps the rapid response of PPE (their high growth rates) to 'high frequency' perturbations in the lower euphotic zone results in competitive exclusion, while the stable, nutrient-limited upper ocean leaves the community in a state of constant competition for growth-limiting nutrients, resulting in niche expansion and divergence into many species using distinct resources.

In summary, picoeukaryotes at Station ALOHA were found to be highly diverse, including known phototrophs and presumed mixotrophs, parasites, and heterotrophs. While Alveolata, which dominated the picoeukaryotes, exhibited minimal depth and temporal variability, members of other picoeukaryotes were highly variable over depth and time. The highly stable temporal and vertical dynamic of alveolates suggest that their unique trophic mode, parasitism, may be ubiquitous and an important consideration in our planktonic food web at Station ALOHA. In addition, the highly depth-variable distributions of Rhizaria and MAST communities indicate that there may be taxa-specific interactions that are of significant top-down control for cyanobacteria and PPE. Finally, the PPE community at Station ALOHA was vertically differentiated, as reflected by clear depth-dependent differences in the relative abundances of PPE taxa, with greater diversity in the high-light, low-nutrient regions of the

euphotic zone. We also observed seasonally dependent changes in the PPE community composition, providing insight into the types of taxa that dominate various regions of the euphotic zone at Station ALOHA at different times of the year. The prevalence of presumed mixotrophic PPE taxa in the high-light region (throughout most of the year) points to the importance of alternative modes of nutrient acquisition in low-nutrient environments, thus indicating that future studies examining the impact of mixotrophy in carbon cycling are needed. With the use of high-throughput sequencing, we were able to examine broad-scale patterns of total and detailed groups of picoeukaryote taxa at Station ALOHA, providing insight into potential pathways of the flux of energy and matter in the euphotic zone of the oligotrophic NPSG.

4.6. Acknowledgments

We acknowledge the HOT program science team for the collection and analyses of various data used in this study. Thanks also to Brianne Maillot for laboratory assistance, to Christine Shulse and Sean Jungbluth for support and advice on Illumina data analyses, and to Edward DeLong and John Eppley for computer server access and support. We also acknowledge Ramiro Logares for running our sequences through his UPARSE pipeline for data comparison. Finally, thanks to the captains and crew of R/V *Kilo Moana* and R/V *Ka'imikai-O-Kanaloa* (University of Hawai'i) and R/V *Thomas G. Thompson* (University of Washington). Support for this work derived from U.S. National Science Foundation (NSF) grants OCE-1241263 and OCE-1260164 (MJC), C-MORE (EF-0424599), the Simons Collaboration on Ocean Processes and Ecology (SCOPE), the University of Hawai'i Denise B. Evans Research Fellowship in Oceanography (YMR).

4.7. References

Acosta F, Ngugi DK, Stingl U. (2013). Diversity of picoeukaryotes at an oligotrophic site off the Northeastern Red Sea Coast. *Aquat Biosyst* **9**: 16. doi:10.1186/2046-9063-9-16.

Amaral-Zettler LA, McCliment EA, Ducklow HW, Huse SM. (2009). A method for studying protistan diversity using massively parallel sequencing of V9 hypervariable regions of small-subunit ribosomal RNA genes. *PLoS ONE* **4**: e6372.

Andersen RA, Bidigare RR, Keller MD, Latasa M. (1996). A comparison of HPLC pigment signatures and electron microscopic observations for oligotrophic waters of the North Atlantic and Pacific Oceans. *Deep-Sea Res II* **43**: 517-537.

Arenovski AL, Lim, EL, Caron DA. (1995). Mixotrophic nanoplankton in oligotrophic surface waters of the Sargasso Sea may employ phagotrophy to obtain major nutrients. *J Plankton Res* **17**: 801-820.

Baldauf S. (2003). The deep roots of eukaryotes. *Science* **300**: 1703-1706.

Bidigare RR, Buttler FR, Christensen SJ, Barone B, Karl DM, Wilson ST. (2014). Evaluation of the utility of xanthophyll cycle pigment dynamics for assessing upper ocean mixing processes at Station ALOHA. *J Plankton Res.* doi:10.1093/plankt/fbu069.

Bidigare RR, Ondrusek ME. (1996). Spatial and temporal variability of phytoplankton pigment distributions in the central equatorial Pacific Ocean. *Deep-Sea Res Pt II* **43**: 809-833.

Bidigare RR, Van Heukelem L, Trees CC. (2005). Analysis of algal pigments by high-performance liquid chromatography. In: Andersen RA [ed.], Algal Culturing Techniques, Academic Press: New York, p. 327-345.

Campbell L, Liu H, Nolla HA, Vaulot D. (1997). Annual variability of phytoplankton and bacteria in the subtropical North Pacific Ocean at Station ALOHA during the 1991-1994 ENSO event. *Deep-Sea Res Pt I* **44**: 167-192.

Campbell L, Nolla HA, Vaulot D. (1994). The importance of *Prochlorococcus* to community structure in the central North Pacific Ocean. *Limnol Oceanogr* **39**: 954–961.

Caporaso JG, Bittinger K, Bushman F, DeSantis TZ, Andersen GL, Knight R. (2010a). PyNAST: a flexible tool for aligning sequences to a template alignment. *Bioinformatics* **26**: 266-267.

Caporaso JG, Kuczynski J, Stombaugh J, Bittinger K, Bushman FD, Costello EK et al. (2010b). QIIME allows analysis of high-throughput community sequencing data. *Nat Methods* **7**: 335-336.

Caron DA. (2000). Symbiosis and mixotrophy among pelagic microorganisms. In: Kirchman DL [ed.], Microbial Ecology of the Oceans, Wiley: Hoboken, p. 495-523

Caron DA, Worden AZ, Countway PD, Demir E, Heidelberg KB. (2009). Protists are microbes too: a perspective. *ISME J* **3**: 4-12.

Chambouvet A, Morin P, Marie D, Guillou L. (2008). Control of toxic marine dinoflagellate blooms by serial parasitic killers. *Science* **322**: 1254-1257.

Connell JH. (1978). Diversity in tropical rain forests and coral reefs. *Science **199***: 1302-1310.

Corno G, Letelier RM, Abbott MR, Karl DM. (2008). Temporal and vertical variability in photosynthesis in the North Pacific Subtropical Gyre. *Limnol Oceanogr* **53**: 1252-1265.

Cuvelier ML, Allen AE, Monier A, McCrow JP, Messié M, Tringe SG et al. (2010). Targeted metagenomics and ecology of globally important uncultured eukaryotic phytoplankton. *Proc Natl Acad Sci USA* 107, 14679–14684. doi:10.1073/pnas.1001665107.

Dasilva CR, Li WKW, Lovejoy C. (2013). Phylogenetic diversity of eukaryotic marine microbial plankton on the Scotian Shelf Northwestern Atlantic Ocean. *J Plankton Res* doi:10.1093/plankt/fbt123.

Demir-Hilton E, Sudek S, Cuvelier ML, Gentemann CL, Zehr JP, Worden AZ (2011). Global distribution patterns of distinct clades of the photosynthetic picoeukaryote *Ostreococcus*. *ISME J* **5**: 1095-1107. doi:10.1038/ismej.2010.209.

de Vargas C, Audic S, Henry N, Decelle J, Mahé F, Logares R et al. (2015). Eukaryotic plankton diversity in the sunlit ocean. *Science* **348**: 1261605. doi:10.1126/science.1261605.

Diez B, Pedros-Alio C, Massana R. (2001). Study of genetic diversity of eukaryotic picoplankton in different oceanic regions by small-subunit rRNA gene cloning and sequencing. *Appl Environ Microbiol* **67**: 2932-2941.

Dimier C, Brunet C, Geider R, Raven J (2009). Growth and photoregulation dynamics of the picoeukaryote *Pelagomonas calceolata* in fluctuating light. *Limnol Oceanogr* **54**: 823-836.

Dore, JE, Karl DM. (1996). Nitrification in the euphotic zone as a source for nitrite, nitrate, and nitrous oxide at Station ALOHA. *Limnol Oceanogr* **41**: 1619-1628.

Dunne JA, Lafferty KD, Dobson AP, Hechinger RF, Kuris AM, Martinez ND et al. (2013). Parasites affect food web structure primarily through increased diversity and complexity. *PLoS Biol* **11**: e1001579. doi:10.1371/journal.pbio.1001579

DuPont CL, McCrow JP, Valas R, Moustafa A, Walworth N, Goodenough U, et al. (2014). Genomes and gene expression across light and productivity gradients in eastern subtropical Pacific microbial communities. *ISME J* **9**: 1076-1092. doi:10.1038/ismej.2014.198.

Edgar RC, Haas BJ, Clemente JC, Quince C, Knight R. (2011). UCHIME improves sensitivity and speed of chimera detection. *Bioinformatics* **27**: 2194-2200.

Flöder S, Sommer U. (1999). Diversity in planktonic communities: an experimental test of the intermediate disturbance hypothesis. *Limnol Oceanogr* **44**: 1114-1119.

Fouilland E, Descolas-Gros C, Courties C, Collos Y, Vaquer A, Gasc A. (2004). Productivity and growth of a natural population of the smallest free-living eukaryote under nitrogen deficiency and sufficiency. *Microb Ecol* **48**: 103-110.

Frias-Lopez J, Thompson A, Waldbauer J, Chisholm SW. (2009). Use of stable isotope-labelled cells to identify active grazers of picocyanobacteria in ocean surface waters. *Environ Microbiol* **11**: 512-525.

Fuller NJ, Pitt FD, Le Gall F, Vaulot D, Scanlan DJ. (2006). Analysis of photosynthetic picoeukaryote diversity at open ocean sites in the Arabian Sea using a PCR biased towards marine algal plastids. *Aquat Microb Ecol* **43**: 79-93. doi:10.3354/ame043079.

Garside C. (1982). A chemiluminescent technique for the determination of nanomolar concentrations of nitrate and nitrite in seawater. *Mar Chem* **11**: 159-167.

Gómez F, Moreira D, Benzerara K, López-García P. (2011). *Solenicola setigera* is the first characterized member of the abundant and cosmopolitan uncultured marine stramenopile group MAST-3. *Environ Microbiol* **13**: 193-202.

Guillou L, Alves-de-Souza C, Siano R, Gonzalez H. (2010). The ecological significance of small, eukaryotic parasites in marine ecosystems. *Microbiology Today* 92-95.

Guillou L, Bachar D, Audic S, Bass D, Berney C, Bittner L et al. (2012). The Protist Ribosomal Reference database (PR2): a catalog of unicellular eukaryote small subunit rRNA sequences with curated taxonomy. *Nucleic Acids Res* **41**: D597–D604. doi:10.1093/nar/gks1160.

Guillou L, Viprey M, Chambouvet A, Welsh RM, Kirkham AR, Massana R et al. (2008). Widespread occurrence and genetic diversity of marine parasitoids belonging to Syndiniales (Alveolata). *Environ Microbiol* **10**: 3349-3365.

Harada A, Ohtsuka S, Horiguchi T. (2007). Species of the parasitic genus *Duboscquella* are members of the enigmatic Marine Alveolate Group I. *Protist* **158**: 337-347.

Hardin G. (1960). The competitive exclusion principle. *Science* **131**: 1292-1297.

Hartmann M, Grob C, Tarran GA, Martin AP, Burkill PH, Scanlan DJ et al. (2012). Mixotrophic basis of Atlantic oligotrophic ecosystems. *Proc Nat Acad Sci USA* **109**: 5756-5760.

Hulburt EM. (1963). The diversity of phytoplanktonic populations in oceanic, coastal, and estuarine regions. *J Mar Res* **21**: 81-93.

Hutchinson E. (1961). The paradox of the plankton. *Am Nat* **95**: 137-145.

Jardillier L, Zubkov MV, Pearman J, Scanlan DJ. (2010). Significant CO_2 fixation by small prymnesiophytes in the subtropical and tropical northeast Atlantic Ocean. *ISME J* **4**: 1180-1192.

Jones RI. (2000). Mixotrophy in planktonic protists: an overview. *Freshwater Biol* **45**: 219-226.

Karl DM. (2002). Nutrient dynamics in the deep blue sea. *Trends Microbiol* **10**: 410-418.

Karl DM, Church MJ. (2014). Microbial oceanography and the Hawaii Ocean Time-series programme. *Nat Rev Microbiol* **12**: 699-713.

Karl DM, Lukas R. (1996). The Hawaii Ocean Time-series (HOT) program: Background, rationale and field implementation. *Deep-Sea Res Pt II* **43**: 129-156.

Karl DM, Tien G. (1992). MAGIC: A sensitive and precise method for measuring dissolved phosphorus in aquatic environments. *Limnol Oceanogr* **37**: 105-116.

Kirkham AR, Lepère C, Jardillier LE, Not F, Bouman H, Mead A et al. (2013). A global perspective on marine photosynthetic picoeukaryote community structure. *ISME J* **7**: 922-936. doi:10.1038/ismej.2012.166.

Kunin V, Engelbrektson A, Ochman H, Hugenholtz P. (2010). Wrinkles in the rare biosphere: pyrosequencing errors can lead to artificial inflation of diversity estimates. *Environ Microbiol* **12**: 118-123.

Lane DJ. (1991).16S/23S rRNA sequencing. In: Stackebrandt E, Goodfellow M [eds.] Nucleic Acid Technologies in Bacterial Systematics, Wiley: New York, p. 115-175.

Letelier RM, Bidigare RR, Hebel DV, Ondrusek M, Winn CD, Karl DM. (1993). Temporal variability of phytoplankton community structure based on pigment analysis. *Limnol Oceanogr* **38**: 1420-1437.

Letelier RM, Karl DM, Abbott MR, Bidigare RR. (2004). Light driven seasonal patterns of chlorophyll and nitrate in the lower euphotic zone of the North Pacific Subtropical Gyre. *Limnol Oceanogr* **49**: 508-519.

Li WKW. (1994). Primary production of prochlorophytes, cyanobacteria, and eukaryotic ultraphytoplankton - measurements from flow cytometric sorting. *Limnol Oceanogr* **39**: 169-175.

Lima-Mendez G, Faust K, Henry N, Decelle J, Colin S, Carcillo F et al. (2015). Determinants of community structure in the global plankton interactome. *Science* **348**. Doi:10.1126/science.1262073.

Liu H, Probert I, Uitz J, Claustre H, Aris-Brosou S, Frada M et al. (2009). Extreme diversity in noncalcifying haptophytes explains a major pigment paradox in open oceans. *Proc Natl Acad Sci USA* **106**: 12803-12808.

Logares R, Audic S, Santini S, Pernice MC, de Vargas C, Massana R. (2012). Diversity patterns and activity of uncultured marine heterotrophic flagellates unveiled with pyrosequencing. *ISME J* **6**: 1823-1833.

Longhurst AR. (1967). Diversity and trophic structure of zooplankton communities in the California Current. *Deep-Sea Res Oceanographic Abstracts* **14**: 393-408.

Mackey DJ, Blanchot J, Higgins HW, Neveux J. (2002). Phytoplankton abundances and community structure in the equatorial Pacific. *Deep-Sea Res Pt II* **49**: 2561-2582.

Mahaffey C, Björkman KM, Karl DM. (2012). Phytoplankton response to deep seawater nutrient addition in the North Pacific Subtropical Gyre. *Mar Ecol Prog Ser* **460**: 13-34. doi:10.3354/meps09699.

Massana R. 2011. Eukaryotic picoplankton in surface oceans. *Annu Rev Microbiol* **65**: 91-110.

Massana R, Pernice M, Bunge JA, del Campo J. (2011). Sequence diversity and novelty of natural assemblages of picoeukaryotes from the Indian Ocean. *ISME J* **5**: 184-195.

Massana R, Unrein F, Rodríguez-Martínez R, Forn I, Lefort T, Pinhassi J et al. (2009). Grazing rates and functional diversity of uncultured heterotrophic flagellates. *ISME J* **3**: 588-596.

McAndrew PM, Björkman KM, Church MJ, Morris PJ, Jachowski N, le B Williams PJ et al. (2007). Metabolic response of oligotrophic plankton communities to deep water nutrient enrichment. *Mar Ecol Prog Ser* **332**: 63-75.

McGowan JA, Walker PW. (1985). Dominance and diversity maintenance in an oceanic ecosystem. *Ecol Monogr* **55:** 103-118.

Medinger R, Nolte V, Pandey RV, Jost S, Ottenwälder B, Schlötterer C et al. (2010). Diversity in a hidden world: potential and limitation of next-generation sequencing for surveys of molecular diversity of eukaryotic microorganisms. *Mol Ecol* **19**: 32-40.

Medlin L, Elwood HJ, Stickel S, Sogin ML. (1988). The characterization of enzymatically amplified eukaryotic 16S-like rRNA-coding regions. *Gene* **71**: 491-499.

Moon-van der Staay SY, van der Staay GWMG, Guillou L, Vaulot D, Claustre H, Medlin LK. (2000). Abundance and diversity of prymnesiophytes in the picoplankton community from the equatorial Pacific Ocean inferred from 18S rDNA sequences. *Limnol Oceanogr* **45**: 98-109.

Moon-van der Staay SY, Watcher RD, Vaulot D. (2001). Oceanic 18S rDNA sequences from picoplankton reveal unsuspected eukaryotic diversity. *Nature*. **409**: 607-610.

Not F, Balagué V, de Vargas C, Massana R. (2009). New insights into the diversity of marine picoeukaryotes. *PLoS ONE* **4** e7143. doi:10.1371/journal.pone.0007143.t001.

Not F, Siano R, Kooistra WHCF, Simon N, Vaulot D, Probert I. (2012). Diversity and ecology of eukaryotic marine phytoplankton. *Adv Bot Res* **64**: 1-53.

Oksanen J, Blanchet FG, Kindt R, Legendre P, Minchin PR, O'Hara RB et al. (2013). Package 'vegan': community ecology package. R package version 2.0-10. http://cran.r-project.org/web/packages/vegan/.

Paerl RW, Foster RA, Jenkins BD, Montoya JP, Zehr JP. (2008). Phylogenetic diversity of cyanobacterial *narB* genes from various marine habitats. *Environ Microbiol* **10**: 3377-3387. doi:10.1111/j.1462-2920.2008.01741.x.

Pasulka AL, Landry MR, Taniguchi DA, Taylor AG, Church MJ. (2013). Temporal dynamics of phytoplankton and heterotrophic protists at station ALOHA. *Deep-Sea Res Pt II* **93**: 44-57.

Quast C, Pruesse E, Yilmaz P, Gerken J, Schweer T, Yarza P et al. (2013). The SILVA ribosomal RNA gene database project: improved data processing and web-based tools. *Nucl Acids Res* **41**: D590-D596.

R Core Development Team. (2014). R: A Language and Environment for Statistical Computing. https://cran.r-project.org/.

Richerson P, Armstrong R, Goldman CR. (1970). Contemporaneous disequilibrium, a new hypothesis to explain the "Paradox of the Plankton." *Proc Natl Acad Sci*, **67**: 1710-1714.

Rii YM, Duhamel S, Bidigare RR, Karl DM, Repeta DJ, Church MJ. (2016). Diversity and productivity of photosynthetic picoeukaryotes in biogeochemically distinct regions of the South East Pacific Ocean. *Limnol Oceanogr* doi:10.1002/lno.10255.

Rodriguez F, Derelle E, Guillou L, Le Gall F, Vaulot D, Moreau H. (2005). Ecotype diversity in the marine picoeukaryote *Ostreococcus* (Chlorophyta, Prasinophyceae). *Environ Microbiol* **7**: 853-859.

Rusch DB, Halpern AL, Sutton G, Heidelberg KB, Williamson S, Yooseph S et al. (2007). The Sorcerer II global ocean sampling expedition: northwest Atlantic through eastern tropical Pacific. *PLoS Biol* **5**: e77. doi:10.1371/journal.pbio.0050077

Sherr EB, Sherr BF. (2002). Significance of predation by protists in aquatic microbial food webs. *Anton Leeuw* **81**: 293-308. doi:10.1023/A:1020591307260.

Shi XL, Marie D, Jardillier L, Scanlan DJ, Vaulot D. (2009). Groups without cultured representatives dominate eukaryotic picophytoplankton in the oligotrophic South East Pacific Ocean. *PLoS ONE* **4**: e7657.

Sieburth JM, Smetacek V, Lenz J. (1978). Pelagic ecosystem structure: Heterotrophic compartments of the plankton and their relationship to plankton size fractions. *Limnol Oceanogr* **23**: 1256-1263.

Stockner JG. (1988). Phototrophic picoplankton: an overview from marine and freshwater ecosystems. *Limnol Oceanogr* **33**: 765-775.

Stoeck T, Bass D, Nebel M, Christen R, Jones MDM, Breiner HW, Richards TA. (2010). Multiple marker parallel tag environmental DNA sequencing reveals a highly complex eukaryotic community in marine anoxic water. *Mol Ecol* **19**: 21–31.

Suzuki R, Shimodaira H. (2006). Pvclust: an R package for assessing the uncertainty in hierarchical clustering. *Bioinformatics* **22**: 1540-1542.

Thompson JD, Higgins DG, Gibson TJ. (1994). ClustalW: Improving the sensitivity of progressive multiple sequence alignment through sequence weighting, position-specific gap penalties and weight matrix choice. *Nucl Acids Res* **22**: 4673-4680.

Timmermans KR, Van der Wagt B, Veldhuis MJW, Maatman A, De Baar HJW. (2005). Physiological responses of three species of marine pico-phytoplankton to ammonium, phosphate, iron and light limitation. *J Sea Res* **53**: 109-120.

Timonin AG. (1969). Structure of pelagic associations – quantitative relationship between different trophic groups of plankton in frontal zones of tropical ocean. *Oceanology-USSR* **9**: 686.

Treusch AH, Demir-Hilton E, Vergin KL, Worden AZ, Carlson CA, Donatz MG et al. (2011). Phytoplankton distribution patterns in the northwestern Sargasso Sea revealed by small subunit rRNA genes from plastids. *ISME J* **6**: 481-492. doi:10.1038/ismej.2011.117.

Van de Peer Y, Jansen J, De Rijk P, De Wachter R. (1997). Database on the structure of small ribosomal subunit RNA. *Nucl Acids Res* **25**: 111-116.

Vaulot D, Eikrem W, Viprey M, Moreau H. (2008). The diversity of small eukaryotic phytoplankton (≤3 μm) in marine ecosystems. *FEMS Microbiol Rev* **32**: 795-820.

Wickham H. (2009). ggplot2: Elegant graphics for data analysis. Springer: New York. doi:10.1007/978-0-387-98141-3.

Worden A, Nolan J, Palenik B. (2004). Assessing the dynamics and ecology of marine picophytoplankton: The importance of the eukaryotic component. *Limnol Oceanogr* **49**: 168-179.

Worden AZ, Not F. (2008). Ecology and diversity of picoeukaryotes. In: Kirchman DL [ed.], Microbial Ecology of the Oceans, John Wiley & Sons, Inc., New York, p.159-205.

Zhang J, Kobert K, Flouri T, Stamatakis A. (2014). PEAR: a fast and accurate Illumina Paired-End reAd mergeR. *Bioinformatics* **30**: 614-620. doi:10.1093/bioinformatics/btt593.

Zhu F, Massana R, Not F, Marie D, Vaulot D. (2005). Mapping of picoeukaryotes in marine ecosystems with quantitative PCR of the 18S rRNA gene. *FEMS Microbiol Ecol* **52**: 79-92.

Zubkov MV, Tarran GA. (2008). High bacterivory by the smallest phytoplankton in the North Atlantic Ocean. *Nature* **455**: 224-226.

Table 4.1. Sampling dates and biogeochemical properties

Cruise	Date	Season*	Mixed Layer Depth (m)	Surface PAR (mol quanta m^{-2} d^{-1})	Nitrate + Nitrite† (mmol N m^{-2})	PPE† (x10^{11} cells m^{-2})
H230	28 Feb 2011	Winter	40 ± 18‡	34.5	94.1	2.04
H233	19 Jul 2011	Summer	78 ± 9	44.1	25.9	1.85
H234	31 Aug 2011	Summer	48 ± 10	41.7	77.0	1.19
H235	27 Sep 2011	Fall	35 ± 13	36.3	52.2	1.41
H236	4 Nov 2011	Fall	57 ± 9	n/a§	90.2	2.28
H239	18 Jan 2012	Winter	98 ± 27	28.7	45.8	1.38
H240	26 Mar 2012	Spring	64 ± 16	n/a	25.1	n/a
H241	2 May 2012	Spring	114 ± 9	44	11.7	1.66
H242	30 May 2012	Spring	36 ± 6	48.4	22.4	1.89
H243	26 Jun 2012	Summer	73 ± 8	42.8	52.5	2.03
HD5	10, 16, 22 Jul 2012	Summer	58 ± 13	44.3	50.1	1.79
H245	17 Aug 2012	Summer	34 ± 6	n/a	22.7	1.70
H246	14 Sep 2012	Fall	59 ± 7	41.7	15.2	1.66
H247	7 Oct 2012	Fall	60 ± 8	35.8	14.6	1.16
H248	3 Dec 2012	Winter	92 ± 11	15.2	71.1	1.39
H249	12 Feb 2013	Winter	111 ± 37	24.1	17.9	2.53
H250	6-7 Mar 2013	Spring	126 ± 45	39	31.3	2.39
H251	5 Apr 2013	Spring	77 ± 28	38.2	18.9	2.30
H252	17 May 2013	Spring	39 ± 10	n/a	10.8	2.17
		Spring	*76 ± 10*	*42 ± 5*	*18 ± 6*	*2.0 ± 0.3*
		Summer	*58 ± 4*	*43 ± 1*	*46 ± 22*	*1.7 ± 0.3*
		Fall	*53 ± 5*	*38 ± 3*	*43 ± 36*	*1.6 ± 0.5*
		Winter	*85 ± 13*	*26 ± 8*	*57 ± 33*	*1.8 ± 0.6*

*Seasonal designations were: Winter (December, January, February); Spring (March, April, May); Summer (June, July, August); Fall (September, October, November)

†0-175 m depth-integrated

‡Mean ± standard deviation

§n/a = not available

Table 4.2. Sequences recovered based on different similarity thresholds

	% Sequence similarity		
	95%	97%	99%
No. of OTUs retrieved	32,251	82,288	359,609
Singleton OTUs*	12,253 (38%)	39,441 (48%)	228,189 (63%)
Quality-filtered OTUs / reads†	14,254 / 7,674,795	33,342 / 7,649,811	111,964 / 7,481,838
Bacteria OTUs / reads‡	--	3,565 / 1,355,785 (17%)	--
Metazoa OTUs / reads‡	--	536 / 310,636 (4%)	--
Total picoeukaryote OTUs / reads§	--	**29,241 / 5,983,390**	--
Unassigned OTUs / reads†	--	8,943 / 955,354 (16%)	--
Alveolata OTUs / reads†	--	14,767 / 3,481,018 (58%)	--
Het OTUs / reads†	--	3,921 / 1,041,375 (17%)	--
PPE OTUs / reads†	--	1,610 / 505,643 (8%)	--

*Singleton OTUs + OTUs present in only one sample (% of total OTUs retrieved)
†No. of OTUs / no. of reads with singletons and alignment failures removed
‡No. of OTUs / no. of reads (% of quality-filtered reads)
§No. of OTUs / no. of reads after removal of Metazoa and Bacteria OTUs.
†No. of OTUs / no. of reads (% of total picoeukaryote sequences) per OTU category: Unassigned = taxonomy unassigned based on BLAST ($<1e^{-30}$); Alveolata = OTUs asigned as Alveolata only; Het = OTUs assigned as Excavata, Marine Stramenopiles, Rhizaria, Picozoa, Opisthokonta, and Amoebozoa/Apusozoa only, PPE = OTUs assigned as Archaeplastida, Cryptophyta, Haptophyta, Chlorachniophyceae, and Ochrophyta only

Table 4.3. Pearson r correlation values describing relationships between picoeukaryote community composition and various environmental properties (Mantel test*)

Environmental parameter	Total picoeukaryote OTUs	Alveolata OTUs	Het OTUs	PPE OTUs
Temperature	0.73	0.73	0.67	0.68
σ-t	0.62	0.60	0.57	0.70
Daily integrated PAR	0.42	0.40	0.44	0.36
Nitrate + Nitrite	0.60	0.64	0.52	0.27
Phosphate	0.27	0.31	0.20	0.11
Silicic acid	0.56	0.59	0.49	0.32
TChl *a*	0.16	0.14	0.16	0.09
Fucoxanthin	--	--	--	0.10
19'-hexanoyloxyfucoxanthin	--	--	--	0.03
19'-butanoyloxyfucoxanthin	--	--	--	0.34
Zeaxanthin	--	--	--	0.03
Divinyl chlorophyll *a*	--	--	--	0.07

*All properties were significantly correlated (P = 0.001).

Table 4.4. Relative abundances (%) of picoeukaryote supergroups (total picoeukaryote OTUs) and of detailed taxa per OTU category for the full (5-175 m), upper (5-75 m), and lower (100-175 m) regions of the euphotic zone.

		Relative abundance per OTU table (%)		
OTU category	Assigned taxa	5-175 m	5-75 m	100-175 m
Total picoeukaryote OTUs	Amoebozoa/Apusozoa	<0.1	<0.1	<0.1
	Archaeplastida	0.9	0.4	1.3
	Alveolata	58.1	63.6	52.6
	Excavata	1.2	1.0	1.5
	Hacrobia	4.6	5.9	3.3
	Opisthokonta	0.9	0.9	0.9
	Rhizaria	9.1	2.6	15.4
	Stramenopiles	10.0	10.6	9.4
	Unassigned	15.8	15.3	16.3
Alveolate OTUs	Syndiniales Amoebophora	12.9	12.6	13.3
	Syndiniales Group I	24.7	21.7	27.8
	Syndiniales Group II	38.4	38.7	38.2
	Syndiniales Groups III, IV, V	3.8	4.5	3.1
	Syndiniales Others	3.5	3.6	3.4
	Dinophyceae	13.1	15.4	10.7
	Ciliophora	3.2	3.5	2.9
	Apicomplexa	<0.1	<0.1	<0.1
Het OTUs	Amoebozoa/Apusozoa	<0.1	<0.1	<0.1
	Excavata	7.8	9.0	6.7
	Hacrobia	7.5	9.9	5.1
	Opisthokonta: Fungi	3.6	4.4	2.9
	Opisthokonta: Choanoflagellata	1.8	2.8	0.8
	Rhizaria: Radiolaria Acantharea	1.5	0.5	2.5
	Rhizaria: Radiolaria Polycystinea	20.3	6.9	33.5
	Rhizaria: Others	15.4	8.8	21.8
	Rhizaria: Cercozoa	0.9	1.1	0.7
	Stramenopiles: MAST-1	9.0	14.1	4.0
	Stramenopiles: MAST-3	17.2	24.0	10.6
	Stramenopiles: MAST-2, -4, -7-9, -11	10.6	15.1	6.1
	Stramenopiles: Others	3.0	2.7	3.3
PPE OTUs	Archaeplastida	9.3	4.3	14.2
	Cryptophyta	6.6	6.0	7.1
	Haptophyta	34.1	45.9	22.5
	Chlorarachniophyceae	1.0	1.2	0.7
	Bacillariophyceae	0.4	0.5	0.3
	Chrysophyceae	10.6	17.7	3.7
	Dictyochophyceae	5.3	7.1	3.5
	Pelagophyceae	25.4	7.9	42.8
	Bolidophyceae	4.0	6.3	1.8
	Stramenopiles: Others	3.3	3.2	3.4

Table 4.5. Twenty most abundant PPE OTUs, their assigned taxonomy, and % of PPE relative abundances

	OTU ID	% of PPE rel. abund.	BLAST E Value	Accession ID	% Identity	Taxonomy
1.	AL-KC001[A]	23.9	$1e^{-58}$	LC012594	100	Pelagophyceae; *Pelagomonas calceolata*
2.	AL-AB002[D]	11.4	$2e^{-61}$	AJ246261	97.7	Prymnesiophyceae; *Coccolithus pelagicus*
3.	AL-FR003[E]	4.9	$2e^{-67}$	FR874277	100	Mamiellophyceae; *Bathycoccus*
4.	AL-1473	3.6	$8e^{-64}$	FJ537352	99.2	Prymnesiophyceae; Clone OLI16010
5.	AL-AB004[B]	3.5	$1e^{-58}$	KC583002	100	Dictyochophyceae; *Florenciella*
6.	AL-KC005	3.1	$2e^{-67}$	KC582977	100	Bolidophyceae; *Bolidomonas*
7.	AL-GQ006[G]	3.0	$2e^{-67}$	GQ426331	100	Mamiellophyceae; *Ostreococcus tauri*
8.	AL-769	2.3	$5e^{-59}$	AJ246261	96.9	Prymnesiophyceae; *Coccolithus pelagicus*
9.	AL-FJ007	2.1	$8e^{-64}$	FJ537322	99.2	Chrysophyceae; Clone LG01-09
10.	AL-EU008	2.0	$3e^{-66}$	EU561701	100	Chrysophyceae; Clone E222
11.	AL-AF009[C]	1.8	$5e^{-68}$	AF107080	100	Prymnesiophyceae; Clone OLI16029
12.	AL-1453	1.7	$1e^{-56}$	FJ537338	97.6	Chrysophyceae; Clone LG01-09
13.	AL-235[F]	1.2	$7e^{-52}$	FR874689	95.3	Chrysophyceae; Clone E222
14.	AL-256	1.2	$2e^{-58}$	AM491017	96.9	Prymnesiophyceae; *Chrysochromulina leadbeateri*
15.	AL-344	1.2	$7e^{-61}$	GU825016	96.9	Prymnesiophyceae; Clone AI5F14RJ2A07
16.	AL-JF010	1.1	$2e^{-58}$	JF791095	97.6	Cryptophyceae; Kathablepharidae; *Leucocryptos marina*
17.	AL-JF011	1.0	$2e^{-67}$	JF791065	100	Cryptophyceae; Clone P1-31; uncultured *Proteomonas*
18.	AL-507	0.8	$4e^{-47}$	FR874689	95.3	Chrysophyceae; Clone E222
19.	AL-2762[H]	0.8	$1e^{-59}$	EF172963	100	Cryptophyceae; Clone P1-31
20.	AL-1359	0.7	$3e^{-54}$	AJ246261	95.4	Prymnesiophyceae; *Coccolithus pelagicus*

[A, B, C, D, E, F, G, H]: OTUs plotted in Figure 8; letter corresponds to panel in figure.

Figure 4.1. Contour plots of euphotic zone (0-175 m) temperature (color, A), $NO_3^- + NO_2^-$ (B), and TChl *a* (C) concentrations between February 2011 and May 2013. Superimposed contour lines (dashed) indicate sigma-t (A and B) and downwelling PAR (C). Black circles indicate discrete depths where samples for subsequent 18S rRNA gene sequencing were collected. Black stars in panel C depict the depths of the 1% surface PAR isopleth.

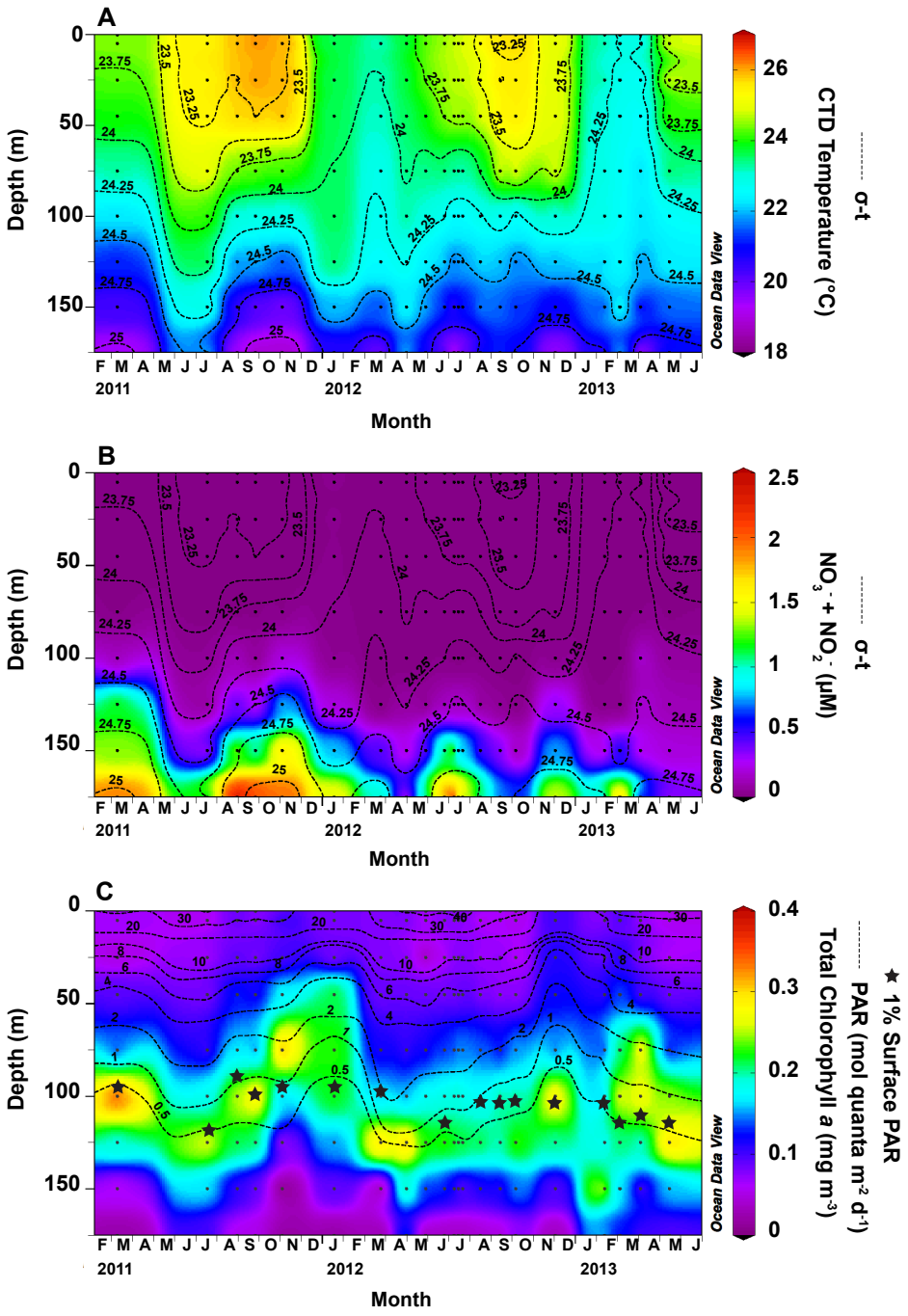

Figure 4.2. Variability in alpha diversity (Shannon Index) of total picoeukaryote OTUs and the three additional OTU categories, binned by depth: Total picoeukaryote OTUs (A), Alveolata OTUs (B), Het OTUs (C), and PPE OTUs (D). For each boxplot, median is indicated by the dark horizontal line, box spans the 1st (Q1; 25th percentile) to the 3rd quartile (Q3, 75th percentile), with the whiskers extending to the maximum (Q3 + 1.5*(Q3-Q1)) and minimum (Q1-1.5*(Q3-Q1)). Outlier observations, considered to be beyond the maximum and minimum limits of the observations, are depicted as open circles.

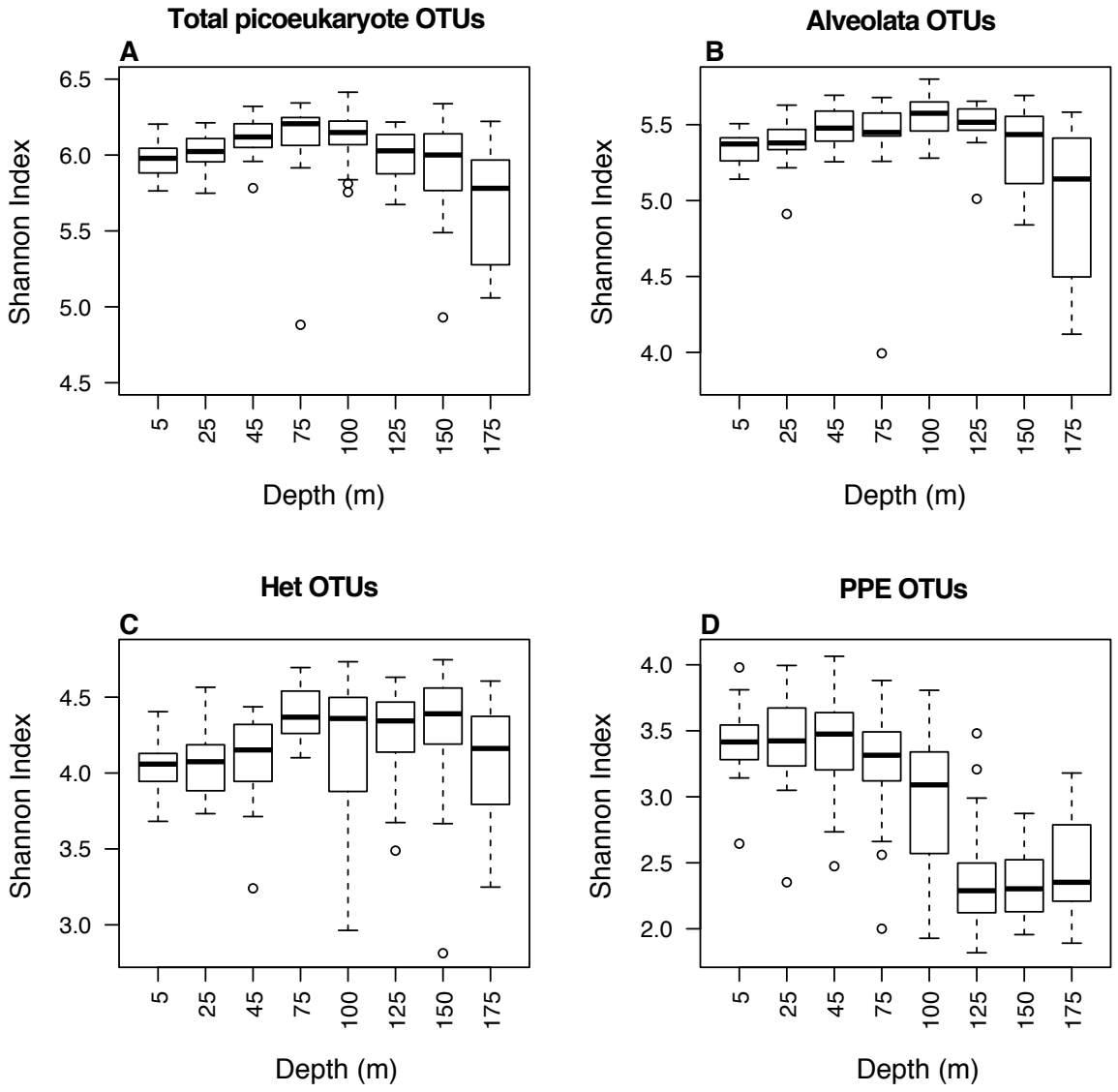

Figure 4.3. Relative abundances of euphotic zone picoeukaryote taxa (at the phylum level) for total picoeukaryotes OTUs binned by depth (A) and cruise sampled (month and year specified; B).

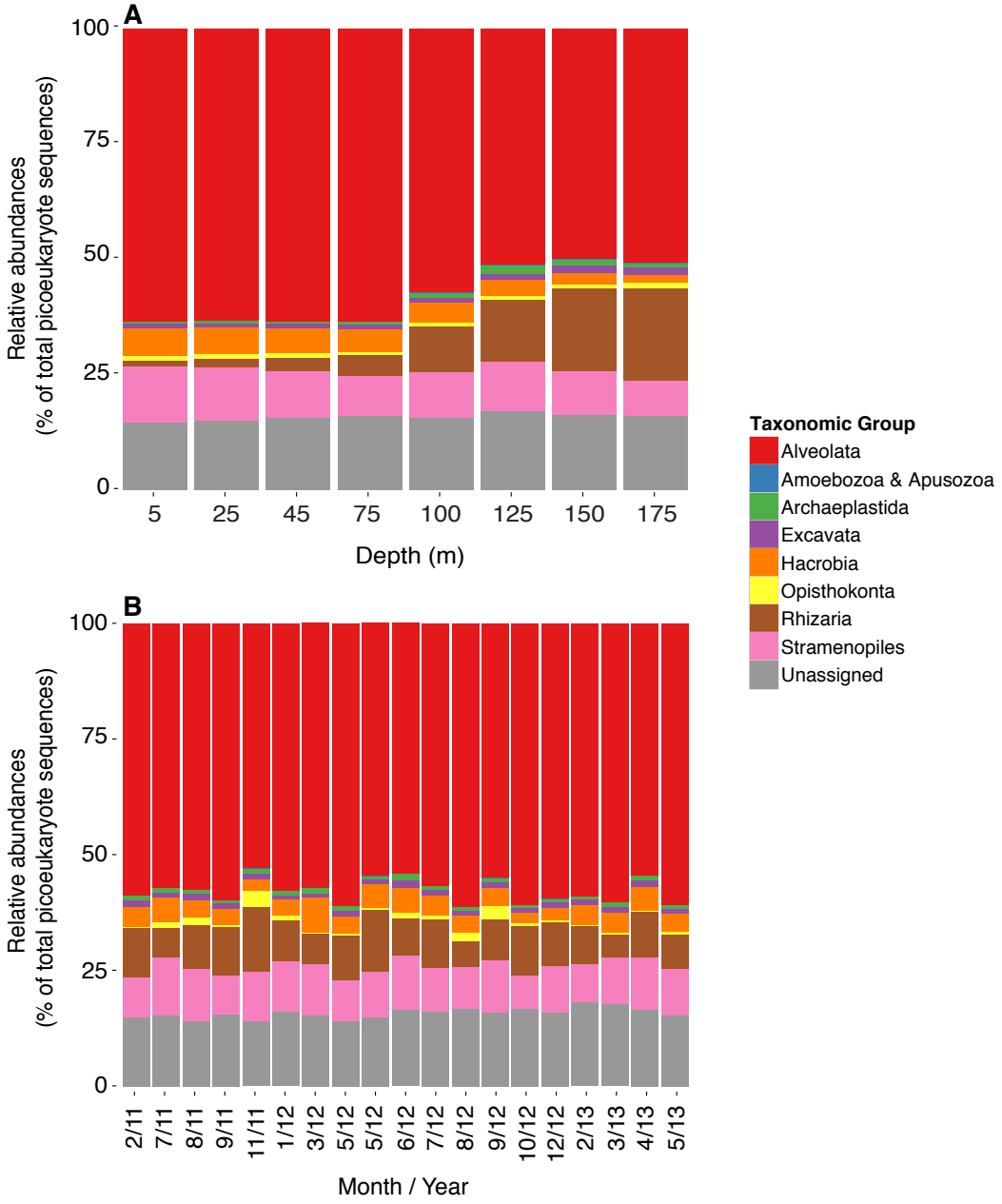

Figure 4.4. Relative abundances of Alveolata OTUs taxa composition binned by depth (A) and cruise sampled (month and year specified; B).

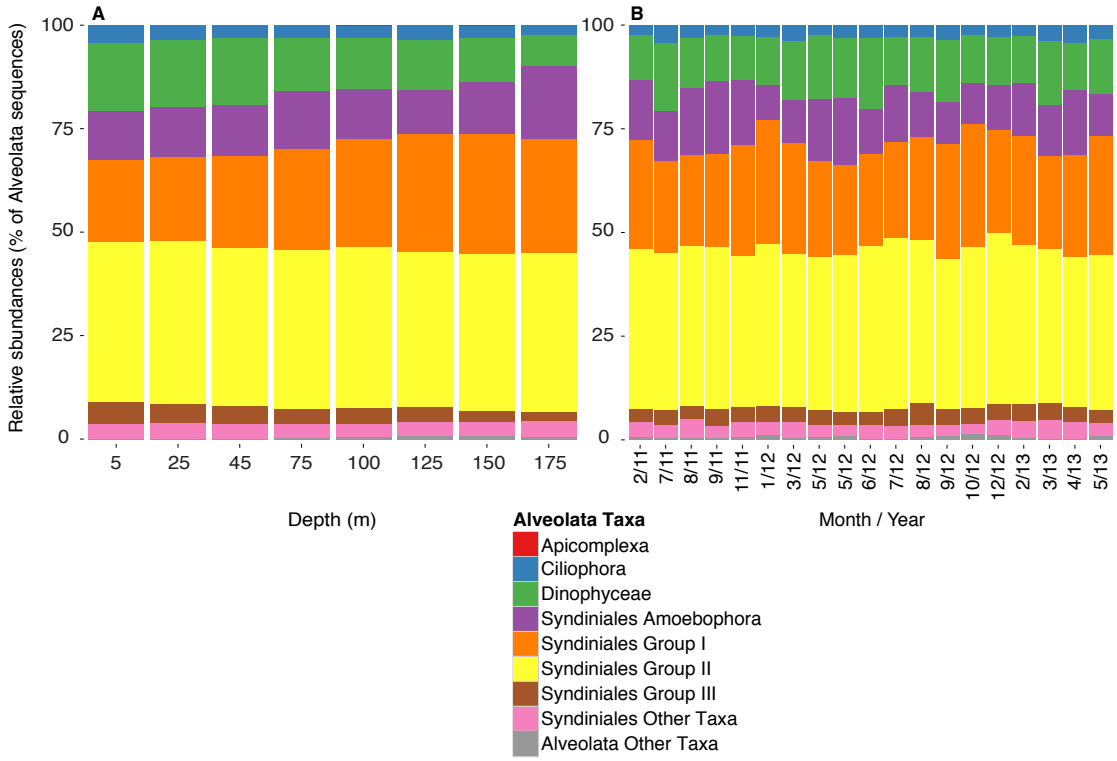

Figure 4.5. Relative abundances of Het OTUs (non-Alveolata, non-photosynthetic) taxa composition binned by depth (A) and cruise sampled (month and year specified; B).

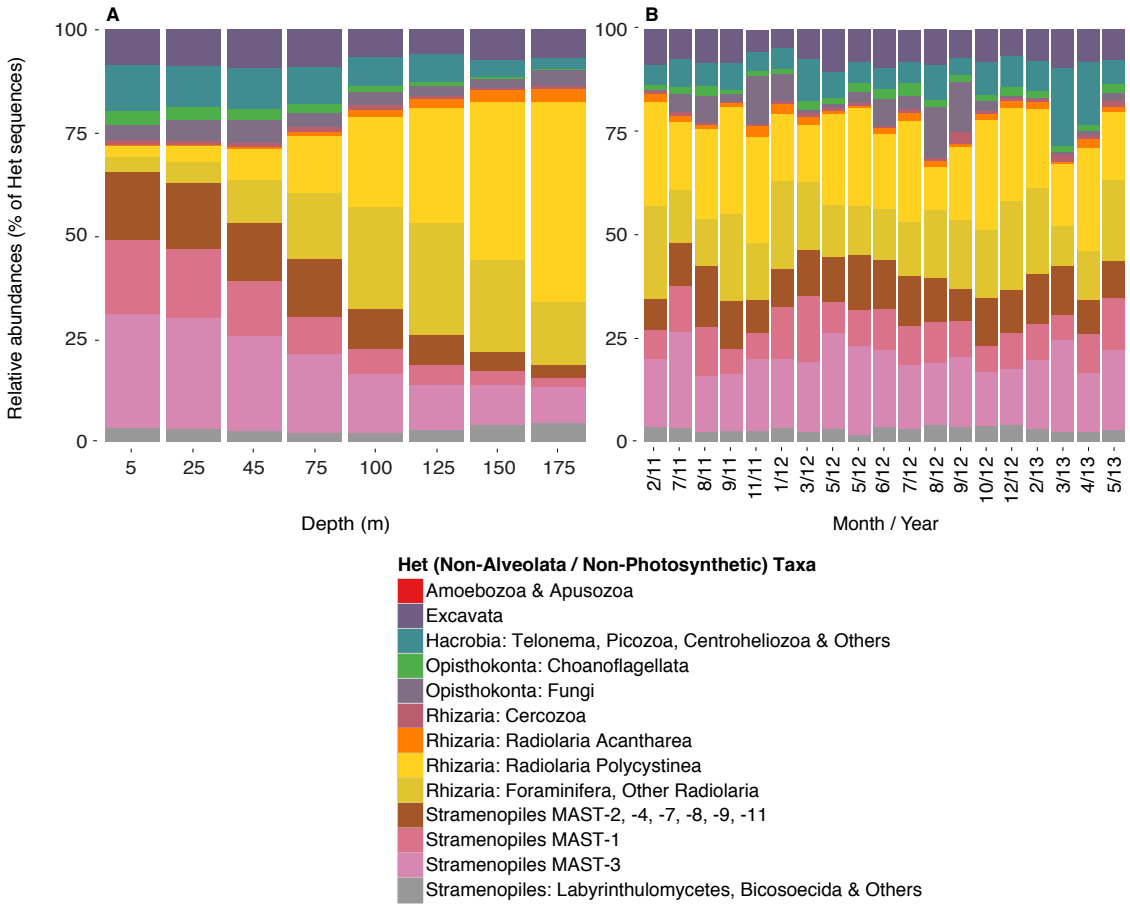

Figure 4.6. Relative abundances of PPE OTUs taxa composition (at the class level) binned by cruise sampled (month and year specified), grouped by depth (5- 175 m).

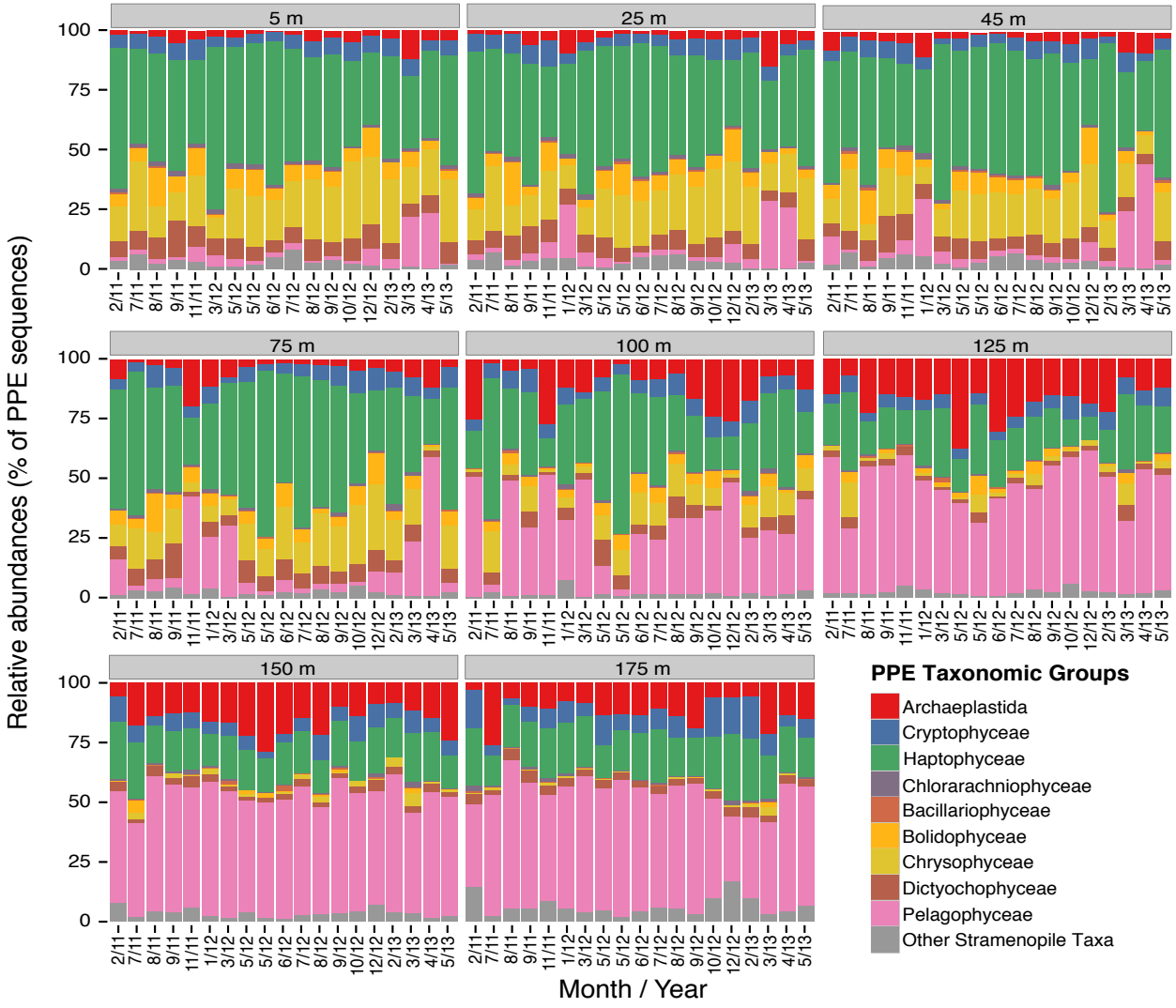

Figure 4.7. Relative abundances of twenty most abundant PPE OTUs sorted by depth. Color key represents relative abundances of each PPE OTU normalized to total picoeukaryote sequences. Within each depth bin, each row indicates the time series of the current study, from February 2011 to May 2013, and color blocks indicate seasons sampled. Bootstrap values on dendrograms were obtained using the R package 'pvclust,' indicating the percent likelihood of repeat occurrence.

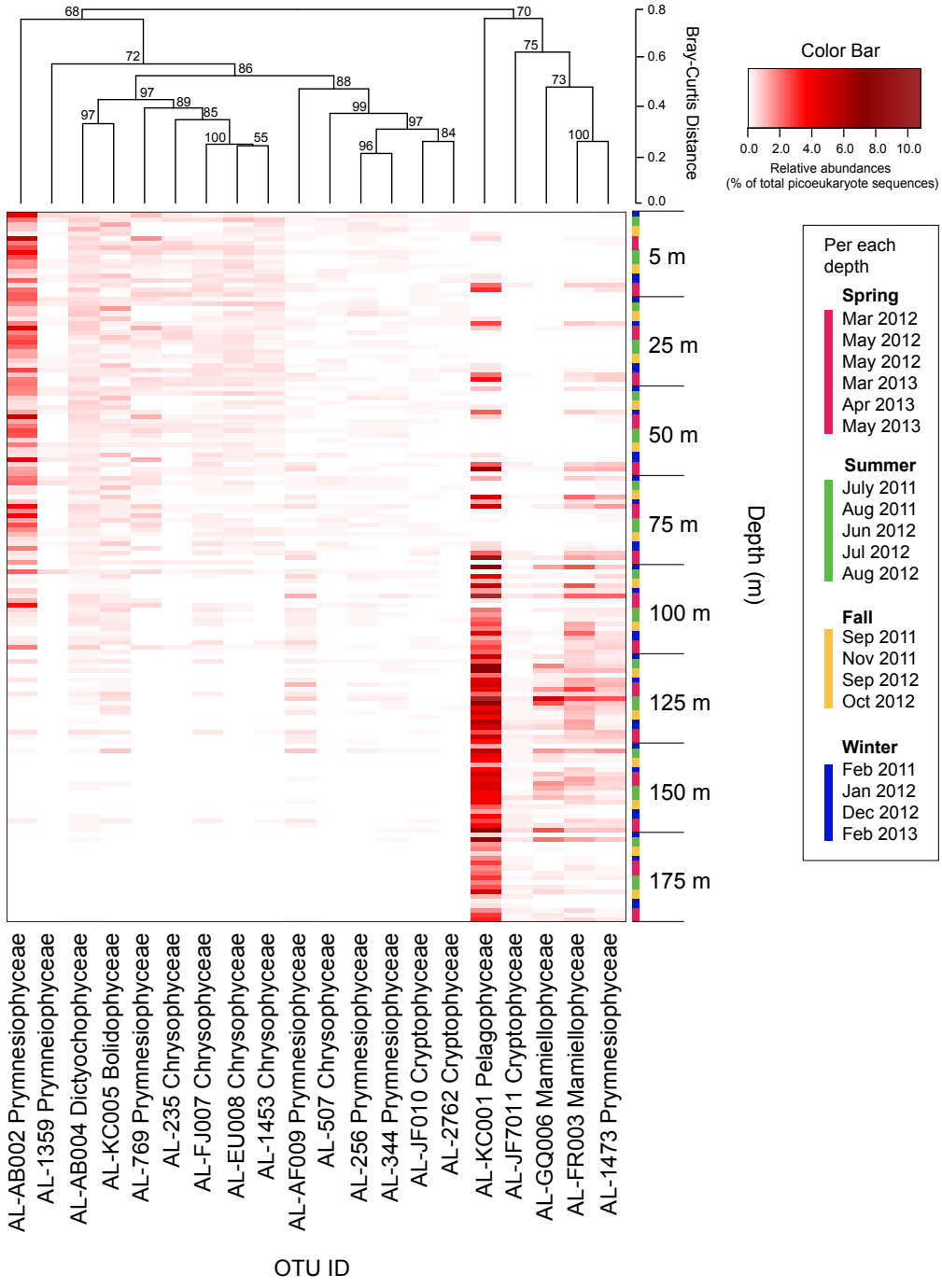

Figure 4.8. Contour plots depicting relative abundances of eight euphotic zone (0-175 m) PPE OTUs from the top 20 most abundant from Feb 2011 to May 2013 Pelagophyceae *Pelagomonas calceolata* (AL-KC001; A), Dictyochophyceae *Florenciella* (AL-AB004; B), Prymnesiophyceae (AL-AF009; C), Prymnesiophyceae (AL-AB002; D), Mamiellophyceae *Bathycoccus* (AL-FR003; E), Chrysophyceae (AL-235; F), Mamiellophyceae *Ostreococcus tauri* (AL-GQ006; G), and Cryptophyceae (AL-2762; H); detailed descriptions of OTUs are provided in Table 5. Sigma-t isopycnal surfaces (from 24.0-24.5) are overlaid on each plot (white dashed lines) and black circles indicate depths of sample taken. Relative abundances of each PPE OUT are normalized to total picoeukaryote sequences. Note differences in z-axis (relative abundance) with each OTU.

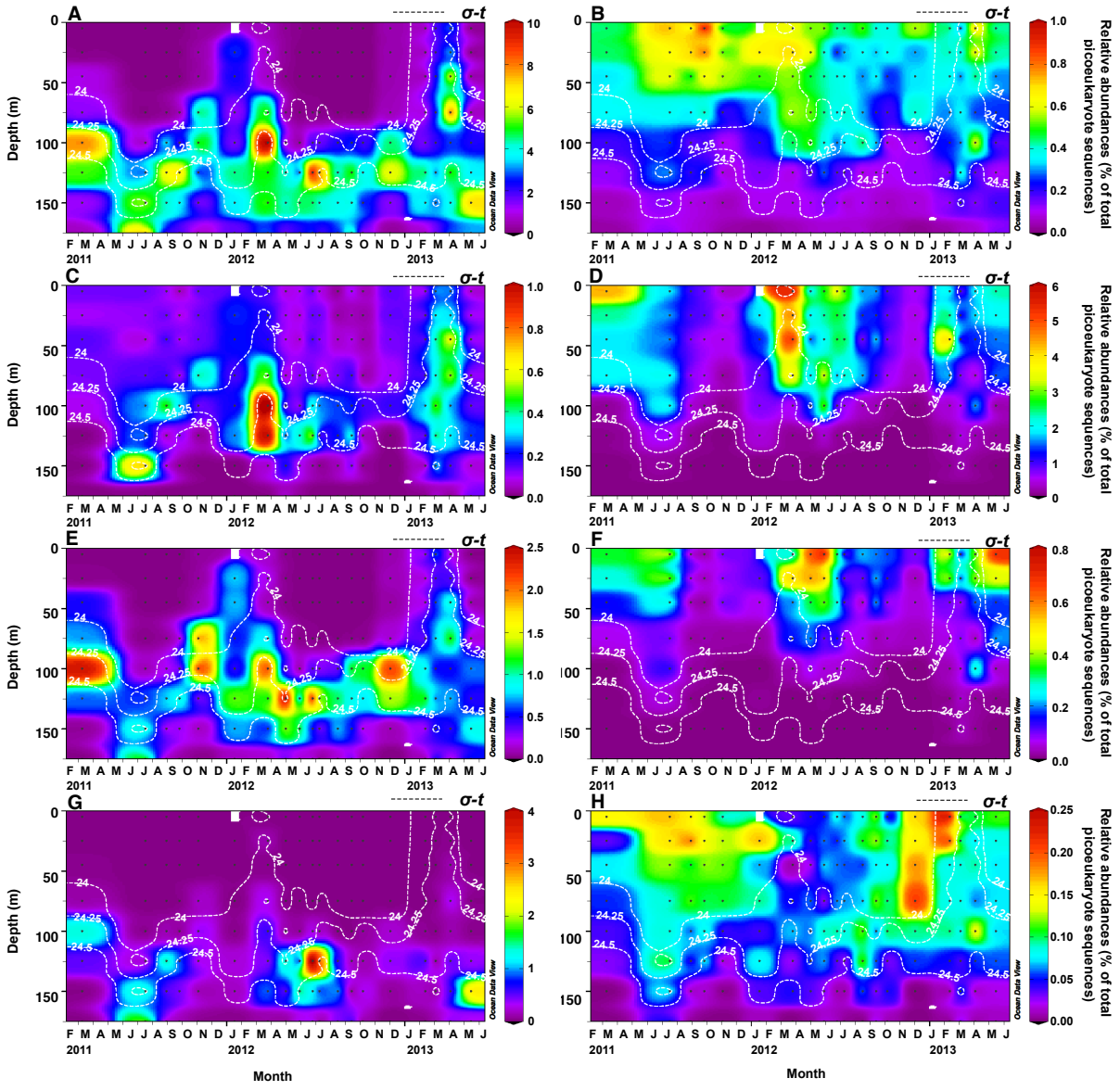

Figure 4.S1. Rarefaction curve of V9 rDNA OTUs delineated at 97% sequence similarity based on mean species richness for each sample up to a subsample of 25,000 sequences. Each line represents a separate sample.

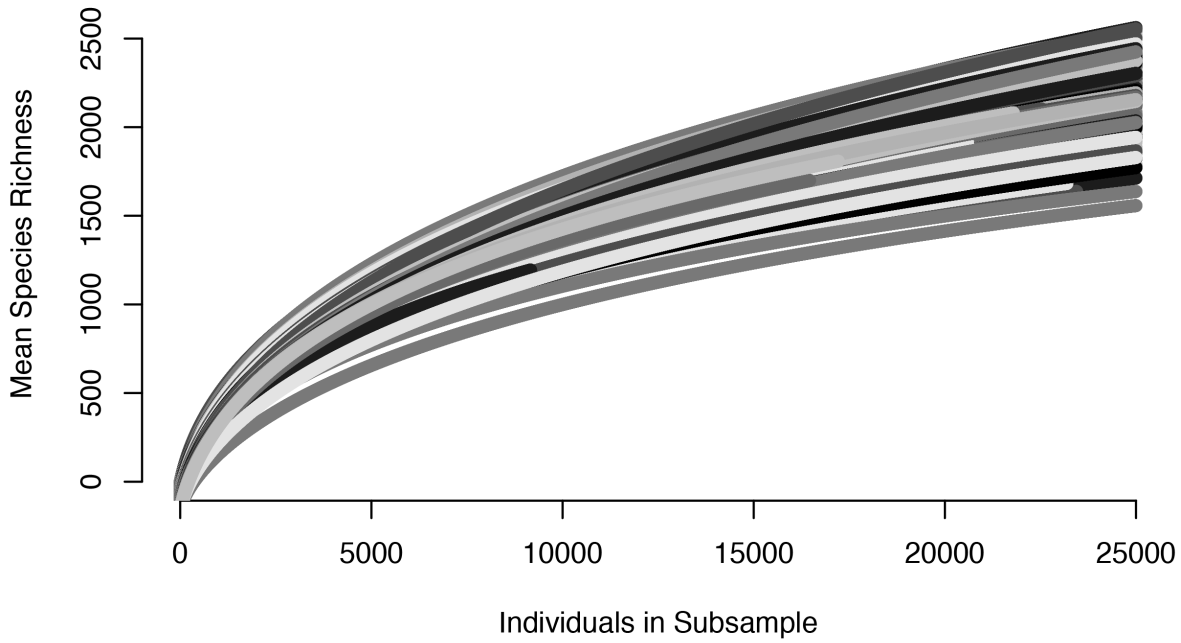

Figure 4.S2. Seasonal variability in alpha diversity (Shannon Index) of the upper (5-75 m; left) and lower (100-175 m; right) euphotic zone PPE communities. Boxplot parameters are the same as described for Fig. 2.

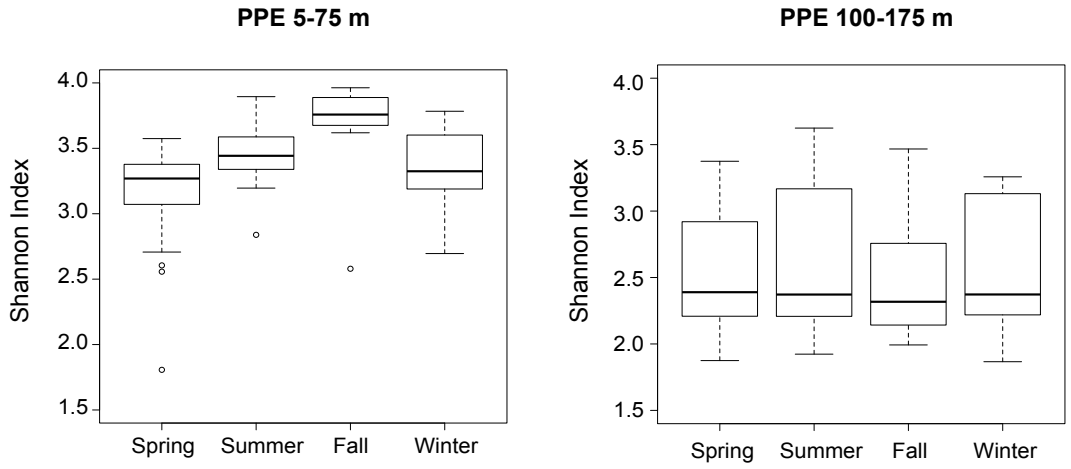

Figure 4.S3. Dendrograms depicting cluster analysis of PPE OTUs obtained per sample, partitioned by season (using Bray-Curtis dissimilarity). Colored lines indicate samples taken within specific depth bins (green: 5-75 m; red: 100-175 m). Bootstrap values (indicating the percentage of likelihood of repeat occurrence) >50 are indicated on dendrograms.

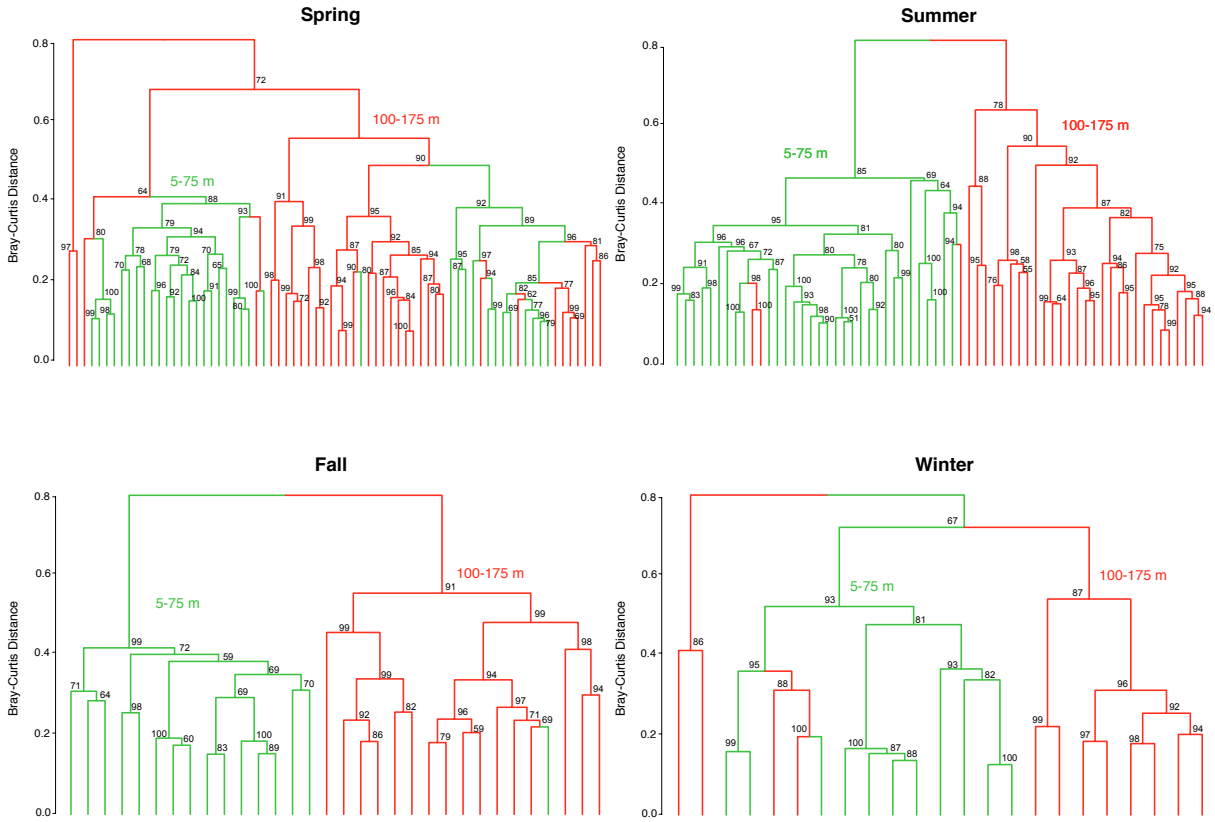

CHAPTER 5

Differential response of eukaryotic phytoplankton to nitrogen substrates

Yoshimi M. Rii, Robert R. Bidigare, David M. Karl, Matthew J. Church

5.1. Abstract

Fixed inorganic nitrogen is persistently scarce in the well-lit regions of the subtropical ocean gyres and its supply plays an important role in controlling phytoplankton productivity. In a series of experiments conducted in the oligotrophic North Pacific Subtropical Gyre (NPSG), we examined changes in phytoplankton productivity and eukaryotic phytoplankton community structure in response to additions of nitrate (NO_3^-), ammonium (NH_4^+), or urea (final concentration = ~3 μM N) in conjunction with phosphate and silicic acid. In general, rates of ^{14}C-primary productivity increased ~2- to 27-fold, coincident with ~2- to 7-fold increases in chlorophyll *a*. Contributions by larger (>3 μm) phytoplankton to rates of ^{14}C-primary production and concentrations of chlorophyll *a* increased from 23-57% to 46-79% and 9-14% to 19-45%, respectively, following additions of nitrogen substrates. Photosynthetic pigment analyses and high-throughput sequencing of the V9 regions of 18S rDNA revealed that pennate diatoms demonstrated large changes following the addition of nitrogen during the two experiments conducted in the summer; concentrations of fucoxanthin increased ~49-fold in the NO_3^- additions and ~23-fold in the NH_4^+ additions, and relative abundances of *Pseudo-nitzschia* increased to ~60% of the >3 μm community in NO_3^- additions and ~30% in NH_4^+ additions. In contrast, smaller eukaryotic phytoplankton increased rapidly (48 h after initial time point) during the experiments conducted in spring and winter, with concentrations of 19'-butanoyloxyfucoxanthin (biomarker for pelagophytes) increasing ~12-fold following nitrogen additions and relative abundances of *Pelagomonas* OTUs increasing to 40-59% of the picophytoplankton (0.2-3 μm) sequences. Examination of alpha diversity metrics revealed that addition of nitrogen substrates decreased diversity for both size fractions throughout most of the year, with significantly lower diversity in the NO_3^- treatments during the summer compared to in winter and spring for larger phytoplankton, likely due to the dominance of diatoms. Overall, our findings revealed that while the responses of phytoplankton biomass, ^{14}C primary production, and eukaryotic community composition appeared independent of the type of nitrogen substrate added, the major taxa responding to nitrogen additions appeared temporally dependent. Our results shed further insight

into the role of nitrogen availability and seasonal-scale differences in shaping eukaryotic phytoplankton diversity in the surface waters of the oligotrophic NPSG.

5.2. Introduction

In oligotrophic marine ecosystems such as the North Pacific Subtropical Gyre (NPSG), less than 10% of organic matter produced is exported out of the euphotic zone as sinking particles, implying rapid remineralization and organic matter turnover (Karl et al., 1996). Such low organic matter export in these regions has been attributed to the restricted supply of inorganic nutrients (nitrogen, phosphorus) to the euphotic zone (Karl, 2002; Arrigo, 2005); for example, concentrations of nitrate + nitrite (N+N) and ammonium (NH_4^+) in the near-surface waters of the NPSG are typically <5 nM and <50 nM, respectively (Wada and Hattori 1990; Karl et al., 2001). Hence, competition for this limiting resource could be central to structuring the productivity and diversity of planktonic communities in this ecosystem.

Nitrogen availability in the euphotic zone of the NPSG varies on seasonal, event-, to interannual scales, exerting important control on plankton community succession, primary productivity, and particulate matter export in this oligotrophic habitat. Seasonal variability, partly in response to variations in the penetration of light to the lower regions of the euphotic zone, permits nitrate (NO_3^-) concentrations to accumulate in the dimly lit lower euphotic zone during the winter with subsequent consumption during the spring (Letelier et al., 2004). Episodic to seasonal-scale supply of NO_3^- to the lower euphotic zone occurs through convective mixing during the winter and through the displacement of isopycnal surfaces due to mesoscale processes such as eddies and planetary waves (Dandonneau et al., 2003; Sakamoto et al., 2004; Johnson et al., 2010). In addition, activities of nitrogen-fixing microorganisms increase during the warm stratified summer months (Church et al. 2009), increasing concentrations of dissolved organic nitrogen and NH_4^+ (Karl et al., 1992; 1997), and frequently coinciding with increased biomass of diatoms (Dore et al., 2008; Villareal et al., 2011; Karl et al., 2012).

Picophytoplankton (≤3 μm), including cyanobacteria *Prochlorococcus* and *Synechococcus* and a diverse assemblage of photosynthetic picoeukaryotes, together constitute ~60-90% of phytoplankton biomass and appear to account for >70% of net primary production in the NPSG (Campbell and Vaulot, 1993; Vaulot et al., 1995; Li et al., 2011). While abundances of *Prochlorococcus* exceed photosynthetic picoeukaryotes by two to three orders of magnitude,

photosynthetic picoeukaryotes appear to demonstrate high rates of cell-specific carbon fixation due to their larger cell biovolumes and rapid rates of growth (Li, 1994; Jardillier et al., 2010; Rii et al., 2016), suggesting that they may constitute important roles in carbon cycling.

Past studies have demonstrated preferential uptake of NH_4^+ relative to NO_3^- by phytoplankton, a finding hypothesized to reflect the energetic savings in assimilating reduced forms of nitrogen (*e.g.*, Eppley et al., 1977; Dortch, 1990). A recent field-based study found that cyanobacteria and eukaryotic phytoplankton in the oligotrophic Sargasso Sea rely on different forms of nitrogen to support their growth (Fawcett et al., 2011). These results suggest that the form and availability of nitrogen substrates may influence the temporal and spatial variability in phytoplankton community composition. In the current study, we examined changes in phytoplankton productivity and eukaryotic phytoplankton community structure in response to nitrogen enrichments conducted in the oligotrophic upper ocean waters at Station ALOHA. In five separate experiments, natural seawater plankton communities were enriched with NO_3^-, NH_4^+, or urea and incubated for 5 to 6 days. We sought to determine which eukaryotic phytoplankton assemblages responded to the additions of selected nitrogenous substrates and over what time-scales, providing insight into how variations in the availability of nitrogenous nutrients contribute to variability in phytoplankton community structure and growth in the euphotic zone of oligotrophic subtropical gyres.

5.3. Methods

5.3.1. Experimental design

Experiments were conducted between July 2011 and April 2013 during five research cruises to Station ALOHA (22.75°N, 158°W), the well-characterized study site of the Hawaii Ocean Time-series (HOT) program (Karl and Lukas, 1996). Sampling occurred during four HOT cruises and one Center for Microbial Oceanography: Research and Education (C-MORE) cruise (termed HOE-DYLAN V, HD5) aboard the R/V *Kilo Moana* (Table 1). Seawater was collected in 12-L polyvinylchloride bottles affixed to a 24-bottle rosette sampler equipped with a Sea-Bird 911+ conductivity, temperature, and depth profiler. Nine 20-L polycarbonate carboys were filled with 25 m Station ALOHA seawater pre-filtered off the rosette sampler through a Nitex screen (mesh size ~202 μm) to exclude larger zooplankton. Of these, three carboys received additions of nitrate (target ~2.8 μM N final concentration as $NaNO_3$) and three carboys received additions of

ammonium (target ~2.8 μM N final concentration as NH_4Cl). All carboys, including three 'Control' carboys, received additions of phosphate (target ~0.2 μM P final concentration as KH_2PO_4) and silicic acid (target ~2.8 μM Si final concentration as Na_2SiO_3) to achieve a final N:P:Si stoichiometric ratio (14:1:14) similar to nutrient pools measured in the sub-euphotic zone (~300 m) waters at Station ALOHA (Table 2). For experiment N248, the setup was identical to that described above except 10-L carboys were used and three additional carboys were amended with urea (target ~2.8 μM N final concentration as $CO(NH_2)_2$). Carboys were incubated for 120 to 144 hours and subsampled at approximately daily timescales throughout the experiment (Table 1). All sampling was conducted before sunrise in order to allow productivity rate measurements to span the full photoperiod. Incubators used for the experiments were covered with blue Plexiglas filters shaded to 50% of the surface photosynthetic active radiation (PAR). Temperature and solar irradiance levels were measured continuously throughout the experiment using a waterproof temperature/light logger (HOBO Pendant® UA-002-08). Accompanying physical and biogeochemical properties at the time of sampling for these experiments were obtained from the HOT program database (http://hahana.soest.hawaii.edu/hot/hot-dogs/).

5.3.2. Macronutrients and ammonium analyses

Nutrient samples were collected at each time point in 125-mL or 500-mL acid-washed high density polyethylene (HDPE) bottles and frozen upright at -20°C until analyzed. Nitrate + nitrite (N+N), phosphate (PO_4^{3-}), and silicic acid ($Si(OH)_4$) concentrations in seawater samples were determined using a 3-channel, Bran+Luebbe AA III™ continuous segmented flow autoanalyzer (Armstrong et al., 1967; Bernhardt and Wilhelms, 1967; Atlas et al., 1971). Detection limits for the instrumental settings used, defined as the lowest resolvable concentrations for each analyses, were 0.058 μM N+N, 0.014 μM PO_4^{3-}, and 0.013 μM $Si(OH)_4$. Analysis for NH_4^+ were run on a hybrid SEAL Autoanalyzer 3 coupled with a 2 m liquid waveguide capillary detection cell, with modified chemistry and an indo-phenol blue reaction (Li et al., 2005). The limit of detection for this method was 0.0037 μM NH_4^+.

5.3.3. ^{14}C-based rates of primary production

Rates of size-fractionated (0.2-3 μm and >3 μm) primary production were assessed based on the assimilation of ^{14}C-bicarbonate into particulate organic matter (Steeman Nielsen, 1952).

Seawater was collected into 30-mL polycarbonate centrifuge tubes (Nalgene™ Oak Ridge) before sunrise, spiked under subdued light with 70 µL of $NaH^{14}CO_3^-$ (MP Biomedicals 17441H, stock concentration 2 mCi ml^{-1}) to a final activity of ~0.14 MBq $NaH^{14}CO_3^-$ mL^{-1}. The tubes were placed in white mesh bags in the same incubator as the experiment carboys over the full photoperiod (~12-14 hours). After sundown, 25 µL aliquots from each sample were collected and stored in 20-mL glass scintillation vials containing 500 µL of β–phenylethylamine to determine the total activity of ^{14}C added to each sample. The remaining sample volume (~25 mL) was serially vacuum-filtered, first onto 25 mm diameter, 3 µm pore size polycarbonate membranes (Millipore Isopore™), then onto 25 mm diameter, 0.2 µm pore size membranes (GE Osmonics polycarbonate track-etched). After filtration, each filter was placed in 20-mL glass scintillation vials, to which 1 mL of 2 M hydrochloric acid was added and vented for at least 24 hours to remove adsorbed ^{14}C-bicarbonate. Ten mL of Ultima Gold liquid scintillation cocktail was then added to each vial and placed in a liquid scintillation counter (Packard TRI-Carb 4640) for the determination of ^{14}C activities. ^{14}C-assimilation rates were calculated based on the resulting radioactivity of the filters, total added activity, and dissolved inorganic carbon concentrations derived from respective water depths at Station ALOHA (Letelier et al., 1996).

5.3.4. Photosynthetic picoeukaryote cell abundance

Seawater samples (2 mL) for photosynthetic picoeukaryote cell abundance measurements were collected for each experiment into cryotubes (Corning) containing 30 µl of 16% paraformaldehyde (PFA, in water, Alfa Aesar 43368) for a final concentration of 0.24% (w/v), kept for 15 minutes in the dark, flash-frozen in liquid nitrogen, and stored at -80°C until analyzed. Photosynthetic picoeukaryote cells were distinguished using a BD Influx™ flow cytometer (triggered on forward scatter) with the data acquisition software Spigot. Cells were enumerated based on forward scatter, side scatter, chlorophyll-based red fluorescence (692 ± 20 nm), and phycoerythrin-based orange fluorescence (585 ± 20 nm) on two lasers, 488 and 457 nm. Cell counts were determined using the data analysis software FlowJo 10.0.7.

5.3.5. Photosynthetic pigments

For measurements of size-fractionated chlorophyll *a* (Chl *a*), seawater (250 mL) was collected in amber HDPE bottles and serially filtered using a peristaltic pump, first onto 25 mm

diameter, 3 µm pore size polycarbonate membranes (Millipore Isopore™), then onto 25 mm diameter, GF/F (Whatman®) filters (nominal pore size ~0.7 µm). Though different filters were used for Chl *a* concentrations and ^{14}C primary production measurements, previous analyses at Station ALOHA indicate Chl *a* concentrations estimated using 0.2 µm polycarbonate and GF/F glass fiber filters are comparable (Chavez et al., 1995; Viviani et al., 2015). Filters were immediately submerged in 5 mL of cold 100% acetone in glass culture tubes, tubes were wrapped in aluminum foil, and stored at -20°C for pigment extraction. After seven days, tubes containing the filters were warmed to room temperature, and Chl *a* concentrations in the extracts were quantified using a Turner Designs 10-AU fluorometer (Strickland and Parsons, 1972).

For photosynthetic pigment analyses using high performance liquid chromatography (HPLC), seawater (2 L) was collected into brown, narrow-mouthed HDPE bottles and subsequently filtered using a peristaltic pump onto 25 mm diameter, GF/F (Whatman®) filters. Filters were immediately flash-frozen in liquid nitrogen and stored at -80°C until analyzed. Photosynthetic pigments were extracted from the filters in 3 mL 100% acetone (HPLC grade) in culture tubes along with 50 µL canthaxanthin, an internal standard, and placed at 4°C for 24 hours. Chlorophyll and carotenoid pigments were separated on a Varian 9012 HPLC system (Waters Spherisorb® 5-µm ODS-2 C_{18} column with a corresponding guard cartridge and a Timberline column heater) and analyzed using SpectraSYSTEM Thermo Separation Products dual wavelength UV/VIS UV2000 and fluorescence FL2000 detectors (Wright et al., 1991; Bidigare et al., 2005). Pigment identifications were based on absorbance spectra, co-chromatography with standards, and relative retention time with a monovinyl Chl *a* standard and representative culture extracts, and Spectra-Physics WOW® software was used to calculate peak area.

5.3.6. DNA extraction, PCR, and sequence analyses

Seawater samples (2 L) for subsequent extraction of planktonic DNA were collected into acid-washed low density polyethylene (LDPE) bottles and serially filtered using a peristaltic pump through 25 mm diameter 3 µm pore size polycarbonate membranes (Millipore Isopore™), then onto 25 mm diameter, 0.2 µm pore size polyethersulfone membranes (Pall Supor®). After filtration, filters were placed in 1.5-mL microcentrifuge tubes, immediately flash-frozen in liquid nitrogen, and stored at -80°C until analyzed. DNA was extracted and purified using the QIAGEN

DNeasy Plant Mini Kit, including a bead-beating step (with 0.1 and 0.5 mm beads) and Proteinase K (36 mAU mL^{-1} final activity, QIAGEN) for additional cell disruption and lysing (Paerl et al., 2008). Extracts were eluted in 200 µL of nuclease-free PCR grade water.

The V9 regions of eukaryote 18S rRNA genes were amplified using the PCR primer pairs 1391F (5'-GTACACACCGCCCGTC-3'; *S. cerevisiae* NCBI GenBank Accession #U53879 position 1629-1644; Lane, 1991) and Euk Br (5'-TGATCCTTCTGCAGGTTCACCTAC-3'; *S. cerevisiae* NCBI GenBank Accession #U53879 position 1774-1797; Medlin et al., 1988; Amaral-Zettler et al., 2009). Each PCR reaction contained both primers (0.2 µM final concentration), 1X 5 PRIME HotMasterMix (Cat# 2200410), and ~5 ng of template DNA in a 25 µL reaction (Amaral-Zettler et al., 2009). The thermal cycling conditions consisted of an initial activation step at 94°C for 3 min, followed by 35 cycles of 45 sec at 94°C, 60 sec at 57°C, and 90 sec at 72°C, ending with a final extension of 10 min at 72 °C. The resulting PCR products (344 in total) were run on an agarose gel to verify product amplification, quantified, pooled (~8 ng of each sample into a single tube), and purified using the MoBio UltraClean PCR Clean-Up Kit (Cat# 12500). The quality of the pooled PCR product was evaluated on a BioAnalyser 2100 (Agilent). Sequencing was then conducted (paired end, 300 cycles) from the forward and the reverse primers on an Illumina MiSeq (University of Hawai‘i Core Functional Genomics Facility at the Hawai‘i Institute of Marine Biology), from which 12,193,511 sequence reads were recovered. Paired-end sequencing reads were merged using PEAR (Zhang et al., 2014), quality filtered (reads trimmed to 100-150 bp in size, maximum expected error of 1%, no ambiguous bases allowed, and an average Phred quality threshold >34), and poor quality reads were removed from further analyses. *De novo* and reference-based chimeras were detected and removed using USEARCH v7.0.1090 (Edgar et al., 2011). Sequences were first clustered using UCLUST v1.2.22q (max accepts = 20, max rejects = 500) into operational taxonomic units (OTUs) based on the SILVA 119 (pre-clustered at 97% similarity threshold) database (Quast et al., 2012), clustered *de novo* at the 97% similarity threshold, and the centroid sequence within each OTU was selected as the representative sequence. Sequences that failed to align using PyNAST (minimum percent identification 0.75; Caporaso et al., 2010), singletons, and OTUs present in only one sample were removed. Taxonomy was assigned to representative sequences at 90% similarity with BLAST (max E value at 1 x e^{-30}) based on the SILVA 119 database (pre-clustered at 97%). Bacteria, Archaea, and Metazoa sequences were removed, resulting in

5,820,084 sequence reads and 11,811 total OTUs. Of these, taxonomy was not assigned to 2,800 OTUs consistent with the stringent E value used. OTUs with assigned taxonomy presumed to be photosynthetic, including Archaeplastida, Hacrobia (Cryptophyceae and Haptophyta), Rhizaria (Chlorarachniophyta), Stramenopiles (Ochrophyta), and Alveolata (Dinophyceae), were separated into an OTU table, and this "phytoplankton-only" OTU table was used for subsequent analyses. Final quality-filtered sequences will be deposited into the Sequence Read Archive (NCBI).

5.3.7. Statistical analyses

Nutrient concentrations measured in each treatment and experiment were tested for normality using the Shapiro-Wilk Test (Royston, 1982) and quantile-quantile plots, and analysis of variance (ANOVA) tests were performed. Data not normally distributed were log-transformed for subsequent ANOVA, or non-parametric Kruskal-Wallis tests (Hollander and Wolfe, 1973) were used to test for significant differences between distributions. One-way ANOVA and linear regression analyses were also used to test for significant differences in nutrient concentrations over the duration of the experiment (Faraway, 2002). Community analyses were performed in R 3.1.1. (R Core Development Team, 2014) with the R package *Vegan* (Oksanen et al., 2013) and graphical outputs were constructed with the package *ggplot2* (Wickham, 2009). Subsampling for calculations of alpha diversity was conducted with 150 reads. Differences in eukaryotic phytoplankton community composition and alpha diversity between experiments were statistically tested using Mantel tests on Bray-Curtis derived dissimilarity matrices and paired t-tests on distribution of Shannon indices.

5.4. Results

5.4.1. Station ALOHA biogeochemistry at initial time points

Two experiments (NvN1 and NvN3) were conducted during the summer (July 2011 and July 2012), two (NvN2 and NvN4) were performed during the spring (March 2012 and April 2013), and one (N248) was conducted during the winter (December 2012; Table 1). At the time these experiments were conducted, sea surface temperatures (SST), mixed layer depths (MLD), the flux of PAR at 25 m, and concentrations of N+N were characteristic of the monthly HOT program climatology for Station ALOHA (Fig. 1). During the summer sampling periods, the

near-surface waters were characterized by relatively warm temperatures (24.8-25.3 °C), the MLD ranged between 58 and 78 m, and the daily integrated surface irradiance averaged ~44 mol quanta m^{-2} d^{-1} (Table 1, Fig. 1). In comparison, during the spring experiments, the upper ocean waters exhibited slightly lower temperatures (22.7-23.0 °C), the MLD ranged between 36 and 77 m, and incident PAR was somewhat lower (averaging ~38 mol quanta m^{-2} d^{-1}). For the experiment conducted in December, the near-surface waters were 24.8 °C, the MLD was relatively deep (averaging 92 m), and daily integrated incident PAR was low (averaging ~15 mol quanta m^{-2} d^{-1}. Concentrations of Chl *a* in the near-surface waters ranged 65-111 ng L^{-1} during the study, with no discernible seasonal pattern among the various experiments (Table 1). Similarly, concentrations of N+N were consistently low (<5 nM) throughout the year with no apparent seasonal-scale differences (Fig. 1D, Table 1). Concentrations of PO_4^{3-} and $Si(OH)_4$ also depicted no apparent seasonality, ranging 60-90 nM P and 0.8~1.2 μM Si, respectively (Table 1).

5.4.2. Nutrients, primary production, chlorophyll a, and cell abundances following nitrogen additions

Concentrations of N+N, NH_4^+, PO_4^{3-}, and $Si(OH)_4$ in the control incubations did not vary significantly over time in any of the experiments (one-way ANOVA and linear regression, $p > 0.05$; Table 2). Contributions of picophytoplankton (0.2-3 μm) to >0.2 μm ^{14}C primary production at initial time points ranged 68-77% (with rates of production in the >3 μm size fraction contributing 23-32%) in all experiments except during NvN3, when picophytoplankton were 43-60% of the initial ^{14}C-productivity (and phytoplankton >3 μm comprised 40-57% of the production; Table 3). At the end of the experiments, the size distributions of ^{14}C-primary production in the controls remained dominated by picophytoplankton (44-59% of the total productivity). Similarly, concentrations of Chl *a* remained largely unchanged in the controls in all of the experiments, with the majority (75-78% of the total Chl *a*) attributed to the picophytoplankton fraction (Table 3). Photosynthetic picoeukaryote abundances were relatively stable over time in the control incubations for all experiments except for NvN1, when cell abundances increased ~3-fold (Table 3).

The addition of either NO_3^- or NH_4^+ of final concentrations ranging ~2.5-3.2 μM N+N and 2.2-5.2 μM NH_4^+ (and PO_4^{3-} and $Si(OH)_4$) resulted in large increases in concentrations of Chl *a* and rates of ^{14}C-production. Over the course of 120 h (5 d) for all experiments, 18-83% of

the added NO_3^- was consumed, resulting in NO_3^- drawdown rates ranging 0.1-0.5 μM N d^{-1} (Table 2). For the NH_4^+ treatments, 32-85% of the added NH_4^+ was consumed over 5 d at rates ranging 0.1-0.9 μM N d^{-1}. For both NO_3^- and NH_4^+ treatments, $Si(OH)_4$ was consumed at 0.06-0.24 μM Si d^{-1} during the summer experiments and ~0.02 μM Si d^{-1} during the spring experiments (Table 2). PO_4^{3-} was consumed in the NO_3^- treatments at rates ranging from ~0.01 to 0.03 μM P d^{-1} (N:P = ~14-21), and at rates ranging from 0.002-0.03 μM P d^{-1} for the NH_4^+ treatments. Urea (target concentration of ~2.8 μM N) was also included as one of the treatments in an experiment conducted in December 2012; however, urea concentrations were not measured during the experiment so rates of consumption or production could not be evaluated.

Rates of ^{14}C primary production (sum of >3 μm and 0.2-3 μm filter size classes) increased ~17- and 27-fold in the NO_3^- and NH_4^+ treatments over 5 d, respectively, during NvN2, with contributions by the >3 μm fraction in the NO_3^- treatment comprising 75 ± 5% (mean of triplicate carboys) of the sum of two fractions, and rates of production by the >3 μm size class comprising 48 ± 14% (mean of triplicate carboys) of the sum of fractions in the NH_4^+ treatment. During NvN3, however, rates of >0.2 μm ^{14}C primary production increased ~21- and 15-fold in the NO_3^- and NH_4^+ treatments, respectively, with contributions by the >3 μm fraction increasing 2- and 1.5-fold for both treatments, respectively. Chl *a* concentrations during NvN3 also increased ~5-fold in NO_3^- treatments and ~3-fold in NH_4^+ treatments over 5 d. Approximately 2- to 4-fold increases in rates of >0.2 μm ^{14}C primary production were observed for all nitrogen additions during N248 and NvN4, with a ~2-fold shift towards >3 μm organisms (Table 3, Fig. 2). Concentrations of Chl *a* increased modestly (~1.9- to 2.3-fold) during the winter experiment (N248) in all nitrogen addition treatments, while ~3- to 4-fold increases in Chl *a* concentrations were observed in both NO_3^- and NH_4^+ treatments during NvN4 over 5 d (Table 3, Fig. 3A, 3B). For both N248 and NvN4, moderate (~2- to 3-fold) increases in the contributions by the >3 μm size fraction to Chl *a* concentrations were observed. Cell abundances of photosynthetic picoeukaryotes increased ~3- to 5-fold in all nitrogen additions during all experiments, except for a ~12-fold increase in the NO_3^- treatment during NvN1 (Table 3).

5.4.3. Changes in eukaryotic phytoplankton community composition

Photosynthetic pigments

Photosynthetic pigments measured during NvN3 (July 2012) and NvN4 (April 2013) revealed variations in the timing and magnitude of the responses by different phytoplankton taxa to the various nitrogen additions (Fig. 3). Concentrations of fucoxanthin, a pigment biomarker diagnostic of diatoms, exhibited large increases during NvN3, with 49- and 23-fold increases in the NO_3^- and NH_4^+ treatments, respectively (Fig. 3C). In contrast, fucoxanthin concentrations increased ~9-fold in both NO_3^- and NH_4^+ additions during NvN4 (Fig. 3D), though the final concentration of fucoxanthin was considerably lower than that observed during NvN3. Pigments diagnostic of pelagophytes and prymnesiophytes, 19'-butanoyloxyfucoxanthin (19'-But) and 19'-hexanoyloxyfucoxanthin (19'-Hex), respectively, displayed the opposite pattern as fucoxanthin. During NvN3, 19'-But and 19'-Hex increased 5- and 3-fold, respectively, by 96 h in both NO_3^- and NH_4^+ treatments and decreased subsequently (Fig. 3E, G). During NvN4, both 19'-But and 19'-Hex reached maximum concentrations (11-fold and 6-fold, respectively) in the NO_3^- and NH_4^+ treatments after 48 h and remained elevated through the remainder of the experiment (Fig. 3F, H). Concentrations of peridinin, a pigment biomarker diagnostic of dinoflagellates, increased steadily throughout both NvN3 and NvN4 (Fig. 3I and J), with larger responses in the NH_4^+ treatments (increasing 7- to 9-fold in NvN3 and NvN4, respectively, compared to 4- to 5-fold increases observed in the NO_3^- treatments) for both experiments.

18S rDNA sequences

The V9 region of 18S rRNA genes was sequenced from size-fractionated samples collected during our experiments to assess possible time-varying changes in phytoplankton community structure following additions of nitrogenous substrates (Fig. 4). Analyses of the resulting relative abundances of phytoplankton OTUs revealed differences in the initial composition of the eukaryotic picophytoplankton (0.2-3 μm) among the different experiments; in contrast, the initial community composition of larger (>3 μm) phytoplankton appeared very similar between experiments. Dinoflagellates dominated the relative abundances (ranging 50-62% of the picophytoplankton 18S rRNA gene sequences) during the summer experiments (NvN1 and NvN3), with haptophytes and chrysophytes also relatively abundant (ranging ~11-16% and ~5-14%, respectively) in the picophytoplankton size fraction. In addition,

phytoplankton belonging to the dictyochophytes, bolidophytes, and eustigmatophytes were present at low relative abundances in the picophytoplankton size fraction (Fig. 6A). The initial picophytoplankton composition during the experiments conducted in the winter and spring months (NvN2, N248, and NvN4) included relative abundances of dinoflagellates lower than that during the summer (ranging 28-39% of picophytoplankton sequences), with greater contributions by pelagophytes (7-21%), haptophytes (5-27%), chrysophytes (6-21%) and dictyochophytes (5-9%). During the December experiment (N248), members of the Rhodophyta and marine ochrophytes (MOCH) were also present (~10% of picophytoplankton 18S rRNA gene sequences). For the larger phytoplankton (>3 μm), dinoflagellates (~76-88% on average) and diatoms (~5-12% on average) comprised a majority of the >3 μm sequences in all experiments, with no discernible seasonal variability. The taxonomic composition of the control carboys remained relatively constant for experiments N248 and NvN4 (Fig. 4B); however, in experiments NvN1, NvN2, and NvN3, members of the Bacillariophyceae increased in the >3 μm size fraction (Fig. 4B), and taxa belonging to the Eustigmatophyceae and Bolidophyceae increased slightly in the picophytoplankton fraction in NvN1 and NvN3, respectively (Fig. 4A).

While changes in phytoplankton community composition were very similar in the various nitrogen treatments (NO_3^-, NH_4^+, or urea), there were apparent differences in the resulting phytoplankton responses to the additions of nitrogen depending on the time of year that the experiments were conducted. For the picophytoplankton, members of the Bacillariophyceae demonstrated the largest increases in relative abundances experiments conducted in the summer (NvN1 and NvN3), increasing from 0.8-1.4% at the onset of the experiments to ~38-59% of the picophytoplankton sequences by the end of the experiments. In contrast, for those experiments conducted in the winter and spring months (N248, NvN2, and NvN4), members of the Pelagophyceae comprised ~7-21% of the picophytoplankton sequences at the onset of the experiments and increased to 34-39% following the additions of nitrogen by the end of the experiments, while diatom composition remained fairly low (~0-1% at onset to ~5-14% at end; Fig. 4A, 5). In the >3 μm size fraction, various taxa of diatoms were the dominant responders to nitrogen additions during all experiments (30-60% of >3 μm sequences), though the magnitude of response by diatoms was greatest during those experiments conducted in the summer (4-6% at onset of experiment to 57-60% of >3 μm sequences at final time point) compared to the response observed during those experiments conducted in the spring and winter months (6-12% to 30-49%

of >3 μm sequences at final time point; Fig. 4B, 5). In addition, the increase in the relative abundances of diatoms in the larger fraction during the summer was more rapid (occurring in the initial 48-96 h) compared to the responses observed in those experiments conducted in the spring and winter (Fig. 4B).

Changes in the relative abundances of the five most abundant OTUs for both size fractions were examined for the NO_3^- and NH_4^+ treatments by comparing relative abundances at the beginning of each experiment to the results at the end of the experiments (Fig. 5). Seasonal binning (winter, spring, and summer) of the experiments emphasized that the resulting trajectory of picophytoplankton community response appeared to depend on when the experiment was conducted. The dominant picophytoplankton at initial time points during the winter and spring included the pelagophyte *Pelagomonas* (averaging ~7% of picophytoplankton sequences in winter and ~19% in spring), dictyochophyte *Florenciella* (averaging ~8% of picophytoplankton sequences in winter and ~4% in spring), chrysophytes (averaging ~4-6% of picophytoplankton sequences in both winter and spring), and *Pfiesteria*-like dinoflagellates (averaging ~5-6% of picophytoplankton sequences in both winter and spring). During the spring months, the haptophyte *Prymnesium* also comprised ~5% of the picophytoplankton sequences, while members of the Raphidophyceae comprised ~7% of the picophytoplankton community during the winter experiment (Table 4). In contrast, during those experiments conducted in the summer, all of the most abundant picophytoplankton OTUs at the beginning of the experiments clustered among the Dinophyceae, including OTUs classified as *Gymnodinium*, *Gyrodinium*, *Karldonium*, *Pfiesteria*-like, and *Azadinium*.

By the end of the experiments, *Pelagomonas* demonstrated the largest increases in relative abundances of picophytoplankton sequences during those experiments initiated in the winter and spring, with smaller contributions by diatoms *Pseudo-nitzschia* and *Nitzschia*, dictyochophyte *Florenciella*, and Prasinophyceae Clade VII-A. In experiments conducted during the summer, diatoms *Pseudo-nitzschia*, *Nitzschia*, and *Minutocellus* demonstrated the largest increases in relative abundances of picophytoplankton (Table 4, Fig. 5). In the >3 μm fraction, the most dominant OTUs at the beginning of the experiments were members of the Dinophyceae irrespective of when the experiments were conducted (Table 4, Fig. 5). Following the addition of nitrogen substrates, the relative contributions by these dinoflagellates decreased, with correspondingly large increases in relative abundances of OTUs closely related to the diatoms

Pseudo-nitzschia and *Nitzschia* (Table 4). Despite often being undetectable at the onset of the experiments, relative abundances of OTUs belonging to these diatom genera comprised ~20 to 60% of the >3 μm phytoplankton sequences (Table 4).

Alpha diversity (assessed by the Shannon Index) of the picophytoplankton communities at the end of the experiments after nitrogen additions was significantly different from communities in the control carboys (paired t-test, $p < 0.05$; Fig. 6). For the larger phytoplankton, the diversity of communities at the end of the experiments was significantly different from that of the initial communities for nitrogen addition treatments only during the summer (paired t-test, $p < 0.05$). Alpha diversity for both pico- and larger phytoplankton did not differ between the NO_3^-, NH_4^+, and urea treatments amongst various seasons (paired t-test, $p > 0.1$; Fig. 6). Significant differences (paired t-test, $p < 0.05$) were observed between the alpha diversity of both pico- and larger phytoplankton communities in the NO_3^- treatments, between spring and summer. Higher Shannon index values were generally observed for both size fractions during the winter and spring compared to the summer experiments, regardless of treatment, likely reflecting the dominance of diatoms in the nitrogen amended treatments during the summer (Fig. 6).

5.5. Discussion

We conducted five experiments during the winter, spring, and summer months between July 2011 to April 2013 to examine the responses of the eukaryotic phytoplankton community to additions of NO_3^-, NH_4^+, or urea (along with PO_4^{3-} and $Si(OH)_4$). We assessed how the addition of nutrients with varying nitrogenous substrates influenced size-dependent responses in rates of primary production and concentrations of Chl *a*, and altered eukaryotic phytoplankton community structure based on changes in concentrations of photosynthetic pigments and analyses of 18S rDNA sequences. In three of the five experiments (NvN3, N248, NvN4), rates of NO_3^- and NH_4^+ drawdown were roughly equivalent between the nitrogen addition treatments. In addition, contributions of pico- and larger phytoplankton to ^{14}C primary production and Chl *a* concentrations did not differ significantly based on the type of nitrogen substrates added, except in NvN2. Thus, our results from five experiments suggest that the oxidation state of the inorganic nitrogen substrate (oxidized NO_3^- or reduced NH_4^+) did not play a major role in shaping the resulting phytoplankton response. A number of previous studies have demonstrated preferential assimilation of NH_4^+ relative to NO_3^- by phytoplankton, a response generally attributable to the

energetic savings associated with assimilation of reduced nitrogen substrates (Glibert and Goldman, 1981; Syrett, 1981; Horrigan and McCarthy, 1982). However, while early studies comparing NO_3^- and NH_4^+ (Strickland et al., 1969; Eppley et al., 1971) and urea (Newell et al., 1967) showed that elemental composition (C:N) and C:Chl ratio of phytoplankton changed depending on nitrogen source used, species composition and growth rates did not appear to be influenced by the type of nitrogen source added (Eppley et al., 1971).

Although our experiments were not designed to examine competition among phytoplankton for differing nitrogen substrates (*e.g.*, through additions of both NO_3^- and NH_4^+ to the same carboy), our results do provide insight into taxa best poised to respond to relatively large changes in nitrogen availability in this ecosystem. Two of our observations, 1) that the timing and response of phytoplankton to both NO_3^- and NH_4^+ were similar, and 2) that no significant changes were observed in our "control" carboys amended with only PO_4^{3-} and $Si(OH)_4$ (except for ~3-fold increase in photosynthetic picoeukaryote cell abundances during NvN1), likely reflect the chronic nitrogen limitation of the oligotrophic upper ocean waters of the NPSG. In these well-lit upper ocean waters, phytoplankton production is consistently light-saturated (Li et al. 2011, White et al. 2015), while concentrations of inorganic nitrogen are proportionately much lower than required for net growth (NO_3^-:PO_4^{3-} ratios of the upper ocean <1). Hence, our results suggest that energetic limitations likely do not restrict eukaryotic phytoplankton consumption of available nitrogen substrates in this habitat.

We observed moderate to large increases in the phytoplankton community response to nitrogen additions, shifting from a picophytoplankton-dominated community (43-77% picophytoplankton contribution to ^{14}C-primary production and 86-91% contribution of picophytoplankton to Chl *a*) to one with a greater representation by the larger (>3 μm) phytoplankton (46-79% contribution to ^{14}C-primary production and 19-45% contribution to Chl *a* by the end of the experiments). Sequencing of 18S rRNA genes provided insight into the types of eukaryotic phytoplankton in these size classes. The larger (>3 μm) phytoplankton community was comprised mainly of dinoflagellates at the onset of the experiment; however, following the addition of nitrogen substrates, diatom composition rapidly (within 5-6 days) expanded, contributing 30-60% of the >3 μm sequences. The diatom response was most significant during those experiments conducted in the summer, particularly in the NO_3^- treatment, where diatoms comprised ~90% of the >3 μm sequences by the end of the experiments. Such observations are

consistent with those of Mahaffey et al. (2012), who observed greater responses (> ~2-fold) in phytoplankton biomass following nutrient enrichment with deep sea water during the summer months than in other times of the year. Consistent with microscopic observations at Station ALOHA (Venrick, 1993; 1999; Scharek et al., 1999), diatoms were present in low concentrations (~1% of total sequences) at the onset of our experiments. The large response by diatoms following the addition of nitrogen may reflect their physiological capacity to outcompete other phytoplankton for available nitrogen when concentrations of NO_3^- and NH_4^+ are relatively high (Eppley et al., 1969). The large diatom response observed in the picophytoplankton size class during those experiments conducted in the summer suggests there are season-specific conditions at Station ALOHA that favor diatom growth during periods when incident light flux is elevated and upper ocean temperatures are warm. Furthermore, iron concentrations, which are not typically limiting in the near-surface waters at Station ALOHA, appear greatest at times when the mixed layer is shallowest, starting from spring into summer months (Boyle et al., 2005). Because iron requirements for diatoms exceed that of other phytoplankton (Sunda and Huntsman, 1995), elevated concentrations of iron may provide diatoms the competitive advantage during the summer. The availability of micronutrient requirements for growth, including vitamins, is an important point to consider in evaluating the differential response of phytoplankton to nitrogen additions in our experiments.

While diatoms were the dominant phytoplankton to respond to nitrogen additions in the >3 μm fraction in all of the experiments, differential response between seasons was observed among the picophytoplankton. Diatoms were still the major responders to nitrogen additions in the picophytoplankton fraction during the summer; however, the pelagophyte *Pelagomonas* responded significantly to additions of nitrogen substrates in the winter and spring. The observed differences in the resultant phytoplankton community composition in response to nitrogen may reflect differing diversity and composition of the communities at the start of the experiments. While pelagophytes comprised 0.8-1.4% of the picophytoplankton sequences at the onset of the summer experiments, they comprised a much larger fraction (6-21%) of the sequences when the winter and spring experiments were conducted. As *Pelagomonas* is typically found in greatest abundances in the low-lit regions of the euphotic zone (Timmermans et al., 2005), its higher relative abundances during the winter and spring months in the surface waters at Station ALOHA was surprising. However, our results are in agreement with a study that examined 18S rRNA

gene distributions over a two-year period at Station ALOHA, which found OTUs clustering closely among *Pelagomonas* in the upper euphotic zone (0-75 m) during winter and spring (Rii et al., in prep). These periods of elevated *Pelagomonas* relative abundance in the upper ocean coincided with periods where the mixed layer extended into the lower region of the euphotic zone (90-110 m), presumably entraining organisms typically found in the dimly-lit regions of the euphotic zone into regions of higher light (Rii et al., in prep). The pelagophytes' survival in the upper euphotic zone during this period of deeper mixing may reflect their flexible photophysiology (Dimier et al., 2009; Bidigare et al., 2014) compared to other phytoplankton, such as some diatoms, whose growth rates often decrease under fluctuating light conditions (van de Poll et al., 2007). In addition, their success may reflect their ability to acquire nitrogen through the increased supply of NO_3^- to the euphotic zone during periods of deeper mixing, as revealed by elevated expression of nitrate transporter genes for *Pelagomonas* suggesting high reliance on nitrate assimilation for nutritional demands (Dupont et al., 2014). Hence, we suspect that the rapid response by pelagophytes (specifically *Pelagomonas*) during spring and winter resulted from the relatively elevated abundances of these organisms at the beginning of the experiments, together with their ability to grow rapidly following the input of bioavailable nitrogen.

When examining alpha diversity, we observed a differential response in the size structure of eukaryotic phytoplankton diversity with the addition of nitrogen substrates, indicating varying degrees of resource competition amongst the different size classes. While the addition of nitrogen substrates induced 'bloom'-like conditions in picophytoplankton (thereby significantly decreasing alpha diversity), nitrogen addition induced growth in many different taxa in the larger (>3 μm) phytoplankton throughout the year (alpha diversity of the nitrogen treatments remained similar to the controls), except in summer when diatoms dominated. This suggests that competition for nutrients influences diversity more significantly for picophytoplankton than for larger phytoplankton.

The proliferation of different taxa in our experiments during different times of the year could also be influenced by top-down controls such as predation, viruses, or parasites. Our experiments excluded large grazers (>202 μm) from our carboys, presumably eliminating the influences of larger mesozooplankton as potential controls on phytoplankton diversity and community structure. However, microzooplankton and heterotrophic and mixotrophic protists

were likely retained in our experimental carboys, and they can be significant grazers of phytoplankton biomass (>40% of Chl *a* per day) in the open ocean (Calbet and Landry, 2004). Though diatoms are typically considered too large to be consumed efficiently by nano- and micro-predators (Frost, 1991; Cullen, 1995), smaller pennate diatoms (typically 2-15 µm in length) can be readily consumed by microzooplankton (Latasa et al., 1997). However, Latasa et al. (1997) observed uncoupling between growth and grazing in the upper 50 m, specifically for diatoms and pelagophytes, accounting for a majority of the net phytoplankton growth in the central equatorial Pacific. Thus, the rapid turnover of fast-growing species through active removal processes may maintain greater diversity (such as among the larger phytoplankton during the spring), despite the availability of nutrients (Longhurst, 1967; Timonin, 1969).

Interestingly, the initial eukaryotic phytoplankton communities (in the larger size class but also during the summer in the picophytoplankton size class) were dominated by dinoflagellates. Autotrophic dinoflagellates such as *Gymnodinium* are reported to lack peridinin, while containing fucoxanthin-related carotenoids (Millie et al., 1993). Such findings may explain why we observed high relative abundances of dinoflagellate OTUs in our study, while observations at Station ALOHA indicate low concentrations of peridinin (Letelier et al. 1993, Bidigare and Ondrusek 1996). Alternatively, the dominance of dinoflagellates in 18S rDNA sequences may be due to high rRNA gene copy numbers previously described among the dinoflagellates (Zhu et al., 2005; Not et al., 2009; Medinger et al., 2010). Moreover, the primers targeting the region (V9) of the 18S rRNA gene amplified in the current study may preferentially amplify dinoflagellates (Stoeck et al., 2010), biasing the sequence results toward these organisms. However, a recent PCR-independent metatranscriptome approach found that dinoflagellates dominated (36-40%) the mapped eukaryote transcripts at Station ALOHA (Alexander et al., 2015), suggesting that dinoflagellates are indeed important contributors to phytoplankton biomass in this ecosystem. In the current study, despite their initial dominance, dinoflagellates did not respond significantly to additions of NO_3^-, NH_4^+, or urea. Concentrations of peridinin increased gradually in two of the experiments (NvN3 and NvN4), but to a lesser extent than other measured pigments. Consistent with these results, additions of nutrient-enriched deep sea water to upper ocean plankton assemblages resulted in a minimal transcriptional response by dinoflagellates (Alexander et al., 2015). Such results, and those observed in the current study, may suggest that the dominant dinoflagellates at Station ALOHA

are heterotrophic or mixotrophic, thereby decreasing their dependence on inorganic nitrogen substrates. Consistent with this hypothesis is the observation that several of the taxa that predominated at the beginning of the experiments appear capable of mixotrophy, including dinoflagellates, haptophytes, chrysophytes, and dictyochophytes (Rothhaupt, 1996; Frias-Lopez et al., 2009; Liu et al., 2009). However, following nitrogen additions, many of these taxa decreased in relative abundance, with organisms not previously known to demonstrate mixotrophic growth (namely diatoms and pelagophytes) becoming increasing dominant. Such results provide support to the hypothesis that limiting nutrients are crucial to shaping plankton metabolism, including promoting mixotrophic modes of nutrient acquisition (Zubkov and Tarran, 2008; Hartmann et al., 2012).

After addition of inorganic nitrogen substrates, we observed a general shift in the size structure of the phytoplankton community from a picophytoplankton-dominated one to a community dominated by larger (>3 μm) phytoplankton. In our experiments, responses in ^{14}C-primary production, photosynthetic pigment biomass, and phytoplankton community composition appeared independent of the type of nitrogen substrate added. However, the picophytoplankton community response appeared seasonally dependent, with diatoms dominating the response during the summer while pelagophytes responded most significantly in the winter and spring. Diatoms in the larger fraction appear to be poised for rapid net growth throughout the year, while smaller, pennate diatoms appeared best able to capitalize on added nitrogen during the summer months. The variability in the responses by phytoplankton appear to stem from differences in initial picophytoplankton populations, which are likely a result of seasonal environmental changes such as mixed layer depth, light, and supply of nitrogen. Our findings provide insight into how abrupt changes in the availability of fixed nitrogen influences successional patterns in eukaryotic phytoplankton assemblages, and highlight those organisms poised for rapid growth when fixed nitrogen is available.

5.6. Acknowledgments

We thank the HOT program science team for the collection and analyses of some of the data used in this study. We would also like to acknowledge Donn Viviani and Brenner Wai for help with sample collection during the experiments. In addition, Brianne Maillot provided laboratory assistance, Susan Curless and Alexa Nelson contributed nutrient analyses, Markus

Lindh assisted with R, and Edward DeLong enabled use of a computer server for the Illumina sequence analyses. We also appreciate the support of the captain and crew of R/V *Kilo Moana*. Support for this work derived from U.S. National Science Foundation (NSF) grants OCE-1241263 and OCE-1260164 (MJC), the Center for Microbial Oceanography: Research and Education (C-MORE; EF-0424599, DMK), the Simons Collaboration on Ocean Processes and Ecology (SCOPE, DMK & MJC), and the University of Hawai‘i Denise B. Evans Research Fellowship in Oceanography (YMR).

5.7. References

Alexander, H., Rouco, M., Haley, S., Wilson, S., Karl, D.M., and Dyhrman, S. T. (2015). Functional group-specific traits drive phytoplankton dynamics in the oligotrophic ocean. *Proc. Natl. Acad. Sci. U.S.A.* 112, E5972-E5979. doi: 10.1073/pnas.1518165112

Amaral-Zettler, L. A., McCliment, E. A., Ducklow, H. W., and Huse, S. M. (2009). A method for studying protistan diversity using massively parallel sequencing of V9 hypervariable regions of small-subunit ribosomal RNA genes. *PLoS ONE* 4, e6372. doi:10.1371/journal.pone.0006372.t003

Armstrong, F. A. J., Stearns, C. R., and Strickland, J. D. H. (1967). The measurement of upwelling and subsequent biological processes by means of the Technicon AutoAnalyzerTM and associated equipment. *Deep-Sea Res.* 14, 381-389.

Arrigo, K. R. (2005). Marine microorganisms and global nutrient cycles. *Nature* 437, 349–355.

Atlas, E. L., Hager, S. W., Gordon, L. I., and Park, P. K. (1971). A practical manual for use of the Technicon AutoanalyzerTM in seawater nutrient analyses; revised. *Technical Report 215, Ref. No. 71-22,* Oregon State University, Dept. of Oceanography, 1–48.

Bernhardt, H., and Wilhelms, A. (1967). The continuous determination of low level iron, soluble phosphate and total phosphate with the AutoAnalyzer. *Technicon Symposium Vol I*, 386.

Bidigare, R. R., Buttler, F. R., Christensen, S. J., Barone, B., Karl, D. M., and Wilson, S. T. (2014). Evaluation of the utility of xanthophyll cycle pigment dynamics for assessing upper

ocean mixing processes at Station ALOHA. *J. Plankton Res.* 36, 1423-1433. doi:10.1093/plankt/fbu069.

Bidigare, R. R., and Ondrusek, M. E. (1996). Spatial and temporal variability of phytoplankton pigment distributions in the central equatorial Pacific Ocean. *Deep-Sea Res. II* 43, 809–833.

Bidigare, R. R., Van Heukelem, L., and Trees, C. C. (2005). "Analysis of algal pigments by high-performance liquid chromatography," in *Algal Culturing Techniques*, ed R. A. Andersen (New York: Academic Press), 327–345.

Boyle, E. A., Bergquist, B. A., Kayser, R. A., and Mahowald, N. (2005). Iron, manganese, and lead at Hawaii Ocean Time-series station ALOHA: Temporal variability and an intermediate water hydrothermal plume. *Geochim. Cosmochim. Acta* 69, 933–952. doi:10.1016/j.gca.2004.07.034.

Calbet, A., and Landry, M. R. (2004). Phytoplankton growth, microzooplankton grazing, and carbon cycling in marine systems. *Limnol. Oceanogr.* 49, 51-57.

Campbell, L., and Vaulot, D. (1993). Photosynthetic picoplankton community structure in the subtropical North Pacific Ocean near Hawaii (station ALOHA). *Deep-Sea Res. I* 40, 2043–2060.

Caporaso, J. G., Bittinger, K., Bushman, F. D., DeSantis, T. Z., Andersen, G. L., and Knight, R. (2010). PyNAST: a flexible tool for aligning sequences to a template alignment. *Bioinformatics* 26, 266–267.

Chavez, F. P., Buck, K. R., Bidigare, R. R., Karl, D. M., Hebel, D., Latasa, M., et al. (1995). On the chlorophyll a retention properties of glass-fiber GF/F filters. *Limnol. Oceanogr.* 40, 428-433.

Church, M. J., Mahaffey, C., Letelier, R. M., Lukas, R., Zehr, J. P., and Karl, D. M. (2009). Physical forcing of nitrogen fixation and diazotroph community structure in the North Pacific subtropical gyre. *Glob. Biogeochem. Cycle* 23, GB2020. doi:10.1029/2008GB003418.

Cullen, J. J. (1995). Status of the iron hypothesis after the open-ocean enrichment experiment. *Limnol. Oceanogr.* 47, 1336-1343.

Dandonneau, Y., Vega, A., Loisel, H., Penhoat, Y. D., and Menkes, C. (2003). Oceanic Rossby waves acting as a "hay rake" for ecosystem floating by-products. *Science* 302, 1548–1551.

Dimier, C., Giovanni, S., Ferdinando, T., and Brunet, C. (2009). Comparative ecophysiology of the xanthophyll cycle in six marine phytoplanktonic species. *Protist* 160, 397–411. doi:10.1016/j.protis.2009.03.001.

Dore, J. E., Letelier, R. M., Church, M. J., Lukas, R., and Karl, D. M. (2008). Summer phytoplankton blooms in the oligotrophic North Pacific Subtropical Gyre: Historical perspective and recent observations. *Prog. Oceanogr.* 76, 2–38. doi:10.1016/j.pocean.2007.10.002.

Dortch, Q. (1990). The interaction between ammonium and nitrate uptake in phytoplankton. *Mar. Ecol. Prog. Ser.* 61, 183–201. doi:10.3354/meps061183.

DuPont, C. L., McCrow, J. P., Valas, R., Moustafa, A., Walworth, N., Goodenough, U., et al. (2014). Genomes and gene expression across light and productivity gradients in eastern subtropical Pacific microbial communities. *ISME J.* 9, 1076-1092. doi:10.1038/ismej.2014.198.

Edgar, R. C., Haas, B. J., Clemente, J. C., Quince, C., and Knight, R. (2011). UCHIME improves sensitivity and speed of chimera detection. *Bioinformatics* 27, 2194–2200. doi:10.1093/bioinformatics/btr381.

Eppley, R. W., Carlucci, A. F., Holm-Hansen, O., Kiefer, D., McCarthy, J. J., Venrick, E., et al. (1971). Phytoplankton growth and composition in shipboard cultures supplied with nitrate, ammonium, or urea as the nitrogen source. *Limnol. Oceanogr.* 16, 741–751.

Eppley, R. W., Rogers, J. N., and McCarthy, J. J. (1969). Half-saturation constants for uptake of nitrate and ammonium by marine phytoplankton. *Limnol. Oceanogr.* 14, 912–920.

Eppley, R. W., Sharp, J. H., Renger, E. H., Perry, M. J., and Harrison, W. G. (1977). Nitrogen assimilation by phytoplankton and other microorganisms in the surface waters of the central North Pacific Ocean. *Mar. Biol.* 39, 111–120.

Faraway, J. J. (2002). Practical regression and ANOVA using R. 128-129. http://cran.r-project.org/doc/contrib/Faraway-PRA.pdf

Fawcett, S. E., Lomas, M. W., Casey, J. R., Ward, B. B., and Sigman, D. M. (2011). Assimilation of upwelled nitrate by small eukaryotes in the Sargasso Sea. *Nat. Geosci.* 4, 717–722. doi:10.1038/ngeo1265.

Frias-Lopez, J., Thompson, A., Waldbauer, J., and Chisholm, S. W. (2009). Use of stable isotope-labelled cells to identify active grazers of picocyanobacteria in ocean surface waters. *Environ. Microbiol.* 11, 512–525. doi:10.1111/j.1462-2920.2008.01793.x.

Frost, B. W. (1991). The role of grazing in nutrient-rich areas of the open sea. *Limnol. Oceanogr.* 36, 1616-1630.

Glibert, P. M., and Goldman, J. C. (1981). Rapid ammonium uptake by marine phytoplankton. *Mar. Biol. Lett*. 2, 25-31.

Hartmann, M., Grob, C., Tarran, G. A., Martin, A. P., Burkill, P. H., Scanlan, D. J., et al. (2012). Mixotrophic basis of Atlantic oligotrophic ecosystems. *Proc. Natl. Acad. Sci. U.S.A.*109, 5756–5760. doi:10.1073/pnas.1118179109.

Hollander, M., and Wolfe, D. A. (1973). Nonparametric statistical procedures. New York: Wiley.

Horrigan, S. G., and McCarthy, J. J. (1982). Phytoplankton uptake of ammonium and urea during growth on oxidized forms of nitrogen. *J. Plankton Res.* 4, 379–389.

Jardillier, L., Zubkov, M. V., Pearman, J., and Scanlan, D. J. (2010). Significant CO2 fixation by small prymnesiophytes in the subtropical and tropical northeast Atlantic Ocean. *ISME J.* 4, 1180–1192. doi:10.1038/ismej.2010.36.

Johnson, K. S., Riser, S. C., and Karl, D. M. (2010). Nitrate supply from deep to near-surface waters of the North Pacific subtropical gyre. *Nature* 465, 1062–1065. doi:10.1038/nature09170.

Karl, D. M. (2002). Nutrient dynamics in the deep blue sea. *Trends Microbiol.* 10, 410–418.

Karl, D. M., and Lukas, R. (1996). The Hawaii Ocean Time-series (HOT) program: Background, rationale and field implementation. *Deep-Sea Res. II* 43, 129–156.

Karl, D. M., Björkman, K. M., Dore, J. E., and Fujieki, L. (2001). Ecological nitrogen-to-phosphorus stoichiometry at station ALOHA. *Deep-Sea Res. II* 48, 1529–1566.

Karl, D. M., Christian, J., Dore, J. E., Hebel, D. V., Letelier, R. M., Tupas, L. M., et al. (1996). Seasonal and interannual variability in primary production and particle flux at Station ALOHA. *Deep-Sea Res. II* 43, 539–568.

Karl, D. M., Church, M. J., Dore, J. E., Letelier, R. M., and Mahaffey, C. (2012). Predictable and efficient carbon sequestration in the North Pacific Ocean supported by symbiotic nitrogen fixation. *Proc. Natl. Acad. Sci. U.S.A.* 109, 1842–1849. doi:10.1073/pnas.1120312109.

Karl, D. M., Letelier, R., Hebel, D., Bird, D. F., and Winn, C. (1992). "Trichodesmium blooms and new nitrogen in the North Pacific gyre," in *Marine Pelagic Cyanobacteria: Trichodesmium and Other Diazotrophs*, eds. E. J. Carpenter and D. G. Capone (Neterlands: Springer), 219-237.

Karl, D. M., Letelier, R., Tupas, L., Dore, J. E., Christian, J., and Hebel, D. (1997). The role of nitrogen fixation in biogeochemical cycling in the subtropical North Pacific Ocean. *Nature* 388, 533-538.

Lane, D. J. (1991). "16S/23S sequencing," in *Nucleic Acid Technologies in Bacterial Systematic*, eds. E. Stackebrandt and M. Goodfellow (New York: Wiley), 115–175.

Latasa, M., Landry, M. R., Schluter, L., and Bidigare, R. R. (1997). Pigment-specific growth and grazing rates of phytoplankton in the central equatorial Pacific. *Limnol. Oceanogr.* 42, 289–298.

Letelier, R. M., Bidigare, R. R., Hebel, D. V., Ondrusek, M. E., Winn, C. D., and Karl, D. M. (1993). Temporal variability of phytoplankton community structure based on pigment analysis. *Limnol. Oceanogr.* 38, 1420–1437.

Letelier, R. M., Dore, J. E., Winn, C. D., and Karl, D. M. (1996). Seasonal and interannual variations in photosynthetic carbon assimilation at Station. *Deep-Sea Res. II* 43, 467–490. doi:10.1016/0967-0645(96)00006-9.

Letelier, R. M., Karl, D. M., Abbott, M. R., and Bidigare, R. R. (2004). Light driven seasonal patterns of chlorophyll and nitrate in the lower euphotic zone of the North Pacific Subtropical Gyre. *Limnol. Oceanogr.* 49, 508–519.

Li, B., Karl, D. M., Letelier, R. M., and Church, M. J. (2011). Size-dependent photosynthetic variability in the North Pacific Subtropical Gyre. *Mar. Ecol. Prog. Ser* 440, 27–40. doi:10.3354/meps09345.

Li, Q. P., Zhang, J.-Z., Millero, F. J., and Hansell, D. A. (2005). Continuous colorimetric determination of trace ammonium in seawater with a long-path liquid waveguide capillary cell. *Mar. Chem.* 96, 73–85. doi:10.1016/j.marchem.2004.12.001.

Li, W. K. W. (1994). Primary Production of Prochlorophytes, Cyanobacteria, and Eukaryotic Ultraphytoplankton - Measurements From Flow Cytometric Sorting. *Limnol. Oceanogr.* 39, 169–175.

Liu, H., Probert, I., Uitz, J., Claustre, H., Aris-Brosou, S., Frada, M., et al. (2009). Extreme diversity in noncalcifying haptophytes explains a major pigment paradox in open oceans. *Proc. Natl. Acad. Sci. U.S.A.* 106, 12803–12808.

Longhurst, A. R. (1967). Diversity and trophic structure of zooplankton communities in the California Current. *Deep-Sea Res.* 14, 393-408.

Mahaffey, C., Björkman, K. M., and Karl, D. M. (2012). Phytoplankton response to deep seawater nutrient addition in the North Pacific Subtropical Gyre. *Mar. Ecol. Prog. Ser.* 460, 13–34. doi:10.3354/meps09699.

Medinger, R., Nolte, V., Pandey, R. V., Jost, S., Ottenwälder, B., Schlötterer, C., et al. (2010). Diversity in a hidden world: potential and limitation of next-generation sequencing for surveys of molecular diversity of eukaryotic microorganisms. *Mol. Ecol.* 19, 32–40. doi:10.1111/j.1365-294X.2009.04478.x.

Medlin, L., Elwood, H. J., Stickel, S., and Sogin, M. L. (1988). The characterization of enzymatically amplified eukaryotic 16S-like rRNA-coding regions. *Gene* 71, 491–499.

Millie, D. F., Paerl, H. W., Hurley, J. P., and Kirkpatrick, G. J. (1993). Algal pigment determinations in aquatic ecosystems: analytical evaluations, applications and recommendations. *Curr. Top. Bot. Res.* 1, 1–13.

Newell, B. S., Morgan, B., and Cundy, J. (1967). The determination of urea in seawater. *J. Mar. Res.* 25, 201-202.

Not, F., del Campo, J., Balagué, V., de Vargas, C., and Massana, R. (2009). New insights into the diversity of marine picoeukaryotes. *PLoS ONE* 4, e7143. doi:10.1371/journal.pone.0007143.t001.

Oksanen, J., Blanchet, F. G., Kindt, R., Legendre, P., Minchin, P. R. , O'Hara, R. B. et al. (2013). Package 'vegan': community ecology package. R package version 2.0-10. http://cran.r-project.org/web/packages/vegan/.

Paerl, R. W., Foster, R. A., Jenkins, B. D., Montoya, J. P., and Zehr, J. P. (2008). Phylogenetic diversity of cyanobacterial *narB* genes from various marine habitats. *Environ. Microbiol.* 10, 3377–3387. doi:10.1111/j.1462-2920.2008.01741.x.

Quast, C., Pruesse, E., Yilmaz, P., Gerken, J., Schweer, T., Yarza, P., et al. (2012). The SILVA ribosomal RNA gene database project: improved data processing and web-based tools. *Nucl. Acids Res.* 41, D590-D596..

R Core Development Team (2014). R: A language and environment for statistical computing. *Vienna: R Foundation for Statistical Computing*. https://cran.r-project.org/.

Rii, Y. M., Duhamel, S., Bidigare, R. R., Karl, D. M., Repeta, D., and Church, M. J. (2016). Diversity and productivity of photosynthetic picoeukaryotes in biogeochemically distinct regions of the South East Pacific Ocean. *Limnol. Oceanogr*. doi:10.1002/lno.10255.

Rii, Y. M., Lindh, M. V., and Church, M. J., in prep. Diversity and dynamics of eukaryotic picoplankton in the North Pacific Subtropical Gyre.

Rothhaupt, K. O. (1996). Laboratorary experiments with a mixotrophic chrysophyte and obligately phagotrophic and photographic competitors. *Ecology* 77, 716–724.

Royston, J. P. (1982). An extension of Shapiro and Wilk's W test for normality to large samples. *Appl. Stat.* 31, 115–124.

Sakamoto, C. M., Karl, D. M., Jannasch, H. W., Bidigare, R. R., Letelier, R. M., Walz, P. M., et al. (2004). Influence of Rossby waves on nutrient dynamics and the plankton community structure in the North Pacific subtropical gyre. *J. Geophys. Res.* 109, C05032. doi:10.1029/2003JC001976.

Scharek, R., Latasa, M., Karl, D. M., and Bidigare, R. R. (1999). Temporal variations in diatom abundance and downward vertical flux in the oligotrophic North Pacific gyre. *Deep-Sea Res. I* 46, 1051–1075.

Steeman Nielsen, E. (1952). The use of radioactive carbon (^{14}C) for measuring organic production in the sea. *J. Cons, Cons. Int. Explor. Mer* 18, 117–140.

Stoeck, T., Bass, D., Nebel, M., Christen, R., Jones, M. D. M., Breiner, H.-W., et al. (2010). Multiple marker parallel tag environmental DNA sequencing reveals a highly complex eukaryotic community in marine anoxic water. *Mol. Ecol.* 19, 21–31. doi:10.1111/j.1365-294X.2009.04480.x.

Strickland, J. D. H., Holm-Hansen, O., Eppley, R. W., and Linn, R. J. (1969). The use of a deep tank in plankton ecology. *Limnol. Oceanogr*. 14, 23-34.

Strickland, J. D. H., and Parsons, T. R. (1972). A practical handbook of seawater analysis. Bull. Fish. Res. Bd. Canada 167.

Sunda, W. G., and Huntsman, S. A. (1995). Iron uptake and growth limitation in oceanic and coastal phytoplankton. *Mar. Chem.* 50, 189-206.

Syrett, P. J. (1981). "Nitrogen metabolism of microalgae," in *Physiological basis of phytoplankton ecology*, ed. T. Platt (Quebec: Canadian Bulletin of Fisheries and Aquatic Sciences), 182–210.

Timmermans, K. R., Van der Wagt, B., Veldhuis, M. J. W., Maatman, A., De Baar, H. J. W. (2005). Physiological responses of three species of marine pico-phytoplankton to ammonium, phosphate, iron and light limitation. *J. Sea. Res.* 53, 109-120.

Timonin, A. G. (1969). Structure of pelagic associations – quantitative relationship between different trophic groups of plankton in frontal zones of tropical ocean. *Oceanology-USSR* 9, 686.

van de Poll, W. H., Vissier, R. J. W., and Buma, A. G. J. (2007). Acclimation to a dynamic irradiance regime changes excessive irradiance sensitivity of *Emiliana huxleyi* and *Thalassiosira weissflogii*. *Limnol. Oceanogr.* 52, 1430-1438.

Vaulot, D., Marie, D., Olson, R. J., and Chisholm, S. W. (1995). Growth of *Prochlorococcus*, a photosynthetic prokaryote, in the Equatorial Pacific Ocean. *Science* 268, 1480–1482.

Venrick, E. (1999). Phytoplankton species structure in the central North Pacific 1973-1996: variability and persistence. *J. Plankton Res.* 21, 1029–1042. doi:10.1093/plankt/21.6.1029.

Venrick, E. L. (1993). Phytoplankton seasonality in the central North Pacific: the endless summer reconsidered. *Limnol. Oceanogr*. 38, 1135-1149.

Villareal, T. A., Adornato, L., Wilson, C., and Schoenbaechler, C. A. (2011). Summer blooms of diatom-diazotroph assemblages and surface chlorophyll in the North Pacific gyre: A disconnect. *J. Geophys. Res* 116, C03001. doi:10.1029/2010JC006268.

Viviani, D. A., Karl, D. M., and Church, M. J. (2015). Variability in photosynthetic production of dissolved and particulate organic carbon in the North Pacific Subtropical Gyre. *Front. Mar. Sci.* 2, 763. doi:10.1029/95GB02149.

Wada, E., and Hattori, A. (1990). Nitrogen in the sea: Forms, abundance, and rate processes. Boca Raton: CRC Press.

White, A. E., Letelier, R. M., Whitmire, A. L., Barone, B., Bidigare, R. R., Church, M. J., et al. (2015). Phenology of particle size distributions and primary productivity in the North Pacific subtropical gyre (Station ALOHA). *J. Geophys. Res. Oceans* 120, 7381–7399. doi:10.1002/2015JC010897.

Wickham, H. (2009). *ggplot2: elegant graphics for data analysis*. New York: Springer Science & Business Media.

Wright, S. W., Jeffrey, S. W., Mantoura, R. F. C., Llewellyn, C. A., Bjornland, T., Repeta, D., et al. (1991). Improved HPLC method for the analysis of chlorophylls and carotenoids from marine phytoplankton. *Mar. Ecol. Prog. Ser.* 77, 183–196.

Zhang, J., Kobert, K., Flouri, T., and Stamatakis, A. (2014). PEAR: a fast and accurate Illumina Paired-End reAd mergeR. *Bioinformatics* 30, 614–620. doi:10.1093/bioinformatics/btt593.

Zhu, F., Massana, R., Not, F., Marie, D., and Vaulot, D. (2005). Mapping of picoeucaryotes in marine ecosystems with quantitative PCR of the 18S rRNA gene. *FEMS Microbiol. Ecol.* 52, 79–92. doi:10.1016/j.femsec.2004.10.006.

Zubkov, M. V., and Tarran, G. A. (2008). High bacterivory by the smallest phytoplankton in the North Atlantic Ocean. *Nature* 455, 224–226. doi:10.1038/nature07236.

Table 5.1. Sea surface temperature (SST), mixed layer depth (MLD), day length, surface PAR, and concentrations of chlorophyll *a* (Chl *a*), nitrate + nitrite (N+N), phosphate (PO_4^{3-}), and silicic acid ($Si(OH)_4$) at 25 m when experiments were conducted. Properties measured in each experiment are also indicated. n/a = not available.

	Experiment				
Parameter	NvN1	NvN2	NvN3	N248	NvN4
Dates	22-27 Jul 2011	27 Mar-1 Apr 2012	11-17 Jul 2012	7-13 Dec 2012	9-14 Apr 2013
Cruise #	HOT 233	HOT 240	HOE-DYLAN 5	HOT 248	HOT 251
Exp. duration (h)	120	120	144	144	120
SST (°C)	25.3	23.0	24.8	24.8	22.7
MLD (m)	78 ± 9	36 ± 6	58 ± 13	92 ± 11	77 ± 28
Day length (hh:mm)†	13:11	12:14	13:23	10:50	12:20
Surface PAR (mol quanta m^{-2} d^{-1})	44.1	n/a	44.3	15.2	38.2
Chl *a* (ng L^{-1})	65.0	77.0	81.6	111.4	68.0
N+N (µM N)	0.003	0.004	0.002	0.004	0.004
PO_4^{3-} (µM P)	0.090	0.089	0.060	0.091	0.070
$Si(OH)_4$ (µM Si)	1.050	1.159	0.850	1.122	1.210
Properties measured‡:					
Nutrients	+	+	+	+	+
Chl *a*/Sz fx Chl *a*	+/-	-/-	+/-	-/+	+/+
Pigments/FCM	-/+	-/+	+/+	-/+	+/+
^{14}C PP	-	+	+	+	+
DNA	+	+	+	+	+

†Day length obtained from www.solartopo.com

‡Nutrients = nitrate + nitrite, ammonium, phosphate, and silicic acid; Sz fx Chl *a* = Size-fractionated chlorophyll *a*; FCM = flow cytometric cell abundances; ^{14}C PP = ^{14}C primary production

Table 5.2. Target and actual concentrations of added nitrate + nitrite, ammonium, phosphate, and silicic acid at initial time point (T_0) of experiments. Concentrations of urea were not measured. Values shown are mean ± standard deviation of the triplicate carboys for each treatment. Drawdown rates were calculated as the daily nutrient consumption over a 120 h (5 d) period. nd: not determined. ∗ indicates no significant difference in concentrations over time (one-way ANOVA, Kruskal-Wallis, and linear regression model against null hypothesis of slope = 0, p > 0.05)

		$NO_3^- + NO_2^-$		NH_4^+		$PO4^{3-}$		$Si(OH)_4$	
Experiment	Treatment	Actual T_0 (μM)	Drawdown rate (μM d^{-1}) / % of initial	Actual T_0 (μM)	Drawdown rate (μM d^{-1}) / % of initial	Actual T_0 (μM)	Drawdown rate (μM d^{-1})	Actual T_0 (μM)	Drawdown rate (μM d^{-1})
NvN1	CON	--	∗	--	nd	0.3 ± 0.00	∗	2.7 ± 0.01	∗
	+NIT	3.2 ± 0.01	0.53 / 83%	--	nd	0.3 ± 0.00	0.03	2.8 ± 0.01	0.24
	+AMM	--	--	nd	nd	0.3 ± 0.00	0.03	2.7 ± 0.01	0.23
NvN2	CON	--	∗	--	∗	0.1 ± 0.00	∗	1.3 ± 0.00	∗
	+NIT	2.5 ± 0.00	0.14 / 28%	--	--	0.3 ± 0.00	0.01	2.5 ± 0.00	0.02
	+AMM	--	--	5.2 ± 0.02	0.89 / 85%	0.3 ± 0.00	0.02	2.5 ± 0.00	0.01
NvN3	CON	--	∗	--	∗	0.1 ± 0.01	∗	2.3 ± 0.03	∗
	+NIT	2.6 ± 0.07	0.16 / 32%	--	--	0.1 ± 0.01	0.01	2.3 ± 0.05	0.07
	+AMM	--	--	2.2 ± 0.01	0.14 / 32%	0.2 ± 0.03	0.002	2.3 ± 0.03	0.06
N248	CON	--	∗	--	∗	0.2 ± 0.00	∗	2.8 ± 0.01	∗
	+NIT	2.9 ± 0.02	0.11/ 18%	--	--	0.1 ± 0.01	∗	3.7 ± 0.01	∗
	+AMM	--	--	3.0 ± 0.02	0.19/ 32%	0.1 ± 0.00	∗	2.5 ± 0.01	∗
	+UREA	--	--	--	--	0.2 ± 0.00	∗	4.1 ± 0.00	∗
NvN4	CON	--	∗	--	∗	0.2 ± 0.00	∗	2.4 ± 0.00	∗
	+NIT	2.8 ± 0.01	0.21 / 38%	--	∗	0.2 ± 0.00	0.01	2.5 ± 0.01	0.02
	+AMM	--	∗	2.7 ± 0.01	0.22 / 41%	0.2 ± 0.00	0.004	2.5 ± 0.00	0.02

Table 5.3. Ratios of change from T_0 (initial time point) to T_{120} (120 h time point) in >0.2 µm ^{14}C-based carbon fixation rates, chlorophyll *a*, and photosynthetic picoeukaryote (PPE) cell abundances for each treatment per experiment. Percentage contribution of the pico- (0.2-3 µm) and larger (>3 µm) fractions to >0.2 µm ^{14}C carbon fixation rates and chlorophyll *a* at T_0 and T_{120} are also noted. Values indicate mean ± standard deviation of triplicate carboys per treatment. nd: not determined.

		^{14}C-primary production					Chlorophyll *a*					
		>0.2 µm*	0.2-3 µm (%)		>3 µm (%)		>0.7 µm	0.7-3 µm (%)		>3 µm (%)		PPE
Experi-ment	Treat-ment	T_{120}:T_0	T_0	T_{120}	T_0	T_{120}	T_{120}:T_0	T_0	T_{120}	T_0	T_{120}	T_{120}:T_0
NvN1	CON	nd	nd	nd	nd	nd	nd	nd	nd	nd	nd	3.2 ± 0.5
	+NIT	nd	nd	nd	nd	nd	nd	nd	nd	nd	nd	12 ± 3.6
	+AMM	nd	nd	nd	nd	nd	nd	nd	nd	nd	nd	8.5 ± 1.6
NvN2	CON	2.4 ± 0.3	69 ± 5	57 ± 10	31 ± 5	43 ± 10	nd	nd	nd	nd	nd	0.9 ± 0.2
	+NIT	17.1 ± 3.1	72 ± 1	25 ± 5	28 ± 1	75 ± 5	nd	nd	nd	nd	nd	3.7 ± 1.3
	+AMM	27.1 ± 28.1	68 ± 7	52 ± 14	32 ± 7	48 ± 14	nd	nd	nd	nd	nd	3.5 ± 1.3
NvN3	CON	1.8 ± 0.6	43 ± 10	59 ± 10	57 ± 10	41 ± 10	0.6 ± 0.1†	nd	nd	nd	nd	1.9 ± 0.3
	+NIT	21.1 ± 10.7	60 ± 4	21 ± 15	40 ± 4	79 ± 15	6.5 ± 2.3†	nd	nd	nd	nd	2.6 ± 0.6
	+AMM	15.4 ± 12.3	55 ± 9	34 ± 14	45 ± 9	66 ± 14	4.5 ± 1.4†	nd	nd	nd	nd	3.4 ± 0.8
N248	CON	0.6 ± 0.4	76 ± 3	47 ± 12	24 ± 3	53 ± 12	0.6 ± 0.3‡	90 ± 5	78 ± 2	10 ± 5	22 ± 2	0.9 ± 0.1
	+NIT	3.0 ± 1.4	71 ± 9	52 ± 3	29 ± 9	48 ± 3	1.9 ± 0.7‡	89 ± 1	73 ± 4	11 ± 1	27 ± 4	2.7 ± 0.6
	+AMM	2.8 ± 2.3	77 ± 5	42 ± 8	23 ± 5	58 ± 8	2.3 ± 0.8‡	91 ± 3	76 ± 2	9 ± 3	24 ± 2	4.8 ± 1.0
	+UREA	2.4 ± 1.1	77 ± 0	54 ± 15	23 ± 0	46 ± 15	1.9 ± 1.2‡	91 ± 1	78 ± 18	9 ± 1	22 ± 18	3.0 ± 1.6
NvN4	CON	0.4 ± 0.2	70 ± 2	44 ± 8	30 ± 2	56 ± 8	1.0 ± 0.3‡	90 ± 1	75 ± 4	10 ± 1	25 ± 4	0.9 ± 0.1
	+NIT	3.6 ± 1.5	72 ± 2	36 ± 4	28 ± 2	64 ± 4	3.1 ± 0.6‡	87 ± 2	81 ± 5	13 ± 2	19 ± 5	3.1 ± 1.5
	+AMM	3.9 ± 1.7	68 ± 2	48 ± 13	32 ± 2	52 ± 13	3.9 ± 0.4‡	86 ± 3	55 ± 1	14 ± 3	45 ± 1	2.8 ± 0.9

*Sum of 0.2-3 µm and >3 µm fractions

†Chl *a* measured on GF/F glass fiber filters (>~0.7 µm)

‡Chl *a* as sum of ~0.7-3 µm and >3 µm fractions

Table 5.4. Mean relative abundances (and standard deviations) of most abundant OTUs at initial (T_0) and final timepoints (T_f) for NO_3^- (+NIT) and NH_4^+ (+AMM) treatments in winter, spring, and summer

					0.2-3 µm						>3 µm					
					Winter (W) / Spring (S)			Summer			Winter (W) / Spring (S)			Summer		
OTU ID	Phylum	Class	Genus / Clone ID	Accession # (% Identity)	T_0	+NIT T_f	+AMM T_f	T_0	+NIT T_f	+AMM T_f	T_0	+NIT T_f	+AMM T_f	T_0	+NIT T_f	+AMM T_f
NR817	Archaeplastida	Prasinophyceae	Clade VII Subclade A	KF031914 (99.2)	--	3.4 (0.5)W 2.1 (2.2)S	--	--	--	--	--	--	--	--	--	--
FJ947	Alveolata	Dinophyceae	*Gymnodinium*	AY664983 (100)	--	--	--	--	--	--	4.4 (2.8)S	--	--	4.6 (2.1)	--	--
AY421	Alveolata	Dinophyceae	*Gymnodinium*	KJ763663 (100)	--	--	--	6.1 (2.4)	--	--	17.1 (2.2)W 22.3 (3.1)S	6.8 (5.2)W	7.0 (4.0)W 5.9 (3.2)S	23.0 (2.2)	--	5.0 (2.3)
NR371	Alveolata	Dinophyceae	*Gyrodinium*	EU793388 (100)	--	--	--	--	--	--	5.6 (0.9)W 4.4 (1.3)S	--	--	--	--	--
EU371	Alveolata	Dinophyceae	*Gyrodinium*	GU824196 (100)	--	--	--	4.2 (1.7)	--	--	13.1 (3.5)W 10.7 (2.7)S	4.8 (3.1)W	4.9 (2.9)W	8.2 (1.5)	--	--
NR766	Alveolata	Dinophyceae	*Gyrodinium*	KJ763375 (100)	--	--	--	--	--	--	--	--	--	4.4(3.0)	--	--
FJ832	Alveolata	Dinophyceae	*Gyrodinium*	KJ763897 (100)	--	--	--	--	--	--	5.1 (0.1)W	--	--	--	--	--
JF791	Alveolata	Dinophyceae	*Karlodinium* clone 3521	JF791085 (100)	--	--	--	4.2 (1.3)	--	--	--	--	--	--	--	--
NR151	Alveolata	Dinophyceae	*Protoperidinium*	AY665007 (96%)	--	--	--	--	--	--	5.6 (7.9)W	--	--	--	--	--
EU048	Alveolata	Dinophyceae	*Scrippsiella*	EF492513 (99.2)	--	--	--	--	--	--	--	--	--	--	1.2 (2.1)	--
NR54	Alveolata	Dinophyceae	*Pfiesteria*-like	KJ763477 (100)	5.1 (1.7)W 6.4 (0.7)S	--	--	8.0 (1.6)	--	--	--	--	--	--	--	--
NR95	Alveolata	Dinophyceae	*Azadinium*	KJ763656 (100)	--	--	--	5.3 (1.8)	--	--	6.3 (1.2)S	--	--	9.0 (2.4)	--	--
JQ616	Alveolata	Dinophyceae	*Prorocentrum*	KF032443 (100)	--	--	--	--	--	--	--	--	6.2 (5.1)W	--	--	--
NR445	Haptophya	Prymnesiophyceae	Uncultured, clone OLI16010	HM581633 (100)	--	2.5 (1.6)S	--	--	--	--	--	--	--	--	--	--
AHAL	Haptophyta	Prymnesiophyceae	*Emiliana huxleyi*	AHALO10037 37 (100)	--	--	--	--	--	--	--	4.6 (1.7)S	--	--	--	--
AB183	Haptophyta	Prymnesiophyceae	*Prymnesium*	AJ246271 (100)	4.6 (3.1)S	--	--	--	--	--	--	--	--	--	--	--
KC771	Ochrophyta	Bacillariophyceae	*Nitzschia*	KC771161 (100)	--	5.9 (5.6)W	11.6 (4.6)W	--	29.1 (24.1)	40.8 (28.6)	--	28.8 (24.3)W 7.0 (5.0)S	23.4 (9.4)W	--	12.1 (9.9)	25.2 (18.6)
NR672	Ochrophyta	Bacillariophyceae	*Pseudo-nitzschia*	JN091708 (96.9)	--	2.7 (1.9)S	3.5 (6.1)S	--	38.1 (22.3)	15.3 (16.0)	--	19.8 (8.5)W 23.0 (11.8)S	14.9 (19.0)W 15.1 (15.5)S	--	60.2 (27.2)	29.5 (30.9)
GU823	Ochrophyta	Bacillariophyceae	*Pseudo-nitzschia*	GU823170 (98.4)	--	--	8.4 (12.9)S	--	--	--	--	7.8 (7.8)S	16.3 (23.2)S	--	--	--
JF790	Ochrophyta	Bacillariophyceae	*Minutocellus* clone 1103	JF790976 (100)	--	--	3.4 (6.0)S	--	8.9 (10.7)	--	--	--	6.4 (9.9)S	--	9.9 (12.7)	4.5 (7.6)
NR813	Ochrophyta	Bolidophyceae	*Bolidomonas*	AF123596 (100)	--	--	--	--	5.7 (6.6)	10.5 (13.8)	--	--	--	--	--	--
KC583	Ochrophyta	Bolidophyceae	*Bolidomonas*	KC583013 (100)	--	--	2.6 (2.1)W	--	--	3.5 (4.3)	--	--	--	--	--	--
NR757	Ochrophyta	Bolidophyceae	*Bolidomonas pacifica*	HQ912557 (100)	--	2.0 (0.7)W	--	--	--	--	--	--	--	--	--	--

EU561	Ochrophyta	Chrysophyceae	Uncultured, clone E222	EU561701 (100)	5.6 (1.0)W 4.4 (1.3)S	--	--	--	--	--	--	--	--	--	--	--
AB217	Ochrophyta	Dictyochophyceae	*Florenciella*	KC583002 (100)	8.3 (2.9)W 3.8 (0.7)S	2.2 (0.6)W 8.7 (8.6)S	8.0 (2.4)W 6.4 (4.3)S	--	--	--	--	--	--	--	--	--
GU474	Ochrophyta	Eustigmatophyceae	uncultured, BCB5F14RJ2C0	GU474113 (100)	--	--	3.2 (0.4)W	--	2.0 (1.5)	4.0 (4.5)	--	--	--	--	2.6 (5.0)	4.9 (6.5)
LC012	Ochrophyta	Pelagophyceae	*Pelagomonas*	LC012594 (100)	6.6 (0.1)W 18.5 (5.0)S	59.1 (2.9)W 51.6 (6.9)S	45.3 (8.3)W 40.0 (8.0)S	--	--	--	--	3.3 (0.3)W 8.1 (3.1)S	6.3 (4.2)S	--	--	--
KC582	Ochrophyta	Raphidophyceae	Uncultured	KC582978 (100)	6.7 (0.02)W	--	--	--	--	--	--	--	--	--	--	--

Figure 5.1. Climatological variability in (A) sea surface temperature (°C; 1988-2014), (B) mixed layer depth (m; 1988-2014), (C) daily integrated PAR at 25 m (mol quanta m^{-2} d^{-1}; 1998-2013), and (D) concentrations of nitrate + nitrite at 25 m (nM N; 1989-2013) at Station ALOHA. Measurements from those occasions when experiments for the current study were conducted are denoted with black triangles. For each boxplot: dark horizontal line indicates the median, the box boundaries represent the 25th and the 75th percentile, and the whiskers extend to the maximum and minimum (boundary +/- 1.5*interquartile range) of the selected observations. Outlier observations, considered to be beyond the maximum and minimum limits of the observations, are depicted as open circles.

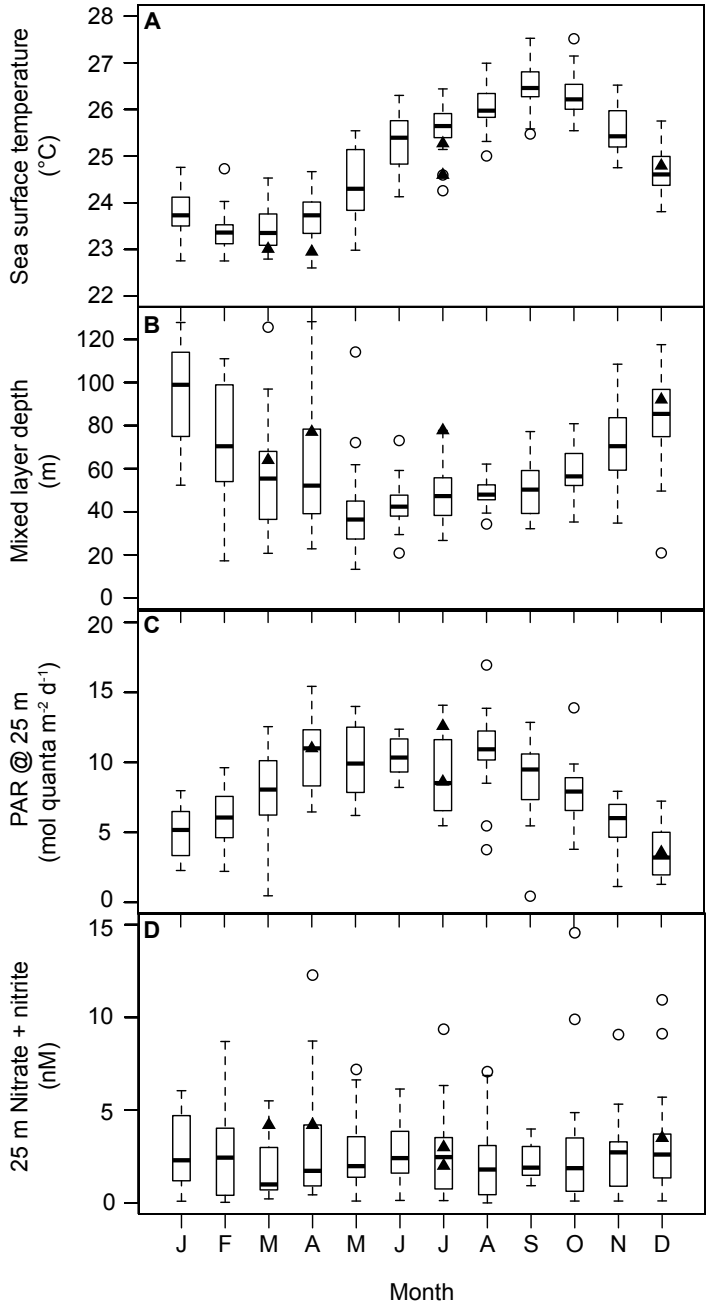

Figure 5.2. Time dependence in rates of ^{14}C-primary production (mmol C m^{-3} d^{-1}) by pico- (0.2-3 µm) and larger (>3 µm) phytoplankton during (A-B) NvN2, (C-D) NvN3, (E-F) N248, and (G-H) NvN4. Colors of lines indicate different treatments: CON = control, +NIT = NO_3^- treatment, +AMM = NH_4^+ treatment, and +UREA = urea treatment. Data points and whiskers indicate means and standard deviations of triplicate carboys. Note differences in y-axis scales for panels A, B, and D.

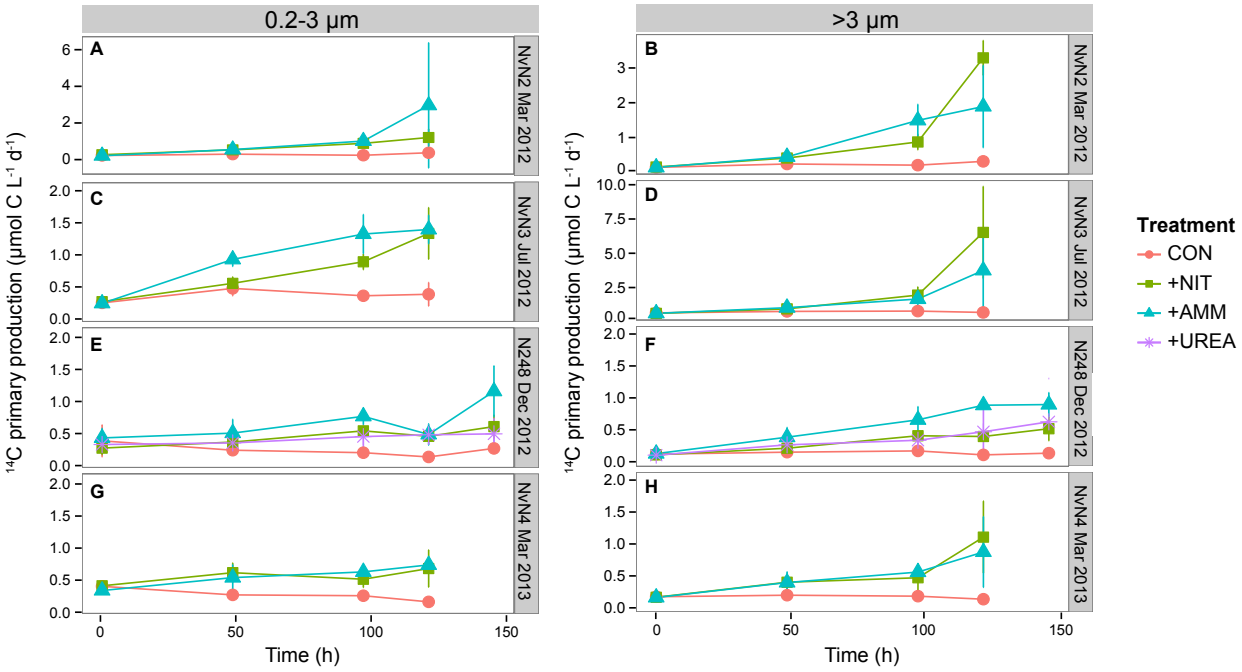

Figure 5.3. Photosynthetic pigment concentrations (ng L^{-1}) during NvN3 and NvN4 from time 0 to end of experiment (120 or 144 h): (A-B) Chl *a*, (C-D) fucoxanthin (Fuco), (E-F) 19'-butanoyloxyfucoxanthin (19'-But), (G-H) 19'-hexanoyloxyfucoxanthin (19'-Hex), (I-J) peridinin (Peri). Note differences in y-axis scales. Line colors indicate different treatments: CON = control, +NIT = NO_3^- treatment, and +AMM = NH_4^+ treatment. Data points and whiskers indicate means and standard deviations of triplicate carboys.

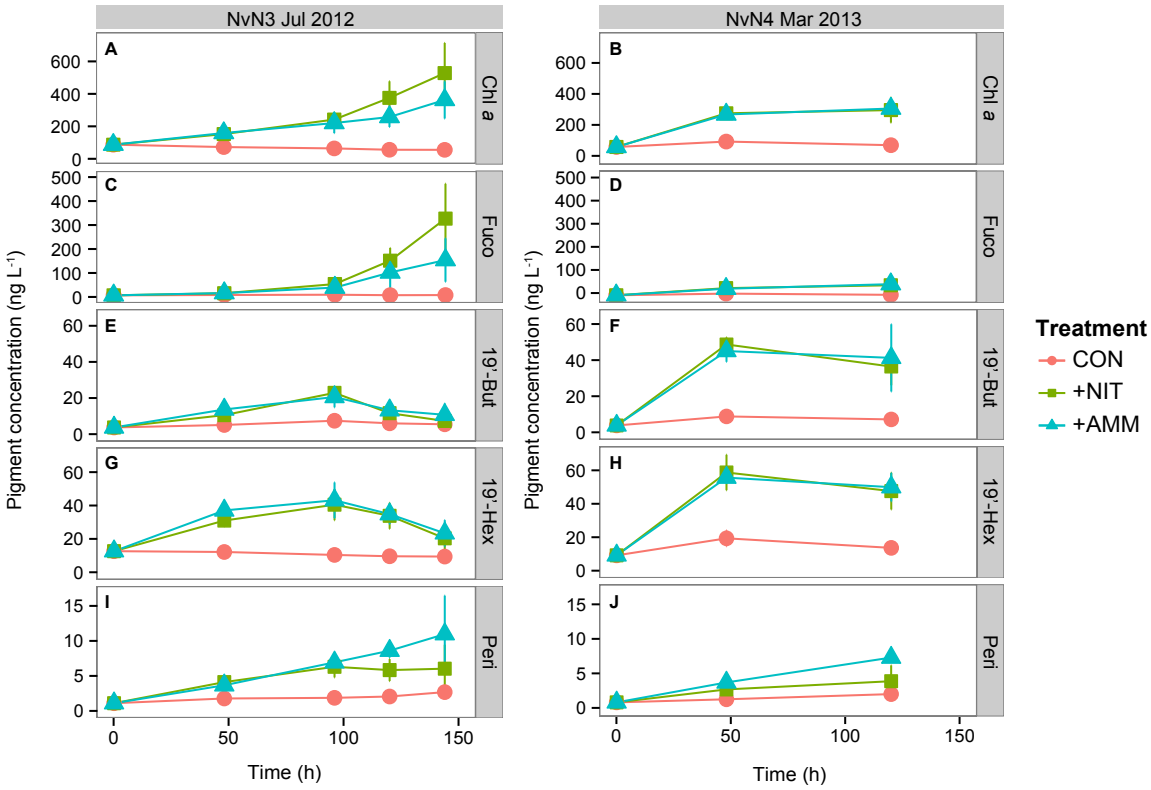

Figure 5.4. Relative abundances (%) of (A) picophytoplankton and (B) >3 µm phytoplankton taxa, binned by time point sampled. Columns indicate mean (of triplicate carboys) relative abundances for different experiments and rows specify the different treatments: CON = control, +NIT = NO_3^- treatment, +AMM = NH_4^+ treatment, and +UREA = urea treatment. Colors indicate various phytoplankton taxa.

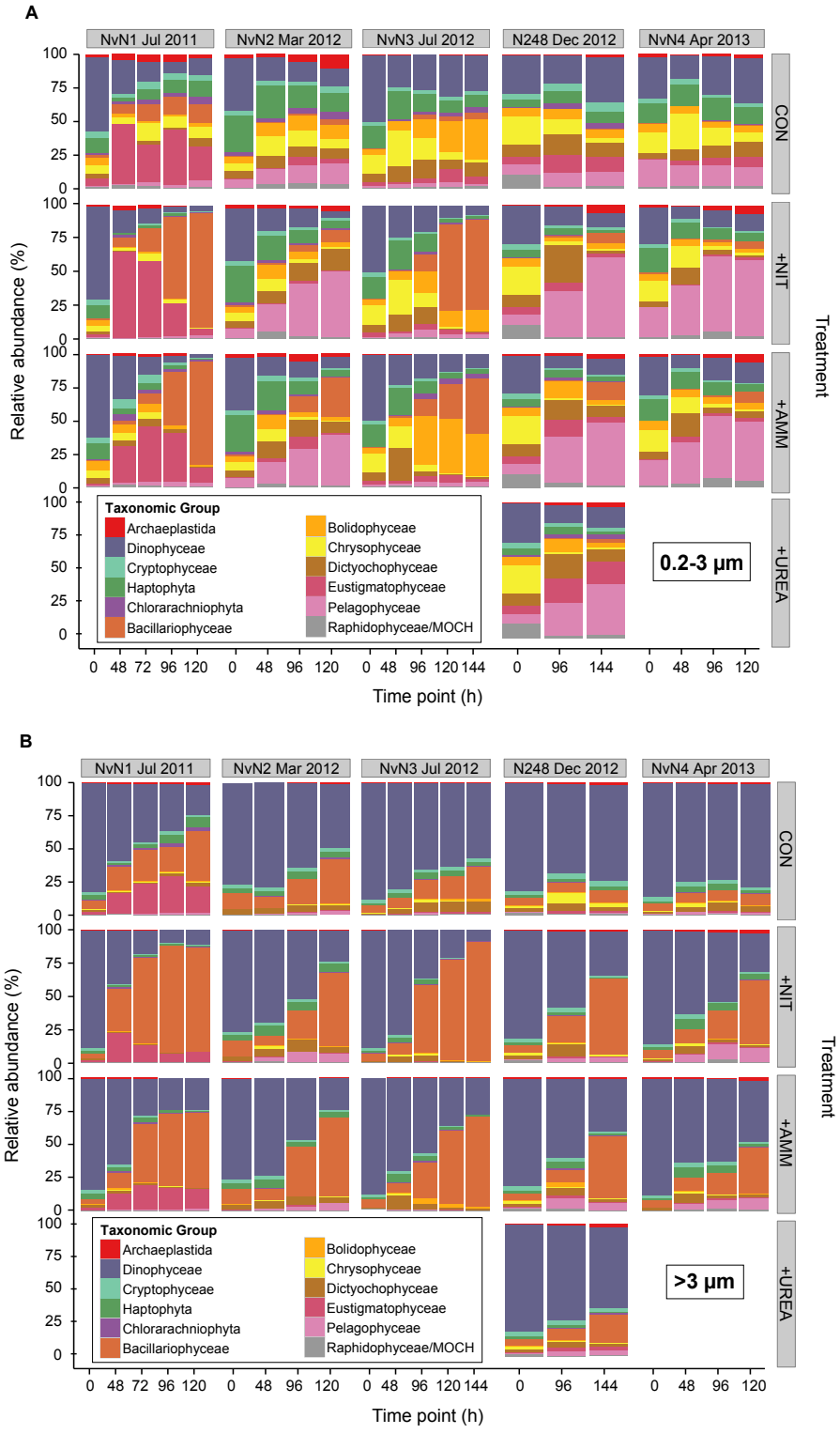

Figure 5.5. Mean relative abundances (%) of the most abundant pico- and >3 µm phytoplankton at initial (T_0) time points and final (T_f) time points for NO_3^- (+NIT) and NH_4^+ (+AMM) treatments during experiments binned by season when experiment was conducted (winter, spring, and summer). Mean relative abundances of phytoplankton taxa depicted using different colors and bubble sizes (size reflects relative abundance). Detailed information on the OTUs listed is listed in Table 4.

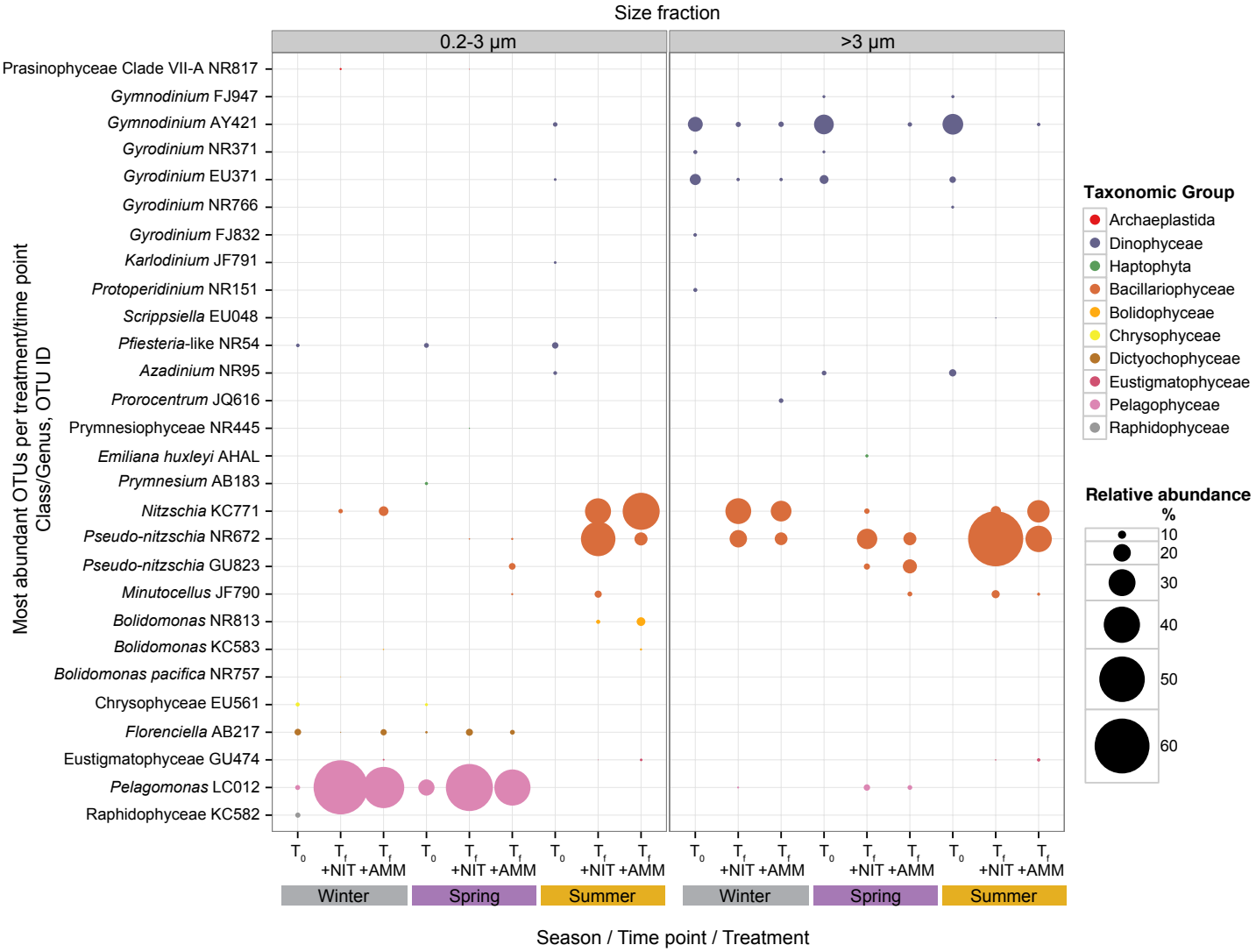

Figure 5.6. Alpha diversity (Shannon index) of the pico- and >3 µm phytoplankton V9 18S rDNA OTUs at final time points for control (CON), NO_3^- (+NIT) and NH_4^+ (+AMM) treatments binned by winter, spring, and summer. Boxplot parameters are the same as described for Fig. 1.

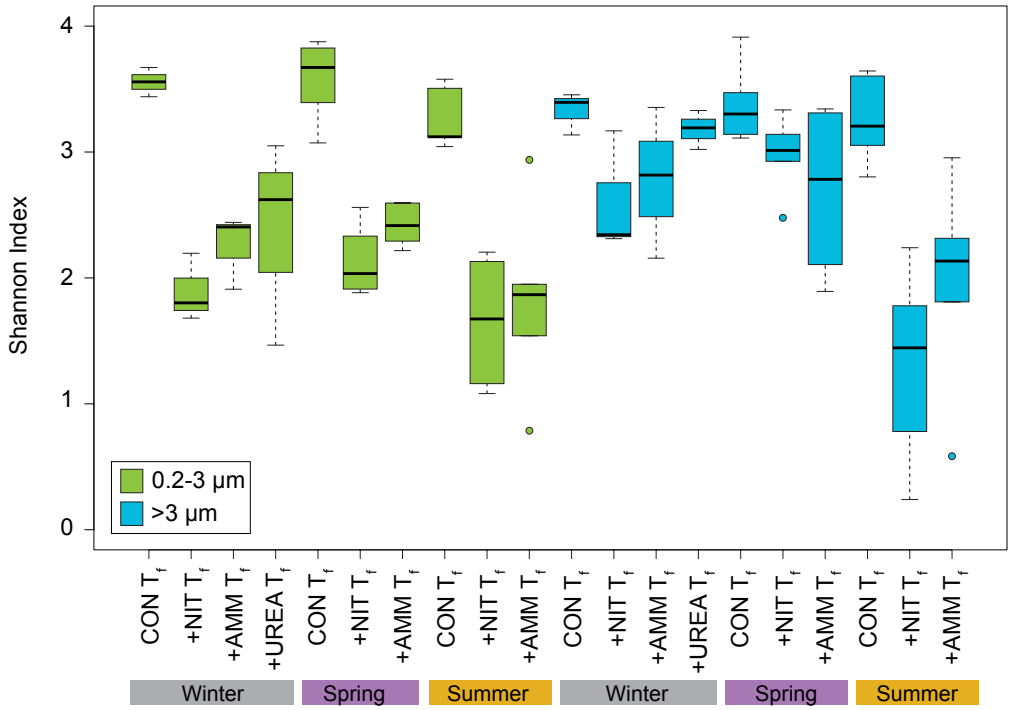

CHAPTER 6 – Conclusions and Future Directions

This dissertation research explored the diversity and activity of photosynthetic picoeukaryotes (PPE) in the oligotrophic North Pacific Subtropical Gyre (NPSG) and the South East Pacific Ocean (SEP). I utilized a suite of approaches, including size-fractionated photosynthetic pigments and rates of ^{14}C primary productivity, flow cytometric sorting of ^{14}C-radiolabeled picoplankton cells, and 18S rRNA gene amplification and sequencing of PPE cells to describe the temporal and vertical dynamics associated with these microorganisms. My research revealed that PPE are highly active on a per cell basis in the oligotrophic ocean, especially in the well-lit regions of the euphotic zone. I also observed diverse and distinct PPE taxa composition between the well-lit and low-light regions of the euphotic zone at Station ALOHA in the NPSG and along biogeochemically distinct regions in the SEP. In the NPSG, variability in PPE taxa composition in the euphotic zone was seasonally dependent. This chapter provides a synthesis of findings from each research unit and identifies important questions that merit future research.

6.1. Research synthesis

To better understand picophytoplankton productivity and the role of PPE in carbon cycling, PPE contributions to primary production were evaluated in the oligotrophic South Pacific Subtropical Gyre (SPSG, near Rapa Nui, or Easter Island) and in the eutrophic stations influenced by coastal upwelling (near Arica, Chile; Chapter 2). Large differences in phytoplankton community structure (both size and taxonomic affiliation) were observed between the gyre and the coastal station, with diatoms and dinoflagellates comprising the community at the coastal station (>3 μm fraction making up 45% of total chlorophyll *a*, or TChl *a*) and picophytoplankton dominating in the gyre station (0.2-3 μm fraction comprising 82-92% of TChl *a*). Despite this large difference in chlorophyll concentrations between the stations, the fractional contribution of picophytoplankton to ^{14}C primary production remained largely invariant (>60%), suggesting picoplankton remained active components of the microbial food web across widely varying trophic conditions sampled along the transect. Such results are consistent with previous studies suggesting that in regions where nutrients are actively supplied to the upper ocean, contributions by larger phytoplankton to productivity and biomass are superimposed on the

microbial food web (Margalef, 1969; Yentsch and Phinney, 1989; Chisholm, 1992). Closer examination of the picophytoplankton fraction revealed that PPE contributed 17-25% to the sum of 0.2-3 μm and >3 μm size fractionated ^{14}C primary production along the transect, equivalent to contributions by *Prochlorococcus*. This was due to high cell-specific rates of production by PPE, particularly in the well-lit upper region (>15% surface photosynthetically active radiation, or PAR). Our results are in agreement with past studies in the Atlantic Ocean (Li, 1994; Jardillier et al., 2010) and indicate that PPE are highly active in the high-light, low-nutrient regions of the SPSG. The lack of concomitant accumulation of PPE biomass, however, may indicate that PPE are closely regulated by an analogous mortality rate. Worden et al. (2004) found that more than 2.5 times the carbon equivalent to the visible PPE standing stock was produced and consumed without changes in standing stock measurements.

In the NPSG, however, *Prochlorococcus* dominated (63-86%) picophytoplankton production, and comprised ~39% of the total ^{14}C-based rates of primary production (Chapter 3). PPE contributions were ~22% of picophytoplankton production, and their cell-specific rates of primary production were, similar to measurements in the SPSG, one to two orders of magnitude greater than those of *Prochlorococcus*. Similar to SPSG, PPE assemblages exhibited higher rates of activity in the upper 45 m in the euphotic zone throughout the year, suggesting that PPE appear adapted to rapid growth in warmer, well-lit regions of the euphotic zone.

This differential contribution of PPE between the North and South Pacific may be due to differences in the food web structure between the two gyres. Atmospheric iron deposition is reported to be an order of magnitude lower in the SPSG compared to the NPSG (Mahowald et al., 2005), limiting primary productivity and nitrogen fixation, resulting in elevated phosphate concentrations in the South Pacific (Bonnet et al., 2008). Low iron concentrations have been shown to limit cell division in *Prochlorococcus* (Mann and Chisholm, 2000), which may explain their lower contributions to primary production in the SPSG. Alternatively, lower cyanobacterial biomass was observed in the SPSG, with *Prochlorococcus* and *Synechococcus* euphotic zone depth-integrated cell inventories being 1.6- to 2.5-fold greater in the NPSG than in the SPSG. However, PPE cell inventories were equivalent between the two gyres, resulting in a two-fold lower *Prochlorococcus*-to-PPE ratio in the SPSG. Such results suggest that there may be greater top-down control by microbial grazers (on bacteria) in the SPSG due to lower abundance and/or activity of omnivorous zooplankton (Rivkin and Legendre, 2002).

Assessments of both ocean gyres revealed diverse and distinct PPE assemblages vertically in the water column, with greater diversity in the upper euphotic zone waters (<75 m). The highly active PPE in the well-lit upper euphotic zone regions of the oligotrophic gyres appeared to be haptophytes, dictyochophytes, and chrysophytes in both North and South Pacific, bolidophytes in the North Pacific, and prasinophytes Clade VII and IX in the South Pacific Subtropical Gyres (Chapters 2 and 4). The PPE community in the deeper euphotic zone surrounding the deep chlorophyll maximum (DCM) were different from the community in the well-lit region, with the low-light PPE community dominated by the pelagophyte *Pelagomonas* and various haptophytes in both North and South Pacific. In addition, the prasinophyte *Bathycoccus* and several cryptophytes appeared elevated in the lower euphotic zone waters of the North Pacific. These findings are broadly consistent with past studies which reported that oligotrophic ocean ecosystems support greater plankton diversity compared to more nutrient-enriched waters (Hulburt, 1963; Longhurst, 1967; McGowan & Walker, 1985). In addition, lower diversity of PPE observed in the deeper euphotic zone and in the eutrophic coastal region off Chile may reflect competitive exclusion due to the selective pressures imposed by higher nutrient concentrations (Hardin, 1960). Thus, such results suggest that in oligotrophic gyres, diversity is promoted to a greater extent by competition for nutrients than for light, and that removal processes promoting rapid turnover of species likely help to maintain elevated diversity in the upper euphotic zone. In addition, the diverse PPE taxa in the upper euphotic zone appeared to be closely related to organisms with previously reported capability for mixotrophy (Frias-Lopez et al., 2009; Acosta et al., 2013), which may help to acquire nutrition for cell maintenance (Mitra et al., 2014) and provide a competitive edge in low-nutrient regions.

Alternatively, PPE in the lower euphotic zone (near the DCM) may rely on seasonal inputs of nitrate due to convective mixing in the winter. Fawcett et al. (2011; 2014) reported that $\delta^{15}N$ signature of eukaryotes showed a greater seasonal reliance on assimilation of nitrate introduced from below the euphotic zone than on nitrogen recycled in the upper euphotic zone. Consistent with these findings, the strong vertical structuring of PPE taxa at Station ALOHA in the NPSG varied temporally, with PPE taxa that typically appeared to reside near the DCM (*e.g.*, *Pelagomonas*, *Bathycoccus*, haptophytes) occurring repeatedly in the upper euphotic zone between November through April. This redistribution of PPE taxa between the upper and lower euphotic zones resulted in altered taxa compositions at seasonal scales.

Consequently, these temporally dependent PPE communities responded differently to nutrient additions, as determined experimentally in Chapter 5. While diatoms were the dominant responders to nutrient additions in the larger size fraction throughout the year, diatoms in the picophytoplankton fraction responded significantly to nutrient additions only during the summer. In contrast, pelagophytes were the dominant responders to nutrient additions in the winter and spring, presumably due to their higher relative abundances during those times of the year. Pelagophyte growth in the upper euphotic zone during these spring periods may have been fueled by increased supply of nutrients with the seasonal deepening of the mixed layer. Such results indicate that changes in PPE taxa composition, influenced by seasonally variable environmental conditions, may significantly alter food web structure and impact contributions to export at seasonal scales in the NPSG.

6.2. Future research

This doctoral research has shown that PPE assemblages in the oligotrophic ocean are diverse, spatially distinct, and highly active in the euphotic zone, which may influence food web dynamics and successive processes. Their apparently high growth rates but relatively low biomass suggests PPE have rapid turnover times in the upper ocean (Calbet and Landry, 2004), contributing either to the dissolved organic matter pool or to the transfer of carbon up the food web. Though small in size, removal from the upper ocean as a result of viral lysis (Baudoux et al., 2008; Bidle and Vardi, 2011) and other causes of mortality, such as accelerated sinking through particle aggregation and mesozooplankton grazing, could contribute to carbon export (Richardson and Jackson, 2007). Consistent with such dynamics, *Pelagomonas* sequences have been retrieved from marine sediments, suggesting they may be significant transporters of carbon to the deep sea (Worden et al., 2012). Thus, understanding the removal processes of PPE and further characterizing the fate of PPE carbon is key to determining the further role of PPE in carbon cycling in the oligotrophic ocean.

In addition, several members of the PPE have been reported to be important consumers of picocyanobacteria, specifically *Prochlorococcus* (Frias-Lopez et al., 2009). If so, this result has large implications for the role of PPE in the food web structure of oligotrophic ecosystems. Hence, determining the timing and expression of phagotrophy in PPE, as well as the trajectory of consumed cell matter (*e.g.*, incorporation into biomass or nutrition for cell maintenance) is key to

further understanding the complicated networks of picoplankton in the oligotrophic ocean. Along these lines, teasing apart the activities of other (non-photosynthetic) picoeukaryotes such as MAST groups and Syndiniales parasites are also crucial in contributing future knowledge to understanding the functional role of picoeukaryotes in the ocean gyres. Though next generation sequencing techniques are prevalent and popular, classic methods such as cell culture isolation and culture-based competition experiments may allow focused evaluation of the ecology of PPE in the oligotrophic subtropical ocean gyres.

6.3. References

Acosta F., D. K. Ngugi, and U. Stingl. 2013. Diversity of picoeukaryotes at an oligotrophic site off the Northeastern Red Sea Coast. Aquat. Biosyst. **9**: 16. doi:10.1186/2046-9063-9-16.

Baudoux, A. C., Veldhuis, M., A. Noordeloos, G. van Noort, and C. Brussaard. 2008. Estimates of virus-vs. grazing induced mortality of picophytoplankton in the North Sea during summer. Aquat. Microb. Ecol. **52**: 69-82.

Bidle, K. D., and A. Vardi. 2011. A chemical arms race at sea mediates algal host–virus interactions. Curr. Opin. Microbiol. **14**, 449-457.

Bonnet, S., G. Guieu, F. Bruyant, and others. 2008. Nutrient limitation of primary productivity in the Southeast Pacific (BIOSOPE cruise). Biogeosciences **5**: 215-225.

Calbet, A., and M. R. Landry. 1999. Mesozooplankton influences on the microbial food web: direct and indirect trophic interactions in the oligotrophic open ocean. Limnol. Oceanogr. **44**: 1370-1380.

Chisholm, S. W. 1992. Phytoplankton size, p. 213-237. In P. G. Falkowski and A. D. Woodhead [eds.], Primary productivity and biogeochemical cycles in the sea. Springer.

Fawcett, S. E., M. W. Lomas, J. R. Casey, B. B. Ward, and D. M. Sigman. 2011. Assimilation of upwelled nitrate by small eukaryotes in the Sargasso Sea. Nature Geosci. **4**: 717-722.

Fawcett, S. E., M. W. Lomas, B. B. Ward, and D. M. Sigman. 2014. The counterintuitive effect of summer-to-fall mixed layer deepening on eukaryotic new production in the Sargasso Sea. Glob. Biogeochem. Cycle **28**: 86-102.

Frias-Lopez, J., A. Thompson, J. Waldbauer, and S. W. Chisholm. 2009. Use of stable isotope-labelled cells to identify active grazers of picocyanobacteria in ocean surface waters. Environ. Microbiol. **11**: 512-525.

Hardin G. 1960. The competitive exclusion principle. Science **131**: 1292-1297.

Hulburt, E. M. 1963. The diversity of phytoplanktonic populations in oceanic, coastal, and estuarine regions. J. Mar. Res. **21**: 81-93.

Jardillier, L., M. V. Zubkov, J. Pearman, and D. J. Scanlan. 2010. Significant CO_2 fixation by small prymnesiophytes in the subtropical and tropical northeast Atlantic Ocean. ISME J. **4**: 1180-1192.

Li, W. K. W. 1994. Primary production of prochlorophytes, cyanobacteria, and eukaryotic ultraphytoplankton: measurements from flow cytometric sorting. Limnol. Oceanogr. **39**: 169-175.

Longhurst, A. R. 1967. Diversity and trophic structure of zooplankton communities in the California Current. Deep-Sea Res.: Oceanogr. Abstr. **14**: 393-408.

Mahowald, N. M., A. R. Baker, G. Bergametti, and others. 2005. Atmospheric global dust cycle and iron inputs to the ocean. Glob. Biogeochem. Cycle **19**: GB4025. doi:10.1029/2004GB002402.

Mann, E. L., and S. W. Chisholm. 2000. Iron limits the cell division rate of *Prochlorococcus* in the eastern equatorial Pacific. Limnol. Oceanogr. **45**: 1067-1076.

Margalef, R. 1969. Size of centric diatoms as an ecological indicator. Mitt. Internat. Verein. Limnol. **17**: 202-210.

McGowan, J. A., and P. W. Walker. 1985. Dominance and diversity maintenance in an oceanic ecosystem. Ecol. Monogr. **55**: 103-118.

Mitra, A., K. J. Flynn, J. M. Burkholder, and others. 2014. The role of mixotrophic protists in the biological carbon pump. Biogeosciences **11**: 995-1005. doi:10.5194/bg-11-995-2014.

Richardson, T. L., and G. A. Jackson. 2007. Small phytoplankton and carbon export from the surface ocean. Science **315**: 838-840. doi:10.1126/science.1133471.

Rivkin, R. B., and L. Legendre. 2002. Roles of food web and heterotrophic microbial processes in upper ocean biogeochemistry: Global patterns and processes. Ecol. Res. **17**: 151-159.

Worden, A. Z., J. Janouskovec, D. McRose, A. Engman, R. M. Welsh, S. Malfatti, S. G. Tringe, and P. J. Keeling. 2012. Global distribution of a wild alga revealed by targeted metagenomics. Curr. Biol. **22**: R675-R677. doi:10.1016/j.cub.2012.07.054.

Worden, A.Z., J. K. Nolan, and B. Palenik, 2004. Assessing the dynamics and ecology of marine picophytoplankton: The importance of the eukaryotic component. Limnol. Oceanogr. **49**: 168-179.

Yentsch, C. S, and D. A. Phinney. 1989. A bridge between ocean optics and microbial ecology. Limnol. Oceanogr. **34**: 1694-1705.